

FACULDADE DE ENGENHARIA DA UNIVERSIDADE DO PORTO

Use of Cork Byproducts as Sorbents for Oil and Grease Removal from Industrial Wastewaters

Ariana Maciel Abranches Pintor



A thesis submitted to the Faculty of Engineering, University of Porto for the PhD degree
in Environmental Engineering

Supervisors: Doutor Rui Alfredo da Rocha Boaventura
Doutora Cidália Maria de Sousa Botelho
Doutor Vítor Jorge Pais Vilar

LSRE-Laboratory of Separation and Reaction Engineering - Associate Laboratory LSRE/LCM
Department of Chemical Engineering, Faculty of Engineering, University of Porto
October, 2014

Use of Cork Byproducts as Sorbents for Oil and Grease Removal from Industrial Wastewaters

Ariana Maciel Abranches Pintor

A thesis submitted to the Faculty of Engineering, University of Porto for
the PhD degree in Environmental Engineering

Abstract

Cork is a natural, renewable material whose extraction and processing is one of the most important industries in Portugal and other Mediterranean countries. From the total weight in cork harvested from the tree, around 80% ends up as cork byproducts. The majority consists of cork granulates, particles of 0.25-8 mm size whose main application is in the production of agglomerates. Emerging studies in the last decade reflect a trend in research for added value applications for this byproduct, namely in environmental remediation. Cork granulates have been shown to be good biosorbents or precursors of activated carbons for the removal of a variety of pollutants from water, and a recent commercial development is the line of products CORKSORB, which consists of granule-filled pillows, socks and booms for oil spill management. The success of this product prompts the study of the application of cork granulates for the removal of oil and grease (O&G) in industrial wastewaters.

O&G is a widespread pollutant which presents the biggest concern in the emulsified form. The most common treatments for emulsified O&G removal include coagulation/flocculation with dissolved air flotation (DAF) and membrane separation. However, the former leads to the production of large amounts of hazardous sludge while the latter is expensive and prone to fouling problems. In this context, sorption onto natural organic materials, such as cork byproducts, is emerging as a simpler and cleaner technology.

Several materials were initially considered for O&G sorption, including raw cork granulates and regranulated cork granulate (RCG), with different particle sizes. These materials were further modified with cationic surfactant hexadecyltrimethylammonium (HDTMA) bromide and used as precursors for the production of activated carbons by impregnation with phosphoric acid. The latter were also pyrolysed with propene to improve hydrophobicity. Textural and surface characterisation of cork biosorbents and cork-based activated carbons was carried out by helium pycnometry, nitrogen adsorption isotherms, temperature-programmed desorption (TPD), Fourier transform infrared spectroscopy (FTIR), potentiometric titration and immersion calorimetry. It was found that activation increased the surface area and developed micro and mesoporosity and this resulted in increased sorption capacity towards sunflower oil. However, when accounting for the yields of carbonisation, the sorption capacity of regranulated cork was the same as that of the best performing activated carbons.

The chosen case study consisted in the treatment of vegetable oil refinery wastewaters (VORWs), namely those from chemical refining of sunflower oil. Two wastewater samples were collected, one was the wastewater from the homogenisation tank of the industrial wastewater treatment plant (TH) and the other was the wastewater from the removal of waxes line (AW), and both were characterised according to the most relevant physicochemical parameters. Due to high contents of chemical oxygen demand (COD) and O&G, a primary treatment was applied in order to precede the sorption treatment. After 30 min in quiescence, O&G removals over 80% in both VORW samples was achieved. Using an empirical hyperbola model and the theoretical principles for droplet motion in a fluid (Newton's and Stokes' equations), it was verified that all "free oil" (droplets with

size under 150 μm) could be removed within the 30-min separation time.

Sorption treatment using regranulated cork granulates was first evaluated in batch mode in sunflower oil-in-water emulsions. A kinetically stable emulsion during 24 h could be produced by adjusting the shearing protocol for emulsification. Droplet size distributions and zeta potential measurements allowed to confirm electrostatic repulsion between oil droplets in stable emulsions and also the occurrence of destabilisation by charge neutralisation when lowering the pH. A 3^2 full factorial design was used to evaluate the influence of pH and NaCl concentration in O&G removal by sorption onto regranulated cork. It was found that the increase of ionic strength by the presence of NaCl caused a double layer compression effect which decreased the zeta potential and allowed for high removals ($\approx 90\%$) at higher values of pH. A 3^3 Box-Behnken design considered also the soap/O&G ratio as a factor. In these conditions, only strong acidification could guarantee effective O&G removal; the presence of saponified matter was inhibitory up to 60 – 70% ratio, due to adsorption of surface-active sodium oleates at the oil-water interface, forming micelles and increasing the electrokinetic potential.

At the conditions of 0.2 M NaCl and pH 6.0 in the absence of soap or pH 2.0 in the presence of 60% soap ratio, the sorption isotherms and kinetics were determined. Equilibrium was well described by both the Freundlich and linear isotherm models, indicating that the uptake mechanism was organic-organic partitioning. Kinetics were described by a mass transfer model with the assumptions of homogeneous oil dispersion in solution and the existence of an external sublayer around the cork particles in which the oil diffuses from the bulk to the solid surface. It was found that increased agitation slowed down the sorption kinetics due to the stabilising influence of turbulence in the emulsion.

Treatment of real VORW samples by sorption onto regranulated cork granulates was successful in batch mode as long as acid conditions (pH lower than 2.0) were provided. The addition of NaCl within practical limits did not contribute significantly to O&G removal. The sorbent dosage could be adjusted to improve removal efficiency further; in AW sample this resulted in a sorption isotherm, while in TH wastewater, the removal efficiency could not go beyond a final O&G concentration of $40 \pm 10 \text{ mg L}^{-1}$ due to the presence of dissolved organic matter.

A continuous stirred-tank reactor unit was operated with a simulated wastewater containing 0.2 M NaCl, 60% soap (to a total O&G concentration of $\approx 200 \text{ mg L}^{-1}$) and adjusted to pH 2.0. At a flowrate of 10 mL min^{-1} , solid/liquid ratio of 3.4 g L^{-1} and with a mechanical stirring speed of 250 rpm, it was possible to treat 4.8 L of wastewater to values below the discharge limit for O&G defined in the Portuguese legislation (15 mg L^{-1}).

Finally, exploratory studies were carried out on oil recovery and sorbent regeneration using desorption by elution and mechanical compression in an extruder. The regranulated cork sorbents were impregnated in pure sunflower oil medium and mechanical compression at 7 bar, with a mass load of 10 g and a compression procedure of four 1-min compressions could achieve the maximum recovery of $67 \pm 1\%$. Using this method, the cork granulates remained stable over 10 cycles of sorption and recovery, suffering only partial fragmentation.

The study demonstrated the feasibility of using regranulated cork sorbents for the removal of O&G from VORWs at lab scale. The methodology has the potential to become a cheaper and more environmentally friendly technology for secondary treatment of oily wastewaters, while providing added value to byproducts from the cork industry.

Resumo

A cortiça é um material natural renovável cuja extração e processamento constitui uma das mais importantes indústrias em Portugal e outros países Mediterrânicos. Do total em peso de cortiça retirada do sobreiro, cerca de 80% passa a constituir subprodutos. A maioria destes consiste em granulados de cortiça, partículas com tamanho entre 0.25-8 mm cuja principal aplicação é a produção de aglomerados. Estudos realizados na última década refletem uma tendência na investigação com vista à aplicação deste subproduto com um valor acrescentado, nomeadamente em remediação ambiental. Já foi demonstrado que os granulados de cortiça são bons biossorventes ou precursores de carvões ativados para a remoção de uma variedade de poluentes em solução aquosa. Um desenvolvimento comercial recente é a linha de produtos CORKSORB que consiste em almofadas, bóias e barreiras preenchidas com grânulos para contenção de derrames de petróleo ou produtos petrolíferos. O sucesso deste material evidencia o potencial para a aplicação de granulados de cortiça na remoção de óleos e gorduras (O&G) em águas residuais industriais.

Os óleos e gorduras são poluentes muito difundidos que causam maior preocupação quando se encontram na forma emulsionada. Os tratamentos mais utilizados para a remoção de O&G emulsionados incluem coagulação/floculação com flutuação por ar dissolvido e separação por membranas. No entanto, o primeiro conduz à produção de grandes quantidades de lama potencialmente tóxica enquanto o último é dispendioso e propenso a problemas de colmatagem. Neste contexto, a sorção por materiais orgânicos naturais, como os subprodutos de cortiça, está a surgir como uma tecnologia mais simples e mais limpa.

Vários materiais foram considerados inicialmente para a remoção de O&G: granulados de cortiça natural e granulados de cortiça aglomerada expandida, com diferentes granulometrias. Estes materiais foram ainda modificados com o surfactante catiónico brometo de hexadeciltrimetilamónio e utilizados como precursores na produção de carvões ativados por impregnação com ácido fosfórico. A caracterização das propriedades de textura e superfície dos biossorventes de cortiça e dos carvões ativados baseados em cortiça foi realizada através de picnometria de hélio, isotérmicas de adsorção de azoto, dessorção a temperatura programada, espectroscopia de absorção no infravermelho, titulação potenciométrica e calorimetria de imersão. Verificou-se que a ativação aumentou a área de superfície e provocou o desenvolvimento de micro e mesoporosidade e isto resultou num aumento da capacidade de sorção de óleo de girassol. No entanto, quando se teve em conta os rendimentos de carbonização, a capacidade de adsorção da cortiça expandida foi a mesma que a dos carvões ativados com melhor desempenho.

O caso de estudo escolhido consistiu no tratamento de águas residuais de refinaria de óleo vegetal (ARROV), nomeadamente da refinação de óleo de girassol. Foram recolhidas duas amostras de águas residuais, uma no tanque de homogeneização da estação de tratamento de águas residuais industriais (TH) e a outra na linha de remoção de ceras (AW), e ambas foram caracterizadas relativamente aos parâmetros físico-químicos. Devido aos elevados valores de carência química de oxigénio (CQO) e de O&G, foi aplicado um tratamento primário antes do tratamento de sorção. Depois de 30 min em repouso, foram atingidas remoções de O&G acima de 80% em ambas as

amostras de ARROV. Utilizando um modelo empírico e os princípios teóricos para o movimento de gotículas num fluido (equações de Newton e Stokes), verificou-se que todo o “óleo livre” (gotículas com tamanho inferior a $150 \mu\text{m}$) pôde ser removido dentro do tempo de separação de 30 min. O tratamento de sorção utilizando granulado de cortiça aglomerada expandida foi primeiro avaliado em modo “batch” utilizando emulsões de óleo de girassol em água. Obteve-se uma emulsão cineticamente estável durante 24 h ajustando o protocolo de mistura para a emulsificação. As distribuições de tamanho de partícula e as medições de potencial zeta puderam confirmar a repulsão eletrostática entre gotículas de óleo em emulsões estáveis e ainda a ocorrência de destabilização através da neutralização de carga quando se baixa o pH. Foi utilizado um desenho experimental fatorial 3^2 para avaliar a influência do pH e da concentração de NaCl na remoção de O&G por sorção em cortiça expandida, e verificou-se que o aumento da força iônica, pela presença de NaCl, causou um efeito de compressão da dupla camada que diminuiu o potencial zeta e permitiu a obtenção de remoções elevadas ($\approx 90\%$) a valores de pH mais altos. Um desenho fatorial Box-Behnken 3^3 considerou ainda como fator a razão sabão/O&G. Nestas condições, só uma acidificação forte garantiu uma remoção de O&G eficaz; a presença de matéria saponificada foi inibidora até uma razão de 60-70%, devido à adsorção de oleatos de sódio na interface óleo/água, formando micelas e aumentando o potencial elétrico.

Para uma concentração de NaCl 0,2 M e pH 6,0 na ausência de sabão, ou pH 2,0 na presença de 60% de sabão, foram determinadas as isotérmicas e cinética de sorção. O equilíbrio foi bem descrito pelas isotérmicas de Freundlich e linear, indicando que o mecanismo de sorção foi a partição orgânica. A cinética foi descrita por um modelo de transferência de massa com assumindo dispersão homogênea de óleo na água e a existência de uma subcamada externa à volta das partículas de cortiça na qual o óleo se difunde do líquido para a superfície sólida. Verificou-se que um aumento da agitação prejudicou a cinética de sorção devido à influência estabilizadora da turbulência na emulsão.

O tratamento de amostras reais de ARROV foi bem sucedido em modo “batch” desde que fossem garantidas condições ácidas (pH igual ou menor que 2,0). A adição de NaCl, dentro de limites práticos, não contribuiu significativamente para a remoção de O&G. A dosagem de sorvente pode ser ajustada para aumentar ainda mais a eficiência de remoção; na amostra AW tal permitiu a obtenção de uma isotérmica de sorção, enquanto na amostra TH a eficiência de remoção não foi além duma concentração final de O&G de $40 \pm 10 \text{ mg L}^{-1}$ devido à presença de matéria orgânica dissolvida.

Um reator contínuo perfeitamente agitado foi operado com uma água residual simulada contendo 0,2 M NaCl, 60% sabão (para uma concentração de O&G total de $\approx 200 \text{ mg L}^{-1}$) e ajustada a pH 2,0. Para um caudal de 10 mL min^{-1} , razão sólido/líquido de $3,4 \text{ g L}^{-1}$ e com uma velocidade de agitação mecânica de 250 rpm, foi possível tratar 4,8 L de água residual de modo a obter valores abaixo do limite de descarga para O&G definido na legislação portuguesa (15 mg L^{-1}).

Por fim, foram realizados estudos exploratórios para a recuperação de óleo e regeneração do sorvente através de dessorção por eluição e compressão mecânica numa extrusora. Os sorventes de cortiça aglomerada expandida foram impregnados em óleo de girassol puro e a compressão mecânica a 7 bar, com uma massa de 10 g e um procedimento de quatro compressões de 1 min permitiu atingir uma recuperação máxima de $67 \pm 1\%$. Com este método, os granulados de cortiça permaneceram estáveis ao longo de 10 ciclos de sorção e recuperação, sofrendo apenas uma fragmentação parcial.

O estudo demonstrou a viabilidade da utilização de cortiça aglomerada expandida para a remoção de O&G de ARROV à escala laboratorial. A metodologia tem potencial para se tornar numa tecnologia mais barata e mais amiga do ambiente para o tratamento secundário de águas residuais com óleo, ao mesmo tempo que acrescenta valor a subprodutos da indústria corticeira.

Acknowledgements

First of all, I would like to thank the institution which made this work possible, the Laboratory of Separation and Reaction Engineering - Associate Laboratory LSRE/LCM and the Faculty of Engineering of the University of Porto. A big thank you goes to my supervisors: Professor Rui Boaventura, for his patience and understanding, for being available to discuss all my ideas, for providing me with the necessary materials for carrying out the experimental work and the opportunities to publish and attend conferences and for always being supportive of my work; Professor Cidália Botelho, for always having a kind listening ear, for all the support and encouragement and for giving me the opportunity to collaborate and supervise younger students; and Doutor Vítor Vilar, for encouraging me to pursue PhD studies and consider this topic, for pushing me to go abroad to learn, for all the insights provided with the collaboration with project HIDROCORK, and for all the valuable suggestions and analyses of my results and papers.

Second, I must acknowledge the financial support of FCT - Fundação para a Ciência e a Tecnologia with my PhD scholarship (SFRH/BD/70142/2010). I would like to acknowledge also QREN - Quadro de Referência Estratégico Nacional, AdI - Agência de Inovação and Corticeira Amorim, S. G. P. S. for the financial support of the HIDROCORK Project (“Use of cork wastes and byproducts for elimination of oils and fats from water”) with which I collaborated and from which I gained valuable insights for my work. I would like to thank the involvement and support of Dr. Susana Silva, mainly directed towards the HIDROCORK Project but always available to help with matters related to this thesis. An acknowledgement also goes to Patrícia Correia who collaborated with the HIDROCORK Project at Corticeira Amorim.

Through the efforts of Dr. Susana Silva I had the opportunity to meet with Eng. Rui Ramos of SOVENA Portugal, whom I acknowledge for the availability to provide the vegetable oil refinery wastewaters for this study and for receiving us at Barreiro back in 2012. I’d also like to thank Eng. Sérgio Palma of SOVENA for all the patience in scheduling and collecting the samples for transport to Porto.

A major acknowledgement goes to Professor Francisco Rodríguez-Reinoso for receiving me for an internship at the University of Alicante in 2011. I was probably more work than value to the laboratory there and I must thank all the patience and kindness with which I was received; in particular to Dr. Ana María Silvestre-Albero, who was a helping hand and teacher from start to finish in all aspects of my stay there. I’d like to thank all my lab mates at Alicante who made me feel welcome and gave me true friendship, in special Erika, Mateus and Robison.

I’d also like to give thanks to all those who helped in little ways to make this work richer. To Alexandra Gonçalves of LCM for helping me with TPD interpretation and deconvolution. To Raquel Cristóvão for teaching me how to work with Statistica software and answering my questions regarding experimental design. To Professor Arminda Alves for answering my questions regarding analytical method validation. To Professor Cheng Chia-Yau, for providing some lab space for my writing in 2012. To Professor Fernão Magalhães and Eng. Luís Carlos Matos, for providing the equipment for droplet size distribution measurements and all the technical assis-

tance. The same goes to Professor Maria do Carmo Pereira and her students Joana Loureiro, Sílvia Coelho, Manuela Frasco and Bárbara Gomes with the zeta potential measurements and equipment. To Eng. Sónia, Eng. Arminda and Eng. Luís Martins who first taught me the FTIR method for O&G determination at E001. To Eng. Liliana Pereira for helping me with small measurements and technical problems at E007/E002.

Not less important in any way, I must thank everyone who collaborated with me at laboratory E404 in this project. A big thank you goes to Catarina Ferreira and Joana Pereira, who were not only my lab mates, colleagues and companions for two years, but have also become friends. Another goes to Renata Souza, for giving me a helping hand in the laboratory when time was running short and for discussing ideas with me in the last year. Finally, thank you Andreia Martins, for being such a dedicated student so we could make a great collaboration at the laboratory.

To everyone else at E404 who put up with me for the past four years, especially those who were always friendly to me even in my bad days. Thanks to those who shared many everyday moments, lab routines, coffees and lunches: Tânia Silva, Tatiana Pozdniakova, João Pereira, Daniel Queirós, Petrick Soares, Rui Ribeiro, Filipe Lopes and Gabriela Ungureanu. A special thank you goes to André Monteiro and Livia Xerez who, beyond that, gave me true friendship, encouragement and support. Finally, my deepest gratitude to André Fonseca, without whose heartfelt friendship and companionship I might have not been able to complete writing in the last two months; thank you for sharing this challenge with me.

Last, but not least, I must thank those who, on a very personal level, contributed toward this work by being there for me. To my parents, thank you for being there in all the hard times, for raising me up when I'm breaking down, for fighting for me and still letting me fly. To João, for all the love and support, for asking about my day, for listening when I needed to vent about my problems and for making me think outside of the box. To my dear friend Susana, for all her messages and chats of encouragement and for putting up with my 'thesis unavailability' for almost a year now. And thank you to everyone who is my friend and crossed my path during these four years with positive messages of encouragement and strength. None of this would have been possible without your love.

To my family

“It is not our part to master all the tides of the world, but to do what is in us for the succour of those years wherein we are set, uprooting the evil in the fields that we know, so that those who live after may have clean earth to till.”

*J. R. R. Tolkien, in *The Lord of the Rings**

Contents

Abbreviations and Symbols	xix
1 Introduction	1
1.1 Motivation and Relevance	1
1.2 Objectives and Outline	3
1.3 References	4
2 Literature Review	7
2.1 Use of cork powder and granulates in the removal of pollutants by sorption	7
2.1.1 Introduction	7
2.1.2 Cork and cork byproducts	7
2.1.3 Application and transformation of cork powder and granulates for sorption	17
2.1.4 Conclusions	28
2.2 Oil and grease (O&G): a common pollutant in wastewaters	28
2.2.1 Introduction	28
2.2.2 The O&G class of pollutants	29
2.2.3 Treatment of wastewaters with O&G	31
2.2.4 Treatment of wastewaters with O&G by sorption	41
2.2.5 Conclusions	48
2.3 References	49
3 Textural and surface characterisation of cork-based sorbents	63
3.1 Introduction	63
3.2 Experimental	64
3.2.1 Biosorbents preparation	64
3.2.2 Activated carbon production	64
3.2.3 Characterisation of materials	65
3.2.4 Potentiometric titration	66
3.2.5 Sorption tests	66
3.3 Results and discussion	67
3.3.1 Physical and chemical characterisation	67
3.3.2 Textural characterisation	68
3.3.3 Surface characterisation	71
3.3.4 Application to the sorption of oil from water	79
3.4 Conclusions	80
3.5 References	81

4	Optimisation of a primary gravity separation treatment for vegetable oil refinery wastewaters	85
4.1	Introduction	85
4.2	Theoretical framework	86
4.3	Experimental	87
4.3.1	Gravity separation column	87
4.3.2	Wastewater samples	87
4.3.3	Experimental methodology	88
4.3.4	Analysis methods	88
4.3.5	Determination of oil and water properties	89
4.4	Results and discussion	89
4.4.1	Characterisation of the wastewaters	89
4.4.2	Gravity separation kinetics	91
4.4.3	Fitting of empirical model and optimisation of retention time	93
4.4.4	Influence of particle size vs. initial height and treatment time	93
4.4.5	Optimal treatment time	97
4.5	Conclusions	99
4.6	References	100
5	The role of emulsion properties and stability on vegetable oil uptake by regranulated cork sorbents	103
5.1	Introduction	103
5.2	Experimental	104
5.2.1	Materials	104
5.2.2	Analytical methods	104
5.2.3	Emulsion stability tests	104
5.2.4	Sorption tests	105
5.3	Results and discussion	106
5.3.1	Production of a stable oil-in-water emulsion	106
5.3.2	Emulsion stability after pH adjustment	107
5.3.3	Influence of pH on oil sorption capacity	108
5.3.4	Influence of ionic strength	111
5.3.5	Sorption kinetics and isotherm	116
5.4	Conclusions	120
5.5	References	120
6	Treatment of vegetable oil refinery wastewater by sorption of oil and grease onto regranulated cork – a study in batch and continuous mode	123
6.1	Introduction	123
6.2	Experimental	124
6.2.1	Materials	124
6.2.2	Analytical methods	124
6.2.3	Experimental set-up	125
6.2.4	Experimental procedure	126
6.3	Results and discussion	127
6.3.1	Real VORWs	127
6.3.2	Influence of saponified matter on O&G sorption onto regranulated cork	132
6.3.3	Continuous sorption tests	137
6.4	Conclusions	141

6.5	References	141
7	Oil desorption and recovery from cork sorbents	143
7.1	Introduction	143
7.2	Experimental	143
7.2.1	Materials	143
7.2.2	Analytical methods	144
7.2.3	Impregnation of cork granules	144
7.2.4	Desorption by elution	144
7.2.5	Recovery by compression	145
7.3	Results and discussion	146
7.3.1	Desorption by elution	146
7.3.2	Recovery by compression	148
7.4	Conclusions	152
7.5	References	153
8	Conclusions and Future Work	155
8.1	General conclusions	155
8.2	Suggestions for future work	157
A	Uncertainty in the analytical method used for O&G determination	159
A.1	Introduction	159
A.2	Experimental	159
A.3	Results	161
A.3.1	Carbon tetrachloride - low range	161
A.3.2	Carbon tetrachloride - high range	162
A.3.3	Tetrachloroethylene - low range	164
A.3.4	Tetrachloroethylene - high range	164
A.3.5	Comparison between methods with CTC and PCE	170
A.4	References	170

List of Figures

2.1	Evolution of the number of publications on indexed journals (source: Scopus) containing the keyword “cork” between 1990 and 2013.	8
2.2	Cork oaks after harvest, with the cork planks at rest in the soil around them. . . .	8
2.3	Scanning electron microscopy (SEM) micrograph of cork cells.	9
2.4	Cork planks piled after boiling.	12
3.1	SEM micrographs of cork granulates.	67
3.2	N ₂ adsorption isotherms at -196 °C for raw cork biosorbents of different granulometry (FCG, ICG, CCG), regranulated cork granules (RCG), and washed cork biosorbents (W-ICG).	69
3.3	N ₂ adsorption isotherms at -196 °C for cork-based activated carbons.	71
3.4	Experimental data and model curves (bimodal Sips distribution of affinity constants combined with local Langmuir-Freundlich isotherm) for particle charge data obtained from potentiometric titration of cork biosorbents ICG, W-ICG and RCG.	73
3.5	TPD profiles of cork biosorbents.	74
3.6	FTIR spectra.	76
3.7	TPD profiles of cork-based activated carbons.	78
3.8	Sorption capacities and removal efficiencies of cork-based sorbents for sunflower oil emulsified in water, at pH 7.2 and 25 °C (error bars: standard uncertainty).	79
4.1	Graphical depiction of experimental removals and the corresponding empirical models adjusted by non-linear regression.	94
4.2	3D surface plots of treatment time t (min) as a function of h and D . Colour legend: brown for time of removal lower than 30 min; yellow for time of removal above 30 min.	96
4.3	3D surface plots of O&G removal (%) as a function of the treatment of particles with initial height h and diameter D	98
5.1	Changes (Δ) between final and initial values of oil concentration (C (O&G)), median droplet diameter (d_{50}), and the opposite of the change in hydrogen ion concentration (C_H), as a function of initial pH after acidification, in the study of emulsion stability with varying pH.	108
5.2	Sorption capacities (q) and removal efficiencies (R) of sunflower oil in water (initial concentration: 150-200 mg L ⁻¹) onto cork granules (dosage 1 g L ⁻¹) as a function of initial pH, along with the opposite of the change in hydrogen ion concentration between final and initial values in control and sorption assays.	109
5.3	Evolution of zeta potential (ζ) (initial, and final in control assays and sorption assays) during 24-h sorption experiments at different pH.	110

5.4	Evolution of particle size distribution measurements (initial, and final in control assays and sorption assays), represented by the median droplet diameter d_{50} , during 24-h sorption experiments at different pH.	111
5.5	Cumulative particle size distributions (initial, and final in control assay and sorption assay) in the 24-h sorption experiment at pH 6.	112
5.6	3D response surface of O&G removal efficiency in function of NaCl concentration and pH, as determined by the quadratic regression model. The experimental points are represented in white circles bordered in blue.	114
5.7	Evolution of zeta potential (ζ) (initial, and final in control assays and sorption assays) at the selected operating conditions of 0.2 M NaCl and pH 6, and its comparison with measurements in the absence of salt at pH 5.6 and 2.	115
5.8	Experimental data for isothermal equilibria at 25 °C of the sorption of sunflower oil from water by cork granules, at the selected operating conditions of 0.2 M NaCl and pH 6, along with fitted curves of the Freundlich equation and linear partitioning model.	117
5.9	Experimental data for the kinetic studies for both rotating speeds of 2 and 20 rpm of the sorption of sunflower oil from water by cork granules (dosage: 1.6 g L ⁻¹), at the selected operating conditions of 0.2 M NaCl and pH 6, along with the fitted curves of the mass transfer model.	119
6.1	Schematic representation of the continuous sorption unit.	125
6.2	Kinetics of O&G sorption by cork granules in real VORW samples AW and TH without chemical adjustment.	129
6.3	O&G removal efficiency R obtained at equilibrium with sorption treatment (cork dosage: 1 g L ⁻¹) after pH adjustment of AW and TH real VORW samples.	130
6.4	Effect of NaCl addition on O&G removal efficiency obtained at equilibrium with sorption treatment (cork dosage: 1 g L ⁻¹) in both VORW samples AW and TH, the latter with or without acidification to pH 2.0.	131
6.5	Isothermal equilibria at 25 °C for sorption of O&G on regranulated cork in AW sample: experimental data and fitted curves of the Freundlich and linear models.	132
6.6	3D response surface, determined by the second-order regression model, of O&G removal efficiency as a function of pH and soap ratio (%), at a fixed NaCl concentration of 0.11 M. Experimental points are represented in white circles bordered in blue.	135
6.7	Isothermal equilibria at 25 °C for sorption of O&G on regranulated cork in simulated wastewater: experimental data and fitted curves of the Freundlich and linear models.	136
6.8	Kinetics of O&G sorption by cork granules in simulated wastewater: experimental data and fitted curve of mass transfer model.	137
6.9	Evolution of normalised responses $\frac{C_{out}}{C_0}$ for the step experiment and the two sorption experiments in the continuous reactor, along with the fitted Danckwerts curve (Equation 6.3 and the model curves of the continuous stirred-tank operation, using the partition coefficient K_p of batch sorption equilibria (6.5) and an adjusted value (16.8) to the experimental data of the best performing sorption experiment (stirring speed 250 rpm).	138
7.1	Extruder CAMOZZI 368-905 used in compression tests along with its three types of metallic conical heads.	145

7.2	Recovery efficiencies for the different aqueous solution elutions, along with the recovery efficiency of the most successful compression procedure (4 compressions of 1 min at 7 bar).	147
7.3	Sorbed amount in total and recovery efficiency by compression during 4 cycles of sorption/compression at three different pressures (2, 5 and 7 bar) ($m_{oc} = 0.5$ g, 2 compressions of 1 min per cycle).	148
7.4	Recovery efficiency during interrupted compression and with continuous compression for 4 min.	149
7.5	Recovery efficiencies according to the mass load of oil-saturated sorbent in the extruder at the operating pressures of 2 bar and 7 bar (four 1-min compressions).	150
7.6	Overall sorption capacity (q_{total}), sorption capacity per cycle (q_{cycle}) and recovery efficiency by compression (R) ($m_{oc} = 10$ g, $P = 7$ bar, four 1-min compressions) during 10 cycles of sorption/recovery.	151
7.7	Visual aspect of the cork sorbents after the first (left) and the tenth (right) cycles of sorption/recovery.	152
A.1	Comparison between FTIR spectra of AW and TH VORW samples, a reference oil standard of 50 mg L^{-1} and a sunflower oil standard of 130 mg L^{-1}	160
A.2	Calibration curve for the CTC-LR method.	161
A.3	Estimation of uncertainty for the CTC-LR method.	163
A.4	Calibration curve for the CTC-HR method.	164
A.5	Estimation of uncertainty for the CTC-HR method.	166
A.6	Calibration curve for the PCE-LR method.	166
A.7	Estimation of uncertainty for the PCE-LR method.	167
A.8	Calibration curve for the PCE-HR method.	168
A.9	Estimation of uncertainty for the PCE-HR method.	169

List of Tables

2.1	Summary of proportions reported by different authors for the chemical composition of cork (Adapted from Silva et al. (2005)).	11
2.2	Chemical structures on cork surface identified by ^{13}C -cross polarization with magic angle spinning (CP/MAS) nuclear magnetic resonance (NMR) and FTIR spectra (based on data from Neto et al. (1995) , Lopes et al. (2001) and Prades et al. (2010)).	13
2.3	Maximum sorption capacities (q_{max}) by adjustment to the Langmuir model reported in the literature for the sorption of toxic metals on raw and regranulated cork granulates.	18
2.4	Maximum sorption capacities by adjustment to the Langmuir model reported in the literature for the sorption of organic pollutants on raw cork granulates.	20
2.5	Summary of chemical activation methods of cork powder and granulates reported in the literature.	23
2.6	Summary of physical activation methods of cork powder reported in the literature.	24
2.7	Limiting adsorbed amounts expressed in liquid volume (w_0) and maximum sorption capacities reported in the literature for the adsorption of pollutants from the gas phase on activated carbons derived from cork.	25
2.8	Maximum sorption capacities reported in the literature for the adsorption of pollutants from water on activated carbons derived from cork.	26
3.1	Elemental analysis, ash content, bulk and structural density of cork biosorbent samples.	68
3.2	Yields of carbonisation, BET surface area and total, micropore, and mesopore volume as determined from N_2 isotherms at $-196\text{ }^\circ\text{C}$ for all the samples studied.	70
3.3	Intrinsic constants and surface charges for carboxylic and hydroxyl groups obtained through the applied model using potentiometric titration data of cork biosorbents.	73
3.4	Total amounts of CO_2 and CO evolved in TPD analysis, respective CO_2/CO ratio, and immersion enthalpies in water and methanol for cork-based materials.	75
4.1	Characterisation of the wastewater samples under study.	90
4.2	Results of O&G and COD monitoring over time and corresponding removal efficiency in gravity separation experiments.	92
4.3	Values of model parameters and corresponding correlation coefficients, obtained for O&G and COD removal from two VORWs.	93
4.4	Physical properties used in theoretical and empirical correlations (ρ_w , ρ_o , μ , h_0 and g).	95
5.1	Factor levels used in the 3^2 full factorial design.	105

5.2	Median droplet diameter, measured right after mixing and following 24 h at rest, of emulsions produced during different protocols of mechanical shear.	107
5.3	Runs and experimental responses in terms of O&G removal efficiency for the 3^2 full factorial design, along with the predicted values obtained by the quadratic regression model and the corresponding residuals.	113
5.4	ANOVA table of the full factorial design, with F -values and p -values for estimating the statistical significance of factors. In bold, significant factors with $p < 0.05$. 113	113
6.1	Factor levels used in the Box-Behnken design.	126
6.2	Characterisation of pretreated wastewater samples according to pH, conductivity, O&G, COD, DOC, and inorganic ions.	128
6.3	O&G removal efficiency results for the 15 runs of the Box-Behnken design, along with the predicted values obtained by the second-order regression model and the corresponding residuals.	133
6.4	ANOVA table of the Box-Behnken design with F -values and p -values. Significant factors, with $p < 0.05$, are emphasized in bold.	134
A.1	Calibration parameters for the CTC-LR method.	162
A.2	Determination of the uncertainty associated to the calibration, for the analytical method CTC-LR.	163
A.3	Calibration parameters for the CTC-HR method.	165
A.4	Determination of the uncertainty associated to the calibration, for the analytical method CTC-HR.	165
A.5	Calibration parameters for the PCE-LR method.	165
A.6	Determination of the uncertainty associated to the calibration, for the analytical method PCE-LR.	167
A.7	Calibration parameters for the PCE-HR method.	168
A.8	Determination of the uncertainty associated to the calibration, for the analytical method PCE-HR.	169
A.9	Comparison between the intermediate precision measurements using PCE and CTC. 170	170

Abbreviations and Symbols

Acronyms

0-CCG carbonised coarse cork granulate

0.11-CCG activated carbon produced from coarse cork granulate by phosphoric acid activation with an X_P ratio of 0.11

0.11-RCG activated carbon produced from regranulated cork granulate by phosphoric acid activation with an X_P ratio of 0.11

0.25-0-CCG activated carbon produced from carbonised coarse cork granulate by phosphoric acid activation with an X_P ratio of 0.25

0.25-CCG activated carbon produced from coarse cork granulate by phosphoric acid activation with an X_P ratio of 0.25

0.25-RCG activated carbon produced from regranulated cork granulate by phosphoric acid activation with an X_P ratio of 0.25

3D 3-dimensional

4,4'-DDT 4,4'-dichlorodiphenyltrichloroethane

ANOVA analysis of variance

AOP advanced oxidation process

API American Petroleum Institute

AW wastewater from the removal of waxes line

BET Brunauer-Emmett-Teller

BOD₅ 5-day biochemical oxygen demand

CCG coarse cork granulate

COD chemical oxygen demand

CP/MAS cross polarization with magic angle spinning

CPI corrugated-plate interceptor

CSTR continuous stirred-tank reactor

- CTC** carbon tetrachloride
- CTC-HR** carbon tetrachloride - high range
- CTC-LR** carbon tetrachloride - low range
- DAF** dissolved air flotation
- DN** dissolved nitrogen
- DOC** dissolved organic carbon
- DR** Dubinin-Radushkevich
- FCG** fine cork granulate
- FTIR** Fourier transform infrared spectroscopy
- GAC** granular activated carbon
- GC** gas chromatography
- HDTMA** hexadecyltrimethylammonium
- IAF** induced air flotation
- ICG** intermediate cork granulate
- IGC** inverse gas chromatography
- IUPAC** International Union of Pure and Applied Chemistry
- LOD** limit of detection
- LOQ** limit of quantification
- MF** microfiltration
- MFC** mechanically agitated flotation cell
- NF** nanofiltration
- NMR** nuclear magnetic resonance
- O&G** oil and grease
- P-0.25-CCG** activated carbon pyrolysed with propene, previously produced from coarse cork granulate by phosphoric acid activation with an X_p ratio of 0.25
- P-0.25-RCG** activated carbon pyrolysed with propene, previously produced from regranulated cork granulate by phosphoric acid activation with an X_p ratio of 0.25
- PAC** polyaluminium chloride
- PAH** polycyclic aromatic hydrocarbon
- PCE** tetrachloroethylene

- PCE-HR** tetrachloroethylene - high range
- PCE-LR** tetrachloroethylene - low range
- PH** peak height
- PIDS** polarization intensity differential scattering
- POME** palm oil mill effluent
- PPI** parallel-plate interceptor
- PVC** polyvinyl chloride
- R&D** research and development
- RCG** regranulated cork granulate
- RO** reverse osmosis
- S-CCG** surfactant-treated coarse cork granulate
- S-FCG** surfactant-treated fine cork granulate
- S-RCG** surfactant-treated regranulated cork granulate
- SDS** sodium dodecyl sulphate
- SEM** scanning electron microscopy
- TDS** total dissolved solids
- TH** wastewater from the homogenisation tank of the industrial wastewater treatment plant
- TPD** temperature-programmed desorption
- TSS** total suspended solids
- UF** ultrafiltration
- UV** ultraviolet
- VOC** volatile organic compound
- VORW** vegetable oil refinery wastewater
- W-CCG** washed coarse cork granulate
- W-FCG** washed fine cork granulate
- W-ICG** washed intermediate cork granulate
- W-RCG** washed regranulated cork granulate
- WWTP** wastewater treatment plant

Latin symbols

a slope of the calibration curve

$\text{adj-}r^2$ adjusted regression coefficient

a_p external surface area per unit particle volume ($\text{cm}^2 \text{cm}^{-3}$)

b intercept of the calibration curve

C_0 initial/feed concentration of O&G or COD (mg L^{-1} ; $\text{mg O}_2 \text{L}^{-1}$)

C_{av} average concentration of standards in the calibration curve (mg L^{-1})

C_b O&G concentration in the bulk liquid (mg L^{-1})

C_{b_0} initial O&G concentration in the bulk liquid (mg L^{-1})

C_c final O&G concentration in the control experiment (mg L^{-1})

C_{eq} concentration of O&G at equilibrium (mg g^{-1})

C_f final O&G concentration in the sorption experiment (mg L^{-1})

C_H hydrogen ion concentration (M)

C (**O&G**) concentration of oil and grease (mg L^{-1})

C_{out} outlet O&G concentration (mg L^{-1})

C_p O&G concentration in the liquid phase at the sorbent surface (mg L^{-1})

C_{pred} predicted concentration of standard according to the calibration curve (mg L^{-1})

C_{std} concentration of standard (mg L^{-1})

C_t concentration of O&G or COD at time t (mg L^{-1} ; $\text{mg O}_2 \text{L}^{-1}$)

D diameter of the oil droplet (μm ; m)

d_{50} median droplet diameter (μm)

D_f particle's resistance to motion (drag force) (N)

df degrees of freedom

f_{oc} fraction of organic carbon

$F(t)$ normalised response to a step experiment

g acceleration of gravity (m s^{-2})

h initial height of the oil droplet (m)

h_0 height of the separating column (m)

ΔH (**CH₃OH**) enthalpy of immersion in methanol (J g^{-1})

ΔH (**H₂O**) enthalpy of immersion in water (J g^{-1})

- K_F Freundlich constant ($\text{mg}^{(1-1/n)}\text{L}^{1/n}\text{g}^{-1}$)
- k_f film mass transfer coefficient ($\text{cm}^3 \text{cm}^{-2} \text{s}^{-1}$)
- $K'_{j,H}$ median value for the affinity distribution for the proton to the binding group j
- K_{oc} organic-carbon-normalized partition coefficient (L kg^{-1})
- K_{ow} octanol-water partition coefficient (commonly expressed as $\log K_{ow}$)
- K_p partition/sorption coefficient (L g^{-1} ; L kg^{-1})
- k_t time interval required to achieve half the maximum removal efficiency (min)
- m_1 mass of cylinder with sample (kg)
- m_2 mass of cylinder (kg)
- m_c mass of cork (g)
- $m_{H,j}$ width of the peak in the Sips distribution ($(0 < m_{H,j} < 1)$)
- m_o mass of oil initially sorbed by cork (mg)
- m_{oc} mass of oil-impregnated cork (g)
- m_{ocd} mass of oil-impregnated cork after the previous desorption cycle (g)
- n dimensionless parameter related to sorbate-sorbent affinity
- N_f number of mass transfer units by film diffusion
- n_{std} number of standards used in the calibration curve
- P pressure (Pa; bar; atm)
- p_{rep} number of repetitions of each analysis
- Q flowrate (mL min^{-1} ; L s^{-1})
- q sorption capacity/sorbed amount per unit mass of sorbent (mg g^{-1})
- q_{cycle} sorption capacity in each cycle (g g^{-1})
- q_{eq} sorbed amount at equilibrium (mg g^{-1})
- Q_H adsorbed amount of protons per unit mass of biosorbent (mmol g^{-1})
- q_{max} maximum sorption capacity (mg g^{-1} ; $\mu\text{g g}^{-1}$)
- $Q_{max,j}$ overall charge of the binding group j (mmol g^{-1})
- q_{total} total sorption capacity (mg g^{-1})
- R removal efficiency (%)
- r^2 correlation coefficient
- R_{max} maximum removal efficiency (%)

- r_p particle radius (cm)
- S_{BET} BET surface area ($\text{m}^2 \text{g}^{-1}$)
- S_r^2 sum of the residual sum of squares (mmol g^{-1})
- S_a standard deviation of the slope
- S_b standard deviation of the intercept
- S_{x_0} uncertainty from the calibration curve
- $S_{y/x}$ standard deviation of the residuals
- T temperature ($^{\circ}\text{C}$)
- t time (s; min; h)
- u uncertainty
- V volume (L; m^3)
- V_{meso} mesopore volume ($\text{cm}^3 \text{g}^{-1}$)
- V_{micro} micropore volume ($\text{cm}^3 \text{g}^{-1}$)
- V_{total} total pore volume ($\text{cm}^3 \text{g}^{-1}$)
- v_t terminal velocity of the oil droplet in water (m s^{-1})
- W mass of sorbent (g)
- w_0 limiting adsorbed amount expressed in liquid volume ($\text{cm}^3 \text{g}^{-1}$)
- W_{eff} effective weight (N)
- X_P mass of phosphorus/mass of precursor ratio
- x_1 independent variable, coded as NaCl concentration (M)
- x_2 independent variable, coded as pH
- x_3 independent variable, coded as soap ratio (%)
- \hat{y} predicted response in O&G removal efficiency (%)

Greek symbols

- α significance level
- β_0 regression coefficient for the intercept
- β_1 regression coefficient for the linear effect of x_1
- β_{11} regression coefficient for the quadratic effect of x_1
- β_{12} regression coefficient for the two-way linear interaction effect of x_1 and x_2

β_{13} regression coefficient for the two-way linear interaction effect of x_1 and x_3

β_2 regression coefficient for the linear effect of x_2

β_{22} regression coefficient for the quadratic effect of x_2

β_{23} regression coefficient for the two-way linear interaction effect of x_2 and x_3

β_3 regression coefficient for the linear effect of x_3

β_{33} regression coefficient for the quadratic effect of x_3

Δ change between final and initial values of a same parameter

ε_b bulk porosity

ζ zeta potential (mV)

θ dimensionless time

λ_1 coefficient of the resolution of a second order homogeneous differential equation

λ_2 coefficient of the resolution of a second order homogeneous differential equation

μ absolute viscosity of the wastewater (Pa s)

ξ mass capacity of the reactor

ξ_m batch mass capacity factor

ρ density (kg m^{-3})

ρ_{ap} apparent density of the sorbent particles (kg m^{-3} ; g L^{-1})

ρ_o density of oil (kg m^{-3})

ρ_w density of water (kg m^{-3})

τ_{exp} experimental mean residence time (h)

τ mean residence time (s; h)

τ_f time constant for film diffusion (s)

Chapter 1

Introduction

1.1 Motivation and relevance¹

Cork consists in the outer bark of the cork oak tree, known botanically as *Quercus suber* L. (Silva et al., 2005). Cork harvest and subsequent transformation supports one of the most important industries in the Mediterranean region. Portugal is the leading country in both cork forest (32% of total worldwide area) and cork processing (52.5% of annual average production in weight) (Cork Information Bureau, 2010). The cork sector is therefore very significant in the Portuguese economy; net exports in this country have totalled 754.3 million euros in 2010 (Lima, 2011).

The traditional use of cork has been on stoppers for wine bottling, which covered around 61% of sales in 2013 of the largest cork company in the world (Corticeira Amorim, 2014). However, many other applications for cork and cork-derived materials have been developed, such as agglomerates, insulation corkboard, cork/rubber composites and ecoceramics (Gil, 2007). More recently, due to its reputation as a renewable material, cork is being used in innovative ecodesign, incorporated in furniture, kitchen utensils, accessories and toys (SusDesign, 2008). Since the beginning of the 21st century, the Portuguese cork industry has been increasing the investment on research and development (R&D) (APCOR, 2011).

From the raw cork materials extracted from the tree, only around 19% are transformed into cork stoppers, the most valuable product of the industry (Rives et al., 2013). The remaining 80% are cork byproducts, of which a significant part (around 25% weight from total) are cork powder wastes, particles with less than 0.25 mm with low commercial value which are generated in operations such as pre-grinding, cutting and polishing (Gil et al., 1986). The larger byproducts suffer grinding to granule sizes between 0.25 and 8 mm and are designated as *cork granulates* (Rives et al., 2012). Their most common applications are in the manufacture of agglomerates and composites (Silva et al., 2005; Rives et al., 2012). Recently, their potential in the removal of pollutants by biosorption and as precursors of activated carbons has been gaining attention from the research community (Silva et al., 2005). A Portuguese patent (no. 103286) was issued for the

¹Part of this section is adapted from the journal article: Pintor, A. M. A., Ferreira, C. I. A., Pereira, J. P. C., Correia, P., Silva, S. P., Vilar, V. J. P., Botelho, C. M. S., Boaventura, R. A. R. Use of cork powder and granules for the adsorption of pollutants: a review. *Water Research*, 46(10):3152-3166, 2012.

bioremoval of Pb(II) from waters using cork byproducts. Cork granule-filled pillows, socks and booms for oil spill management, marketed as CORKSORB, have enjoyed commercial success (Corticeira Amorim, 2009).

The effectiveness of CORKSORB in oil spill cleanup derives from the hydrophobicity of cork, a characteristic that results from its chemical composition and cellular structure. This affinity of cork granules for oil and organics prompts the premise of this study, which consists in their use as sorbents of oily substances emulsified or dispersed in wastewaters. *Oil and grease (O&G)*, as it is called, is the class of pollutants that comprises such substances, along with many others bearing the similar characteristic of having a very low affinity for water.

The O&G definition includes compounds like hydrocarbons, fatty acids, soaps, lipids and waxes (Patterson, 1985); most of these substances have very low biodegradability, and therefore their release to the environment may impact the biosphere (Wahi et al., 2013). As a result of lower density, they will float in water, and once at the surface, they may spread in very thin films and cover large reservoir areas. Even the thinnest layer of oil will affect aquatic life by decreasing both the penetration of light and the oxygen transfer between air and water (Roques and Aurelle, 1991).

In addition to its ecological impact, O&G affects the operation of traditional wastewater treatment plants (WWTPs), inhibiting biological activity in activated sludge reactors and causing clogging and fouling of pumps and piping (Rhee et al., 1989). Furthermore, the presence of oily matter in wastewaters is often indicative of the occurrence of toxic micro pollutants, especially those which are also hydrophobic. High concentrations of benzene, toluene and xylene have been associated with discharges of petroleum refinery wastewaters in the municipal system (Rhee et al., 1989), and mono- and polyaromatics have been detected alongside other long-chain hydrocarbons in stormwater runoff (Stenstrom et al., 1984). For the aforementioned reasons, wastewaters heavily loaded with O&G can neither be directly discharged onto the environment nor collected by the municipal system; an alternative treatment strategy must be sought.

There is a large body of literature on how to remove O&G from water, including many studies on the application of several technologies; still, oily wastewaters remain a challenge, because O&G may vary in chemical composition, physical properties and industrial source. Treatment design depends on the specifications of each wastewater and the characteristics of oily substances present in its constitution. Rhee et al. (1989) consider O&G “one of the most complicated pollutants to remove” in oil processing wastewaters.

One of the most promising technologies for the removal of O&G from wastewaters is sorption. The use of organic sorbents is particularly relevant because these materials are easily accessible, cost-effective and present reduced environmental impact (Wahi et al., 2013). Aquatic plant *Salvinia* sp. (Ribeiro et al., 2003), chitosan powder and flake (Ahmad et al., 2005; Pitakpoolsil and Hunsom, 2014), kapok fibre (Abdullah et al., In Press) and non-viable fungal cultures (Srinivasan and Viraraghavan, 2010, 2014) are examples of natural sorbents which have successfully been employed in the uptake of O&G from synthetic or real wastewaters. Using this technology with cork granulates is an innovative approach which attempts to take advantage of the favourable

characteristics of this material towards oil uptake.

1.2 Objectives and Outline

The main goal of this thesis is to establish a treatment methodology for O&G removal in industrial wastewaters using sorption onto cork granulates. First of all, a literature review on both the applications of cork granules in environmental technology and the available treatments for oily wastewaters was carried out to establish the context for the development of the study. Afterwards, experimental work using cork granulates and vegetable oil refinery wastewater (VORW) samples (real and simulated) was executed, with the following objectives in mind:

- To characterise the textural and surface properties of cork granulates and investigate possible pretreatments that could enhance their affinity towards O&G;
- To select and optimise a pretreatment for real wastewaters able to remove free oil and reduce the organic load for the sorption treatment;
- To identify the chemical parameters that influence sorption of O&G from real wastewater samples onto cork granules;
- To investigate the electrostatic mechanisms and chemical interactions which affect the uptake of oil by hydrophobic sorbents such as cork granules, by examining the influence of operating parameters like pH, ionic strength, and soap content, in vegetable oil sorption by cork granules in synthetic oil-in-water emulsions;
- To establish the best operating conditions for successful lab scale treatment of real and simulated wastewater by O&G sorption onto cork granules;
- To determine the most efficient method for oil recovery and sorbent regeneration.

This thesis is divided into eight chapters. After the present introductory chapter, a second one discusses the current literature in two themes: the characterisation of cork byproducts and their current applications, and the state-of-the-art in O&G removal and oily wastewater treatment.

In the third chapter, several types of cork granulates collected at a Portuguese cork company are thoroughly characterised, in both textural and surface properties, using a wide range of techniques (N_2 adsorption isotherms, temperature-programmed desorption (TPD), Fourier transform infrared spectroscopy (FTIR), potentiometric titration and immersion calorimetry, among others). The effect of washing and surface modification with cationic surfactant on these materials is also studied. Activated carbons were produced using cork granulates as precursors and analysed using the same methods. A screening of the sorption capacity of the materials is done through sorption tests using sunflower oil-in-water emulsions.

The fourth chapter presents the case study of VORW and the characterisation of the selected wastewater samples. An optimisation of a gravity separation pretreatment is carried out with the

objective of completing removal of free O&G, thus preventing overload in the sorption treatment. In the fifth chapter, an in-depth study of the chemistry of electrostatic interactions affecting sorption of vegetable oil onto cork granules in batch mode is presented. The influence of pH and ionic strength is investigated by analysing not only sorption capacity under different conditions but also by measuring properties of the oil-in-water emulsion, such as particle size and zeta potential. Kinetics and equilibria at maximized sorption capacity are experimentally determined and modelled according to theoretical and empirical equations.

The sixth chapter deals with the application of the sorption technology to real VORW, by examining the best operating conditions for treatment. Differences between studying oil-in-water emulsions and real wastewaters are explored by examining the influence of soap content in sorption performance. The continuous treatment of simulated wastewater in a stirred tank is demonstrated as a conclusion to the experimental work.

In the seventh chapter, the recovery of oil from cork sorbents is tested using methodologies of elution with aqueous solutions and mechanical compression. The possibility of reusing cork granules in oil sorption is also investigated by analysing the performance of cork sorbents throughout several cycles of sorption and regeneration.

Finally, the eighth chapter summarizes the conclusions of this thesis. Some suggestions for future work are also given in this last chapter.

1.3 References

Abdullah, M. A., Afzaal, M., Ismail, Z., Ahmad, A., Nazir, M. S., and Bhat, A. H. Comparative study on structural modification of *Ceiba pentandra* for oil sorption and palm oil mill effluent treatment. *Desalination and Water Treatment*, In Press.

Ahmad, A. L., Sumathi, S., and Hameed, B. H. Adsorption of residue oil from palm oil mill effluent using powder and flake chitosan: equilibrium and kinetic studies. *Water Research*, 39(12):2483–2494, 2005.

APCOR. I&D na indústria corticeira, 2011. URL <http://www.apcor.pt/artigo/296.htm>. accessed September 2014.

Cork Information Bureau. Cork sector in numbers, 2010. URL <http://www.apcor.pt/userfiles/File/Cork%20Statistics.pdf>. accessed September 2014.

Corticeira Amorim, S.G.P.S. CORKSORB - sustainable absorbents, 2009. URL <http://www.corksorb.com/>. accessed September 2014.

Corticeira Amorim, S.G.P.S. Annual report and accounts 2013, 2014. URL http://www.amorim.com/xms/files/Investidores/5_Relatorio_e_Contas/PT_R_C_Corticeira_Amorim2013.pdf. accessed September 2014.

Gil, L. Technical manual: Cork as a building material, 2007. URL <http://apcor.pt/userfiles/File/Caderno%20Tecnico%20F%20EN.pdf>. accessed September 2014.

- Gil, L., Santos, J., and Florêncio, M. I. Identificação e caracterização de vários tipos de pó obtidos no processamento industrial da cortiça. *Boletim do Instituto dos Produtos Florestais - Cortiça*, 575:255–261, 1986.
- Lima, J. A importância da cortiça no panorama nacional, 2011. URL <http://ae.isa.utl.pt/attachments/article/123/Apresenta%C3%A7%C3%A3o%20JL%20ISA%2021%20Mar%C3%A7o%202011.pdf>. accessed September 2014.
- Patterson, J. W. *Industrial Wastewater Treatment Technology*. Butterworth Publishers, 1985.
- Pitakpoolsil, W. and Hunsom, M. Treatment of biodiesel wastewater by adsorption with commercial chitosan flakes: Parameter optimization and process kinetics. *Journal of Environmental Management*, 133: 284–292, 2014.
- Rhee, C. H., Martyn, P. C., and Kremer, J. G. Removal of oil and grease in oil processing wastewater. Technical report, Sanitation District of Los Angeles County, 1989.
- Ribeiro, T. H., Rubio, J., and Smith, R. W. A dried hydrophobic aquaphyte as an oil filter for oil/water emulsions. *Spill Science & Technology Bulletin*, 8(5–6):483–489, 2003.
- Rives, J., Fernandez-Rodriguez, I., Gabarrell, X., and Rieradevall, J. Environmental analysis of cork granulate production in Catalonia – Northern Spain. *Resources, Conservation and Recycling*, 58:132–142, 2012.
- Rives, J., Fernandez-Rodriguez, I., Rieradevall, J., and Gabarrell, X. Integrated environmental analysis of the main cork products in southern Europe (Catalonia – Spain). *Journal of Cleaner Production*, 51: 289–298, 2013.
- Roques, H. and Aurelle, Y. Oil-water separations oil recovery and oily wastewater treatment. In Turkman, Aysen and Uslu, Orhan, editors, *New Developments in Industrial Wastewater Treatment*, volume 191 of *NATO ASI Series*, pages 155–174. Springer Netherlands, 1991.
- Silva, S. P., Sabino, M. A., Fernandes, E. M., Correló, V. M., Boesel, L. F., and Reis, R. L. Cork: properties, capabilities and applications. *International Materials Reviews*, 50(6):345–365, 2005.
- Srinivasan, A. and Viraraghavan, T. Oil removal from water using biomaterials. *Bioresource Technology*, 101(17):6594–6600, 2010.
- Srinivasan, A. and Viraraghavan, T. Oil removal in a biosorption column using immobilized *M. rouxii* biomass. *Desalination and Water Treatment*, 52(16-18):3085–3095, 2014.
- Stenstrom, M. K., Silverman, G. S., and Bursztynsky, T. A. Oil and grease in urban stormwaters. *Journal of Environmental Engineering*, 110(1):58–72, 1984.
- SusDesign. Corque, 2008. URL <http://www.corquedesign.com/>. accessed September 2014.
- Wahi, R., Chuah, L. A., Choong, T. S. Y., Ngaini, Z., and Nourouzi, M. M. Oil removal from aqueous state by natural fibrous sorbent: An overview. *Separation and Purification Technology*, 113:51–63, 2013.

Chapter 2

Literature Review

2.1 Use of cork powder and granulates in the removal of pollutants by sorption¹

2.1.1 Introduction

This first section of the literature review chapter aims to summarize recent research developments on the properties of cork and on the use of cork byproducts on sorption technologies for the removal of pollutants.

The study of cork has drawn the attention of many scholars across the years. The chemical composition of cork has been studied since the 18th century (Conde et al., 1998), but the total knowledge of cork's properties, potential applications and transformations is far from complete. The increasing investment from private companies in R&D and the public financing of cork research in Mediterranean countries has led to a steady increase in publications about cork in indexed journals over the last three decades (Figure 2.1).

Part of this research focuses on cork byproducts, such as powder and granulates, and the possibilities of creating added-value products from these materials. A growing field of application for cork powder and granulates is in the purification of waters and treatment of wastewaters and gaseous emissions by sorption. Cork presents advantages for environmental technology, because it is a renewable resource and a natural material.

2.1.2 Cork and cork byproducts

2.1.2.1 Properties of cork

The bark of the cork oak (*Quercus suber* L., Figure 2.2), commonly named *cork*, grows as a continuous and thick circular layer around the tree (Pereira, 1988) and is harvested at intervals of 9 to 12 years (Silva et al., 2005). This periodical harvest is possible because the cork oak's bark

¹This section is adapted from the paper: Pintor, A. M. A., Ferreira, C. I. A., Pereira, J. P. C., Correia, P., Silva, S. P., Vilar, V. J. P., Botelho, C. M. S., Boaventura, R. A. R. Use of cork powder and granules for the adsorption of pollutants: a review. *Water Research*, 46(10):3152-3166, 2012.

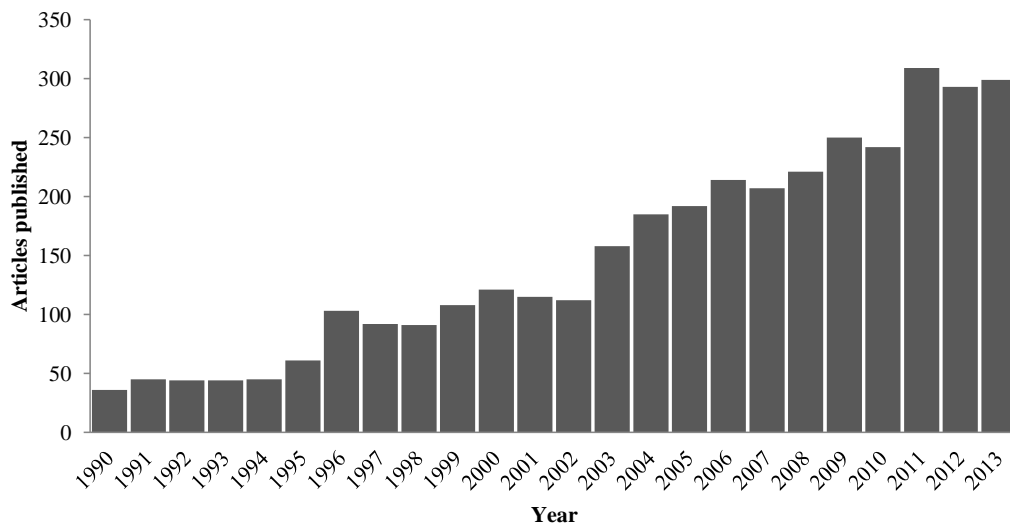


Figure 2.1: Evolution of the number of publications on indexed journals (source: Scopus) containing the keyword “cork” between 1990 and 2013.

has the ability to regenerate. It is said to be the only tree with this peculiarity, and that is the reason why cork is often heralded as a “truly renewable, environmentally friendly resource” (Fernandes et al., 2010).



Figure 2.2: Cork oaks after harvest, with the cork planks at rest in the soil around them.

The cork oak grows mostly in the Mediterranean region, where ideal climatic conditions occur: dry summers and mild winters (Barberis et al., 2003; Jové et al., 2011). In the beginning of its life cycle, the tree generates two kinds of cork which have inferior quality than the subsequent harvests. The first extraction of the bark is denominated *virgin cork* and is produced by the original phellogen of the tree (Pereira, 1988). It is stripped from the cork oak when it is 20-30 years

old (Lopes et al., 2001) and it is irregular in structure, thickness and density. For this reason, it can only be used for cork board, insulation, and similar applications (Cumbre et al., 2000). The following layer, that corresponds to the second stripping, is the first to be called *reproduction cork*, even though it is similarly unfit for the production of stoppers. Afterwards, the periodical harvest of high quality reproduction cork begins, repeating itself for around 15 to 18 times during the lifespan of the cork oak tree (170-200 years) (Fialho et al., 2001; Lopes et al., 2001; Jové et al., 2011). This reproduction cork is suitable for cork stoppers' production due to its more regular cellular structure (Silva et al., 2005).

Cork has microscopic features different from other lignocellulosic materials. It is formed by hollow polyhedral prismatic cells, which, from the radial direction (relative to the tree trunk), form an unique honeycomb structure. From transversal directions, the rectangular laterals can be observed to be stacked upon each other like a brick wall (Silva et al., 2005; Carrott et al., 2006; Lequin et al., 2009). Generally, the lateral faces of cork cells are corrugated (Figure 2.3), possibly resulting from compression during bark growth (Silva et al., 2005). On average, cork cells are 45 μm tall, with a hexagonal face of 15-20 μm and a thickness of 1-2 μm (Carrott et al., 1999; Lequin et al., 2009), but their dimensions vary with the season when they are generated: spring cells are longer with thin walls, while autumn cells are smaller with thicker walls (Gomes et al., 1993).

In terms of chemical composition, cork consists primarily of suberin and lignin, and, in smaller

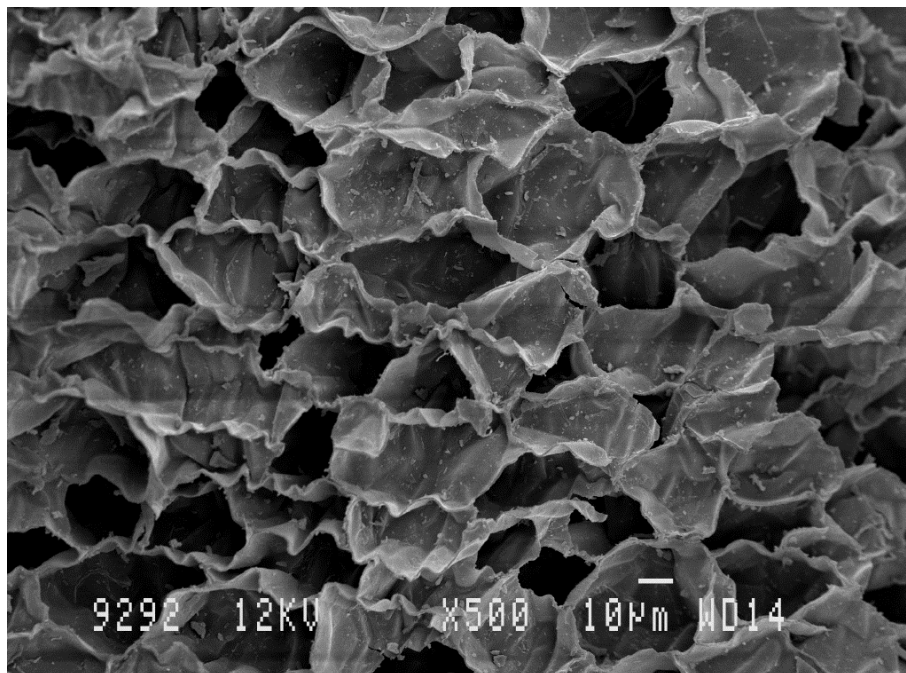


Figure 2.3: SEM micrograph of cork cells.

proportions, of polysaccharides (cellulose and hemicellulose) and extractives (waxes and tannins) (Pereira, 1979, 1988; Bento et al., 2001). These organic constituents make up three layers at the cell wall. The internal primary lamella is rich in lignin and the outward tertiary wall is thin and made of polysaccharides. Between these two thin layers stands a thick secondary wall, believed to

be composed of alternating wax and suberin (Bernards, 2002; Silva et al., 2005), although Pereira (1988) has suggested that it may also contain lignin. Internally, cork cells enclose cerin crystals, fridelin, and a large quantity of gas, presumably similar to air (Silva et al., 2005).

The proportion in which the chemical components of cork appear in cell constitution can be influenced by a variety of factors, such as the extract's morphological location on the tree, the cork quality, and the geographical origin of the cork oak from whence it came. Results from studies by Pereira (1988) on Portuguese cork and by Conde et al. (1998) on Spanish cork showed a constancy in the structural components of cork (suberin, lignin, and polysaccharides) in samples from the same geographical origin. Between samples of different origin, differences were found in the proportion of minor constituents (extractives and polyphenols). However, a clear relationship between geographical proximity and chemical similarity could not be established. This difficulty stems from the natural heterogeneity of the material, which leads to the occurrence of chemical differences in samples from the same provenance and even from the same tree (Pereira, 1984, 2013). The latter instances were ascribed by Conde et al. (1998) to morphological disparities, such as the North or South orientation of the sample, its distance from the base of the tree and its situation on the stem or branch. However, while in that study such differences were simply reflected in the quantity of minor chemical components, Jové et al. (2011) also reported same-tree variability, related to the cork bark layer, but in the major contents of suberin and holocellulose. In another survey, samples with geographical proximity exhibited large fluctuations in major components suberin and polysaccharides (Lopes et al., 2001). Nevertheless, these and other authors (Prades et al., 2010) were able to establish a qualitative relationship between the contents of primary constituents suberin and lignin and cork quality. In general, higher suberin contents were found to correspond to increased quality standards.

As a result of such diverseness in the chemical composition of cork, precise values for the proportions of its components cannot be established. Instead, there is a range of likely percentages of each constituent, which can be estimated from the different measures reported by researchers who have addressed this issue. A summary of the values found in the literature is presented in Table 2.1.

Moisture is also an important characteristic of cork which is related to its quality. The hygroscopic moisture balance under stable ambient conditions of temperature and relative humidity is approximately 6% for good quality cork. According to Prades et al. (2010), it can reach as high as 10% when the quality is poorer, due to a greater presence of lignin tissue.

As far as physical properties are concerned, cork exhibits some unique features, such as high coefficient of friction, resilience, imperviousness to liquids, low thermal conductivity, low density, high energy absorption, excellent insulation properties, near-zero Poisson coefficient, and resistance to fire, among others (Pereira, 1988; Fernandes et al., 2010). The density of cork is expressed by a wide range of values, from 120 to 240 kg m⁻³. Since the density of the cell wall materials is believed to be constant (estimated as 1200 kg m⁻³), the variations within the aforementioned interval are caused by irregular cell dimensions and wall corrugation. Generally, higher densities correspond to cells with thicker, heavily corrugated walls.

Table 2.1: Summary of proportions reported by different authors for the chemical composition of cork (Adapted from [Silva et al. \(2005\)](#)).

Reference	%Suberin	%Lignin	%Polysac.	%Extract.	%Ash
<i>Virgin cork</i>					
Caldas et al. (1986) (from Silva et al. (2005))	45	27	12	10	5
Pereira (1982)	45	21	13	19	1.2
Pereira and Marques (1988)	38.6	21.7	18.2	15.3	0.7
<i>Reproduction cork (“amadia”)</i>					
Gil (1998)	42	21.5	16	13	
Caldas et al. (1986) (from Silva et al. (2005))	48	29	12	8.5	2.1
Pereira (1982)	33.5	26	26	13	2.5
Parameswaran (1981) (from Pereira (1984))	33	13	6	24	
Holloway (1972)	37	14.8		15.8	
Carvalho (1978) (from Pereira (1979))	50	19	13	15	3
Conde et al. (1998)	62	23	21	11	
Jové et al. (2011)	40	21	11	15	0.85
Pereira (2013)	42.8	22		16.2	

Cork is not a porous material. The interior of the cellular structure is only accessible by lenticular channels, hollow cylinders that cross planks radially. The prevalence of these channels varies between trees and between different ages of cork. Nevertheless, the existence of a small microporosity in cork ($0.026 \text{ cm}^3 \text{ g}^{-1}$) has been reported by [Hanzlík et al. \(2004\)](#) following assays of adsorption of carbon dioxide ([Lequin et al., 2009](#)).

The industrial processing of cork is responsible for several changes in its chemical composition and physical properties ([Conde et al., 1998](#)). After harvesting from the tree, the cork bark is left to rest for about 5 months, after which it is submitted to boiling for 1 hour in water. While initially cork cell walls are collapsed and wrinkled ([Figure 2.3](#)), after boiling, the gas inside the cells expands, creating a very tight and uniform cell structure ([Silva et al., 2005](#)). [Figure 2.4](#) shows the homogeneity of cork planks after this treatment. The reduction in the corrugation of cell walls, along with the expansion in volume inside the cells, leads to a decrease in density for the cork product ([Fortes and Rosa, 1988](#); [Silva et al., 2005](#)). Furthermore, boiling also reduces mechanical strength as the water absorption softens the cell walls ([Silva et al., 2005](#)).

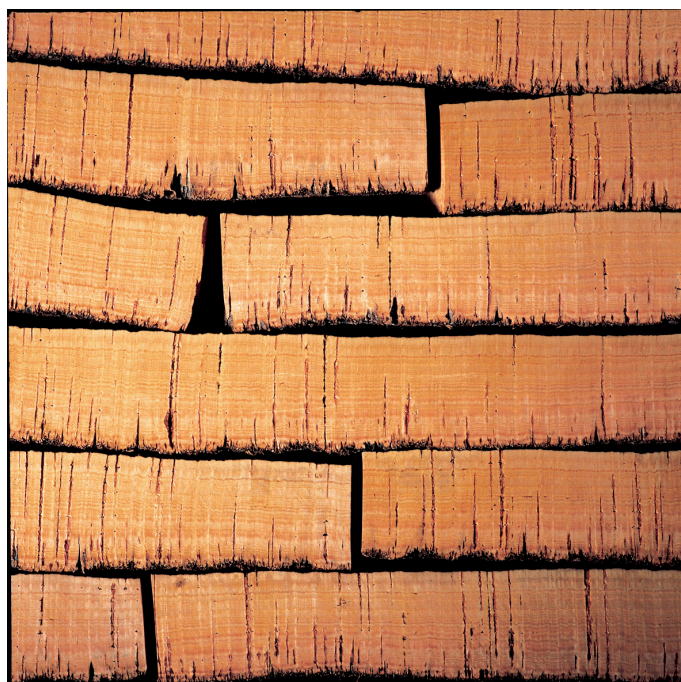


Figure 2.4: Cork planks piled after boiling.

At its surface, cork shows high affinity for non-polar liquids (zero contact angle observed for *n*-alkanes) and very low polarity. The cork surface is amphoteric, i.e., compatible with both acidic and basic polymeric functional groups ([Silva et al., 2005](#)). The chemical characteristics of the cork's surface are intimately connected to its chemical composition, which has been studied both by ^{13}C solid-state NMR and FTIR. [Table 2.2](#) summarizes the chemical structures found on cork surface through the interpretation of the peaks in NMR and FTIR spectra.

Exposition of cork to rising temperature can induce thermal decomposition of its chemical constituents and transformation of the material. Thermal degradation of cork has also been studied by

Table 2.2: Chemical structures on cork surface identified by ^{13}C -CP/MAS NMR and FTIR spectra (based on data from Neto et al. (1995), Lopes et al. (2001) and Prades et al. (2010)).

Peak	Surface group/structure	Constituent
<i>^{13}C-CP/MAS NMR</i>		
21 ppm	$\text{CH}_3\text{-COO-}$	hemicellulose
25-33 ppm	methylene ($-(\text{CH}_2)_n-$)	suberin
56 ppm	methoxyl ($-\text{OCH}_3$)	lignin, suberin, hemicellulose
65-105 ppm	carbohydrates	cellulose
110-155 ppm	aromatic carbons	lignin
172 ppm	ester ($-\text{COO-}$)	suberin
<i>FTIR</i>		
3425 cm^{-1}	$-\text{OH}$ “stretching”	water, hemicellulose, cellulose
2919, 2854-2849 cm^{-1}	$-\text{CH}_3$ aliphatic “stretching”	suberin
1749-1747, 1719 cm^{-1}	$\text{C} = \text{O}$ “stretching”	suberin, hemicellulose, cellulose
1635, 1607, 1513 cm^{-1}	$\text{C} = \text{C}$ “stretching”	suberin, lignin, extractives
1466 cm^{-1}	CH asymmetric deformation	lignin
1366 cm^{-1}	CH symmetric deformation	extractives
1267 cm^{-1}	CO “stretching”	suberin, hemicellulose, cellulose, lignin
1164 cm^{-1}	CO asymmetric “stretching”	suberin, hemicellulose, cellulose, lignin
1101, 1036 cm^{-1}	CH , CO deformation	hemicellulose, cellulose

NMR and FTIR methods.

Up to 150 °C, it is believed that cork maintains its characteristics, since its spectra at ambient conditions and after exposure until this temperature are identical. There is only a small mass reduction to register, after heating between 100 and 150 °C, which can be attributed to the loss of water (Rosa and Fortes, 1988). At 150 °C, however, the NMR spectrum suggests that waxes and other extractives are decomposed, and that suberin starts to break down, probably at points of attachment to the cell wall. Moreover, at 200 °C, decomposition of carbohydrates begins (Neto et al., 1995).

At 200-350 °C the most significant transformations occur. The expansion of the cells increases their volume by about 100%, and the cell walls are thermochemically degraded, due to a combined loss of polysaccharides above 200 °C and degradation of hemicelluloses and carbohydrates in the range 180-360 °C. This process leads to the conversion of raw cork into a material with a dark appearance and 30% of the initial weight (Silva et al., 2005). Heating at over 200 °C causes such a loss in mass and an increase in volume that density may decrease to half the original values. At 200-250 °C the colour of cork is still dark brown, but it changes to black at 300 °C (Rosa and Fortes, 1988). At a temperature of 350 °C, decomposition of lignin has already begun and suberin is degraded further.

Finally, at 400 °C and above, a broad peak characteristic of aromatic carbon dominates the spectra, indicating that the material is now a mixture of coke (formed from the decomposition of suberin from 250 °C upward) and lignin (Neto et al., 1995).

2.1.2.2 Properties of cork powder and granulates

As it has been mentioned in chapter 1, cork powder production accounts to up to 25% in weight of the raw cork material (Gil et al., 1986; Silva et al., 2005), while cork granulates correspond to about 50% (Rives et al., 2012). According to Portuguese Standards NP-114 and NP-273, cork powder is a material having dimensions lower than 0.25 mm (Gil, 1997). Cork granulates consist of granules in a larger size range, from 0.25 to 8 mm (Rives et al., 2012).

Cork powder is a material with low commercial value, and is often considered as “burning powder”, and used to feed boilers due to its high heating value (Gil, 1997; Fernandes et al., 2010). Other applications include the use as a filling agent (mixed with glues, for enhancement of the quality of cork stoppers), the production of linoleum, the use as an agricultural substrate and, more recently, agglomeration with polymers (Fernandes et al., 2010). Cork granulates’ traditional application is in the agglomerate industry, for instance for the production of champagne stoppers, wall and floor coverings, shoesoles and memo boards (Rives et al., 2012).

Cork powder and granulates can also be used to prepare activated carbons with high specific surface areas, comparable to commercial activated carbons, or they can be used directly as biosorbents for pollutants removal, in both cases with environmental and cost reduction advantages. In chapter 1, it has been mentioned that cork granulates have enjoyed commercial success as the CORKSORB absorbents for oil spill management (Corticeira Amorim, 2009).

Any granular or powder sorbent material should be characterised in structural, textural and surface

properties in order to optimise the study of suitable sorption applications. Such a characterisation for cork sorbents has been tentatively carried out by [Domingues \(2005\)](#) on cork granulates with dimensions between 1-2 mm and 3-4 mm. In that work, the surface area was estimated by mercury porosimetry and iodine number, the latter a measure which gives the quantity of iodine sorbed by unit mass of sorbent material. Surface area for 1-2 mm granulates was $16.3 \text{ m}^2 \text{ g}^{-1}$ with an iodine number of 83.9 mg g^{-1} and for 3-4 mm granulates $10.7 \text{ m}^2 \text{ g}^{-1}$ with an iodine number of 33.6 mg g^{-1} .

From mercury porosimetry results the study could also provide an estimate of pore size distributions. The mean pore diameter was calculated to be around $1\text{-}1.34 \text{ }\mu\text{m}$, which indicates the presence of macropores, and the pore volumes obtained were $2.83 \text{ cm}^3 \text{ g}^{-1}$ for 1-2 mm granulates and $2.24 \text{ cm}^3 \text{ g}^{-1}$ for 3-4 mm granulates. The decrease of both surface area and pore volume with particle size indicates that the cork surface is essentially external, confirming the notion that cork cells are closed and the interior spaces are inaccessible.

[Gomes et al. \(1993\)](#), [Cordeiro et al. \(1995\)](#) and [Domingues \(2005\)](#) have determined the surface tension of cork by contact angle measurements and inverse gas chromatography (IGC). The former estimate the surface tension of the solid through the calculation of the work of adhesion and the surface tension of the wetting liquid; using different wetting liquids, the two main components of surface tension, dispersive and polar, can be obtained ([Domingues, 2005](#)). IGC is an analogous technique to traditional analytical gas chromatography (GC) in which the mobile phase is constituted by a single substance injected to probe the properties of a solid stationary phase. It is believed to be a more adequate technique for materials with heterogeneous, rough surfaces, such as cork.

In both studies by [Gomes et al. \(1993\)](#) and [Domingues \(2005\)](#), the determination of surface tension by contact angle measurements was done using water and methylene iodide as liquid probes, for the determination of polar and dispersive components, respectively. The sum of both components yielded $32 \pm 3 \text{ mN m}^{-1}$ in the first study and 20.2 mN m^{-1} in the latter. However, while the determination of the first value implied 75% of dispersion forces, in the latter 98% corresponds to the dispersive component. Quantification by IGC with *n*-alkanes as probes resulted in a higher value of the dispersive component, 42 mN m^{-1} ; the tendency of this technique to yield higher results when compared to contact angle measurements had also been observed for other materials, such as cellulose ([Cordeiro et al., 1995](#)).

Additionally, [Gomes et al. \(1993\)](#) studied the dispersion of *n*-alkanes on the cork surface and found that both *n*-heptane, *n*-decane and *n*-hexadecane spread spontaneously with zero contact angle. [Cordeiro et al. \(1995\)](#) have also observed, using IGC with polar probes (tetrahydrofuran, chloroform and ethyl acetate), that the surface of cork exhibits an amphoteric nature, as it has been mentioned in section 2.1.2.1.

As far as chemical composition is concerned, [Domingues \(2005\)](#) has determined organic carbon by the Tinsley's method (titration with ammonium iron sulfate) and nitrogen content by the Kjeldahl method, with the results of $68 \pm 8\%$ and $0.38 \pm 0.09\%$, respectively. Even though the value of organic carbon determined in this study was well beyond the usual carbon contents of

other lignocellulosic materials, this can be easily explained by the fact that these materials tend to have a much higher content of cellulose than cork, whose main components are suberin and lignin. Since it is believed that suberin has an aromatic domain in its structure as well as carbon double bonds, this increases the carbon content in comparison to cellulose, which has no carbon double bonds (Domingues, 2005).

In terms of moisture, i.e., water content, cork powder and granulates usually present values in the range of 6 to 10%, the same range that has been mentioned for cork planks (section 2.1.2.1). Nevertheless, Gil and Cortiço (1998) have established the cork hygroscopic equilibrium moisture content curves for a range of temperature between 5 and 40 °C and relative humidity between 20 and 90%, concluding that in this range moisture varies between 4 and 13%.

Furthermore, Gonzalez Adrados and Calvo Haro (1994) mention that these products can swell to a moisture content around 50% when submerged in water; this is believed to be the original moisture content of cork upon extraction from the tree. Lequin et al. (2010) describe the water sorption mechanism in two steps: in the first step, water forms clusters around hydrophilic sites on the surface; and in the second step, water diffuses into the cell wall, leading to a swelling of the material. This transformation on the wall structure leads to a hysteresis loop on water vapor adsorption isotherms. These authors further state that water vapor isotherms reinforce the notion that cork is hydrophobic, since it presents slightly higher Henry's constant than the most hydrophobic materials (activated carbons, pure siliceous materials) but much lower than hydrophilic ones such as silica gels. Further studies by Gil et al. (2000) confirm, with a NMR microscopy study on both natural and desuberized cork samples, that hydrophobicity can be attributed to suberin and that hydrophilicity, on the other hand, is higher on lenticels, which are the main sites responsible for the macroporosity of cork.

Domingues (2005) and Fiol and Villaescusa (2009) have also determined the value of the point of zero-charge for cork granulates. This is an important parameter to evaluate surface charge and the presence of alkaline and acidic surface groups. In both studies, it was concluded that the pH of zero charge of cork falls in the acidic range, between 2.1 and 4.6 for 0.5-1.0 mm granulates (Domingues, 2005) and between 3.5 and 3.7 for 0.75-1.5 mm granulates (Fiol and Villaescusa, 2009). More recently, Olivella et al. (2011b) have determined the quantity of acidic functional groups in 0.25-0.42 mm grain size cork granules by Boehm titration (Boehm, 1994). A value of 1.88 mmol g⁻¹ of total acidic groups was obtained, of which 0.73 mmol g⁻¹ corresponded to strong acids and 0.92 mmol g⁻¹ to phenolic OH groups.

Finally, Olivella et al. (2011b) have also analysed the potential of cork to leach toxic components when in contact with water. This is very important to evaluate the feasibility of applying cork granulates as sorbents. Using Microtox Toxicity Analyzer (luminescence inhibition of bacteria *Vibrio fischeri* as the indicator of ecotoxicity), no toxicity was found in water made to contact with cork in similar conditions as a batch sorption test (3 g L⁻¹ cork in deionized water, 1 h stirring).

2.1.3 Application and transformation of cork powder and granulates for sorption

2.1.3.1 Biosorption

One of the main applications of cork powder and granulates has been in biosorption, i.e. using dead biomass or waste products of agricultural or industrial operations to remove pollutants by sorption, without major structural modification of the raw material. Since these products usually have low commercial value, their use for water purification presents advantages over other technological options which require high capital investment (Fiol et al., 2003).

Biosorption of toxic metals Toxic “heavy” metals compose the main target class of pollutants which has been the focus of cork biosorption research, as has been the case for other biomaterials. Metals whose studies of adsorption on cork granules have been published at least once include copper (Villaescusa et al., 2000, 2002; Chubar et al., 2003, 2004; Hanzlík et al., 2004), zinc (Chubar et al., 2003, 2004), nickel (Villaescusa et al., 2000, 2002; Chubar et al., 2003, 2004), lead (Mota et al., 2006; López-Mesas et al., 2011), trivalent chromium (Machado et al., 2002), hexavalent chromium (Fiol et al., 2003; Sen et al., 2012; Sfaksi et al., 2014), silver (Hanzlík et al., 2004), cadmium (Hanzlík et al., 2004; López-Mesas et al., 2011; Krika et al., 2011), uranium (Psareva et al., 2005) and mercury (Lopes et al., 2014). While most of these studies focus on raw cork granulates, a recent one (Sen et al., 2012) also provides data for “regranulated cork” or “black agglomerate” granules, which are byproducts of agglomerate production with injection of steam over 300 °C.

Biosorption can be an advantageous method for eliminating toxic metals at low concentration from waters and wastewaters for which the traditional methods such as chemical precipitation or reverse osmosis become inefficient, and adsorption with polymer resins, activated carbon or activated alumina is too expensive (Villaescusa et al., 2002; Fiol et al., 2003). Several mechanisms have been proposed to explain the sorption of metals from water, like complexation, ion exchange and inorganic microprecipitation (Machado et al., 2002; Villaescusa et al., 2002). It is likely that a combination of all is involved, but ion exchange is usually considered the main mechanism for metal sorption (Machado et al., 2002). Villaescusa et al. (2000) have demonstrated that electrostatic attraction plays a part in metal uptake, since metal sorption decreases in the presence of sodium chloride, i.e. when the ionic strength of the solution increases.

pH is a very important factor on sorption performance, since competition between metals and ions, inclusively hydrogen ions (H^+), may occur (Mota et al., 2006). Some studies (Villaescusa et al., 2000; Machado et al., 2002; Chubar et al., 2003) show that cationic metals' uptake is maximum at pH values near neutrality, as metal removal increases with pH due to the competition between H^+ and metals at low pH. For metals which occur mostly in the anionic form, such as Cr(VI), however, it has been shown that sorption is enhanced at acidic pH, due to the electrostatic attraction between positively charged groups at the biomaterial surface and the chromium anions (Fiol et al., 2003; Sen et al., 2012; Sfaksi et al., 2014).

Chubar et al. (2003, 2004) have demonstrated that the main active sites responsible for cationic

metal sorption are carboxylic groups; in the sorption of zinc, they have even been shown to be the sole functional group responsible for uptake. The affinity of surface groups toward each metal can significantly influence their uptake, namely when several elements are present in solution. [Hanzlík et al. \(2004\)](#) have shown that cork has higher affinity to copper than to silver and cadmium; however, both synergistic and antagonistic effects can occur between these three metals. In another study on metal competition, [López-Mesas et al. \(2011\)](#) observed a reduction of cadmium uptake in the presence of lead.

Most studies on metal sorption by cork present isotherms with a good adjustment to the Langmuir (1918) model, however, isotherms with two iso-capacity zones, for the adsorption of Cu(II) and Zn(II), have also been reported ([Chubar et al., 2003](#)). The Langmuir model indicates a monolayer coverage of the sorbent surface by the metal ions, while the existence of two iso-capacity zones can be attributed to a two-step adsorption mechanism in which the first step corresponds to the saturation of easily available sites and the second one to the saturation of the less available ones ([Chubar et al., 2003](#)). Additionally, [Sfaksi et al. \(2014\)](#) uses the Brunauer-Emmett-Teller (BET) isotherm ([Brunauer et al., 1938](#)) to describe the adsorption of Cr(VI).

Based on the different adjustments to the Langmuir model reported in the literature for the adsorption of different toxic metals, Table 2.3 summarizes the values of maximum sorption capacity (q_{max}) presented by each author, along with the optimum pH considered for sorption. The differences between studies on the same metal by different authors might be explained by variations in pH, granulometry or concentration range used in the experimental tests. These influence ionic competition and available active sites on the surface area.

Kinetics of metal sorption have been studied by [Machado et al. \(2002\)](#) for trivalent chromium,

Table 2.3: Maximum sorption capacities by adjustment to the Langmuir model reported in the literature for the sorption of toxic metals on raw and regranulated cork granulates.

Metal	Cork type and size	Optimum pH	q_{max} (mg g ⁻¹)	Reference
Cu(II)	raw, 0.425-0.85 mm	6-7	2.96	Villaescusa et al. (2000)
	raw, 50-100 μ m	5	20	Chubar et al. (2003)
Zn(II)	raw, 50-100 μ m	5	25	Chubar et al. (2003)
Ni(II)	raw, 0.425-0.85 mm	6-7	4.1	Villaescusa et al. (2000)
	raw, 50-100 μ m	5	10	Chubar et al. (2003)
Cr(III)	raw, 0.200-0.355 mm	4	6.3	Machado et al. (2002)
Cr(VI)	raw, 1.0-1.5 mm	2.0-4.7	17	Fiol et al. (2003)
	regranulated, 0.25-0.42 mm	2	22.98	Sen et al. (2012)
Pb(II)	raw, 1-2 mm	3.0-3.5	5.3	Mota et al. (2006)
	raw, 0.5-1 mm	5	13.6	López-Mesas et al. (2011)
Cd(II)	raw, 0.5-1 mm	5	2.4	López-Mesas et al. (2011)
	raw, < 80 μ m	6	9.65	López-Mesas et al. (2011)

Psareva et al. (2005) for uranium and Krika et al. (2011) for cadmium and in both cases it was observed that a second-order model was the best fit to the experimental data.

Desorption of metals from cork has been studied for chromium (Machado et al., 2002; Fiol et al., 2003) and copper and nickel (Villaescusa et al., 2000). HCl and H₂SO₄ have been selected as eluting agents, as lowering the pH causes protons to compete with the metals for the active sites. While trivalent chromium and copper could be eluted at high rates (over 50%), hexavalent chromium and nickel could not be desorbed over 30% even using stronger acid solutions.

Cork powder and granules have also been submitted to pretreatments to enhance their adsorptive properties toward toxic metals. Mota et al. (2006) tested pretreatment with solvents to extract phenols, tannins, waxes and fats from cork granules, using deionized water, ethanol and ethyl acetate. However, such pretreatments were unsuccessful in improving cork granules' uptake of Pb(II). Pretreatment with acids was tested by both Machado et al. (2002) and Chubar et al. (2004) with the objective of increasing the number of active sites by the introduction of sulfonic groups by sulfonation or of carboxylic groups by oxidation of aliphatic sites. However, this did not lead to an increase on the sorption capacity of cork neither for copper and zinc nor for chromium(III). A similar kind of pretreatment uses sorbent contact with calcium or sodium chloride aiming at converting the active binding sites at the cork surface from H⁺ to Na⁺ or Ca²⁺. If the substitution is successful, it avoids a decrease in pH during sorption when the H⁺ ions are exchanged for the metal and tends to favour the sorption reaction because the exchange with sodium or calcium for the metal is easier due to the size of the ions and lower affinity of these alkaline/alkaline earth ions to the binding sites. Chubar et al. (2004) report an increase in sorption capacity for copper on Na-saturated cork biomass, but Machado et al. (2002) did not find significant improvements in Cr(III) sorption following the same pretreatment. Alkaline pretreatment with 0.5 M NaOH at 90 °C was successful in increasing the sorption capacity to a similar extent as the aforementioned NaCl treatment, possibly due to an identical saturation of the active sites with sodium. Nevertheless, treatment of cork granules with alkaline solutions must always be carried out with caution since at high concentrations they may damage the cell structure (Machado et al., 2002). Lastly, other successful pretreatments include boiling in commercial laundry detergent and contact with oxidising agents (e.g. sodium hypochlorite and sodium iodate) (Chubar et al., 2004).

Biosorption of organics Cork has also been used as a biosorbent for organics, such as pyrethroid pesticides (fenprothrin, permethrin, deltamethrin, fenvalerate, λ -cyhalothrin (Domingues, 2005), bifenthrin (Domingues, 2005; Domingues et al., 2005) and α -cypermethrin (Domingues, 2005; Domingues et al., 2007)), 4,4'-dichlorodiphenyltrichloroethane (4,4'-DDT) (Boussahel et al., 2009), volatile phenols (Karbowiak et al., 2010), paracetamol (Villaescusa et al., 2011), ofloxacin (Crespo-Alonso et al., 2013), ibuprofen, carbamazepine and clofibrac acid (Dordio et al., 2011), methylene blue (Olivella et al., 2012), chrysoidine (Nurchi et al., 2014), chloroanisoles (Capone et al., 1999; Barker et al., 2001) and polycyclic aromatic hydrocarbons (PAHs) (Olivella et al., 2011a, 2013). Table 2.4 summarizes the maximum sorption capacities obtained in the literature derived from fitting experimental results of sorption of organic pollutants onto cork granules to the Langmuir

Table 2.4: Maximum sorption capacities by adjustment to the Langmuir model reported in the literature for the sorption of organic pollutants on raw cork granulates.

Pollutant	Cork size	q_{max} ($\mu\text{g g}^{-1}$)	Reference
Bifenthrin	1-2 mm	260	Domingues et al. (2005)
	3-4 mm	55	
α-cypermethrin	1-2 mm	303	Domingues et al. (2007)
	3-4 mm	136	
Acenaphthene	0.25-0.42 mm	46 \pm 25	Olivella et al. (2011a)
Fluorene	0.25-0.42 mm	49 \pm 26	Olivella et al. (2011a)
Phenanthrene	0.25-0.42 mm	32 \pm 5	Olivella et al. (2011a)
Anthracene	0.25-0.42 mm	26 \pm 18	Olivella et al. (2011a)
Pyrene	0.25-0.42 mm	32 \pm 4	Olivella et al. (2011a)
Benz(a)anthracene	0.25-0.42 mm	26 \pm 8	Olivella et al. (2011a)
Chrysene	0.25-0.42 mm	23 \pm 5	Olivella et al. (2011a)
Benzo(b)fluoranthene	0.25-0.42 mm	28 \pm 12	Olivella et al. (2011a)
Benzo(k)fluoranthene	0.25-0.42 mm	21 \pm 7	Olivella et al. (2011a)
Benzo(a)pyrene	0.25-0.42 mm	21 \pm 5	Olivella et al. (2011a)
Indeno(1,2,3-cd)pyrene	0.25-0.42 mm	20 \pm 18	Olivella et al. (2011a)
Dibenz(a,h)anthracene	0.25-0.42 mm	16 \pm 3	Olivella et al. (2011a)
Benzo(ghi)perylene	0.25-0.42 mm	23 \pm 2	Olivella et al. (2011a)
4,4'-DDT	< 0.5 mm	2.03 $\times 10^3$	Boussahel et al. (2009)
	< 0.2 mm	19.08 $\times 10^3$	
Ofloxacin	\leq 0.85 mm	31.1 $\times 10^3$	Crespo-Alonso et al. (2013)
	\leq 0.42 mm	37.9 $\times 10^3$	
Methylene blue	0.63-0.75 mm	30.52 $\times 10^3$	Olivella et al. (2012)
Chrysoidine G	0.42-0.85 mm	44.6 $\times 10^3$	Nurchi et al. (2014)
	\leq 0.42 mm	57.3 $\times 10^3$	

model.

Sorption kinetics of organic pollutants have been shown to fit well to the pseudo-second order kinetic model with varying equilibrium times (Psareva et al., 2005; Dordio et al., 2011; Olivella et al., 2012; Nurchi et al., 2014). Isothermal equilibria could be described not only by the Langmuir model but also, in some cases, by the Freundlich model (Domingues, 2005; Dordio et al., 2011; Olivella et al., 2011a) and by partitioning models (Karbowski et al., 2010; Olivella et al., 2013). Contrary to the Langmuir model, which describes monolayer adsorption, the Freundlich model predicts multilayer adsorption on heterogeneous surfaces, which may be more representative of the process, especially when there are attractive forces between sorbate molecules. On the other hand, partitioning models describe adsorption by weak interactions, especially hydrophobic ones, which can easily be the main forces responsible by sorption in the case of organic non-polar compounds. The predominance of these interactions can also be explained by the cork structure, especially its aromatic domain of suberin and lignin. The hydrophobic regions in these structural components of cork increase the ability of hydrophobic compounds to diffuse into the material (Karbowski et al., 2010). A similar effect was observed in the interaction between lignin and paracetamol on grape stalks (Villaescusa et al., 2011). Since cork is hydrophobic, it has an advantage of affinity over other natural materials for the removal of organic pollutants (Domingues et al., 2007).

Cork granulates have also been used in continuous operation using a packed bed configuration, in the removal of pyrethroids from water (Domingues, 2005) and as a support for biofilms in the degradation of volatile organic compounds (VOCs) (Kwon and Cho, 2009). Cork has good characteristics for biofilm attached growth such as good water holding capacity, durability and ability to attach microorganisms.

As it has been mentioned in chapter 1, cork granulates are also being used commercially as absorbents for oil spills (Corticeira Amorim, 2009). In this application, it was found that cork can absorb up to ten times their own weight in oil.

2.1.3.2 Production of activated carbons

Activated carbons are very important materials: their porous structure and surface properties make them adequate for many applications, from medicine to industrial plants and treatment of wastewaters and gaseous effluents (Carvalho et al., 2006; Cardoso et al., 2008). Using waste residues as carbon precursors has been a recently favoured practice, as it simultaneously deals with the problem of waste disposal while reducing the production costs (Mestre et al., 2009). Cork has the essential features of an activated carbon precursor, having, however, specific structural characteristics which distinguish it from wood and other lignocellulosic materials (Carrott et al., 1999; Carvalho et al., 2003).

Preparation of activated carbons involves physical and/or chemical activation. Physical activation consists of carbonisation under inert atmosphere, followed by gasification under water vapor or carbon dioxide. Chemical activation consists in the impregnation of the precursor with a chemical agent followed by carbonisation. While chemical activation is less energy-consuming than

physical activation, as it only has one calcination step instead of two, it demands more reactant consumption and implies a washing step after carbonisation to remove the reaction products (Cardoso et al., 2008).

The properties of the activated carbon, such as surface area, pore volume and pore distribution, depend on the preparation and activation method, including, for chemical activation, the impregnant used, the degree of impregnation, the experimental procedure for the impregnation and, for both chemical and physical activation, the pyrolysis temperature and flowrate (Carrott et al., 2006).

Chemical activation of cork has been tested by impregnation with phosphoric acid and basic reagents, such as sodium and potassium hydroxides and carbonates. Impregnation can be done in two ways: through immersion in solutions of the activating agent, or by physical mixture of the adsorbent with the impregnant in powder form. Even though physical impregnation is a method rarely used, it is simpler and less time-consuming than impregnation in solutions (Carvalho et al., 2004).

In general, prior to chemical activation, a washing pretreatment of cork, with H₂SO₄ 10% or 20%, is carried out (Carrott et al., 1999; Carvalho et al., 2003; Carrott et al., 2006; Carvalho et al., 2006; Mourão et al., 2006; Cardoso et al., 2008). However, Mestre et al. (2007) have tested samples without this pretreatment, concluding that due to the low ash content of cork, the difference between their properties with or without acid treatment are not significant enough to justify the large quantities of time and reactants spent in this procedure.

Activation methods which have been described in the literature are summarised in Tables 2.5 (chemical activation) and 2.6 (physical activation). Textural properties of these carbons were determined through N₂ and CO₂ adsorption isotherms at -196 °C and 0 °C, respectively. Isotherm analysis by the BET equation allowed the calculation of surface areas, which ranged between 76 and 1616 m² g⁻¹. Pore volume and distribution could be calculated in most instances using the Dubinin-Radushkevich (DR) equation (Dubinin and Stoeckli, 1980). Total pore volume varies between 0.06 and 0.73 cm³ g⁻¹, while micropore volume varies between 0.04 and 0.61 cm³ g⁻¹.

As expected, carbons with high surface area are usually the ones with higher pore volume. Still, the textural properties of each carbon depend on the method of activation. When impregnated with phosphoric acid, materials are activated at the beginning of carbonisation, at lower temperature, and thus result in a more mesoporous material, a final product with larger pores. On the other hand, treatment with basic impregnants results in a denser material, whose formation occurs after the precursor has been partially carbonised, thus at higher temperature (Carrott et al., 2006). Carbons activated by basic impregnants, especially potassium hydroxide, are essentially microporous (Cardoso et al., 2008).

A direct relation between adsorption capacity, impregnant amount and pyrolysis temperature has not been established; the experimental conditions have to be optimised for each type of activated carbon produced. However, higher amount of impregnant and temperature of pyrolysis leads to increased consumption of reactants and energy, turning the process of activated carbon production more expensive. In this sense, researchers have been seeking ways to produce activated carbons with similar properties but with less resource consumption and at lower cost. Carvalho et al.

Table 2.5: Summary of chemical activation methods of cork powder and granulates reported in the literature.

Impregnant	Method	Ratio Imp:cork	Pyrolysis flow	Heating rate	Pyrolysis conditions	Reference
KOH	Solution	1:4, 1:2, 1:1	N ₂ , 120 mL min ⁻¹	5 °C min ⁻¹ up to 300 °C,	300 °C, 3 h; 500-800 °C, 2 h	Cardoso et al. (2008)
	Physical	0:1 – 4:1		then 10 °C min ⁻¹	300 °C, 3 h; 500-900 °C, 2-16 h	Carvalho et al. (2003)
	Solution	1:1 – 2:1		8 °C min ⁻¹	450 or 700 °C; 2 h	Carrott et al. (2006)
	Physical	2:1	N ₂ , 85 mL min ⁻¹			Mourão et al. (2010), Cansado et al. (2012)
	Solution	1:1	N ₂ , 100 mL min ⁻¹	5 °C min ⁻¹	750 °C, 2 h	Atanes et al. (2012)
K ₂ CO ₃		1:1 – 2:1	N ₂ , 300 mL min ⁻¹	10 °C min ⁻¹	700 or 800 °C, 1 h	Mestre et al. (2014)
	Physical	2:1	N ₂ , 85 mL min ⁻¹	8 °C min ⁻¹	450 or 700 °C; 2 h	Carrott et al. (2006)
		1:1	N ₂ , 300 mL min ⁻¹		700 °C, 1 h	Mestre et al. (2007); Neng et al. (2011) and others
		1:1 – 4:1	N ₂ , 120 mL min ⁻¹		500-800 °C, 1 h	Carvalho et al. (2004)
	Solution	1:1 – 2:1	N ₂ , 300 mL min ⁻¹	10 °C min ⁻¹	700 or 800 °C, 1 h	Mestre et al. (2014)
H ₃ PO ₄	Solution	1:1 – 2:1	N ₂ , 85 mL min ⁻¹	8 °C min ⁻¹	450 or 700 °C; 2 h	Carrott et al. (2006)
		2:1			450 °C; 2 h	Carrott et al. (1999); Mourão et al. (2006)
NaOH	Physical Solution	1:1 – 2:1	N ₂ , 85 mL min ⁻¹	8 °C min ⁻¹	450 or 700 °C; 2 h	Carrott et al. (2006)
Na ₂ CO ₃	Physical	1:1 – 2:1	N ₂ , 85 mL min ⁻¹	8 °C min ⁻¹	450 or 700 °C; 2 h	Carrott et al. (2006)

Table 2.6: Summary of physical activation methods of cork powder reported in the literature.

Oxidising agent	Gasification temperature	Carrier flow	Heating rate	Reference
CO ₂	450-900 °C, 30 min	N ₂ , 85 mL min ⁻¹	1, 4, 8 °C min ⁻¹	Carrott et al. (2003)
	700-800 °C, 30 min		8 °C min ⁻¹	Carrott et al. (1999)
	750 °C, 30 min			Mourão et al. (2006)
	750 °C, 2 h	N ₂ , 100 mL min ⁻¹	5 °C min ⁻¹	Atanes et al. (2012)
H ₂ O (vapor)	750 °C, 30 min	N ₂ , 85 mL min ⁻¹	8 °C min ⁻¹	Mourão et al. (2006)
	750 °C, 1 h ¹	N ₂ , 300 mL min ⁻¹	20 °C min ⁻¹	Mestre et al. (2007, 2009, 2010); Neng et al. (2011)
	800 °C, 1 h	N ₂ , 480 mL min ⁻¹	10 °C min ⁻¹	Mestre et al. (2014)

¹ Treatment after chemical activation with K₂CO₃.

(2004), for instance, have suggested the use of potassium carbonate in substitution of potassium hydroxide as impregnating agent, as the impregnation method is faster and the calcination time is shorter, while attaining around 90% of surface area.

Activated carbons from cork have been agglomerated into granular form, through compression into pellets or using binders such as montmorillonite or laponite. In the latter case, the aggregated mixture of activated carbon and clay was shaped onto cylindrical extrudates (4×9 mm) which, in the case of laponite-based samples, suffered additional thermal treatment (10 °C min⁻¹ up to 300-600 °C, 1 h). Extrudates have lower surface area and pore volume when compared to the powdered samples, and therefore decreased adsorption capacity. However, granulated carbons are more suitable for commercialisation than fine powders, especially if they exhibit good thermal and compression resistance and stability in water (Carvalho et al., 2004, 2006).

Finally, besides activated carbons, carbonisation of cork has also been carried out for the preparation of cation exchangers. For this purpose, the cork was first submitted to pyrolysis under nitrogen flow until 300 to 600 °C and then to sulfonation with sulfuric acid or oleum. The best cation exchangers obtained from cork had an exchange capacity around 2 meq g⁻¹ (Valenzuela Calahorra et al., 1993).

2.1.3.3 Application of activated carbons in adsorption

Activated carbons have several applications in environmental technology, and those produced from cork have been used in the treatment of water, wastewater and gaseous effluents in order to remove a wide range of pollutants. Their application is usually selected according to the surface properties

Table 2.7: Limiting adsorbed amounts expressed in liquid volume and maximum sorption capacities reported in the literature for the adsorption of pollutants from the gas phase on activated carbons derived from cork.

Pollutant	Activation method	w_0 or q_{max}	Reference
Ethanol	K ₂ CO ₃ , 700 °C, 1 h, Agglomeration with montmorillonite and laponite	0.3 cm ³ g ⁻¹	Carvalho et al. (2006)
Trichloroethylene		0.34 cm ³ g ⁻¹	
Methylethylketone	K ₂ CO ₃ , 700 °C, 1 h, Agglomeration with montmorillonite and laponite	0.34 cm ³ g ⁻¹	Carvalho et al. (2006)
	KOH, 300 °C, 3 h + 500-800 °C, 2 h	0.10- 0.52 cm ³ g ⁻¹	Cardoso et al. (2008)
1,1,1-trichloroethane	K ₂ CO ₃ , 700 °C, 1 h, Agglomeration with montmorillonite and laponite	0.29 cm ³ g ⁻¹	Carvalho et al. (2006)
	KOH, 300 °C, 3 h + 500-800 °C, 2 h	0.02- 0.58 cm ³ g ⁻¹	Cardoso et al. (2008)
Cyclohexane	K ₂ CO ₃ , 700 °C, 1 h, Agglomeration with montmorillonite and laponite	0.3 cm ³ g ⁻¹	Carvalho et al. (2006)
	KOH, 300 °C, 3 h + 500-800 °C, 2 h	0.03- 0.42 cm ³ g ⁻¹	Cardoso et al. (2008)
n-hexane	KOH, 300 °C, 3 h + 500-800 °C, 2 h	0.14- 0.58 cm ³ g ⁻¹	Cardoso et al. (2008)
Sulfur dioxide (in N₂ flow)	CO ₂ , 750 °C, 2 h	61.0 mg g ⁻¹	Atanes et al. (2012)
	KOH, 750 °C, 2 h	95.2 mg g ⁻¹	

and affinities, since removal efficiency depends on adsorbate-adsorbent interaction.

Studied applications found in the literature essentially consist of the removal of emerging micropollutants from water, such as pharmaceuticals (ibuprofen (Mestre et al., 2007, 2009; Neng et al., 2011; Mestre et al., 2014), paracetamol (Cabrita et al., 2010; Mestre et al., 2014), clofibric acid (Mestre et al., 2010; Neng et al., 2011; Mestre et al., 2014), acetylsalicylic acid, caffeine and iopamidol (Mestre et al., 2014)) and phenolic compounds (Mourão et al., 2006, 2010; Cansado et al., 2012), and of VOCs on the gas phase (Carvalho et al., 2004, 2006; Cardoso et al., 2008; Atanes et al., 2012).

A summary of the applications of activated carbons derived from cork in the adsorption of pollutants of environmental significance, along with their limiting adsorbed amounts expressed in liquid volume (w_0), in the case of gaseous adsorbates, and maximum sorption capacities, in both gaseous and aqueous phases, is presented on Tables 2.7 (gaseous phase) and 2.8 (aqueous phase). Adsorption isotherms for pollutants in the gas phase either follow a linear trend on the lower pres-

Table 2.8: Maximum sorption capacities reported in the literature for the adsorption of pollutants from water on activated carbons derived from cork.

Pollutant	Activation method	q_{max}	Reference
Ibuprofen	K ₂ CO ₃ , 700 °C, 1 h	145.2 mg g ⁻¹ (0.70 mmol g ⁻¹)	Mestre et al. (2007, 2009)
	K ₂ CO ₃ , 700 °C, 1 h + H ₂ O (vapor), 750 °C, 1 h	378.1 mg g ⁻¹ (1.83 mmol g ⁻¹)	
	KOH, 800 °C, 1 h	174.4 mg g ⁻¹ (0.85 mmol g ⁻¹)	Mestre et al. (2014)
	H ₂ O (vapor), 800 °C, 1 h	143.1 mg g ⁻¹ (0.69 mmol g ⁻¹)	
P-nitrophenol	CO ₂ , 750 °C, 30 min	1.64-2.13 mmol g ⁻¹	Mourão et al. (2006, 2010)
	KOH, 500 °C, 30 min	1.7-2.4 mmol g ⁻¹	Cansado et al. (2012)
Phenol	CO ₂ , 750 °C, 30 min	1.55-1.99 mmol g ⁻¹	Mourão et al. (2006, 2010)
	KOH, 500 °C, 30 min	1.8-2.0 mmol g ⁻¹	Cansado et al. (2012)
P-chlorophenol	CO ₂ , 750 °C, 30 min	1.58-2.27 mmol g ⁻¹	Mourão et al. (2006, 2010)
P-cresol		1.82-2.88 mmol g ⁻¹	
Clofibric acid	K ₂ CO ₃ , 700 °C, 1 h	139 mg g ⁻¹ (0.65 mmol g ⁻¹)	Mestre et al. (2010)
	K ₂ CO ₃ , 700 °C, 1 h + H ₂ O (vapor), 750 °C, 1 h	295 mg g ⁻¹ (1.37 mmol g ⁻¹)	
Paracetamol	K ₂ CO ₃ , 700 °C, 1 h	200 mg g ⁻¹ (1.32 mmol g ⁻¹)	Cabrita et al. (2010)

sure range (Carvalho et al., 2004) or resemble a type I isotherm according to the International Union of Pure and Applied Chemistry (IUPAC) classification, due to the microporous nature of the adsorbents (Carvalho et al., 2006; Cardoso et al., 2008). Limiting adsorbed amounts expressed in liquid volume were calculated by fitting to the Dubinin-Astakhov (Dubinin, 1979; Carvalho et al., 2006) and the DR (Cardoso et al., 2008) equations, while in the case of the study of SO₂ adsorption in a carrier N₂ flow, the maximum sorption capacity was calculated by fitting the experimental data to the Langmuir isotherm (Atanes et al., 2012). Carvalho et al. (2006) have also studied the adsorption of water vapor on cork-based activated carbons, and the isotherm had the S-shape characteristic of interaction with hydrophobic materials.

Adsorption of organic pollutants in aqueous phase generally follows a pseudo-second order kinetic model (Mestre et al., 2007, 2009, 2010; Cabrita et al., 2010; Mestre et al., 2014). It is usually a fast process, but adsorption rates depend on the porous structure. The presence of mesopores enhances the adsorption process as they help with the penetration of the molecules into the pores (Mestre et al., 2009, 2010, 2014). The presence of a higher volume of supermicropores (0.7-2 nm size) has also been linked to a quicker initial rate of adsorption in the case of ibuprofen (Mestre et al., 2007).

The reported isotherms for the adsorption of phenolic compounds, ibuprofen and paracetamol belong to the L-type, with a steep initial rise and a concave curvature for low concentrations, followed by a plateau at high concentrations (Mourão et al., 2006; Mestre et al., 2009; Cabrita et al., 2010). Equilibrium data have been fitted exclusively to the Langmuir model, in the case of ibuprofen and paracetamol (Mestre et al., 2007, 2009; Cabrita et al., 2010), and to the Langmuir, Freundlich, Dubinin-Radushkevich-Kaganer and Redlich-Peterson (1959) equations, in the case of phenolic compounds (Mourão et al., 2006, 2010; Cansado et al., 2012). In the case of clofibrac acid, the reported isotherms belong to the S-type, indicating lateral interactions between the solute molecules (Mourão et al., 2010).

It is known that adsorption capacity is mainly influenced by the micropore distribution. Narrow micropores are usually considered as sites with high potential of adsorption, but in the case of organic pollutants, they may be too small to accommodate the molecules. Therefore, the governing factor is the existence of larger micropores, such as supermicropores (Mourão et al., 2006; Mestre et al., 2009, 2010).

Furthermore, uptake of organic compounds by activated carbons is also dependent on pH, since it influences the speciation of the molecules and the surface chemistry of the carbons. As cork-derived activated carbons usually result in basic carbons (pH of zero charge below 7), the carbon will be neutral or positively charged when the pH is acid, and negatively charged when the pH is above the point of zero charge. Solutes like ibuprofen, paracetamol and clofibrac acid are weak electrolytes and therefore are neutral at acid pH and dissociate into the anionic form at pH near neutrality and higher. As the neutral molecules are the ones with more affinity for the carbons, adsorption is favoured at acid pH, especially near 2 for both ibuprofen and clofibrac acid (Mestre et al., 2009, 2010), and around 6 for paracetamol (Cabrita et al., 2010).

2.1.4 Conclusions

In this section, the unique properties of cork, a natural, renewable material, were reviewed. It was shown how the main byproducts of the cork industry, powder and granulates, can be transformed into added-value products by application in environmental sorption technologies. This process is twice beneficial since both product recycling and water, wastewater or air purification can be achieved.

Even though the properties of cork powder and granulates are already well known, research about the applications on environmental remediation and industrial pollution abatement are recent and can be developed much further. Other byproducts are also emerging as potential adsorbents, for instance, “regranulated cork”, a byproduct of black agglomerate. Many studies could be found on the biosorption of toxic metals by cork, with results comparable to other biosorbents.

Several studies report on the production of activated carbons using cork byproducts as precursors. Good textural properties such as high surface area and development of micro and mesoporosity could be achieved with adequate activation methods. The application of cork-based activated carbons on environmental technology has been investigated for the removal of VOCs in the gas phase and the adsorption of organic pollutants from water.

Both cork byproducts and cork-based activated carbons exhibit hydrophobic properties which favour the uptake of organic compounds. The most recent research on biosorption has focused on the removal of organic pollutants in low concentrations from water, and cork powder and granulates seem to be particularly suited for this purpose due to the establishment of weak interactions and partitioning with the sorbate molecules. Similar mechanisms could dictate the affinity of cork toward oil molecules in water. This possibility is subject of study in the present work.

2.2 Oil and grease (O&G): a common pollutant in wastewaters

2.2.1 Introduction

This second section of the literature review aims to establish the state-of-the-art on the O&G class of pollutants. Their origins, methods of analysis, composition, and best available technologies for removal are examined. There are numerous studies on O&G removal from wastewaters, and the selected publications for reference try to be as broad as possible in order to point out advantages and disadvantages of proposed methodologies. Special emphasis will be given to sorption, following the lead from a recent review by [Wahi et al. \(2013\)](#) which examines the practical advantages of using low-cost sorbents for O&G removal.

2.2.2 The O&G class of pollutants

2.2.2.1 Types of O&G

O&G substances can be divided into two great classes, differing in origin and in chemical constitution. A first category has mineral provenance, namely from petroleum and its derivatives, and consists of a mixture of hydrocarbons of different chemical configurations; a second group is from biological origin (animal or vegetable), and is mainly composed of triglycerides, i.e. esters of glycerin and fatty acids.

It is not clear whether further chemical differences can be assigned to the two types. [Patterson \(1985\)](#) maintains that there is a dichotomy between mineral and biological oils in which polarity and biodegradability are a characteristic of the latter group. However, it might be an oversimplification to correlate these chemical properties with the previous classification. In fact, [O'Brien \(2003\)](#) points out that “all edible fats and oils are water-insoluble”, because of the large non-polar hydrocarbon tails of fatty acids which govern triglycerides' polarity, despite the slightly polar carbon-oxygen bonds in glycerol. Therefore, as a rule, oils of biological origin behave like nonpolar molecules. Likewise, it is difficult to establish *a priori* whether any O&G present in a wastewater will be biodegradable; it tends to depend on external factors which influence microbiological activity.

Regardless of chemical classification, O&G in water and wastewater can be examined with regards to their physical characteristics, which are fundamental for appropriate treatment design. The level of dispersion and stability of oil droplets in aqueous medium will influence the readiness of separation and the resources which need to be put forward to achieve the treatment objective. Here, [Patterson \(1985\)](#) defines five other classes of O&G, which were later complemented by [Rhee et al. \(1989\)](#) by attributing a droplet size range to each class:

- *Free oil* comprises all droplets with diameter over 150 μm , which will rise quickly to the surface in quiescent conditions, due to the imbalance of forces caused by the differential density between oil and water;
- *Dispersed oil*, which mixed with water consists in a *mechanical dispersion*, is made up of droplets with diameter between 20 and 150 μm , stabilised by electric charges and other interparticle forces;
- *Emulsified oil*, which together with water forms a *chemically stabilised emulsion*, consists of droplets with diameter under 20 μm stabilised by the chemical action of surface active agents;
- *Soluble or “dissolved” oil* includes all particles which are dissolved or very finely dispersed in drops under 5 μm size;
- “*Oil-wet solids*” are suspended solids with oil adhered to their surface.

Other authors who have directly or indirectly classified O&G regarding their physical characteristics (API, 1990; Roques and Aurelle, 1991; Welz et al., 2007) provide only variations of the aforementioned classification, either by considering only a few classes or by giving emphasis on the role of surfactants in the emulsification of oil in water.

2.2.2.2 Sources of O&G

O&G is present in municipal wastewaters, but not in high concentrations: provided industrial discharges are under control, the entrance of oil in the system is restricted to domestic activities such as cooking or cleaning, and the problem is usually controlled at the source through the installation of grease traps. Similarly, O&G in stormwaters, consisting of leached hydrocarbons from automobile vehicles and related activities such as parking lots and gas stations, was rarely found to exceed a few milligrams per liter in a study by Stenstrom et al. (1984).

So how does oil and grease end up in high concentrations in wastewaters? The answer to this question lies in industrial activity. Liquid waste rejected by plants mixes oily matter with water used at all steps of operation, resulting in colloidal suspensions with oil droplets in different physical forms. As far as industrial wastewaters are concerned, O&G concentrations may reach a few dozens of grams per liter.

In his book about industrial wastewater treatment, Patterson (1985) presents a comprehensive list of industrial processes which generate oily wastewater, from which three prevailing activities are singled out as representative of different realities:

- *Petroleum wastewaters* originate from both crude oil extraction and oil refineries. On-field exploitations of crude oil reservoirs originate “oil-field brine”, a wastewater that, besides being loaded with hydrocarbons, presents very high salinity (Dalmacija et al., 1996). Wastewaters from oil refineries also contain other “non-conventional pollutants” such as ammonia, sulphides, chlorides, mercaptans and phenols (Rhee et al., 1989; Hami et al., 2007; Yu et al., 2013);
- *Metalworking wastewaters* result from metal piece manufacturing in materials ranging from aluminum to steel. Cutting, cooling and lubricating oils are often applied in the process to serve as interface between tools and workpieces. These fluids usually do not consist of pure oils, but of oil-in-water emulsions which combine the properties of both liquids under the stabilising action of a surfactant (Benito et al., 2002, 2010). In rinsing, cooling and cleaning operations, they are carried away to the facility’s wastewaters. Moreover, when spent, the diluted metalworking fluids themselves consist in wastewaters with O&G concentrations that may reach dozens of grams per liter only in the emulsified form (Patterson, 1985; MacAdam et al., 2012);
- *Food processing wastewaters* derive from the transformation of both animal and vegetable products. Operations of slaughtering and cleaning generate oily wastewaters in meat processing (Dassey and Theegala, 2012). Extraction and refinery of vegetable oils discharge

great volumes of oily wastewaters as well. In Southern Asia, palm oil mill effluent (POME) is a growing concern (Ahmad et al., 2005c; Ngarmkam et al., 2011; Abdullah et al., *In Press*), while in Mediterranean countries, olive mill wastewaters' production is high, due to strong activity in this sector (Al-Malah et al., 2000; Santi et al., 2008; Michael et al., 2014). Refining of vegetable oils originates vegetable oil refinery wastewaters (VORWs) from different origins, for example, sunflower, cottonseed, soybean and rapeseed (Pandey et al., 2003).

2.2.3 Treatment of wastewaters with O&G

Treatment of oily wastewater is, according to Patterson (1985), "similar in concept to treatment of domestic sewage", since it consists of a primary treatment followed by a secondary step and, when needed, a tertiary stage for the refinement of quality parameters for discharge and/or reuse. However, treatment technology differs in its specifications for each situation.

In wastewaters where O&G is the central pollutant of concern, primary treatment generally consists of a gravity separation tank with quiescent flow conditions which allow free oil to float to the surface. Different tank configurations can be used for this effect, from the traditional American Petroleum Institute (API) separator to parallel-plate interceptors (PPIs) which take advantage of tilted plates inside the tank to promote oil droplet aggregation and ascension. The oil layer which forms at the surface after gravity separation can be skimmed off and sometimes reprocessed, yielding valuable returns for the facility (API, 1990).

For wastewaters with high solids content, sedimentation of solids is also enabled by the stagnant conditions of a gravity separator, or alternatively by sedimentation tanks (Al-Malah et al., 2000; Ahmad et al., 2005b). Separation of settleable solids can also be done by means of magnetic and/or mesh filters (Benito et al., 2002).

After the first step of treatment, the secondary unit aims to separate the remaining oil, which is mostly in the emulsified form and therefore does not spontaneously separate under the action of gravity and buoyancy forces. The breaking of the oil/water emulsion can be externally promoted through a variety of treatment methods, which can be classified as chemical, electrical or physical. Chemical methods are the most common and work by destabilising the emulsified oil droplets through the addition of coagulants such as aluminum or iron salts. The sludge generated in this process can then be separated by a physical method, most commonly sedimentation or flotation. Electrical methods include electroflotation and electrocoagulation: the former replaces traditional flotation by creating gas bubbles by the electrolysis of water, and the latter induces coagulation by means of consumable electrodes, which upon oxidation release metallic coagulants into the wastewater. Finally, physical methods act by changing physical properties or applying forces to promote coalescence and agglomeration of oil droplets. Techniques in this category include heating, centrifugation, filtration, dissolved air flotation (DAF) and coalescing beds (Patterson, 1985; Roques and Aurelle, 1991). Although Yang (2007) considers DAF a primary treatment technique, most authors consider this technology to be most effective in the treatment of emulsified oil, especially when coupled with coagulation and flocculation (Angelidou et al., 1977; Suzuki and Maruyama,

2005).

When biodegradable oil and grease is present in wastewater, the secondary treatment step may be a biological reactor, operating in a very similar way to a municipal WWTP. With this methodology, removal of non-biodegradable oils occurs by sorption or incorporation in the biological sludge (Patterson, 1985). Therefore the presence of the latter type of oils must not be prevailing in order not to interfere with the normal functioning of the process.

After the secondary treatment, the effluent may need refinement if the previous methods were not efficient enough to reduce O&G concentration below the discharge limit, or if a higher water quality is desired to allow reuse. In such cases, a tertiary step will involve a more selective technology, such as adsorption, membrane filtration or advanced oxidation processes (AOPs). As an example, Al-Malah et al. (2000) proposes adsorption in activated clay for the removal of residual O&G at the end of a treatment line composed by previous steps of sedimentation, centrifugation and filtration. In another approach, Taha and Ibrahim (2014) have optimized an aerated heterogeneous Fenton process to complement the treatment of POME after anaerobic biodegradation.

In the next sections the different steps in oily wastewater treatment and the corresponding technologies for O&G removal at each stage will be explored in more detail, referencing previously published studies in each segment as appropriate.

2.2.3.1 Primary treatment

Primary treatment of oily wastewaters aims for both the removal of O&G in free oil form and the sedimentation of solids and unstable colloidal particles. Separation of these substances from the aqueous matrix is usually performed by taking advantage of gravitational forces and differential densities, which cause oil globules to float and solid granules to settle (Patterson, 1985).

Quiescence of the wastewater can be achieved in gravity separators, which consist in tanks and/or channels where horizontal flows are low enough not to interfere with oil rise or solid deposition. The first separator to be designed for this effect, back in the 1950s, was the API separator. It consists in a simple rectangular channel coupled with an oil skimmer and a sludge pump. The design parameters limit horizontal water velocity to 3 ft min^{-1} (approx. 1.5 cm s^{-1}), hence allowing a reduced surface-loading rate (flowrate divided by surface area) which in turn increases oil removal. Theoretically, any oil droplet whose rise rate exceeds the surface-loading rate will reach the top of the separator and be skimmed off from the surface (API, 1990).

The rise rate of oil globules can be estimated taking into account the balance of the forces that act upon them. The most important factors governing the rise rate are differential density and viscosity. It is clear that the closer the specific gravities of oil and water, the slower the separation. Similarly, the more viscous the fluid the lower the rising rate. The decrease in viscosity can be achieved with an increase in temperature. Therefore, heating is a possible mechanism of enhancing phase separation.

Another possibility for the improvement of separation involves the adoption of a different separator design. Previously, the simple rectangular channel which composes the API separator has been described. However, sometimes, to achieve the desired removal efficiency, large surface areas are

required to decrease the surface-loading rate. With a simple rectangular channel configuration this may involve unfeasible land occupation. In order to solve this problem, plate separators were conceived. The inclined plates added inside this reactor configuration enable an increase in surface area avoiding the enlargement of the reactor itself.

In a PPI, plates are distributed inside the reactor at angles between 45 and 60° from the horizontal and a spacing of 0.75-1.5 in between them (approx. 2 to 4 cm). [Das and Biswas \(2003\)](#) found that a baffled separator with 4 cm spacing between baffles positioned at a 45° angle was the most suitable configuration for the separation of a 5% diesel oil-water mixture. Parallel plates promote collision between oil droplets near the solid surface, leading to the occurrence of coalescence ([Patterson, 1985](#)). The increase in droplet size implies that the rise rate will also increase, speeding up the separation process. Coalescence can be further improved by using corrugated plates in the place of standard smooth parallel plates; this configuration is called a corrugated-plate interceptor (CPI) ([Hydro-Flo Technologies, 2002](#)).

PPI and CPI units present many advantages over the traditional API separator, the most obvious of which is the improvement of efficiency in a same limited space. According to [API \(1990\)](#), plate separators can handle flows two or three times higher than equivalent traditional units. Moreover, these configurations can be designed to remove oil globules as small as 60 μm diameter, often meeting treatment requirements of O&G concentration as low as 50 mg L^{-1} . Traditional separators are dimensioned for a diameter threshold of 150 μm and are only expected to remove O&G down to a concentration of 100 mg L^{-1} .

In all gravity separators, at the end of the quiescence period, both oil and sludge have to be collected, respectively, from the top and bottom of the separator. At the surface, an oil-skimming device gathers the less dense phase, which can be either discarded or reprocessed. The sediment, on the other hand, is removed from the bottom of the separator either manually or using a scraper and a sludge pump, depending on the concentration of solids in the wastewater ([API, 1990](#)).

The effect of gravity separation can be enhanced by several methods, namely DAF, centrifugation, coalescing beds, and heating ([Roques and Aurelle, 1991](#)). [Benito et al. \(2002\)](#) have also improved the removal of settleable solids using filtration with mesh and magnetic filters.

2.2.3.2 Secondary treatment: chemical methods

As it has been covered in the previous section, the removal of free O&G is fairly straightforward once a good grasp of the physical forces acting on the oil droplets is acquired. A bigger challenge remains: the removal of the remaining oil, which is dispersed in very small droplets and stabilised by interparticle forces and/or surface active agents. This type of stable O&G is often found in industrial wastewaters, and must be targeted by a secondary treatment, since gravity separation is ineffective ([Zouboulis and Avranas, 2000](#)).

Chemical methods of secondary treatment consist in the addition of a reagent to remove O&G by taking advantage of a chemical process ([Patterson, 1985](#)). [Ahmad et al. \(2003\)](#) proposes solvent addition (*n*-hexane having the best performance) to extract oil from POME. However, this

methodology seems rather unfeasible in practice due to the high associated costs, unless the recovered product should prove to have very high added value.

The most common reagents used in emulsified O&G treatment aim to break the oil-water emulsion, regardless of the possibility of recovery (Yang, 2007). Emulsion breakage can be achieved using detergents, acids, coagulants and polymers (Eckenfelder, 2000). Acidification, *per se*, is usually not enough to foster the aggregation of oil droplets in a short time frame. Nevertheless, it may prove to be beneficial if it takes advantage of processes already under way at the industrial facility. An example is presented by Boyer (1984) in the treatment of edible oil wastewater, where separation of oil is enhanced at the WWTP by taking advantage of residual acidity and heat from acidulation wastewater. The main disadvantage of acidification may consist in the robust construction materials needed for tanks, which may increase the installation's cost.

Using acidification to break the oil-water emulsion leads us in the right direction towards faster and more effective techniques of oil separation. Zouboulis and Avranas (2000) and Welz et al. (2007) state that oil droplets are stable as a colloidal phase due to the adsorption of surface active agents or hydroxyl ions at their surface, which promote the negative charging of the particles and the occurrence of electrostatic repulsion between them. Therefore, positively charged particles, such as the hydrogen ions released to solution upon the addition of an acid, will destabilise the dispersion by means of charge neutralisation. But while H^+ will only promote coalescence of oil droplets, metallic cations cause a much stronger effect of coagulation, since apart from neutralisation, they can stimulate other mechanisms of destabilisation, such as double layer compression, precipitation and bridging flocculation (Zouboulis and Avranas, 2000; Welz et al., 2007; Yang, 2007; Cañizares et al., 2008). Several authors (Zouboulis and Avranas, 2000; Cañizares et al., 2008; Benito et al., 2010; Karhu et al., 2014) successfully monitor the stability of the oil-water emulsion by measurement of the zeta potential or surface charge, reporting that effective coagulation is achieved when zeta potential is brought to zero. The importance of charge and zeta potential neutralisation in coagulation is further highlighted in the observations of Chi and Cheng (2006) who demonstrated the occurrence of charge reversion and restabilisation of colloids following a positively charged coagulant overdose.

The most common coagulants used in oily wastewater treatment are iron and aluminium salts (Rhee et al., 1989; Zouboulis and Avranas, 2000; Ahmad et al., 2003; Cañizares et al., 2008; Santo et al., 2012), which are cheap and widely available. Chipasa (2001), Pandey et al. (2003) and Benito et al. (2010) have also used calcium salts as coagulants, namely calcium chloride and lime, and Suzuki and Maruyama (2005) the inorganic polymer polyaluminium chloride (PAC). PAC has a higher net charge than monomer aluminium salts, thus being more effective in emulsion breaking; furthermore, polymers promote flocculation by bridging between coagulated particles, forming flocs which are easier to separate from the aqueous phase.

The separation of the coagulated sludge from the supernatant can be achieved by several methods, the most popular of which is DAF (Zouboulis and Avranas, 2000; Dassey and Theegala, 2012; Karhu et al., 2014). This separation technique can, by itself, remove particles over $40 \mu\text{m}$ diameter, but its performance is boosted by the use of coagulant and flocculant aids, with which it is able

to achieve an effluent quality of 1 to 20 mg L⁻¹ O&G. Coagulants not only promote the aggregation of oil droplets, as it has been previously described, but they also increase the adhesion between air bubbles and oil droplets, easing the flotation of oily matter (Rhee et al., 1989). DAF performance can also be enhanced by surfactants, due to the formation of positively charged air bubbles which attract negatively charged flocs and oil droplets (Angelidou et al., 1977; Karhu et al., 2014). A technique with similar characteristics is induced air flotation (IAF), though it relies on the production of larger bubbles and higher turbulence (Meysami and Kasaeian, 2005).

Other flotation techniques which have just recently been introduced in wastewater treatment have been tested. Foam separation, a method widely applied in ore flotation, relies in the spontaneous formation of air bubbles in the presence of a foaming agent that enhances adhesion between flocs and bubbles. The generated foam brings to the surface not only the coagulated oily matter but also suspended solids (Suzuki and Maruyama, 2005). Another technology, mechanically agitated flotation cell (MFC), promotes higher turbulence than DAF or IAF and has higher capacity than those traditional flotation methods. Despite the increase in energy efficiency, MFC treatment could not achieve O&G concentrations below 50 mg L⁻¹ (Welz et al., 2007). In another approach, Santander et al. (2011) could achieve 80 to 85% O&G removal from petroleum wastewaters in conventional and modified jet flotation cells. Finally, it is worth mentioning that centrifugation has also been used to separate coagulated sludge from treated effluent (Benito et al., 2010), but the expensive energy costs associated with this method compare rather unfavorably to flotation techniques.

The biggest disadvantage which is often pointed out in the literature regarding traditional chemical methods such as coagulation with inorganic salts is the production of large amounts of hazardous sludge (Boyer, 1984; Ahmad et al., 2006). Since the oil is trapped among aluminium and iron precipitates, it is unrecoverable (Decloux et al., 2007). The handling of the oily/metallic sludge usually involves costly treatment or deposition. In this sense, organic and biodegradable coagulants have been tested in place of inorganic salts, in order to minimise the hazardousness of the sludge and develop a cleaner process. Synthetic organic polymers have been used by for this purpose by Karhu et al. (2014) and Cristóvão et al. (2014). Boyer (1984) had previously advocated the use of food-grade organic compounds as coagulants, while Benito et al. (2002) have used a biodegradable demulsifier to destabilise oil-water emulsions and separate them by centrifugation. The most popular organic coagulant presented in the literature for the treatment of oily wastewater is chitosan (Ahmad et al., 2005b, 2006; Chi and Cheng, 2006). It is a natural polymer of marine origin with widespread applications. The treatment of oily wastewater by chitosan powder is believed to work by both mechanisms of coagulation and adsorption (Ahmad et al., 2006; Geetha Devi et al., 2012). The positive charge of chitosan particles attracts negatively charged oil droplets and other suspended solids (Ahmad et al., 2005b). Ahmad et al. (2006) have concluded that chitosan is more efficient than traditional coagulants alum and PAC in a study on the treatment of POME: to achieve the same treatment objectives, operation with the natural polymer requires lower coagulant dosage, less mixing time and less sedimentation time. Chi and Cheng (2006) have achieved similar conclusions in the treatment of milk processing wastewater samples; following a cost-benefit analysis, they concluded that the use of chitosan does not increase costs while provid-

ing operating benefits.

Regardless of the type of coagulant used, it must be noted that chemical treatment may not lead to full compliance with discharge limits. For stricter regulations, the remaining O&G will still need further reduction, and coagulation is ineffective in the removal of dissolved organic matter (Chipasa, 2001; Chi and Cheng, 2006). Aslan et al. (2009) have shown, through chemical oxygen demand (COD) fraction analysis, that the effluent of physicochemical treatment of VORW has high biodegradability. For this reason, the coupling of coagulation/flocculation and DAF processes with subsequent biological reactors is a common solution to achieve the desired effluent quality for discharge (Chipasa, 2001; Pandey et al., 2003).

2.2.3.3 Secondary treatment: electrical methods

Electrical methods take advantage of electrochemistry to increase the efficiency of coagulation and flotation processes. In electrocoagulation, the coagulants are generated *in situ*, by means of consumable electrodes. Electroflotation, on the other hand, is the generation of gas bubbles by the electrolysis of water, mimicking an air flotation process (Patterson, 1985). The main advantage of electrical treatment methods derives from the fact that both electrocoagulation and electroflotation often coexist in a treatment process. This leads to high efficiency gains, since while metallic cations are being released to the solution, promoting the aggregation of oil droplets, hydrogen gas bubbles are being formed, improving agitation conditions and carrying the flocs to the surface (Yang, 2007).

The study of electrocoagulation has been carried out mostly in real wastewater matrices, such as refractory wastewater (Xu and Zhu, 2004), olive mill wastewaters (Tezcan Ün et al., 2006), VORW (Tezcan Un et al., 2009), POME (Phalakornkule et al., 2010), biodiesel wastewater (Ngamlerdpokin et al., 2011), slaughterhouse wastewaters (Bayar et al., 2014; Ozyonar and Karagozoglul, 2014) and restaurant wastewater (Ji et al., In Press). Nevertheless, recent studies have also approached the destabilisation of oil-in-water emulsions by this method in order to study more fundamental principles of the technology (Sangal et al., 2013; Fouad, 2014).

Aluminium is the most common material for sacrificial electrodes (Tezcan Un et al., 2009; Phalakornkule et al., 2010; Sangal et al., 2013), even though some studies have found iron electrodes more efficient (Tezcan Ün et al., 2006). The efficacy of a consumable electrode depends on the specifics of each application, including, for instance, the supporting electrolytes. Izquierdo et al. (2010) have found that chlorides are the most advantageous types of salts for energy-efficient dissolution of both aluminium and iron electrodes, while nitrates and sulfates cause large decreases of efficiency for treatment with the latter.

Electrocoagulation has been compared to chemical coagulation with inconclusive results. While some authors report definite efficiency gains with electrocoagulation (Ozyonar and Karagozoglul, 2014), others observe that electro and chemical coagulation lead to similar O&G removals, with other mechanisms coming into play. Cañizares et al. (2008, 2009) have argued that pH is a very important factor when choosing between electrocoagulation and chemical coagulation, since each process causes different variations in this parameter through time. The deviation of pH from an

optimum range of operation can then compromise treatment effectiveness. In another approach, [Phalakornkule et al. \(2010\)](#) demonstrate that, for a similar treatment of POME, electrocoagulation is cheaper than chemical coagulation, due to the elimination of reactant consumption. However, in the same study, it is reported that electrocoagulation generates twice the mass of sludge of chemical coagulation, so this environmental impact is not minimised by the electrical method, but it is even worsened.

The use of electroflotation methods with insoluble electrodes can reduce the production of hazardous sludge ([Hosny, 1996](#); [Mansour and Chalbi, 2006](#)). These processes work solely on the basis of hydrogen and oxygen bubble generation. The size of the bubbles and their surface charge influence strongly the treatment efficiency. Nevertheless, despite attempts to optimise flotation performance, to achieve the desired effluent concentrations coagulant and flocculant agents often need to be added to the electroflotation unit ([Mostefa and Tir, 2004](#); [Mansour and Chalbi, 2006](#)). Recent studies have approached the treatment of oily wastewaters by optimizing both electrocoagulation and electroflotation performance in the same unit ([Ji et al., In Press](#)).

2.2.3.4 Secondary treatment: physical methods

The control of the physical properties of oil and water can be fundamental in devising alternative treatments where gravity separation and chemical and electrochemical methods have proven unsatisfactory or hazardous ([Zhou et al., 2008](#)). One way to achieve this is by tweaking the operating conditions of processes which have been described earlier to separate coagulated flocs from water so that they are able to perform oil droplet separation without coagulant addition. The other option is to apply other physical separation methods, such as heating, coalescence and filtration, and optimise them for oil/water separation ([Rhee et al., 1989](#); [Roques and Aurelle, 1991](#); [Yang, 2007](#)). Instead of working as a method of carrying floatable flocs to the surface, DAF can be used as a method of oil droplet separation alone ([Angelidou et al., 1977](#); [Suzuki and Maruyama, 2005](#)). As it has been mentioned earlier in section 2.2.3.2, [Zouboulis and Avranas \(2000\)](#) have found that the technology is able to separate all droplets with diameters over 40 μm ; however, this did not result in good removal efficiencies in this study. In a previous work, [Angelidou et al. \(1977\)](#) were able to achieve high treatment quality of other oil-water emulsions using DAF, and could even describe the process accurately using theoretical models of first-order kinetics. [Tansel and Pascual \(2011\)](#) also applied DAF without coagulants with success in the treatment of brackish and pond waters contaminated with emulsified oil. One of the parameters often highlighted for optimal performance is the size distribution of air bubbles. In this sense, designs which promote microbubble formation, such as cyclone-based technologies, have been tested ([Le et al., 2013](#); [Ran et al., 2013](#)). Centrifugation is also a method which is used to separate coagulated sludge and treated water that can be applied directly to oil-water emulsions ([Tansel and Regula, 2000](#)). However, without the addition of coagulants or demulsifiers, the technology is unable to remove the smallest emulsified oil particles ([Yang, 2007](#)), nor can it reduce COD levels associated with dissolved organic matter ([Al-Malah et al., 2000](#)).

Vacuum evaporation is a technique that is very effective in producing a purified aqueous phase,

and can be used when there is a goal of water reuse. However, the operating costs are inhibitory for a large-scale application (Benito et al., 2010).

Roques and Aurelle (1991) propose coalescence in a granular medium bed as treatment strategy. This method works by fostering the aggregation of small oil droplets onto larger particles, so that they will easily be separated by gravity once they flow out of the coalescing bed. The mechanism unfolds in three steps: first, the oil droplets are attracted to the granules' surface; then, they adhere to the solids by means of weak interactions; finally, the oil salts out of the bed in larger droplets, which easily float to the surface in a free resting space at the top of the bed. This technology is usually based on resin materials (Maiti et al., 2011), but it has also been done with other granular and fibrous media, such as polypropylene and nylon fibres (Li and Gu, 2005), sand (Multon and Viraraghavan, 2006), polyurethane, poly(ethylene terephthalate) and polypropylene granules (Sećerov Sokolović et al., 2014) and glass microfibres (Ma et al., 2014).

Instead of promoting coalescence in view of downstream gravity separation, a filtration bed will provide oil removal by both retention and coalescence (Patterson, 1985). However, the study of filtration beds is very complex, since several mechanisms occur simultaneously, including sorption, which will be approached in further sections of this chapter. Therefore, in this section only an overview of membrane separation is presented.

Membrane filtration has the ability to achieve high effluent purity, and often allows the recovery of the separated oily phase (Decloux et al., 2007). The biggest constraint to good membrane performance is maintenance and fouling, which can be minimised by adequate pretreatments with high removals of O&G and suspended solids, and by careful choice of the membrane characteristics and operating conditions (Ahmad et al., 2003).

In oil-water separation, the affinity of the membrane material towards oil and water is one of the most important characteristics influencing filtration performance. Membranes can range from superhydrophobic (contact angle with water = 0°) to superhydrophilic (contact angle with water $> 150^\circ$) and from superoleophilic (contact angle with oil = 0°) to superoleophobic (contact angle with oil $> 150^\circ$) (Kota et al., 2012). Another important parameter is the membrane pore size, which determines whether we are working with microfiltration (MF), ultrafiltration (UF), nanofiltration (NF) or reverse osmosis (RO) processes.

Decloux et al. (2007) have accomplished the treatment of a real acidic VORW using a MF hydrophilic mineral membrane and operating it at low transmembrane pressure. Removal efficiencies of over 90% for suspended solids and O&G and 60% for COD were achieved in this study. Good O&G removal efficiencies were also obtained for the treatment of petroleum refinery wastewaters with a MF membrane (Abadi et al., 2011). However, due to its large pores, MF is often used in a two-step membrane treatment as a pretreatment before tighter membranes. Peng and Tremblay (2008) used MF in combination with UF, where the MF membrane works as a coalescence medium for smaller particles and is very effective in the separation of surfactants and detergents. A more recent approach to MF membranes has been to improve their surface properties in order to combine hydrophilicity with oleophobicity and take advantage of these affinities to improve separation performance and avoid fouling problems (Zhu et al., 2014). A remarkable study by

Kota et al. (2012) has reported on the creation of a superhydrophilic/superoleophobic membrane (stainless steel mesh coated with fluorodecyl polyhedral oligomeric silsesquioxane and cross-linked poly(ethylene glycol) diacrylate) which keeps its properties after water wetting. The differential density between water and oil makes it possible for the process to be driven by gravity forces alone. The authors demonstrate the feasibility of the method with successful separations (99.9% purity for each phase) of oil-in-water and water-in-oil emulsions, even when stabilised by surfactants, maintaining operation for over 100 h without fouling or losing membrane permeation.

UF has been used both as secondary and tertiary treatment, for oil-in-water emulsions (Benito et al., 2002; Chakrabarty et al., 2008; Benito et al., 2010) and for oily wastewaters (Mohammadi and Esmaelifar, 2004; Akdemir and Ozer, 2009; Masoudnia et al., In Press). Still, high operating pressures and specific methods of cleaning and regeneration are often needed for UF to run smoothly (Peng and Tremblay, 2008). Therefore, the effectiveness of this technology comes at the expense of elevated costs.

2.2.3.5 Tertiary treatment

Tertiary treatment is often designed with the perspective of water reuse, so a great effluent quality is expected.

NF and RO membranes are in this category, since they can deliver even higher quality permeates than MF and UF systems; however, they are also more expensive to operate. NF membranes have been used successfully at end-of-line treatments of petroleum wastewaters (Mondal and Wickramasinghe, 2008) and olive mill wastewaters (Ochando-Pulido and Stoller, 2014). Mondal and Wickramasinghe (2008) have also shown that RO membranes can achieve greater permeate quality than NF ones. Al-Jeshi and Neville (2008) have achieved over 99% O&G removal in the separation of oil-in-water emulsions with oil contents ranging from 0.15% to 50% with a RO membrane. An advantage of RO membranes is that they also enable the separation of salts, which are commonly found in oily wastewaters from the petroleum and food industries. However, the efficiency of salt rejection is influenced by the feed's oil concentration.

Oxidation technologies, namely AOPs, are also emerging as tertiary treatment alternatives for oily wastewaters, in particular due to their ability to destroy dissolved organic matter and thus reduce the remaining COD content after secondary treatment. Many methodologies, from chemical oxidation to solar ultraviolet (UV) radiation photocatalysis, have been studied for this purpose, for instance, Fenton's reagent ($\text{Fe}^{2+}/\text{H}_2\text{O}_2$) (Dincer et al., 2008; Kalyanaraman et al., 2012), $\text{H}_2\text{O}_2/\text{UV}$ (Dincer et al., 2008; Souza et al., 2011; Kalyanaraman et al., 2012), photo-Fenton ($\text{Fe}^{2+}/\text{H}_2\text{O}_2/\text{UV}$) (Dincer et al., 2008), O_3/UV (Souza et al., 2011), aerated heterogeneous Fenton with nano zero-valent iron (Taha and Ibrahim, 2014) and solar photo-Fenton (Michael et al., 2014).

2.2.3.6 Biological treatment

The use of biological reactors in wastewater treatment is very common, since it is a very cheap and easily accessible technology. Previously, on section 2.2.1, the reasons why O&G is not so easily

treated by biological methods and how it interferes with their normal functioning have been presented. Nevertheless, in a few particular cases, it is possible to use biological treatment to remove O&G from wastewaters.

Untreated industrial wastewater containing high concentrations of oil is rarely fit for biological degradation. [Aslan et al. \(2009\)](#) evaluated the biodegradability of VORWs, inferring that they cannot be treated by biological methods alone, due to their low BOD₅/COD ratio. Biodegradable O&G is, therefore, mostly constituted by soluble substances and very finely divided droplets at very low concentration ([Rhee et al., 1989](#); [Chipasa, 2001](#)). Oils of biological origin (such as vegetable and animal oils) are, in general, easier to biodegrade than those of mineral origin ([Patterson, 1985](#)).

For proper functioning of a biological reactor as a secondary treatment, upstream treatments must enable removal of all coarse O&G and substances which are not subject to biodegradation. It is a common strategy to use a typical sequence of industrial WWTPs: physicochemical treatment (coagulation/flocculation followed by sedimentation/flotation) preceding an activated sludge reactor. This has been successfully used for the treatment of VORWs ([Chipasa, 2001](#); [Pandey et al., 2003](#)). [Aslan et al. \(2009\)](#) have confirmed that the effluent of a physicochemical treatment leads to increased biodegradability in these types of wastewaters.

Other typologies of biological reactors have also been tested for oily wastewater remediation, such as biological filters with supported biomass on granular activated carbon (GAC) ([Dalmacija et al., 1996](#); [Souza et al., 2011](#)), biological aerated filters ([Zhao et al., 2006](#); [Tong et al., 2013](#)) and membrane biological reactors ([Sharghi et al., 2013](#)).

2.2.3.7 Combination of treatment strategies

As it has been introduced in the beginning of this section ([2.2.3](#)), the removal of O&G and the full decontamination of wastewaters is only achieved by a combination of different methodologies in sequential steps. In the literature, it is more common to find studies exploring the possibilities of each technology at once, but a few authors have proposed combinations of treatment strategies which have proved successful in the removal of O&G from oil-in-water emulsions and real wastewaters.

[Pandey et al. \(2003\)](#) have examined a real VORW treatment plant, giving suggestions to improve its operation and performance. The basis of the proposed treatment is the common combination of physicochemical and biological treatment, which has been mentioned in section [2.2.3.6](#) and studied by other authors ([Chipasa, 2001](#); [Aslan et al., 2009](#)). Upstream from the coagulation/flocculation unit, the industrial WWTP has an equalisation tank, and downstream from two activated sludge processes, the plant completes treatment with secondary clarification and disinfection by chlorination. The final effluent is compliant with limits of discharge.

In a different study, [Benito et al. \(2002\)](#) report on the design of a pilot plant for the treatment of a cutting oil residue from metalworking with very high levels of O&G and COD. The authors were able to achieve quality for discharge into the local drainage system by a sequence of filtration, demulsification/centrifugation, UF and peat bed filtration.

Ahmad et al. (2003) and Peng and Tremblay (2008) also advocate treatment strategies centered on one or more membrane separation units. But while the first group of authors recommends the use of different pretreatments to remove suspended solids and O&G and prevent fouling, the latter combines different types of membranes for more efficient operation.

In another study with more sophisticated technologies, Souza et al. (2011) have combined AOPs with a biological filter supported on GAC for the treatment of petroleum wastewaters. The effluent after both units had enough quality for water reuse.

Finally, there are many authors that center the treatment line on a sorption unit. This methodology, which is the main focus of this thesis, will be covered in greater detail in the next section. Al-Malah et al. (2000) propose treatment of olive mill effluent by sequential sedimentation, centrifugation, filtration and sorption onto activated clay. Previously, Alther (1995) had suggested that sorption of O&G onto organoclays could be positioned either as a pretreatment for more sensitive adsorption and membrane separation or as a post treatment for primary units such as gravity separators. Ahmad et al. (2005a) have studied O&G removal by sorption as a follow-up to coagulation and sedimentation. Dalmacija et al. (1996) and Hami et al. (2007) have used sorbents as a direct complement to other technologies, such as activated sludge processes and DAF, with improvements in O&G and COD removal efficiency.

2.2.4 Treatment of wastewaters with O&G by sorption

Thirty years ago, in an overview of O&G removal methodologies in industrial wastewater treatment, Patterson (1985) mentioned adsorption as an emerging technology, mostly used in tertiary treatment. In the past two decades the importance of (ad)sorption in oily wastewater treatment has changed immensely. Alther (1995) was a pioneer in this matter, demonstrating the versatility of organoclays in oil removal, either as a pretreatment for membrane separation processes or as a secondary treatment following gravity separators. These sorbents can be used both in the powdered and granular forms, the former in batch systems and the latter in filtration units, mixed with other clay media, such as anthracite.

In more recent studies, activated clay and other mineral sorbents have been shown to provide successful treatment for olive mill wastewaters (Al-Malah et al., 2000; Santi et al., 2008). Besides capturing O&G, they also sorb other organics, such as polyphenols. Santi et al. (2008) have tested both batch and percolating column configurations, finding no difference between them in terms of treatment efficiency. The authors tried to improve effluent quality by performing sequential sorption treatments, but it was ineffective.

The concept of coupling sorption units toward a better overall treatment result is more valuable when each unit is designed with a different objective in mind. Zhou et al. (2008) performed a successful two-step treatment of a synthetic oil-in-water emulsion using modified resin for removing high concentrations of oil and GAC for treatment polishing. Dalmacija et al. (1996) and Hami et al. (2007) have used activated carbon in the powdered form as an aid of coagulation/flocculation/DAF and activated sludge processes, and in the granular form as a tertiary step, in refinery wastewater treatment. However, despite the demonstrated increase in efficiency in 5-day biochemical oxygen

demand (BOD₅) and COD removal, adsorption onto activated carbon can be an expensive technology. If higher O&G concentrations are present, pore clogging effects can occur (Mowla et al., 2013).

The use of granular media in a column configuration also needs to take into account the occurrence of coalescence (Roques and Aurelle, 1991). Wang et al. (2010) have tried to circumvent this problem by using a fluidised bed of hydrophobic nanogels. Since nanogels are less dense than water, the configuration used was inverse fluidisation. In order to improve operation, the authors tested combinations of both fixed and fluidised bed in the same run, by switching between flowrates under and above the minimum fluidisation velocity. The main disadvantage of a fluidised bed is the high flowrate it requires for proper bed expansion.

Since activated carbon and other synthetic materials such as nanogels are expensive to manufacture, many authors have been turning to natural materials, including agro-industrial wastes, in the search for a cheaper technology of O&G removal by sorption. Most of these low-cost materials have been tested solely on batch mode for a preliminary screening of sorption capacity; examples include rubber powder (Ahmad et al., 2003, 2005a), fungal biomass (Srinivasan and Viraraghavan, 2010), walnut shell (Srinivasan and Viraraghavan, 2010), and chitosan powder and flake (Ahmad et al., 2005b; Geetha Devi et al., 2012; Pitakpoolsil and Hunsom, 2014). Since some materials did not present high affinity for oil by themselves, they have been submitted to pretreatments to improve oil sorption capacity, such as surface modification with cationic surfactant (Ibrahim et al., 2009, 2010). Other treatments, such as the deposition of iron oxide on the sorbents' surface, have aimed to facilitate their separation from water using magnetic properties (Ngarmkam et al., 2011). Finally, sorption units have been designed, such as biosorption columns of *Salvinia* sp. (Ribeiro et al., 2003) and *M. rouxii* (Srinivasan and Viraraghavan, 2014) dead biomass.

Experimental sorption tests have been carried out both in oil-in-water emulsions and in real wastewaters from several provenances. Besides oil sorption, some materials, such as chitosan, also trigger coagulation-like mechanisms. This has been previously addressed in section 2.2.3.2, where chitosan was mentioned as a natural coagulant. Beyond outperforming traditional coagulants PAC and alum, chitosan powder has also been proven to overcome adsorbents bentonite and activated carbon in oil sorption capacity (Ahmad et al., 2005b). Aside from improving oil removal efficiency, chitosan also works at lower dosages than conventional coagulants and sorbents (Ahmad et al., 2006).

Finally, it is worth mentioning that a lot of research in oil-absorbing materials has been done outside of wastewater treatment technologies, with oil spill management applications in mind instead. In this field of research, authors have focused either on increasing oil sorption capacity by improved material synthesis, or in reducing costs of spill decontamination by finding natural high-uptake materials. Sorbents tested with this purpose include carbon fibre felts (Inagaki et al., 2002), vegetable fibres (Annunciado et al., 2005), walnut shell (Srinivasan and Viraraghavan, 2008) and polymers (Atta et al., 2013). These sorbents are of interest since if their high affinity for oil is coupled with durability and high hydrophobicity they may be quite effective for O&G removal in wastewaters.

In the next two sections the properties of oil sorbents and the corresponding uptake mechanisms will be reviewed. A final section will present some examples of desorption and oil recovery found in the literature.

2.2.4.1 Types and characteristics of sorbents

Several materials are reported in the literature as sorbents of O&G. As it has been mentioned, their experimental applications range from separation of synthetic oil-in-water emulsions to real wastewaters of complex composition. Therefore, it is not easy to establish a pattern that identifies the best types of sorbents and the respective physicochemical characteristics and sorption capacities. Nevertheless, a review of the studied sorbents is important to frame the proposal of a new O&G sorption treatment in the context of the existing knowledge.

One of the most common adsorbents, which has been widely tested for many applications, is activated carbon. However, its production is expensive due to low yields of carbonisation coupled to high energy requirements. One of the ways to reduce the cost of activated carbon production is to use natural carbonaceous materials as precursors. [Ngarmkam et al. \(2011\)](#) have used palm shell, a local resource, as a precursor of activated carbons for the treatment of POME. Even though removals of over 90% were achieved for ZnCl₂-treated carbons, the absolute sorption capacity of either the raw palm shell sorbents or the best performing carbons did not exceed 30-90 mg L⁻¹, a low value. Adsorption onto commercial activated carbon has been more successfully used as a complement to other treatment methods, improving BOD₅ and COD removal in refinery wastewaters and oil-field brine ([Dalmacija et al., 1996](#); [Hami et al., 2007](#)).

The main disadvantage of the use of activated carbons in O&G sorption is that oil droplets sit at the entrance of the pores, blocking a great part of available surface area in these materials, and not taking advantage of their most distinct property, the development of microporosity ([Alther, 1995](#); [Mowla et al., 2013](#)). [Zhou et al. \(2008\)](#) have advocated the use of synthetic polymeric sorbents instead, highlighting their higher stability, selectivity and lower cost. They propose a treatment with an organophilic resin modified by cationic surfactant. Other sorbents of the same type include ethanol-grafted polyacrylonitrile ([Ji et al., 2009](#)) and polystyrene resin ([Kundu and Mishra, 2013](#)), which were used in oil-in-water emulsion treatment, and polyurethane foams ([Atta et al., 2013](#)) and polyester non-woven matrices ([Li et al., In Press](#)), which were used for oil spill management. Furthermore, other synthetic materials such as hydrophobic nanogels ([Quevedo et al., 2009](#); [Wang et al., 2010, 2012](#)) have been used.

Other authors have opted for the use of natural mineral sorbents such as bentonite clay ([Al-Malah et al., 2000](#); [Moazed and Viraraghavan, 2005](#)), vermiculite ([Mysore et al., 2005](#)), sepiolite ([Rajaković-Ognjanović et al., 2008](#)), clay soil and zeolite ([Santi et al., 2008](#)). These materials do not present high porosity but, as it has been mentioned, this is not an essential aspect in oil sorption ([Alther, 1995](#)). They work best when modified with surfactants, so that their lipophilicity is enhanced, and in this case they are denominated as *organoclays*. [Alther \(1995\)](#) defines organoclays as clays whose surface sodium and calcium have been exchanged for the nitrogen end of a quaternary amine. The hydrophobic tail of the surfactant is left to contact with the solution or emulsion,

thereby granting organophilic properties to the sorbent. For the removal of oil and organic contaminants, the use of surfactants with a long alkyl chain is preferred, since it is believed that these tails possess more affinity towards these contaminants than short ones (Atkin et al., 2003; Salehi et al., 2013). The modification of clays with quaternary ammonium cations has been extensively studied and several applications have been researched besides the removal of oil and grease (Xi et al., 2007; Gök et al., 2008). These materials can be used both in powdered and granular form (Alther, 1995).

Some authors have applied the idea behind clay modification with cationic surfactants to organic materials. This was first reported by Namasivayam and Sureshkumar (2008) on coconut coir pith but only used later by Ibrahim et al. (2009, 2010) on barley straw with oil sorption in mind. These researchers verified that raw barley straw had a very low affinity towards oil and managed to improve it almost nine-fold through modification with cetylpyridinium chloride.

Organic materials with natural oil affinity can be used as O&G sorbents without any surface modifications. Chitosan powder and flake have both been used in the treatment of POME with better performance than coagulants alum and PAC (Ahmad et al., 2006) and sorbents bentonite and activated carbon (Ahmad et al., 2005b), as it has been previously mentioned in sections 2.2.3.2 and 2.2.4. Chitosan powder seems to work especially well due to its high surface area and charge density (Ahmad et al., 2005c). It has been tested successfully in the removal of COD, turbidity and electrical conductivity from VORWs (Geetha Devi et al., 2012). Chitosan flakes have also been used in the treatment of biodiesel wastewater (Pitakpoolsil and Hunsom, 2014).

Several types of dead biomass have been used in the treatment of oil-in-water emulsions, for instance hydrophobic aquatic plant *Salvinia* sp. (Ribeiro et al., 2003), non-viable fungal cultures *M. rouxii* and *A. coerulea* (Srinivasan and Viraraghavan, 2010, 2014), fruiting bodies of macro-fungus *Auricularia polytricha* (Yang et al., 2014) and kapok (*Ceiba pentandra* (L.) Gaertn.) (Abdullah et al., In Press). Srinivasan and Viraraghavan (2010) have suggested that the affinity of *M. rouxii* towards oil might be partly caused by the presence of chitosan in its constitution. Ribeiro et al. (2003) evaluated sorbent hydrophobicity through a methodology that measures the partition between an organic phase and water. Hydrophobicity has also been used as a justification for the use of rubber powder as a sorbent in POME treatment (Ahmad et al., 2005a). However, the dosages required for effective treatment by sorption onto this material are very high.

In oil spill management, natural fibrous sorbents are an increasingly common option for oil sorption. A recent review by Wahi et al. (2013) highlights the advantages of natural fibrous sorbents, namely their high buoyancy and low processing cost. Abdullah et al. (2010) further point out that natural organic sorbents are easier to dispose after use and can be co-applied with other techniques such as bioremediation. Sorption onto natural fibres has had attention from researchers for several decades (Johnson et al., 1973), but many materials, such as silk floss (Annunciado et al., 2005), walnut shell (Srinivasan and Viraraghavan, 2008), kapok fibres (Abdullah et al., 2010), and rice husks (Bazargan et al., 2014) have only recently been shown to be fit for this application. Common characteristics that are described by the authors as conducive to high oil sorption include hydrophobicity and low specific gravity. This last feature means that the material will have ten-

dency towards floating in water, just like oil, therefore facilitating contact between sorbent and pollutant when the spills occur in aqueous environments (Annunciado et al., 2005). Inagaki et al. (2002) demonstrate, through different types of carbon materials, that there is an inversely proportional correlation between apparent density and sorption capacity.

Both hydrophobicity and low specific gravity are characteristics of cork (section 2.1.2.1). Therefore, this material is also a natural organic sorbent indicated for the clean-up of oil spills. Cork granule-filled pillows, socks and booms are commercialised by Corticeira Amorim under the brand CORKSORB (Corticeira Amorim, 2009). Studies have shown that cork granules can reach sorption capacities of about 10 times their own weight.

2.2.4.2 Oil sorption mechanism onto natural organic materials

There are two great types of oil/sorbent interactions to be taken into account when examining oil sorption: absorption and adsorption. While the latter refers only to surface interactions, namely the accumulation of adsorbate at the liquid/solid interface, the former involves the penetration of the sorbate into the sorbent material, even if just for a few nanometers (Annunciado et al., 2005). When contacting sorbents with pure oil, i.e. in oil spill cleanup, it is believed that both processes occur. In this scenario, oil accumulates almost instantaneously at the surface through lipophilic interactions or coalescence, the latter being prominent in hydrophilic materials, which do not bond easily with oil (Srinivasan and Viraraghavan, 2008). Then, absorption into the material is promoted by capillary forces (Inagaki et al., 2002). These forces are especially relevant in sorbents with hair-like features (Ribeiro et al., 2003; Yang et al., 2014). Wahi et al. (2013) suggest that oil sorption occurs in a three-phase mechanism consisting of diffusion, capillary action and agglomeration in porous and rough structures.

When the contact between oil and sorbent happens in an aqueous medium, competition between water and oil may take place (Annunciado et al., 2005; Srinivasan and Viraraghavan, 2008). Interactions between oil and water must be taken into account, and this is often done by measuring the oil's interfacial tension. Srinivasan and Viraraghavan (2008) suggest that oils with lower interfacial tension exhibit higher uptake because they reach the pores of the sorbent more easily. However, when the oil is emulsified, low interfacial tension will lead to the formation of smaller oil droplets and higher kinetic stability. Emulsion stability is most commonly evaluated through droplet size distribution and zeta potential measurements (Srinivasan and Viraraghavan, 2010). Surface active agents (surfactants) also influence emulsion stability and, as a consequence, oil sorption. Benito et al. (2010) have studied the influence of surfactant type and concentration, observing higher stability in emulsions prepared with increased surfactant dosages. Wang et al. (2010, 2012) have also identified the presence of surfactant as a hindering influence in oil sorption by nanogels.

It has been previously mentioned in section 2.2.3.2 that destabilisation of emulsions can be carried out by charge neutralisation of oil droplets, thus promoting their aggregation. Most authors agree that the decrease of pH contributes to emulsion destabilization, most noticeably by bringing the

zeta potential closer to zero, resulting in an improvement in oil sorption onto several sorbent materials (Ahmad et al., 2005b,c, 2006; Srinivasan and Viraraghavan, 2010). This works even better when the sorbent also becomes positively charged via protonation of surface functionalities, as in the case of amino groups in chitosan (Geetha Devi et al., 2012), thereby attracting negatively charged colloidal particles. In this case, the action of the sorbent resembles that of a coagulant, aggregating the oil droplets at its surface (Ahmad et al., 2005b).

Apart from favourable electrostatic conditions, adequate agitation is also essential to overcome surface film resistance, which is suggested by Ahmad et al. (2003) to be the main factor in the rate of sorption, due to an observation of faster kinetics with higher mixing speed. High agitation velocities and times lead to a desirable breakage of the oil droplets, increasing the surface area available for contact between oil and sorbent (Ahmad et al., 2005c). Nevertheless, speed should not be too intense to avoid redispersion of the oil droplets in a stabilised state (Ahmad et al., 2005b). The risk is higher when there is excess sorbent that may promote charge reversal (Geetha Devi et al., 2012); optimisation of sorbent dosage and mixing conditions should be done for every application. If the film resistance is easily overcome by proper agitation, then oil bonding to the sorbate may consist in the rate-controlling step. Intraparticle diffusion and adsorption onto the porosity is then presented by some authors as the main mass transfer mechanism (Ahmad et al., 2005a,c).

Many researchers agree that chemisorption occurs between oil and most sorbent materials. Hydrophobic interactions lead to the uptake of oil and organics from the aqueous medium by a partitioning process (Alther, 1995). In surfactant-modified materials, these interactions occur between the oil and the oleophilic tails at the solid's surface. These surface-modified sorbents can be regenerated without losing surface properties since the ionic bond between solid and surfactant is stronger than the weak bonds between surfactant and oil (Roques and Aurelle, 1991; Zhou et al., 2008).

Oil sorption equilibria and kinetics have been described using mathematical models which are commonly employed in the literature to interpret adsorption processes. The Freundlich isotherm (Freundlich, 1907), which is illustrative of heterogeneous multilayer adsorption, is the model applied by most authors to describe equilibrium data (Ribeiro et al., 2003; Ahmad et al., 2005a,c). Nevertheless, Ibrahim et al. (2009, 2010) have also successfully fitted the Langmuir isotherm equation (Langmuir, 1918), which represents monolayer adsorption, and Yang et al. (2014) have used the Langmuir-Freundlich isotherm with better results than both Langmuir and Freundlich equations. As far as kinetics are concerned, oil sorption is usually fast. In an aqueous mixture, kinetics can usually be described by pseudo-first-order (Yang et al., 2014) or pseudo-second-order (Ahmad et al., 2005c) empirical equations, or a combination of both (Pitakpoolsil and Hunsom, 2014).

2.2.4.3 Desorption/recovery²

After the oil sorption treatment is completed, it is important to study the desorption or recovery of oil from the sorbent. This is one of the most unexplored topics in both oil spill management with sorbent materials and treatment of oily wastewaters by sorption of O&G. But it is a very important aspect to explore in current times, especially as recycling and reutilisation of materials is encouraged and as we move towards a cradle-to-cradle approach in product design (McDonough and Braungart, 2010). Still, to the best of the authors' knowledge, this aspect is only superficially covered in sections of research papers on the development of oil sorbents.

An important aspect to consider is the release of oil by the sorbent when in contact with clean water, which is a study with other important implications, such as the prediction of the occurrence of leaching after deposition in sanitary landfill. Since most oil sorbents are hydrophobic, contact with water should lead to little release of oil, and this has been shown to occur in vermiculite (Mysore et al., 2005), barley straw (Ibrahim et al., 2009) and dead biomass (Srinivasan and Viraraghavan, 2014). Pitakpoolsil and Hunsom (2014) investigated chitosan sorbent regeneration with aqueous solutions of NaOH, but even though significant removal of oil was reported, the capacity of the sorbent declined greatly in the second sorption cycle. Extraction with organic solvent *n*-hexane showed better results for the recovery of oil from activated carbon (Ngarmkam et al., 2011) and regeneration of carbon fibre felts (Inagaki et al., 2002).

Physical methods, on the other hand, have been studied more often. Inagaki et al. (2002) also show good oil recovery from carbon fibre felts using centrifugation. Srinivasan and Viraraghavan (2008) and Atta et al. (2013) successfully used compression to recover oil from walnut shell and polyurethane foams, respectively, while Johnson et al. (1973) accomplished regeneration of cotton fibres with squeezing in rolls of stainless steel and hard rubber. However, for more fragile sorbents, the techniques of compression and squeezing may be too aggressive and damage the sorbent's structure, affecting its performance in subsequent sorption cycles (Toyoda and Inagaki, 2000; Inagaki et al., 2002; Abdullah et al., 2010). In these cases, researchers have suggested the use of vacuum filtration, a technique with lower oil recovery efficiency but with low to no effect of structural damage to fragile sorbents. Using this method, carbon fibre felts could be fully regenerated for at least 8 cycles (Inagaki et al., 2002), and kapok fibre decreased its uptake on the second cycle but could then be reused without sorption capacity loss for at least 15 cycles (Abdullah et al., 2010). Other sorbents such as exfoliated graphite (Toyoda and Inagaki, 2000) and thermally reduced graphene (Iqbal and Abdala, 2013) lose capacity gradually due to cumulative oil retention in the sorbent after several cycles of sorption and recovery.

As far as the recovered oil is concerned, it may be fit for many purposes, even if it does not possess the quality to be reintroduced into the production line anymore. As long as hazardous trace elements are monitored, the recovered oil can be burned in a thermal power plant as an energy source,

²This section is adapted from the paper: Pintor, A. M. A., Ferreira, C. I. A., Pereira, J. P. C., Souza, R. S., Silva, S. P., Vilar, V. J. P., Botelho, C. M. S., Boaventura, R. A. R. Oil desorption and recovery from cork sorbents. Working paper, 2014.

sometimes along with the spent organic sorbent (Srinivasan and Viraraghavan, 2008; Benito et al., 2010).

2.2.5 Conclusions

O&G is a serious concern in wastewater treatment. Its main sources are industrial wastewaters from petroleum, metalworking and food processing facilities. Conventional wastewater treatment plants do not decontaminate O&G effectively and may even be affected by large concentrations of these pollutants, because they create superficial films that can lead to clogging in pumps and piping and inhibition of microbiological activity in activated sludge reactors.

Therefore, removal of O&G in industrial wastewaters requires specific treatment. It usually consists of two or three sequential steps with different objectives. The primary treatment has the goal of eliminating the free oil and suspended solids which constitute the largest load of organic pollution. Secondary treatment aims at removing the emulsified oil, which is dispersed so finely that it cannot be separated easily only by buoyancy forces. Finally, tertiary treatment separates residual O&G and COD and even other substances such as salts, using more sophisticated technologies.

Primary treatment is, in general, achieved by gravity separation. Secondary treatment, however, comprises many methodologies. Chemical treatment includes coagulation/flocculation with DAF, a common method used in practice. Effluents of such treatment can often be forwarded to biological reactors. Electrical methods are improvements of chemical and physical methods such as electrocoagulation and electroflotation. The main disadvantage of chemical/electro coagulation is the production of large amounts of hazardous sludge, which is unrecoverable and must be disposed of. Physical methods, namely membrane separation, can achieve very high O&G removal rates, and the retained oil in the membrane may be recovered. The main disadvantage of this method consists in the frequent clogging of membrane pores and the high energy demands. Finally, tertiary treatment can be carried out with NF, RO membranes or AOPs, toward a goal of water reuse. Sorption is an emerging technology that can avoid production of hazardous sludge and avoid the large costs associated with membrane operation. Natural sorbents from either mineral or organic provenance have the additional advantage of low cost and environmental friendliness and have been shown to provide good O&G removal efficiencies. High surface area, charge density and hydrophobicity are desirable characteristics of oil sorbents, and corrugations and hair-like features can also be advantageous by promoting oil uptake by capillary forces. Oil sorption usually occurs by partitioning between the sorbent and the sorbate and this process has been enhanced by surface modification of some sorbents. It has been shown that oil droplets in an emulsion exhibit negative charge and are stabilised by the resulting droplet-droplet repulsive forces, and the neutralisation of these droplet surface charges can be done by reducing the pH or by positive charges at the sorbent's surface. Oil sorbents may be regenerated after saturation, especially by solvent extraction or compression.

Finally, it is worth mentioning that cork is one of the materials which has been successfully used for oil sorption in oil spill management, due to its hydrophobic properties and low density, ideal

characteristics for this application. In pure oil medium, cork granules have shown sorption capacities of about 10 times their own weight. This thesis aims to broaden the range of application, by studying the feasibility of using cork granules for O&G sorption in oil-in-water emulsions and oily wastewaters.

2.3 References

- Abadi, S. R. H., Sebzari, M. R., Hemati, M., Rekabdar, F., and Mohammadi, T. Ceramic membrane performance in microfiltration of oily wastewater. *Desalination*, 265(1–3):222 – 228, 2011.
- Abdullah, M. A., Rahmah, A. U., and Man, Z. Physicochemical and sorption characteristics of Malaysian *Ceiba pentandra* (L.) Gaertn. as a natural oil sorbent. *Journal of Hazardous Materials*, 177(1–3):683 – 691, 2010.
- Abdullah, M. A., Afzaal, M., Ismail, Z., Ahmad, A., Nazir, M. S., and Bhat, A. H. Comparative study on structural modification of *Ceiba pentandra* for oil sorption and palm oil mill effluent treatment. *Desalination and Water Treatment*, In Press.
- Ahmad, A. L., Ismail, S., Ibrahim, N., and Bhatia, S. Removal of suspended solids and residual oil from palm oil mill effluent. *Journal of Chemical Technology & Biotechnology*, 78(9):971–978, 2003.
- Ahmad, A. L., Sumathi, S., Bhatia, S., and Ibrahim, N. Adsorption of residual oil from palm oil mill effluent using rubber powder. *Brazilian Journal of Chemical Engineering*, 22(3):371–379, 2005a.
- Ahmad, A. L., Sumathi, S., and Hameed, B. H. Residual oil and suspended solid removal using natural adsorbents chitosan, bentonite and activated carbon: A comparative study. *Chemical Engineering Journal*, 108(1-2):179–185, 2005b.
- Ahmad, A. L., Sumathi, S., and Hameed, B. H. Adsorption of residue oil from palm oil mill effluent using powder and flake chitosan: equilibrium and kinetic studies. *Water Research*, 39(12):2483–2494, 2005c.
- Ahmad, A. L., Sumathi, S., and Hameed, B. H. Coagulation of residue oil and suspended solid in palm oil mill effluent by chitosan, alum and PAC. *Chemical Engineering Journal*, 118(1-2):99–105, 2006.
- Akdemir, E. O. and Ozer, A. Investigation of two ultrafiltration membranes for treatment of olive oil mill wastewater. *Desalination*, 249(2):660 – 666, 2009.
- Al-Jeshi, S. and Neville, A. An experimental evaluation of reverse osmosis membrane performance in oily water. *Desalination*, 228(1-3):287–294, 2008.
- Al-Malah, K., Azzam, M. O. J., and Abu-Lail, N. I. Olive mills effluent (OME) wastewater post-treatment using activated clay. *Separation and Purification Technology*, 20(2-3):225–234, 2000.
- Alther, G. R. Organically modified clay removes oil from water. *Waste Management*, 15(8):623–628, 1995.
- Angelidou, C., Keshavarz, E., Richardson, M. J., and Jameson, G. J. The removal of emulsified oil particles from water by flotation. *Industrial & Engineering Chemistry Process Design and Development*, 16(4): 436–441, 1977.

- Annunciado, T. R., Sydenstricker, T. H. D., and Amico, S. C. Experimental investigation of various vegetable fibers as sorbent materials for oil spills. *Marine Pollution Bulletin*, 50(11):1340–1346, 2005.
- API. *Design and Operation of Oil-Water Separators*. American Petroleum Institute, first edition, February 1990. API Publication 421, Monographs on Refinery Environmental Control - Management of Water Discharges.
- Aslan, S., Alyuz, B., Bozkurt, Z., and Bakaoglu, M. Characterization and biological treatability of edible oil wastewaters. *Polish Journal of Environmental Studies*, 18(4):533–538, 2009.
- Atanes, E., Nieto-Márquez, A., Cambra, A., Ruiz-Pérez, M. C., and Fernández-Martínez, F. Adsorption of SO₂ onto waste cork powder-derived activated carbons. *Chemical Engineering Journal*, 211–212:60 – 67, 2012.
- Atkin, R., Craig, V. S. J., Wanless, E. J., and Biggs, S. Mechanism of cationic surfactant adsorption at the solid-aqueous interface. *Advances in Colloid and Interface Science*, 103(3):219–304, 2003.
- Atta, A. M., Brostow, W., Datashvili, T., El-Ghazawy, R. A., Lobland, H. E. H., Hasan, A. M., and Perez, J. M. Porous polyurethane foams based on recycled poly(ethylene terephthalate) for oil sorption. *Polymer International*, 62(1):116–126, 2013.
- Barberis, A., Dettori, S., and Filigheddu, M. R. Management problems in Mediterranean cork oak forests: post-fire recovery. *Journal of Arid Environments*, 54(3):565–569, 2003.
- Barker, D. A., Capone, D. L., Pollnitz, A. P., McLean, H. J., Francis, I. L., Oakey, H., and Sefton, M. A. Absorption of 2,4,6-trichloroanisole by wine corks via the vapour phase in an enclosed environment. *Australian Journal of Grape and Wine Research*, 7(1):40–46, 2001.
- Bayar, Se., Yildiz, Y., Yilmaz, A., and Koparal, A. S. The effect of initial pH on treatment of poultry slaughterhouse wastewater by electrocoagulation method. *Desalination and Water Treatment*, 52(16-18):3047–3053, 2014.
- Bazargan, A., Hui, C., and McKay, G. Marine residual fuel sorption and desorption kinetics by alkali treated rice husks. *Cellulose*, 21(3):1997–2006, 2014.
- Benito, J. M., Rios, G., Ortea, E., Fernandez, E., Cambiella, A., Pazos, C., and Coca, J. Design and construction of a modular pilot plant for the treatment of oil-containing wastewaters. *Desalination*, 147 (1-3):5–10, 2002.
- Benito, J. M., Cambiella, A., Lobo, A., Gutierrez, G., Coca, J., and Pazos, C. Formulation, characterization and treatment of metalworking oil-in-water emulsions. *Clean Technologies and Environmental Policy*, 12(1):31–41, 2010.
- Bento, M. F., Pereira, H., Cunha, M. A., Moutinho, A. M. C., Van Den Berg, K. J., Boon, J. J., Van Den Brink, O., and Heeren, R. M. A. Fragmentation of suberin and composition of aliphatic monomers released by methanolysis of cork from *Quercus suber* L., analysed by GC-MS, SEC and MALDI-MS. *Holzforschung*, 55(5):487–493, 2001.
- Bernards, M. A. Demystifying suberin. *Canadian Journal of Botany*, 80:227–240, 2002.

- Boehm, H. P. Some aspects of the surface chemistry of carbon blacks and other carbons. *Carbon*, 32(5): 759–769, 1994.
- Boussahel, R., Irinislimane, H., Harik, D., and Moussaoui, K. M. Adsorption, kinetics, and equilibrium studies on removal of 4,4-DDT from aqueous solutions using low-cost adsorbents. *Chemical Engineering Communications*, 196(12):1547–1558, 2009.
- Boyer, M. J. Current pollution control practices in the United States. *Journal of the American Oil Chemists' Society*, 61(2):297–301, 1984.
- Brunauer, S., Emmett, P. H., and Teller, E. Adsorption of gases in multimolecular layers. *Journal of the American Chemistry Society*, 60:309–319, 1938.
- Cabrita, I., Ruiz, B., Mestre, A. S., Fonseca, I. M., Carvalho, A. P., and Ania, C. O. Removal of an analgesic using activated carbons prepared from urban and industrial residues. *Chemical Engineering Journal*, 163(3):249–255, 2010.
- Cañizares, P., Martínez, F., Jiménez, C., Sáez, C., and Rodrigo, M. A. Coagulation and electrocoagulation of oil-in-water emulsions. *Journal of Hazardous Materials*, 151(1):44–51, 2008.
- Cañizares, P., Jiménez, C., Martínez, F., Rodrigo, M. A., and Sáez, C. The pH as a key parameter in the choice between coagulation and electrocoagulation for the treatment of wastewaters. *Journal of Hazardous Materials*, 163(1):158 – 164, 2009.
- Cansado, I. P. P., Mourão, P. A. M., Falcão, A. I., Carrott, M. M. L. Ribeiro, and Carrott, P. J. M. The influence of the activated carbon post-treatment on the phenolic compounds removal. *Fuel Processing Technology*, 103:64–70, 2012.
- Capone, D. L., Skouroumounis, G. K., Barker, D. A., McLean, H. J., Pollnitz, A. P., and Sefton, M. A. Absorption of chloroanisoles from wine by corks and by other materials. *Australian Journal of Grape and Wine Research*, 5(3):91–98, 1999.
- Cardoso, B., Mestre, A. S., Carvalho, A. P., and Pires, J. Activated carbon derived from cork powder waste by KOH activation: Preparation, characterization, and VOCs adsorption. *Industrial & Engineering Chemistry Research*, 47(16):5841–5846, 2008.
- Carrott, P. J. M., Ribeiro Carrott, M. M. L., and Lima, R. P. Preparation of activated carbon “membranes” by physical and chemical activation of cork. *Carbon*, 37(3):515–517, 1999.
- Carrott, P. J. M., Ribeiro Carrott, M. M. L., Mourão, P. A. M., and Lima, R. P. Preparation of activated carbons from cork by physical activation in carbon dioxide. *Adsorption Science & Technology*, 21(7): 669–681, 2003.
- Carrott, P. J. M., Ribeiro Carrott, M. M. L., and Mourão, P. A. M. Pore size control in activated carbons obtained by pyrolysis under different conditions of chemically impregnated cork. *Journal of Analytical and Applied Pyrolysis*, 75(2):120–127, 2006.
- Carvalho, A. P., Cardoso, B., Pires, J., and Carvalho, M. B. Preparation of activated carbons from cork waste by chemical activation with KOH. *Carbon*, 41(14):2873–2876, 2003.

- Carvalho, A. P., Gomes, M., Mestre, A. S., Pires, J., and Carvalho, M. B. Activated carbons from cork waste by chemical activation with K_2CO_3 : Application to adsorption of natural gas components. *Carbon*, 42(3):672–674, 2004.
- Carvalho, A. P., Mestre, A. S., Pires, J., Pinto, M. L., and Rosa, M. E. Granular activated carbons from powdered samples using clays as binders for the adsorption of organic vapours. *Microporous and Mesoporous Materials*, 93(1-3):226–231, 2006.
- Chakrabarty, B., Ghoshal, A. K., and Purkait, M. K. Ultrafiltration of stable oil-in-water emulsion by polysulfone membrane. *Journal of Membrane Science*, 325(1):427 – 437, 2008.
- Chi, F. H. and Cheng, W. P. Use of chitosan as coagulant to treat wastewater from milk processing plant. *Journal of Polymers and the Environment*, 14(4):411–417, 2006.
- Chipasa, K. B. Limits of physicochemical treatment of wastewater in the vegetable oil refining industry. *Polish Journal of Environmental Studies*, 10:141–147, 2001.
- Chubar, N., Carvalho, J. R., and Correia, M. J. N. Cork biomass as biosorbent for Cu(II), Zn(II) and Ni(II). *Colloids and Surfaces A: Physicochemical and Engineering Aspects*, 230(1-3):57–65, 2003.
- Chubar, N., Carvalho, J. R., and Correia, M. J. N. Heavy metals biosorption on cork biomass: effect of the pre-treatment. *Colloids and Surfaces A: Physicochemical and Engineering Aspects*, 238(1-3):51–58, 2004.
- Conde, E., Cadahía, E., Garcia-Vallejo, M. C., and González-Adrados, J. R. Chemical characterization of reproduction cork from Spanish *Quercus suber*. *Journal of Wood Chemistry and Technology*, 18(4):447 – 469, 1998.
- Cordeiro, N., Neto, C. P., Gandini, A., and Belgacem, M. N. Characterization of the cork surface by inverse gas chromatography. *Journal of Colloid and Interface Science*, 174(1):246–249, 1995.
- Corticeira Amorim, S.G.P.S. CORKSORB - sustainable absorbents, 2009. URL <http://www.corksorb.com/>. accessed September 2014.
- Crespo-Alonso, M., Nurchi, V. M., Biesuz, R., Alberti, G., Spano, N., Pilo, M. I., and Sanna, G. Biomass against emerging pollution in wastewater: Ability of cork for the removal of ofloxacin from aqueous solutions at different pH. *Journal of Environmental Chemical Engineering*, 1(4):1199 – 1204, 2013.
- Cristóvão, R. O., Botelho, C. M., Martins, R. J. E., Loureiro, J. M., and Boaventura, R. A. R. Primary treatment optimization of a fish canning wastewater from a Portuguese plant. *Water Resources and Industry*, 6:51–63, 2014.
- Cumbre, F., Lopes, F., and Pereira, H. The effect of water boiling on annual ring width and porosity of cork. *Wood and Fiber Science*, 32(1):125–133, 2000.
- Dalmacija, B., Miskovic, D., Tamas, Z., and Karlovic, E. Tertiary treatment of oil-field brine in a biosorption system with granulated activated carbon. *Water Research*, 30(5):1065–1068, 1996.
- Das, S. K. and Biswas, M. N. Separation of oil-water mixture in tank. *Chemical Engineering Communications*, 190(1):116–127, 2003.

- Dassey, A. J. and Theegala, C. S. Evaluating coagulation pretreatment on poultry processing wastewater for dissolved air flotation. *Journal of Environmental Science and Health, Part A*, 47(13):2069–2076, 2012.
- Decloux, M., Lameloise, M.-L., Brocard, A., Bisson, E., Parmentier, M., and Spiraers, A. Treatment of acidic wastewater arising from the refining of vegetable oil by crossflow microfiltration at very low transmembrane pressure. *Process Biochemistry*, 42(4):693–699, 2007.
- Dincer, A. R., Karakaya, N., Gunes, E., and Gunes, Y. Removal of COD from oil recovery industry wastewater by the advanced oxidation processes (AOP) based on H₂O₂. *Global NEST Journal*, 10(1): 31–38, 2008.
- Domingues, V. *Utilização de um produto natural (cortiça) como adsorvente de pesticidas piretróides em águas*. PhD thesis, University of Porto, 2005.
- Domingues, V., Alves, A., Cabral, M., and Delerue-Matos, C. Sorption behaviour of bifenthrin on cork. *Journal of Chromatography A*, 1069(1):127–132, 2005.
- Domingues, V. F., Priolo, G., Alves, A. C., Cabral, M. F., and Delerue-Matos, C. Adsorption behavior of alpha-cypermethrin on cork and activated carbon. *Journal Of Environmental Science And Health. Part B, Pesticides, Food Contaminants, And Agricultural Wastes*, 42(6):649–654, 2007.
- Dordio, A. V., Gonçalves, P., Texeira, D., Candeias, A. J., Castanheiro, J. E., Pinto, A. P., and Carvalho, A. J. P. Pharmaceuticals sorption behaviour in granulated cork for the selection of a support matrix for a constructed wetlands system. *International Journal of Environmental Analytical Chemistry*, 91(7-8): 615–631, 2011.
- Dubinin, M. M. *Characterization of Porous Solids*. The Society of Chemical Industry, London, 1979.
- Dubinin, M. M. and Stoeckli, H. F. Homogeneous and heterogeneous micropore structures in carbonaceous adsorbents. *Journal of Colloid and Interface Science*, 75(1):34–42, 1980.
- Eckenfelder, W. W. *Industrial Water Pollution Control*. McGraw-Hill, 2000.
- Fernandes, E. M., Correló, V. M., Chagas, J. A. M., Mano, J. F., and Reis, R. L. Cork based composites using polyolefin's as matrix: Morphology and mechanical performance. *Composites Science and Technology*, 70(16):2310–2318, 2010.
- Fialho, C., Lopes, F., and Pereira, H. The effect of cork removal on the radial growth and phenology of young cork oak trees. *Forest Ecology and Management*, 141(3):251–258, 2001.
- Fiol, N. and Villaescusa, I. Determination of sorbent point zero charge: usefulness in sorption studies. *Environmental Chemistry Letters*, 7(1):79–84, 2009.
- Fiol, N., Villaescusa, I., Martínez, M., Miralles, N., Poch, J., and Serarols, J. Biosorption of Cr(VI) using low cost sorbents. *Environmental Chemistry Letters*, 1(2):135–139, 2003.
- Fortes, M. A. and Rosa, M. E. Densidade da cortiça: Factores que a influenciam. *Boletim do Instituto dos Produtos Florestais - Cortiça*, 593:65–68, 1988.
- Fouad, Y. O. Separation of cottonseed oil from oil–water emulsions using electrocoagulation technique. *Alexandria Engineering Journal*, 53(1):199 – 204, 2014.

- Freundlich, H. Ueber die adsorption in loesungen. *Zeitschrift für Physikalische Chemie*, 57:385–470, 1907.
- Geetha Devi, M., Shinoon Al-Hashmi, Z. S., and Chandra Sekhar, G. Treatment of vegetable oil mill effluent using crab shell chitosan as adsorbent. *International Journal of Environmental Science and Technology*, 9(4):713–718, 2012.
- Gil, A. M., Lopes, M. H., Pascoal Neto, C., and Callaghan, P. T. An NMR microscopy study of water absorption in cork. *Journal of Materials Science*, 35(8):1891–1900, 2000.
- Gil, L. Cork powder waste: An overview. *Biomass & Bioenergy*, 13(1-2):59–61, 1997.
- Gil, L. *Cortiça: Produção, tecnologia e aplicação*. INETI, Lisbon, 1998.
- Gil, L. and Cortiço, P. Cork hygroscopic equilibrium moisture content. *European Journal of Wood and Wood Products*, 56(5):355–358, 1998.
- Gil, L., Santos, J., and Florêncio, M. I. Identificação e caracterização de vários tipos de pó obtidos no processamento industrial da cortiça. *Boletim do Instituto dos Produtos Florestais - Cortiça*, 575:255–261, 1986.
- Gök, Ö., Özcan, A. S., and Özcan, A. Adsorption kinetics of naphthalene onto organo-sepiolite from aqueous solutions. *Desalination*, 220(1-3):96–107, 2008.
- Gomes, C. M. C. P. S., Fernandes, A. C., and Almeida, B. J. V. S. The surface tension of cork from contact angle measurements. *Journal of Colloid and Interface Science*, 156(1):195–201, 1993.
- Gonzalez Adrados, J. R. and Calvo Haro, R. M. Variacion de la humedad de equilibrio del corcho en plancha con la humedad relativa. Modelos de regresión no lineal para las isotermas de adsorción. *Investigación Agraria, Sistemas y Recursos Forestales*, 3(2), 1994.
- Hami, M., Al-Hashimi, M. A., and Al-Doori, M. M. Effect of activated carbon on BOD and COD removal in a dissolved air flotation unit treating refinery wastewater. *Desalination*, 216(1-3):116–122, 2007.
- Hanzlík, J., Jehlicka, J., Sebek, O., Weishauptová, Z., and Machovic, V. Multi-component adsorption of Ag(I), Cd(II) and Cu(II) by natural carbonaceous materials. *Water Research*, 38(8):2178–2184, 2004.
- Holloway, P. J. The suberin composition of the cork layers from some ribes species. *Chemistry and Physics of Lipids*, 9(2):171–179, 1972.
- Hosny, A. Y. Separating oil from oil-water emulsions by electroflotation technique. *Separations Technology*, 6(1):9 – 17, 1996.
- Hydro-Flo Technologies, Inc. Oil/water separator theory of operation, 2002. URL <http://www.oil-water-separator.hydroflotech.com/Engineering%20Data/Oil%20Water%20Separator%20Theory%20of%20Operation.htm>. accessed September 2014.
- Ibrahim, S., Ang, H.-M., and Wang, S. Removal of emulsified food and mineral oils from wastewater using surfactant modified barley straw. *Bioresource Technology*, 100(23):5744–5749, 2009.
- Ibrahim, S., Wang, S., and Ang, H. M. Removal of emulsified oil from oily wastewater using agricultural waste barley straw. *Biochemical Engineering Journal*, 49(1):78–83, 2010.

- Inagaki, M., Kawahara, A., Nishi, Y., and Iwashita, N. Heavy oil sorption and recovery by using carbon fiber felts. *Carbon*, 40(9):1487–1492, 2002.
- Iqbal, M. Z. and Abdala, A. A. Oil spill cleanup using graphene. *Environmental Science and Pollution Research*, 20(5):3271–3279, 2013.
- Izquierdo, C. J., Canizares, P., Rodrigo, M. A., Leclerc, J. P., Valentin, G., and Lapicque, F. Effect of the nature of the supporting electrolyte on the treatment of soluble oils by electrocoagulation. *Desalination*, 255(1–3):15 – 20, 2010.
- Ji, F., Li, C., Dong, X., Li, Y., and Wang, D. Separation of oil from oily wastewater by sorption and coalescence technique using ethanol grafted polyacrylonitrile. *Journal of Hazardous Materials*, 164 (2–3):1346 – 1351, 2009.
- Ji, M., Jiang, X., and Wang, F. A mechanistic approach and response surface optimization of the removal of oil and grease from restaurant wastewater by electrocoagulation and electroflotation. *Desalination and Water Treatment*, In Press.
- Johnson, R. F., Manjreker, T. G., and Halligan, J. E. Removal of oil from water surfaces by sorption on unstructured fibers. *Environmental Science & Technology*, 7(5):439–443, 1973.
- Jové, P., Olivella, M. À., and Cano, L. Study of the variability in chemical composition of bark layers of *Quercus suber* L. from different production areas. *BioResources*, 6(2):1806–1815, 2011.
- Kalyanaraman, C., Kanchinadham, S. B. K., Vidya Devi, L., Porselvam, S., and Rao, J. R. Combined advanced oxidation processes and aerobic biological treatment for synthetic fatliquor used in tanneries. *Industrial & Engineering Chemistry Research*, 51(50):16171–16181, 2012.
- Karbowiak, T., Mansfield, A. K., Barrera-García, V. D., and Chassagne, D. Sorption and diffusion properties of volatile phenols into cork. *Food Chemistry*, 122(4):1089–1094, 2010.
- Karhu, M., Leiviskä, T., and Tanskanen, J. Enhanced DAF in breaking up oil-in-water emulsions. *Separation and Purification Technology*, 122:231 – 241, 2014.
- Kota, A. K., Kwon, G., Choi, W., Mabry, J. M., and Tuteja, A. Hygro-responsive membranes for effective oil-water separation. *Nature communications*, 3:1025, 2012.
- Krika, F., Azzouz, N., and Ncibi, M. C. Adsorptive removal of cadmium from aqueous solution by cork biomass: Equilibrium, dynamic and thermodynamic studies. *Arabian Journal of Chemistry*, 2011.
- Kundu, P. and Mishra, I. M. Removal of emulsified oil from oily wastewater (oil-in-water emulsion) using packed bed of polymeric resin beads. *Separation and Purification Technology*, 118:519 – 529, 2013.
- Kwon, S.-H. and Cho, D. A comparative, kinetic study on cork and activated carbon biofilters for VOC degradation. *Journal of Industrial and Engineering Chemistry*, 15(1):129–135, 2009.
- Langmuir, I. The adsorption of gases on plane surfaces of glass, mica and platinum. *Journal of the American Chemical Society*, 40(9):1361–1403, 1918.
- Le, T. V., Imai, T., Higuchi, T., Yamamoto, K., Sekine, M., Doi, R., Vo, H. T., and Wei, J. Performance of tiny microbubbles enhanced with “normal cyclone bubbles” in separation of fine oil-in-water emulsions. *Chemical Engineering Science*, 94:1 – 6, 2013.

- Lequin, S., Karbowski, T., Brachais, L., Chassagne, D., and Bellat, J. P. Adsorption equilibria of sulfur dioxide on cork. *American Journal of Enology and Viticulture*, 60(2):138–144, 2009.
- Lequin, S., Chassagne, D., Karbowski, T., Gougeon, R., Brachais, L., and Bellat, J.-P. Adsorption equilibria of water vapor on cork. *Journal of Agricultural and Food Chemistry*, 58(6):3438–3445, 2010.
- Li, J. and Gu, Y. Coalescence of oil-in-water emulsions in fibrous and granular beds. *Separation and Purification Technology*, 42(1):1 – 13, 2005.
- Li, S., Wu, X., Cui, L., Zhang, Y., Luo, X., Zhang, Y., and Dai, Z. Utilization of modification polyester non-woven as an affordable sorbent for oil removal. *Desalination and Water Treatment*, In Press.
- Lopes, C. B., Oliveira, J. R., Rocha, L. S., Tavares, D. S., Silva, C. M., Silva, S. P., Hartog, N., Duarte, A. C., and Pereira, E. Cork stoppers as an effective sorbent for water treatment: the removal of mercury at environmentally relevant concentrations and conditions. *Environmental Science and Pollution Research*, 21(3):2108–2121, 2014.
- Lopes, M. H., Rutledge, D., Gil, A. M., Barros, A. S., Delgadillo, I., and Neto, C. P. Variability of cork from Portuguese *Quercus suber* studied by solid-state ¹³C-NMR and FTIR spectroscopies. *Biopolymers*, 62(5):268–277, 2001.
- López-Mesas, M., Navarrete, E. R., Carrillo, F., and Palet, C. Bioseparation of Pb(II) and Cd(II) from aqueous solution using cork waste biomass. Modeling and optimization of the parameters of the biosorption step. *Chemical Engineering Journal*, 174(1):9–17, 2011.
- Ma, S., Kang, Y., and Cui, S. Oil and water separation using a glass microfiber coalescing bed. *Journal of Dispersion Science and Technology*, 35(1):103–110, 2014.
- MacAdam, J., Ozgencil, H., Autin, O., Pidou, M., Temple, C., Parsons, S., and Jefferson, B. Incorporating biodegradation and advanced oxidation processes in the treatment of spent metalworking fluids. *Environmental Technology*, 33(24):2741–2750, 2012.
- Machado, R., Carvalho, J. R., and Neiva Correia, M. J. Removal of trivalent chromium(III) from solution by biosorption in cork powder. *Journal of Chemical Technology & Biotechnology*, 77(12):1340–1348, 2002.
- Maiti, S., Mishra, I. M., Bhattacharya, S. D., and Joshi, J. K. Removal of oil from oil-in-water emulsion using a packed bed of commercial resin. *Colloids and Surfaces A: Physicochemical and Engineering Aspects*, 389(1–3):291 – 298, 2011.
- Mansour, L. B. and Chalbi, S. Removal of oil from oil/water emulsions using electroflotation process. *Journal of Applied Electrochemistry*, 36(5):577–581, 2006.
- Masoudnia, K., Raisi, A., Aroujalian, A., and Fathizadeh, M. A hybrid microfiltration/ultrafiltration membrane process for treatment of oily wastewater. *Desalination and Water Treatment*, In Press.
- McDonough, W. and Braungart, M. *Cradle to Cradle: Remaking the Way We Make Things*. Farrar, Straus and Giroux, 2010.
- Mestre, A. S., Pires, J., Nogueira, J. M. F., and Carvalho, A. P. Activated carbons for the adsorption of ibuprofen. *Carbon*, 45(10):1979–1988, 2007.

- Mestre, A. S., Pires, J., Nogueira, J. M. F., Parra, J. B., Carvalho, A. P., and Ania, C. O. Waste-derived activated carbons for removal of ibuprofen from solution: Role of surface chemistry and pore structure. *Bioresource Technology*, 100(5):1720–1726, 2009.
- Mestre, A. S., Pinto, M. L., Pires, J., Nogueira, J. M. F., and Carvalho, A. P. Effect of solution pH on the removal of clofibric acid by cork-based activated carbons. *Carbon*, 48(4):972–980, 2010.
- Mestre, A. S., Pires, R. A., Aroso, I., Fernandes, E. M., Pinto, M. L., Reis, R. L., Andrade, M. A., Pires, J., Silva, S. P., and Carvalho, A. P. Activated carbons prepared from industrial pre-treated cork: Sustainable adsorbents for pharmaceutical compounds removal. *Chemical Engineering Journal*, 253:408 – 417, 2014.
- Meysami, B. and Kasaeian, A. B. Use of coagulants in treatment of olive oil wastewater model solutions by induced air flotation. *Bioresource Technology*, 96(3):303 – 307, 2005.
- Michael, I., Panagi, A., Ioannou, L. A., Frontistis, Z., and Fatta-Kassinos, D. Utilizing solar energy for the purification of olive mill wastewater using a pilot-scale photocatalytic reactor after coagulation-flocculation. *Water Research*, 60:28 – 40, 2014.
- Moazed, H. and Viraraghavan, T. Use of organo-clay/anthracite mixture in the separation of oil from oily waters. *Energy Sources*, 27(1-2):101–112, 2005.
- Mohammadi, T. and Esmaelifar, A. Wastewater treatment using ultrafiltration at a vegetable oil factory. *Desalination*, 166:329 – 337, 2004.
- Mondal, S. and Wickramasinghe, S. R. Produced water treatment by nanofiltration and reverse osmosis membranes. *Journal of Membrane Science*, 322(1):162 – 170, 2008.
- Mostefa, N. M. and Tir, M. Coupling flocculation with electroflotation for waste oil/water emulsion treatment. Optimization of the operating conditions. *Desalination*, 161(2):115 – 121, 2004.
- Mota, D., Marques, P., Pereira, C., Gil, L., and Rosa, M. F. Lead bioremoval by cork residues as biosorbent. In *ECOWOOD 2006 - 2nd International Conference on Environmentally-Compatible Forest Products*, pages 251–264. Fernando Pessoa University, Porto, Portugal, September 20-22 2006.
- Mourão, P. A. M., Carrott, P. J. M., and Ribeiro Carrott, M. M. L. Application of different equations to adsorption isotherms of phenolic compounds on activated carbons prepared from cork. *Carbon*, 44(12): 2422–2429, 2006.
- Mourão, P. A. M., Cansado, I. P. P., Carrott, P. J. M., and Ribeiro Carrott, M. M. L. Designing activated carbons from natural and synthetic raw materials for pollutants adsorption. *Materials Science Forum*, 636-637:1404–1409, 2010.
- Mowla, D., Karimi, G., and Salehi, K. Modeling of the adsorption breakthrough behaviors of oil from salty waters in a fixed bed of commercial organoclay/sand mixture. *Chemical Engineering Journal*, 218:116 – 125, 2013.
- Multon, L. M. and Viraraghavan, T. Removal of oil from produced water by coalescence/filtration in a granular bed. *Environmental Technology*, 27(5):529–544, 2006.

- Mysore, D., Viraraghavan, T., and Jin, Y.-C. Treatment of oily waters using vermiculite. *Water Research*, 39(12):2643 – 2653, 2005.
- Namasivayam, C. and Sureshkumar, M. V. Removal of chromium(VI) from water and wastewater using surfactant modified coconut coir pith as a biosorbent. *Bioresource Technology*, 99(7):2218–2225, 2008.
- Neng, N. R., Mestre, A. S., Carvalho, A. P., and Nogueira, J. M. F. Cork-based activated carbons as supported adsorbent materials for trace level analysis of ibuprofen and clofibrac acid in environmental and biological matrices. *Journal of Chromatography A*, 1218(37):6263–6270, 2011.
- Neto, C. P., Rocha, J., Gil, A., Cordeiro, N., Esculcas, A. P., Rocha, S., Delgadillo, I., De Jesus, J. D. P., and Correia, A. J. F. ¹³C solid-state nuclear magnetic resonance and Fourier transform infrared studies of the thermal decomposition of cork. *Solid State Nuclear Magnetic Resonance*, 4(3):143–151, 1995.
- Ngamlerdpokin, K., Kumjadpai, S., Chatanon, P., Tungmanee, U., Chuenchuanom, S., Jaruwat, P., Lertsathitphongs, P., and Hunsom, M. Remediation of biodiesel wastewater by chemical- and electro-coagulation: A comparative study. *Journal of Environmental Management*, 92(10):2454 – 2460, 2011.
- Ngarmkam, W., Sirisathitkul, C., and Phalakornkule, C. Magnetic composite prepared from palm shell-based carbon and application for recovery of residual oil from POME. *Journal of Environmental Management*, 92(3):472–479, March 2011.
- Nurchi, V. M., Crespo-Alonso, M., Biesuz, R., Alberti, G., Pilo, M. I., Spano, N., and Sanna, G. Sorption of chrysoidine by row cork and cork entrapped in calcium alginate beads. *Arabian Journal of Chemistry*, 7(1):133 – 138, 2014.
- O'Brien, R. D. *Fats and Oils: Formulating and Processing for Applications*. Taylor & Francis, second edition, 2003.
- Ochando-Pulido, J. M. and Stoller, M. Boundary flux optimization of a nanofiltration membrane module used for the treatment of olive mill wastewater from a two-phase extraction process. *Separation and Purification Technology*, 130:124 – 131, 2014.
- Olivella, M. À., Jové, P., and Oliveras, A. The use of cork waste as a biosorbent for persistent organic pollutants—study of adsorption/desorption of polycyclic aromatic hydrocarbons. *Journal of Environmental Science and Health, Part A*, 46(8):824–832, 2011a.
- Olivella, M. À., Jové, P., Sen, A., Pereira, H., Villaescusa, I., and Fiol, N. Sorption performance of *Quercus cerris* cork with polycyclic aromatic hydrocarbons and toxicity testing. *BioResources*, 6(3):3363–3375, 2011b.
- Olivella, M. À., Fiol, N., Torre, F. de la, Poch, J., and Villaescusa, I. A mechanistic approach to methylene blue sorption on two vegetable wastes: Cork bark and grape stalks. *BioResources*, 7(3):3340–3354, 2012.
- Olivella, M. À., Jové, P., Bianchi, A., Bazzicalupi, C., and Cano, L. An integrated approach to understanding the sorption mechanism of phenanthrene by cork. *Chemosphere*, 90(6):1939 – 1944, 2013.
- Ozyonar, F. and Karagozoglu, B. Investigation of technical and economic analysis of electrocoagulation process for the treatment of great and small cattle slaughterhouse wastewater. *Desalination and Water Treatment*, 52(1-3):74–87, 2014.

- Pandey, R. A., Sanyal, P. B., Chattopadhyay, N., and Kaul, S. N. Treatment and reuse of wastes of a vegetable oil refinery. *Resources, Conservation and Recycling*, 37(2):101–117, 2003.
- Patterson, J. W. *Industrial Wastewater Treatment Technology*. Butterworth Publishers, 1985.
- Peng, H. and Tremblay, A. Y. Membrane regeneration and filtration modeling in treating oily wastewaters. *Journal of Membrane Science*, 324(1-2):59–66, 2008.
- Pereira, H. Cosntituição química da cortiça - estado actual dos conhecimentos. *Cortiça*, 483:259–264, 1979.
- Pereira, H. Chemical composition of cork from *Quercus suber* L. *Anais do Instituto Superior de Agronomia*, Vol. XL:9–15, 1982.
- Pereira, H. Composição química da cortiça virgem e da cortiça de reprodução amadia do *Quercus suber* L. *Boletim do Instituto dos Produtos Florestais - Cortiça*, 550:237–240, 1984.
- Pereira, H. Chemical composition and variability of cork from *Quercus suber* L. *Wood Science and Technology*, 22(3):211–218, 1988.
- Pereira, H. Variability of the chemical composition of cork. *BioResources*, 8(2), 2013.
- Pereira, H. and Marques, A. V. The effect of chemical treatments on the cellular structure of cork. *IAWA Bulletin*, 9(4):337–345, 1988.
- Phalakornkule, C., Mangmeemak, J., Intrachod, K., and Nuntakumjorn, B. Pretreatment of palm oil mill effluent by electrocoagulation and coagulation. *ScienceAsia*, 36:142 – 149, 2010.
- Pitakpoolsil, W. and Hunsom, M. Treatment of biodiesel wastewater by adsorption with commercial chitosan flakes: Parameter optimization and process kinetics. *Journal of Environmental Management*, 133: 284–292, 2014.
- Prades, C., Garcia-Olmo, J., Romero-Prieto, T., De Ceca, J. L. G., and Lopez-Luque, R. Methodology for cork plank characterization (*Quercus suber* L.) by near-infrared spectroscopy and image analysis. *Measurement Science & Technology*, 21(6):65602–65602, 2010.
- Psareva, T. S., Zakutevskyy, O. I., Chubar, N. I., Strelko, V. V., Shaposhnikova, T. O., Carvalho, J. R., and Correia, M. J. N. Uranium sorption on cork biomass. *Colloids and Surfaces A: Physicochemical and Engineering Aspects*, 252(2-3):231–236, 2005.
- Quevedo, J. A., Patel, G., and Pfeffer, R. Removal of oil from water by inverse fluidization of aerogels. *Industrial & Engineering Chemistry Research*, 48(1):191–201, 2009.
- Rajaković-Ognjanović, V., Aleksić, G., and Rajaković, Lj. Governing factors for motor oil removal from water with different sorption materials. *Journal of Hazardous Materials*, 154(1–3):558 – 563, 2008.
- Ran, J., Liu, J., Zhang, C., Wang, D., and Li, X. Experimental investigation and modeling of flotation column for treatment of oily wastewater. *International Journal of Mining Science and Technology*, 23 (5):665 – 668, 2013.
- Redlich, O. and Peterson, D. L. A useful adsorption isotherm. *The Journal of Physical Chemistry*, 63(6): 1024–1024, 1959.

- Rhee, C. H., Martyn, P. C., and Kremer, J. G. Removal of oil and grease in oil processing wastewater. Technical report, Sanitation District of Los Angeles County, 1989.
- Ribeiro, T. H., Rubio, J., and Smith, R. W. A dried hydrophobic aquaphyte as an oil filter for oil/water emulsions. *Spill Science & Technology Bulletin*, 8(5–6):483–489, 2003.
- Rives, J., Fernandez-Rodriguez, I., Gabarrell, X., and Rieradevall, J. Environmental analysis of cork granulate production in Catalonia – Northern Spain. *Resources, Conservation and Recycling*, 58:132–142, 2012.
- Roques, H. and Aurelle, Y. Oil-water separations oil recovery and oily wastewater treatment. In Turkman, Aysen and Uslu, Orhan, editors, *New Developments in Industrial Wastewater Treatment*, volume 191 of *NATO ASI Series*, pages 155–174. Springer Netherlands, 1991.
- Rosa, M. E. and Fortes, M. A. Temperature-induced alterations of the structure and mechanical properties of cork. *Materials Science and Engineering*, 100:69–78, 1988.
- Salehi, K., Mowla, D., and Karimi, G. Comparison between long- and short-chain organoclays for oil removal from salty waters. *Journal of Dispersion Science and Technology*, 34(12):1790–1796, 2013.
- Sangal, V. K., Mishra, I. M., and Kushwaha, J. P. Electrocoagulation of soluble oil wastewater: Parametric and kinetic study. *Separation Science and Technology*, 48(7):1062–1072, 2013.
- Santander, M., Rodrigues, R. T., and Rubio, J. Modified jet flotation in oil (petroleum) emulsion/water separations. *Colloids and Surfaces A: Physicochemical and Engineering Aspects*, 375(1–3):237 – 244, 2011.
- Santi, C. A., Cortes, S., D’Acqui, L. P., Sparvoli, E., and Pushparaj, B. Reduction of organic pollutants in olive mill wastewater by using different mineral substrates as adsorbents. *Bioresource Technology*, 99(6):1945–1951, 2008.
- Santo, C. E., Vilar, V. J. P., Botelho, C. M. S., Bhatnagar, A., Kumar, E., and Boaventura, R. A. R. Optimization of coagulation–flocculation and flotation parameters for the treatment of a petroleum refinery effluent from a Portuguese plant. *Chemical Engineering Journal*, 183:117 – 123, 2012.
- Sećerov Sokolović, R. M., Govedarica, D. D., and Sokolović, D. S. Selection of filter media for steady-state bed coalescers. *Industrial & Engineering Chemistry Research*, 53(6):2484–2490, 2014.
- Sen, A., Olivella, A., Fiol, N., Miranda, I., Villaescusa, I., and Pereira, H. Removal of chromium(VI) in aqueous environments using cork and heat-treated cork samples from *Quercus cerris* and *Quercus suber*. *BioResources*, 7(4):4843–4857, 2012.
- Sfaksi, Z., Azzouz, N., and Abdelwahab, A. Removal of Cr(VI) from water by cork waste. *Arabian Journal of Chemistry*, 7(1):37 – 42, 2014.
- Sharghi, E. A., Bonakdarpour, B., Roustazade, P., Amoozegar, M. A., and Rabbani, A. R. The biological treatment of high salinity synthetic oilfield produced water in a submerged membrane bioreactor using a halophilic bacterial consortium. *Journal of Chemical Technology & Biotechnology*, 88(11):2016–2026, 2013.

- Silva, S. P., Sabino, M. A., Fernandes, E. M., Correló, V. M., Boesel, L. F., and Reis, R. L. Cork: properties, capabilities and applications. *International Materials Reviews*, 50(6):345–365, 2005.
- Souza, B. M., Cerqueira, A. C., Sant’Anna, G. L., and Dezotti, M. Oil-refinery wastewater treatment aiming reuse by advanced oxidation processes (AOPs) combined with biological activated carbon (BAC). *Ozone: Science & Engineering*, 33(5):403–409, 2011.
- Srinivasan, A. and Viraraghavan, T. Removal of oil by walnut shell media. *Bioresource Technology*, 99(17):8217–8220, 2008.
- Srinivasan, A. and Viraraghavan, T. Oil removal from water using biomaterials. *Bioresource Technology*, 101(17):6594–6600, 2010.
- Srinivasan, A. and Viraraghavan, T. Oil removal in a biosorption column using immobilized *M. rouxii* biomass. *Desalination and Water Treatment*, 52(16-18):3085–3095, 2014.
- Stenstrom, M. K., Silverman, G. S., and Bursztynsky, T. A. Oil and grease in urban stormwaters. *Journal of Environmental Engineering*, 110(1):58–72, 1984.
- Suzuki, Y. and Maruyama, T. Removal of emulsified oil from water by coagulation and foam separation. *Separation Science and Technology*, 40(16):3407–3418, 2005.
- Taha, M. R. and Ibrahim, A. H. COD removal from anaerobically treated palm oil mill effluent (AT-POME) via aerated heterogeneous Fenton process: Optimization study. *Journal of Water Process Engineering*, 1:8 – 16, 2014.
- Tansel, B. and Pascual, B. Removal of emulsified fuel oils from brackish and pond water by dissolved air flotation with and without polyelectrolyte use: Pilot-scale investigation for estuarine and near shore applications. *Chemosphere*, 85(7):1182 – 1186, 2011.
- Tansel, B. and Regula, J. Coagulation enhanced centrifugation for treatment of petroleum hydrocarbon contaminated waters. *Journal of Environmental Science and Health, Part A*, 35(9):1557–1575, 2000.
- Tezcan Ün, Ü., Uğur, S., Koparal, A.S., and Ögütveren, Ü. B. Electrocoagulation of olive mill wastewaters. *Separation and Purification Technology*, 52(1):136 – 141, 2006.
- Tezcan Ün, U., Koparal, A. S., and Bakir Ogutveren, U. Electrocoagulation of vegetable oil refinery wastewater using aluminum electrodes. *Journal of Environmental Management*, 90(1):428–433, 2009.
- Tong, K., Zhang, Y., Liu, G., Ye, Z., and Chu, P. K. Treatment of heavy oil wastewater by a conventional activated sludge process coupled with an immobilized biological filter. *International Biodeterioration & Biodegradation*, 84:65 – 71, 2013.
- Toyoda, M. and Inagaki, M. Heavy oil sorption using exfoliated graphite: New application of exfoliated graphite to protect heavy oil pollution. *Carbon*, 38(2):199 – 210, 2000.
- Valenzuela Calahorra, C., Bernalte García, A., Preciado Barrera, C., Bernalte García, M. J., and Gómez Corzo, M. Cation exchangers prepared from cork wastes. *Bioresource Technology*, 44:229–233, 1993.
- Villaescusa, I., Martínez, M., and Miralles, N. Heavy metal uptake from aqueous solution by cork and yohimbe bark wastes. *Journal of Chemical Technology & Biotechnology*, 75(9):812–816, 2000.

- Villaescusa, I., Fiol, N., Cristiani, F., Floris, C., Lai, S., and Nurchi, V. M. Copper(II) and nickel(II) uptake from aqueous solutions by cork wastes: a NMR and potentiometric study. *Polyhedron*, 21(14-15):1363–1367, 2002.
- Villaescusa, I., Fiol, N., Poch, J., Bianchi, A., and Bazzicalupi, C. Mechanism of paracetamol removal by vegetable wastes: The contribution of π - π interactions, hydrogen bonding and hydrophobic effect. *Desalination*, 270(1-3):135–142, 2011.
- Wahi, R., Chuah, L. A., Choong, T. S. Y., Ngaini, Z., and Nourouzi, M. M. Oil removal from aqueous state by natural fibrous sorbent: An overview. *Separation and Purification Technology*, 113:51–63, 2013.
- Wang, D., Silbaugh, T., Pfeffer, R., and Lin, Y. S. Removal of emulsified oil from water by inverse fluidization of hydrophobic aerogels. *Powder Technology*, 203(2):298–309, 2010.
- Wang, D., McLaughlin, E., Pfeffer, R., and Lin, Y. S. Adsorption of oils from pure liquid and oil–water emulsion on hydrophobic silica aerogels. *Separation and Purification Technology*, 99:28 – 35, 2012.
- Welz, M. L. S., Baloyi, N., and Deglon, D. A. Oil removal from industrial wastewater using flotation in a mechanically agitated flotation cell. *Water SA*, 33(4):453–458, 2007.
- Xi, Y., Frost, R. L., and He, H. Modification of the surfaces of Wyoming montmorillonite by the cationic surfactants alkyl trimethyl, dialkyl dimethyl, and trialkyl methyl ammonium bromides. *Journal of Colloid and Interface Science*, 305(1):150–158, 2007.
- Xu, X. and Zhu, X. Treatment of refractory oily wastewater by electro-coagulation process. *Chemosphere*, 56(10):889 – 894, 2004.
- Yang, C.-L. Electrochemical coagulation for oily water demulsification. *Separation and Purification Technology*, 54(3):388–395, 2007.
- Yang, X., Guo, M., Wu, Y., Wu, Q., and Zhang, R. Removal of emulsified oil from water by fruiting bodies of macro-fungus (*Auricularia polytricha*). *PLoS ONE*, 9(4):e95162, 2014.
- Yu, L., Han, M., and He, F. A review of treating oily wastewater. *Arabian Journal of Chemistry*, 2013.
- Zhao, X., Wang, Y., Ye, Z., Borthwick, A. G. L., and Ni, J. Oil field wastewater treatment in Biological Aerated Filter by immobilized microorganisms. *Process Biochemistry*, 41(7):1475 – 1483, 2006.
- Zhou, Y.-B., Tang, X.-Y., Hu, X.-M., Fritschi, S., and Lu, J. Emulsified oily wastewater treatment using a hybrid-modified resin and activated carbon system. *Separation and Purification Technology*, 63(2): 400–406, 2008.
- Zhu, X., Tu, W., Wee, K.-H., and Bai, R. Effective and low fouling oil/water separation by a novel hollow fiber membrane with both hydrophilic and oleophobic surface properties. *Journal of Membrane Science*, 466:36 – 44, 2014.
- Zouboulis, A. I. and Avranas, A. Treatment of oil-in-water emulsions by coagulation and dissolved-air flotation. *Colloids and Surfaces A: Physicochemical and Engineering Aspects*, 172(1–3):153–161, 2000.

Chapter 3

Textural and surface characterisation of cork-based sorbents¹

3.1 Introduction

In the previous chapter, namely in section 2.1.3, it has been shown that cork powder and granulates present high potential both as biosorbents and as activated carbon precursors. In this chapter, a comparative study is carried out between several types of cork granulates as biosorbents and cork-based activated carbons produced by phosphoric acid activation.

Surface modifications of cork biosorbents and activated carbons were also studied in order to improve hydrophobicity. As it has been mentioned in section 2.2.4.1, some materials' affinity for oil has been successfully enhanced by treatment with quaternary ammonium surfactants, for instance organoclays (Alther, 1995) and barley straw (Ibrahim et al., 2009, 2010). With the same objective, cork granulates were modified with hexadecyltrimethylammonium (HDTMA) bromide in this study. As far as activated carbons are concerned, Gonçalves et al. (2010) have reported an improvement in hydrophobicity by a second pyrolysis under propene, which leads to inorganic carbon deposition and decrease of affinity for polar liquids, and this procedure has here been applied to cork-based activated carbons.

Textural and surface characterisation of the materials were performed using techniques such as elemental analysis, nitrogen adsorption, TPD, infrared analysis (FTIR), immersion calorimetry and potentiometric titration. Finally, the sorption capacity of these materials was evaluated in the removal of sunflower oil emulsified in water.

¹This chapter is based on the paper: Pintor, A. M. A., Silvestre-Albero, A. M., Ferreira, C. I. A., Pereira, J. P. C., Vilar, V. J. P., Botelho, C. M. S., Rodríguez-Reinoso, F., Boaventura, R. A. R. Textural and surface characterization of cork-based sorbents for the removal of oil from water. *Industrial & Engineering Chemistry Research*, 52(46):16427–16435, 2013.

3.2 Experimental

3.2.1 Biosorbents preparation

The starting material, raw cork byproduct, was provided by Corticeira Amorim, SGPS (Portugal). Two types of cork granulates were used in this study: low-density cork granulate, from rejects of cork plank and stoppers' cutting and polishing operations, and regranulated cork granulate (RCG), a byproduct of cork agglomerate produced inside a closed heating chamber at approximately 380 °C with injection of steam. The former was supplied in three different particle size classes: fine cork granulate (FCG) (0.2-0.3 mm), intermediate cork granulate (ICG) (0.5-0.6 mm), and coarse cork granulate (CCG) (0.8-1.0 mm); RCG had particle size between 1.0-2.0 mm.

The four categories (FCG, ICG, CCG, RCG) of cork granulates were washed with distilled water to remove impurities and water extractables, such as phenolic acids and polyphenols (Conde et al., 1998). Washing was carried out in 2 h cycles, under mechanical stirring between 300 and 500 rpm and at a temperature of 60 °C, until there was no significant release of organic substances (i.e. the value of dissolved organic carbon in the wash water was below 10 mg L⁻¹). The cork granules were subsequently dried overnight in an oven at 100 °C. Cork samples after washing with water are identified with the prefix W (washed fine cork granulate (W-FCG), washed intermediate cork granulate (W-ICG), washed coarse cork granulate (W-CCG) and washed regranulated cork granulate (W-RCG)).

Washed cork granulates were subsequently treated with the cationic surfactant HDTMA bromide (Acrós Organics, > 99% purity). Washed cork granules (W-FCG, W-CCG, W-RCG) were soaked in 0.5 g L⁻¹ HDTMA bromide solution for 24 h, under mechanical stirring (300-500 rpm), at room temperature. After separation, the cork granulates were rinsed with distilled water several times and dried overnight in an oven at 60 °C. Surfactant-treated cork is referred to by using the prefix S (surfactant-treated fine cork granulate (S-FCG), surfactant-treated coarse cork granulate (S-CCG), surfactant-treated regranulated cork granulate (S-RCG)).

3.2.2 Activated carbon production

For the production of activated carbons, original cork granulates CCG and RCG were impregnated with phosphoric acid solution in two different mass of phosphorus/mass of precursor ratios (X_P), 0.11 and 0.25, during 2 h at 85 °C. The impregnated biomass was heated to dryness in an oven and then carbonised in a horizontal tubular furnace under N₂ flow (100 mL min⁻¹). The heating rate was 2 °C min⁻¹ and the maximum temperature was 450 °C and kept for 120 min. After cooling in N₂ flow, the pyrolysed samples were washed with distilled water until neutral pH. Finally, they were dried overnight in an oven at 85 °C and stored in an airtight container. Throughout the paper, these activated carbons are denominated according to phosphorus ratio and precursor (activated carbon produced from coarse cork granulate by phosphoric acid activation with an X_P ratio of 0.11 (0.11-CCG), activated carbon produced from regranulated cork granulate by phosphoric acid activation with an X_P ratio of 0.11 (0.11-RCG), activated carbon produced from coarse cork

granulate by phosphoric acid activation with an X_P ratio of 0.25 (0.25-CCG), activated carbon produced from regranulated cork granulate by phosphoric acid activation with an X_P ratio of 0.25 (0.25-RCG)).

Raw cork granulate CCG was submitted to a simple carbonisation in N_2 flow with the same heating program as described above, producing carbonised coarse cork granulate (0-CCG). This sample was then impregnated with phosphoric acid solution at a X_P of 0.25. Pyrolysis under N_2 flow was carried out in the same conditions as before. The cooled sample was washed with distilled water until neutral pH, oven dried overnight and denominated as activated carbon produced from carbonised coarse cork granulate by phosphoric acid activation with an X_P ratio of 0.25 (0.25-0-CCG).

Based on the methodology developed by [Gonçalves et al. \(2010\)](#), a second pyrolysis of the activated carbons, under propene atmosphere, was carried out on two of the cork-based activated carbons developed in this study (0.25-CCG and 0.25-RCG). The carbonisation was done in an horizontal furnace at a flow rate of 100 mL min^{-1} . Heating rate was $5 \text{ }^\circ\text{C min}^{-1}$ until $350 \text{ }^\circ\text{C}$ and maximum temperature was kept for 30 min. The samples were cooled in propene atmosphere and denominated as activated carbon pyrolysed with propene, previously produced from coarse cork granulate by phosphoric acid activation with an X_P ratio of 0.25 (P-0.25-CCG) and activated carbon pyrolysed with propene, previously produced from regranulated cork granulate by phosphoric acid activation with an X_P ratio of 0.25 (P-0.25-RCG).

3.2.3 Characterisation of materials

Bulk density was determined according to Standard Test ASTM D 2854-89. Structural density was determined by helium pycnometry in a home-made apparatus. Total ash content determination was done according to ASTM D-2866-83. Elemental analysis (carbon, nitrogen, hydrogen, sulphur) was carried out in an Element microanalyzer Thermo Finnigan Flash 1112 equipment. Isotherms of liquid nitrogen (Air Liquide) at $-196 \text{ }^\circ\text{C}$ were performed in a home-made fully automated equipment designed and constructed by the Advanced Materials group (LMA), now commercialized as N2G-sorb-6 (Gas to Materials Technologies; www.g2mtech.com). Prior to isotherm acquisition, samples were outgassed under vacuum at $100 \text{ }^\circ\text{C}$ (for biosorbents) or $250 \text{ }^\circ\text{C}$ (for activated carbons). The N_2 isotherms were analysed using the BET equation ([Brunauer et al., 1938](#)), to calculate specific surface areas (in the range $0.05 < p/p_0 < 0.20$) and total pore volume (at $p/p_0 = 0.99$) ([Marsh and Rodriguez-Reinoso, 2006](#)), and the DR equation ([Dubinin, 1979](#)), to calculate micropore volume.

TPD was carried out in a U-shaped tubular microreactor placed inside an electrical furnace. 100 mg of sample were heated under helium flow (50 mL min^{-1}) at a rate of $10 \text{ }^\circ\text{C min}^{-1}$ up to $1000 \text{ }^\circ\text{C}$. A mass spectrometer (Omnistar Balzer MSC200) was used to monitor the H_2O , CO_2 and CO evolved. The CO and CO_2 spectra were integrated to obtain the values of the total amounts of CO and CO_2 groups.

The enthalpy of immersion of cork granulates and cork-based activated carbons in water and

methanol was determined in a Tian-Calvet immersion calorimeter (Setaram CD80), whose experimental system has been described elsewhere (Silvestre-Albero et al., 2001). The samples were previously outgassed under vacuum at 100 °C (for biosorbents) or 250 °C (for activated carbons) during 4 h.

Infrared spectra of the samples were obtained in a FTIR Spectrophotometer (IRAffinity-1, Shimadzu) equipped with an analysis module for solids (PIKE EasiDiff, PIKE Technologies). Each run was comprised of 30 scans, with a resolution of 4 cm⁻¹, in the range of wavenumbers from 400 to 4000 cm⁻¹.

3.2.4 Potentiometric titration

For potentiometric titration, 150 mg of biosorbent (ICG, W-ICG, RCG) was added to each reaction tube with 45 mL of electrolyte solution (0.1 M KNO₃) and placed in a rotating shaker (VWR) at a fixed velocity of 20 rpm for 2 h. After this period, a known amount of 0.1 M NaOH or HCl was added and the tubes were kept in the shaker for another 24 h, after which the pH was measured (Metrohm 6.0255.100 combined pH glass electrode). A range of pH approximately from 2.5 to 11.5 was covered.

A blank titration was performed in the absence of biosorbent to determine the reference pH titration curve and the experimental surface charge. N₂ was bubbled for 90 s at the beginning of assays corresponding to the basic branch of the titration, to avoid interference of dissolved carbonates.

3.2.5 Sorption tests

Sorption tests were carried out in batch mode by contacting approximately 22.5 mg of sorbent with 45 mL of a sunflower oil-in-water emulsion in a rotating shaker at 20 rpm. Sorbents selected for study were ICG, W-ICG, RCG, S-RCG, 0.25-CCG, 0.25-RCG, P-0.25-CCG and P-0.25-RCG. Experiments were carried out in a thermostatic cabinet at 25 °C during 24 h, a time predicted to reach equilibrium based on examined literature and experimental exploration. The emulsion was produced by adding sunflower oil to water in a proportion of approximately 200 mg L⁻¹ and agitating at 8800 rpm (UltraTurrax MICCRA D-15, ART) during three 10-min cycles alternated with 10-min breaks. It had a pH of approximately 7.2.

The initial and final concentrations of oil in water were determined using Standard Methods (2005) for the determination of O&G in water, namely the partition-infrared method (5520-C), with tetrachloroethylene (PCE) as the extraction solvent and sunflower oil as the reference standard. The infrared absorption in the C-H band was read in the extracts using a FTIR spectrophotometer (IRAffinity-1, Shimadzu), on the range 2700-3200 cm⁻¹ (30 scans, resolution 2.0). The limit of detection was of 1.5 mg L⁻¹. The estimation of uncertainty in the analytical method is presented in Appendix A.

3.3 Results and discussion

3.3.1 Physical and chemical characterisation

Scanning electron microscopy (SEM) images of cork granules (ICG, W-ICG, S-CCG) show that the structure of cork materials is not affected by granulometry (Figure 3.1). The micrographs show an amplification of the cork cells in honeycomb structure which constitute the external macropores. Pre-washing of cork is an important step since it removes the pores' small internal impurities (Figures 3.1a and 3.1b). Regranulated cork (Figure 3.1d), while resembling the raw cork structure, is slightly more compact, reflecting the thermal treatment. The rise in temperature and pressure (up to ≈ 2 bar) results in compression, and lignin helps the particles bond together to agglomerate.

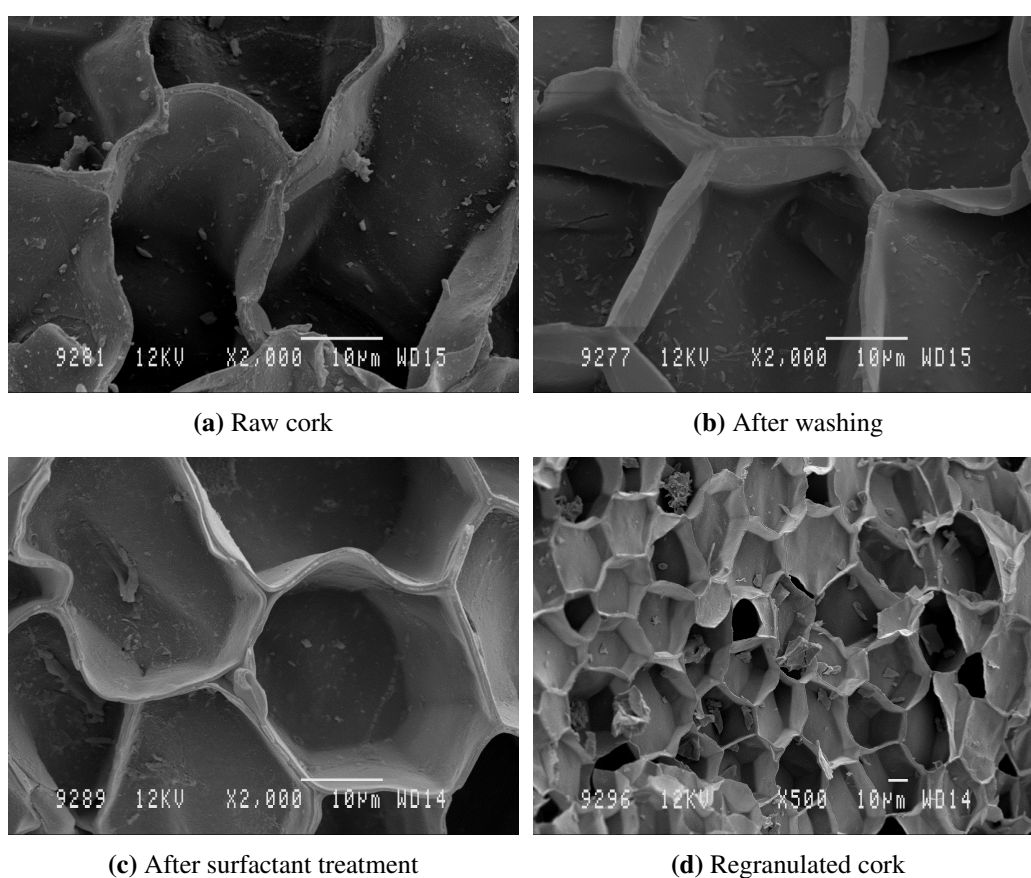


Figure 3.1: SEM micrographs of cork granulates.

Values of bulk density, ash content and elemental analysis of cork biosorbents are presented in Table 3.1. Cork density is variable, as it depends on the cellular features. Cork cell walls are believed to have constant density (around 1.2 g cm^{-3}); however, cork cells are hollow polyhedrons, and there is a large quantity of gas inside these closed compartments (Silva et al., 2005). For the finest particle size (FCG), the observed structural density of 1.32 g cm^{-3} is very similar to the density of cork cell walls. However, an increase in particle size leads to a decrease in structural density, because more cork cells in a same unit weight are closed and incorporating air into the

Table 3.1: Elemental analysis, ash content, bulk and structural density of cork biosorbent samples¹.

Sample	C (%)	H (%)	N (%)	Ash (%)	O (%) (est.)	Bulk density (g cm ⁻³)	Structural density (g cm ⁻³)
FCG	61.90	7.90	0.63	0.93	29.57	0.083	1.32
ICG	62.96	7.97	0.58	0.42	28.07	0.069	0.93
CCG	62.44	7.95	0.63	0.47	28.51	0.069	0.73
RCG	70.22	7.66	0.58	1.24	20.30	0.071	0.54
W-ICG	63.27	8.05	0.55	—	28.13	—	—
S-FCG	60.50	7.73	0.64	—	31.13	—	—
S-CCG	64.68	8.58	0.71	—	26.03	—	—
S-RCG	67.93	6.57	0.66	—	24.84	—	—

¹ Cork biosorbent samples identified as: raw (FCG, ICG, CCG, RCG), washed with water (W-ICG) and surfactant-treated (S-FCG, S-CCG, S-RCG).

structure of the material. Larger cork particles approach the values for cork plank found in the literature (120-240 kg m⁻³ (Fortes and Rosa, 1988)). Bulk density is lower than structural density, and similar for all grain sizes.

Elemental analysis revealed, as expected, that carbon is the main constituent of cork granules (61-63%); it constitutes the basis of structural components (suberin, lignin, polysaccharides and extractives). Hydrogen ($\approx 8\%$) is the counterpart of carbon in the aliphatic chains of suberin and aromatic rings of lignin. Nitrogen content ($\approx 0.6\%$) is low; this element is a component of minor extractives and peptic polysaccharides in the cell wall (Domingues, 2005). Sulphur was not detected in any of the samples. Ash content (0.4-0.5%) is lower than the range reported in the literature (0.9-6.0% (Gil, 1997)), however, it must be taken into account that ash content depends on the temperature used for carbonisation. Oxygen content was estimated by subtracting the sum of carbon, hydrogen, nitrogen and ash contents from total weight.

The elemental composition of regranulated cork differs from raw cork by an increase in carbon content in detriment of oxygen content, along with a slight decrease in hydrogen. This means that carbon remains in the structure of regranulated cork while its bonds with hydrogen and oxygen are partially degraded. This conclusion supports earlier publications that indicate that at 350-400 °C, cork suffers degradation of polysaccharides, carbohydrates and extractives, and partial degradation of suberin and lignin, retaining mostly its aromatic domain and originating coke (Neto et al., 1995). Washing with water does not lead to changes in the elemental ratios of cork granulate. Surfactant-treated biosorbents present slightly different values from raw cork; however, these changes do not follow a clear trend and cannot be correlated to adsorption and/or incorporation of the surfactant in the cork matrix.

3.3.2 Textural characterisation

N₂ adsorption isotherms were determined to evaluate specific surface area and porosity features in all samples. Isotherms of cork granulates (Figure 3.2) are of Type III, the class of nonporous or

macroporous solids, according to Brunauer classification (Gregg and Sing, 1991). Cork cells with 15-20 μm diameter constitute the macropores of granulates, as seen in Figure 3.1. As the interior cells are closed, cork has no available internal porosity, therefore only these external macropores are detected. As the nitrogen-cork interaction is weak, the uptake is very small at low relative pressures, rising only for $p/p_0 > 0.9$, due to condensation phenomenon.

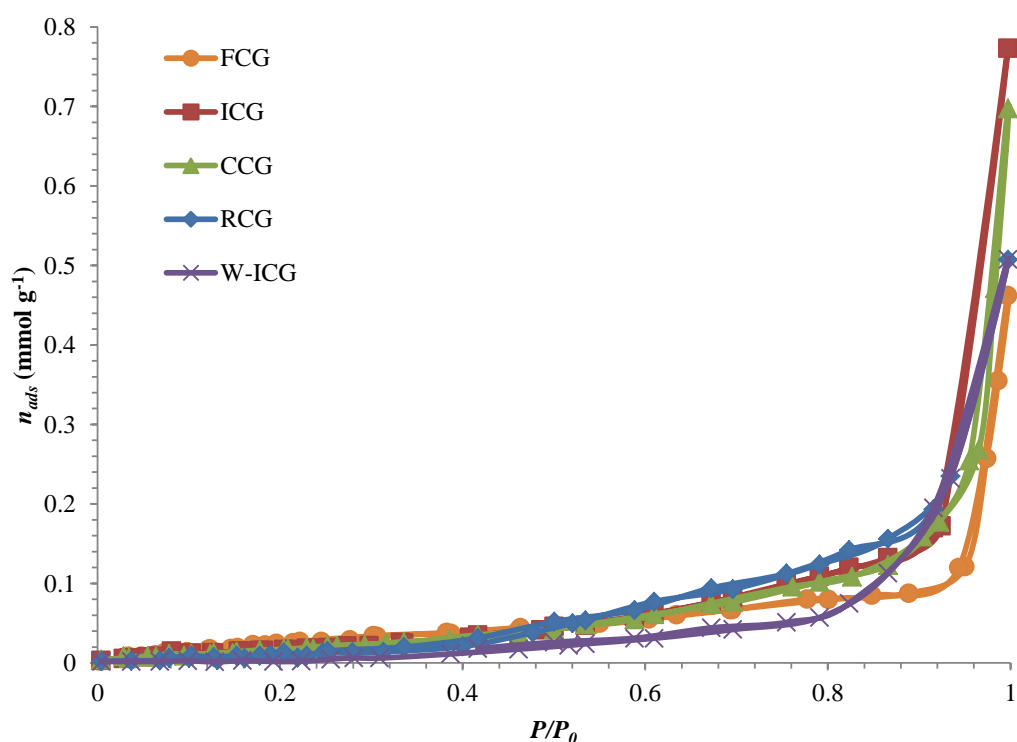


Figure 3.2: N_2 adsorption isotherms at $-196\text{ }^\circ\text{C}$ for raw cork biosorbents of different granulometry (FCG, ICG, CCG), regranulated cork granules (RCG), and washed cork biosorbents (W-ICG).

Similar Type III isotherms were obtained for the surfactant-treated biosorbents. In these materials, adsorption at low relative pressures is even lower. Adsorption of surfactant during the 24-h treatment may have led to coverage of the cork's surface and thus inhibited adsorption of nitrogen.

Table 3.2 presents the parameters obtained through analysis of the N_2 isotherms by the BET and DR equations. The total pore volume can be attributed to macroporosity for cork biosorbents, values ranging between 0.01 and $0.03\text{ cm}^3\text{ g}^{-1}$.

Simple pyrolysis of cork under N_2 flow, at $450\text{ }^\circ\text{C}$, yielded 22.3% of the initial weight, which is within the range (20-30%) predicted by Marsh and Rodriguez-Reinoso (2006) for carbonisation of lignocellulosic materials. The weight loss corresponds, in an early stage, to the evaporation of moisture water and, at higher temperatures, to the degradation of structural components (Neto et al., 1995). The isotherm of carbonized sample 0-CCG (Figure 3.3) shows that uptake of nitrogen by this material is higher than that of the precursor, indicating an increase in specific surface area and total pore volume. The steep rise at high relative pressures that occurs at $p/p_0 > 0.9$ for raw cork granulates disappears, which indicates a lesser incidence of condensation in macropores.

Table 3.2: Yields of carbonisation, BET surface area and total, micropore, and mesopore volume as determined from N₂ isotherms at -196 °C for all the samples studied.

Sample	Yield (%)	S_{BET} (m ² g ⁻¹)	V_{total} (cm ³ g ⁻¹)	V_{micro} (cm ³ g ⁻¹)	V_{meso} (cm ³ g ⁻¹)
FCG	—	< 2	0.03	0.00	0.03
ICG	—	< 2	0.03	0.00	0.03
CCG	—	< 2	0.02	0.00	0.02
RCG	—	< 2	0.02	0.00	0.02
W-ICG	—	< 2	0.02	0.00	0.02
S-FCG	—	< 2	0.01	0.00	0.01
S-CCG	—	< 2	0.01	0.00	0.01
S-RCG	—	< 2	0.01	0.00	0.01
0-CCG	22.3	60	0.09	0.03	0.06
0.11-CCG	30.2	410	0.21	0.16	0.05
0.11-RCG	45.2	270	0.18	0.10	0.08
0.25-CCG	33.2	620	0.34	0.25	0.09
0.25-RCG	43.8	540	0.33	0.21	0.12
0.25-0-CCG	19.2	560	0.32	0.23	0.09
P-0.25-CCG	33.9	360	0.26	0.14	0.12
P-0.25-RCG	43.8	385	0.20	0.14	0.05

The classification according to Brunauer is Type II, typical of nonporous solids (Gregg and Sing, 1991).

Carbon yields are slightly higher when there is a previous impregnation with phosphoric acid. Yields depend on the amount of carbon released with hydrogen and oxygen as CO₂ and hydrocarbons. The activating agent dehydrates the precursor prior to carbonisation, leading to more removal of oxygen and hydrogen as water instead. Phosphoric acid was selected as the impregnant in this study since the objective was to create activated carbons with a greater development of mesoporosity and increased mean pore size. This method of activation also presents cost advantages: it has only one calcination step and the pyrolysis temperature is low (≈ 450 °C) (Carrott et al., 2006; Cardoso et al., 2008).

The N₂ adsorption isotherms of the phosphoric acid cork-based activated carbons are shown in Figure 3.3, and can be classified as Type I (including mesoporosity). The first steep gradient of adsorption, at low relative pressures ($p/p_0 < 0.05$), is not as steep for these isotherms as for those of strictly microporous adsorbents; as such, it may be inferred that the microporosity in these carbons is not very narrow. The following plateau is rising slightly, which corresponds to partial adsorption in the mesoporosity. It can thus be deduced that micro and mesoporosity are developed in the carbons due to the action of phosphoric acid, and not by pyrolysis alone.

For phosphoric acid activated carbons, uptake of nitrogen increased with phosphorus ratio (X_P). Similar increases in BET area and micropore volume were observed for both precursors following an increase in phosphorus ratio from 0.11 to 0.25. Increasing the phosphorus ratio also increased the mesopore volume, agreeing with previous studies that state that mesoporosity development is

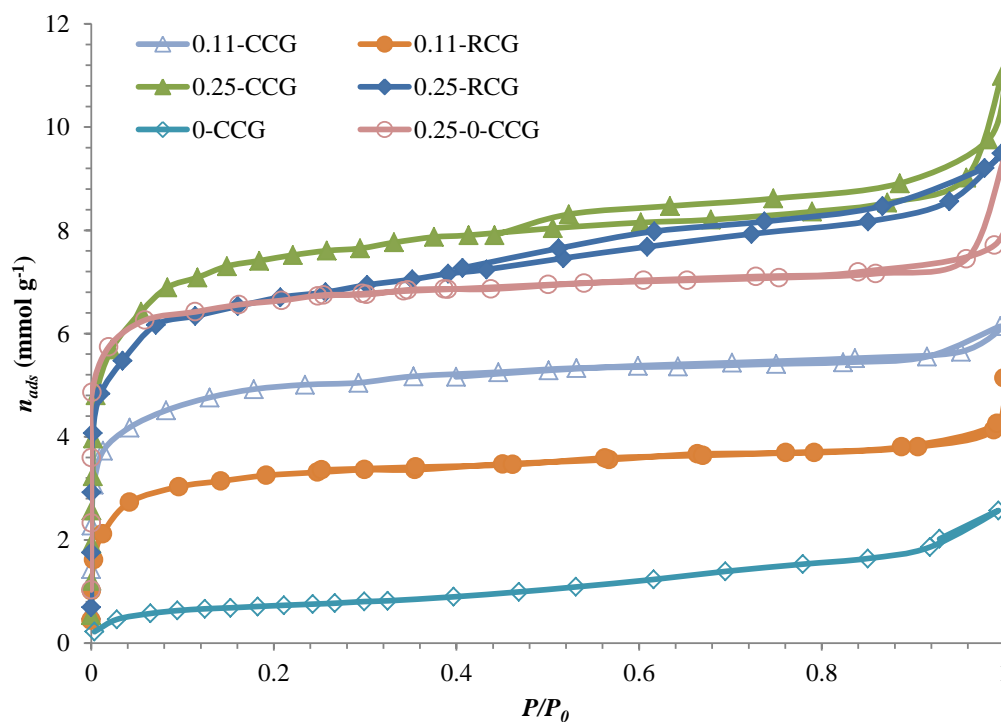


Figure 3.3: N_2 adsorption isotherms at $-196\text{ }^\circ\text{C}$ for cork-based activated carbons.

more significant at higher phosphorus ratios (Molina-Sabio and Rodríguez-Reinoso, 2004). Using raw cork as a precursor resulted in higher uptake of nitrogen than using regranulated cork. This is seen in Table 3.2 through the higher BET area and pore volume of the former samples. Activation of sample 0-CCG resulted in a development of narrower microporosity, but did not lead to higher uptake of nitrogen than that of samples obtained by direct activation of precursors. Isotherms of activated carbons modified by pyrolysis of propene (P-0.25-CCG, P-0.25-RCG, not shown) are similar in shape to those of their activated carbon precursors, only the nitrogen uptake is lower. This occurs due to the formation of carbon deposits on the carbon surface during pyrolysis of propene, which leads to coverage of micropores. In turn, this causes a decrease in BET area and pore volume, and a slight weight gain after the second pyrolysis.

3.3.3 Surface characterisation

Although activated carbons are essentially a carbon matrix of packed aromatic rings organized in graphene layers, there are heteroatoms, such as oxygen and hydrogen, which are incorporated in the structure and affect the adsorption properties of the material (Rodríguez-Reinoso and Molina-Sabio, 1998). The amount of heteroatoms depends on the preparation of the carbon, in particular the precursor and activation method. They are usually present at the surface, in the form of groups analogous to organic species (Salame and Bandosz, 1998).

Oxygen surface groups are the ones which most influence the surface properties of carbons. They determine the acidity/basicity and promote specific interactions with polar molecules. Techniques

used to quantify oxygen surface groups include FTIR, potentiometric titration, TPD and immersion calorimetry.

3.3.3.1 Cork biosorbents

Due to the widespread interest in the characteristics of cork as a natural material, many authors already published studies on its chemical composition, including a FTIR spectrum (Lopes et al., 2001). The band assignments presented in this and other texts of the literature were summarized in the previous chapter, and can be consulted in Table 2.2.

Potentiometric titration aims to quantify surface functionality in cork biosorbents through the protonation and deprotonation of surface groups. The active sites at the surface will capture or release protons according to the intrinsic equilibrium constant of each class of sites. The model fitted to experimental data, which was based on a bimodal continuous distribution of affinity constants (following a quasi-Gaussian Sips distribution function (Sips, 1950)) with a local Langmuir-Freundlich isotherm, can be found explained elsewhere (Milne et al., 1995; Vilar et al., 2009). The surface charge (adsorbed amount of protons per unit mass of biosorbent (Q_H)) corresponds to the weighted sum of the charge of the two classes of sites considered – carboxylic groups, titrated with acid and with low intrinsic constant, and hydroxyl groups, titrated with base and with high intrinsic constant (Eq. 3.1):

$$Q_H = Q_{max,1} \frac{(K'_{1,H} C_H)^{m_{H,1}}}{1 + (K'_{1,H} C_H)^{m_{H,1}}} - Q_{max,2} \left(1 - \frac{(K'_{2,H} C_H)^{m_{H,2}}}{1 + (K'_{2,H} C_H)^{m_{H,2}}} \right) \quad (3.1)$$

where $Q_{max,j}$ is the overall charge of the binding group j (mmol g⁻¹), $K'_{j,H}$ is the median value for the affinity distribution for the proton to the binding group j , C_H is the hydrogen ion concentration (M), and $m_{H,j}$ is the width of the peak in the Sips distribution ($0 < m_{H,j} < 1$). A plotting of the surface charge (experimental and theoretical) as a function of pH, for cork biosorbents, is presented in Figure 3.4.

Although the fitting of the model had some limitations due to the presence of only a dozen of data points, a trend could be clearly identified and some parameters quantified. A non-linear regression was applied to the experimental data according to the methodology explained in Vilar et al. (2008). The values for the affinity constants, overall charge of each binding group, and other parameters are presented in Table 3.3. The sum of the residual sum of squares (S_r^2) and the correlation coefficient (r^2) are also presented.

Table 3.4 presents both the total amounts of CO and CO₂ evolved in TPD analysis of cork biosorbents, calculated by integration of the respective spectra. The CO₂ and CO TPD spectra in graph form can be found in Figure 3.5.

Both potentiometric titration and TPD point to the conclusion that cork has an acidic surface. In the latter technique, CO₂/CO ratio is above unity, and CO₂-evolving groups are usually identified to be carboxylic acids. These are the strongest acidic groups with the lowest intrinsic dissociation

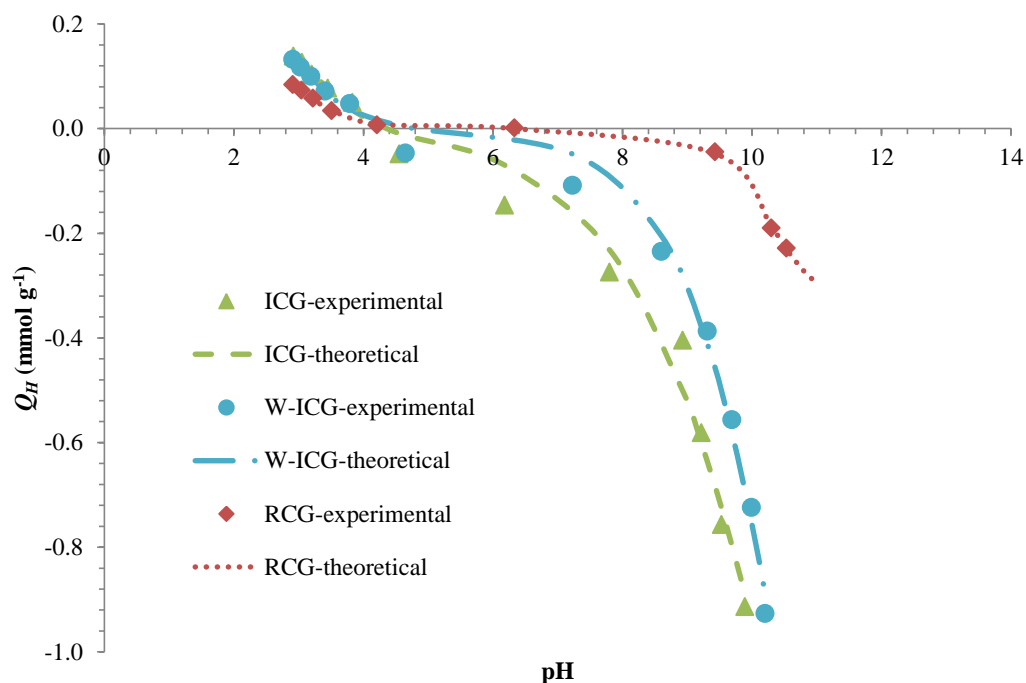
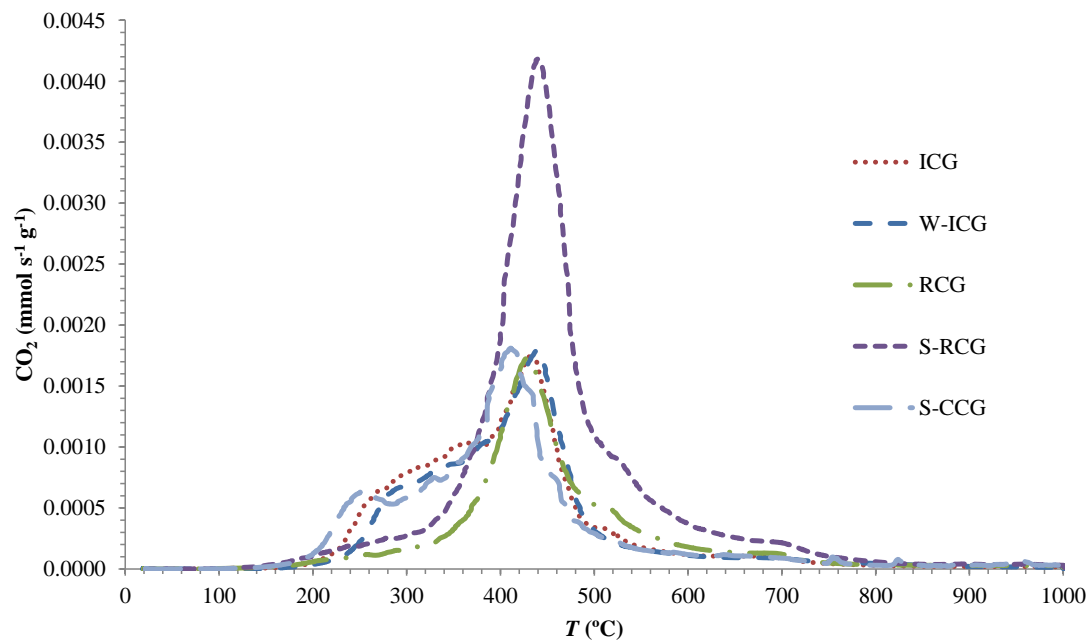
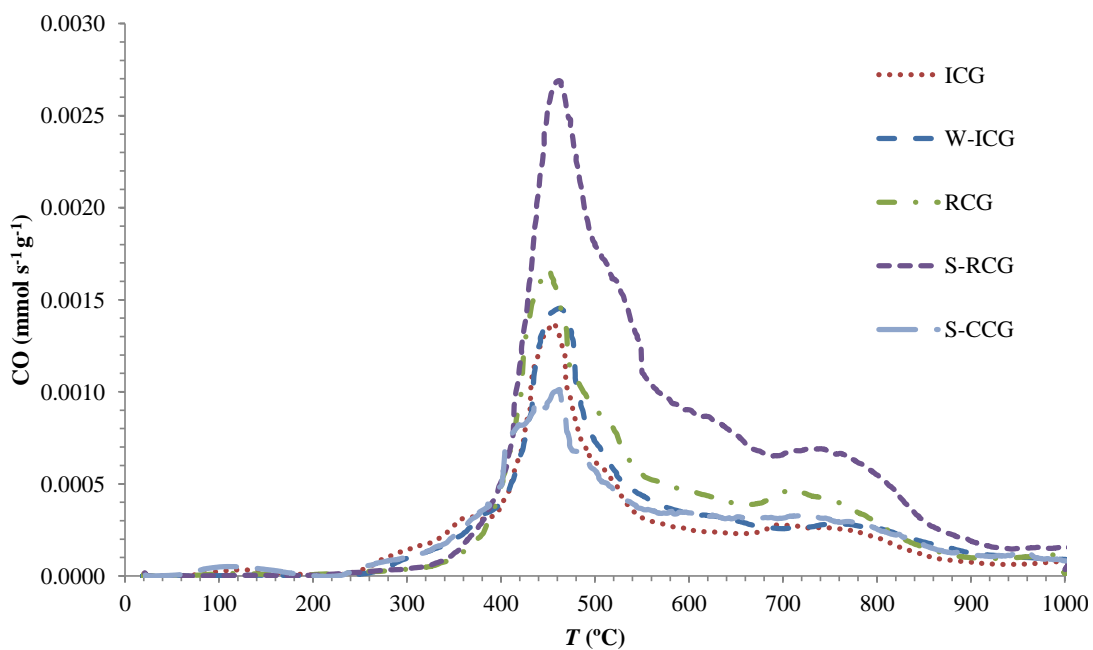


Figure 3.4: Experimental data and model curves (bimodal Sips distribution of affinity constants combined with local Langmuir-Freundlich isotherm) for particle charge data obtained from potentiometric titration of cork biosorbents ICG, W-ICG and RCG.

Table 3.3: Intrinsic constants and surface charges for carboxylic and hydroxyl groups obtained through the applied model using potentiometric titration data of cork biosorbents.

Sample	$pK_{1,H}$	$pK_{2,H}$	$Q_{max,1}$ (mmol g^{-1})	$Q_{max,2}$ (mmol g^{-1})	$m_{H,1}$	$m_{H,2}$	r^2	S_r^2 (mmol g^{-1})
ICG	3.3	11.0	0.20	2.99	1.00	0.34	0.986	3.5×10^{-3}
W-ICG	3.1	11.0	0.21	3.01	1.00	0.47	0.993	1.8×10^{-3}
RCG	2.9	10.2	0.16	0.34	1.00	1.00	1.000	4.7×10^{-6}

(a) CO₂

(b) CO

Figure 3.5: TPD profiles of cork biosorbents.

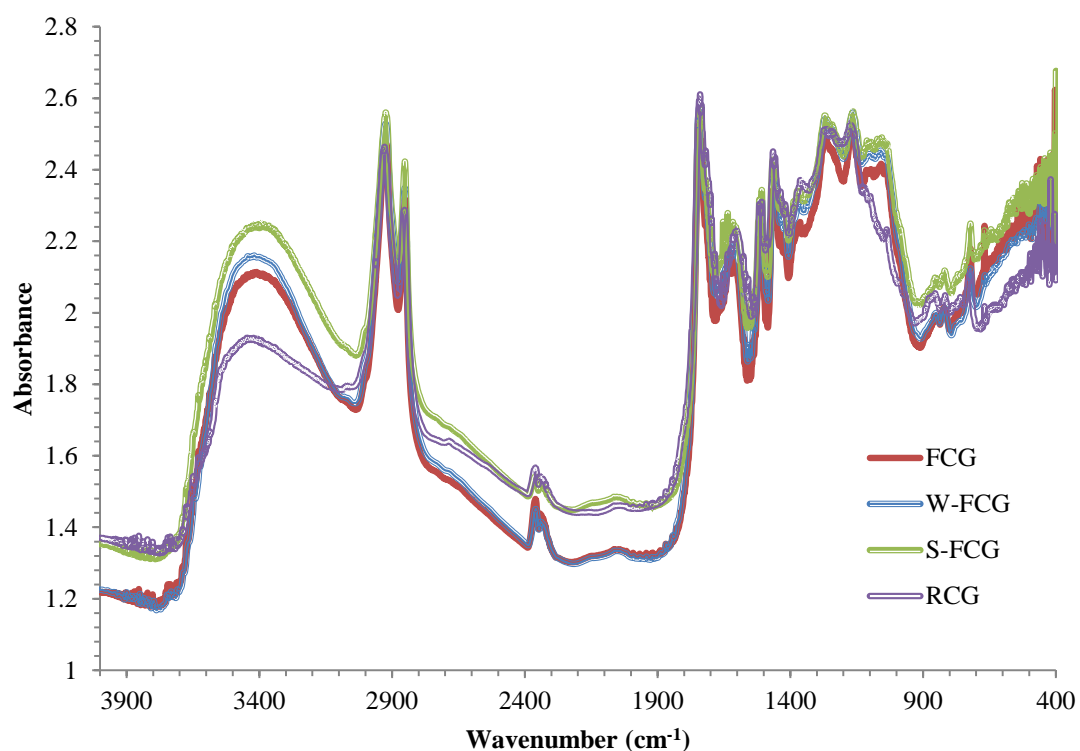
Table 3.4: Total amounts of CO₂ and CO evolved in TPD analysis, respective CO₂/CO ratio, and immersion enthalpies in water and methanol for cork-based materials.

Sample	CO ₂ (mmol g ⁻¹)	CO (mmol g ⁻¹)	CO ₂ /CO	ΔH (H ₂ O) (J g ⁻¹)	ΔH (CH ₃ OH) (J g ⁻¹)
ICG	1.67	1.36	1.23	29.3	31.5
W-ICG	1.67	1.62	1.03	8.2	24.1
RCG	1.39	1.86	0.75	15.5	33.0
S-RCG	3.01	3.24	0.93	4.7	17.9
S-CCG	1.66	1.49	1.11	–	–
0.25-CCG	0.48	1.63	0.29	44.2	79.0
0.25-RCG	0.60	2.25	0.27	46.4	79.8
P-0.25-CCG	0.33	1.03	0.32	36.8	66.6
P-0.25-RCG	0.33	1.14	0.29	54.2	71.1

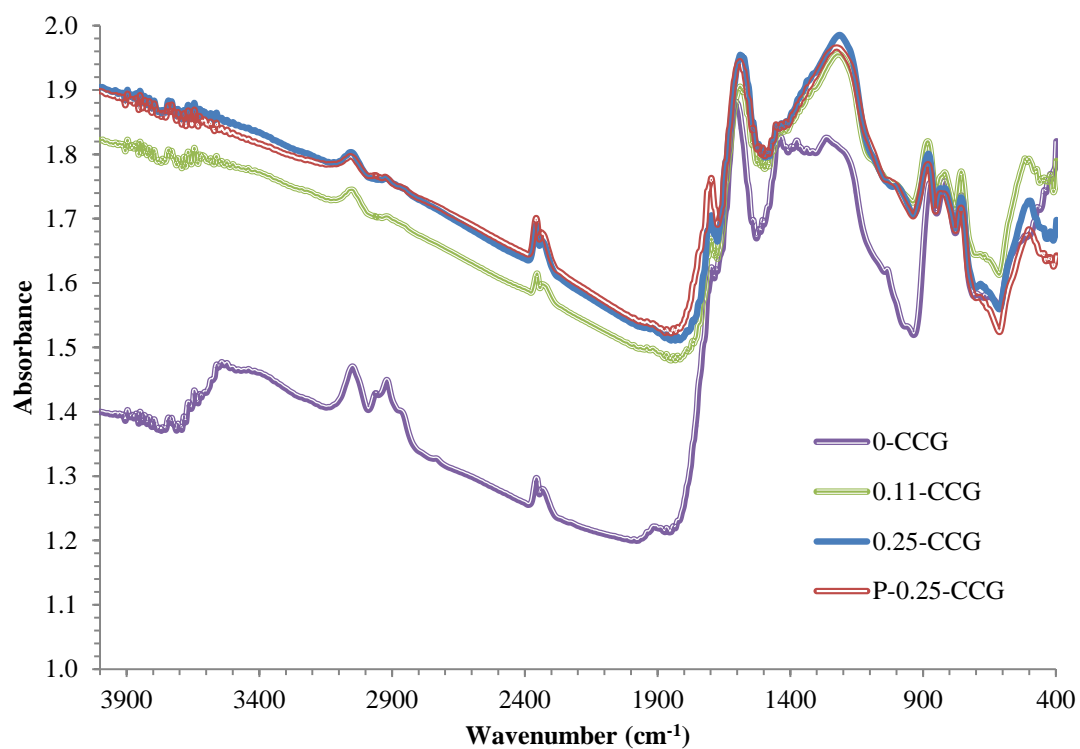
constants ($pK_a < 5$). The intrinsic constant for carboxylic groups determined through potentiometric titration was ≈ 3 (Table 3.3). Cork biosorbents also have a significant portion of weakly acidic groups, with a higher intrinsic affinity constant ($pK_{2,H} \approx 11$, Table 3.3). The hydroxyl functionality appears as part of both phenolic and carboxylic groups (Figueiredo et al., 1999) and is detected in the FTIR spectrum through a broad absorption feature between 3600 – 3100 cm⁻¹. Surface charge for hydroxyl groups is lower in regranulated cork due to decomposition of the more heat-sensitive groups during thermal treatment. There is a decrease in the –OH “stretching” absorption peak in RCG sample’s FTIR spectrum (Figure 3.6a) and in the amount of CO₂-evolving groups in TPD. The latter is coupled with an increase in CO-evolving groups, likely due to the presence of non-acidic groups, such as carbonyls and ethers, formed due to exposure to high temperatures (Bandosz et al., 1997).

The presence of different surface groups also influences the polarity of the surface, as it was verified through immersion calorimetry. For nonpolar liquids, the heat of immersion depends on the porosity (Rodríguez-Reinoso et al., 1997), but the more polar the liquid, the stronger the effect of surface groups. Cork is known to be hydrophobic (Lequin et al., 2010), hence immersion enthalpies for both water and methanol were low (Table 3.4). The removal of phenolic extracts and other water-soluble substances is reflected in a decrease of affinity for both liquids in sample W-ICG. For regranulated cork RCG, the decrease in oxygen surface functionality is responsible for a decrease in affinity for water.

Surfactant treatment on both raw and regranulated cork biosorbents was expected to improve hydrophobicity, since if the hydrophilic ammonium cation adsorbed on the cork’s surface, it would leave the aliphatic hydrophobic tail in contact with the external medium. The observed decrease in the adsorption enthalpy for polar adsorbates points to an improvement towards the intended objective. Adsorbed surfactant is not detected through the FTIR spectrum as the bands usually used to identify its presence, the C-H “stretching” absorption peaks at 2922 and 2853 cm⁻¹ (Ibrahim et al., 2010), are quite prominent in the original cork biosorbents’ spectra (Figure 3.6a and Ta-



(a) cork biosorbents



(b) carbonized cork and cork-based activated carbons

Figure 3.6: FTIR spectra.

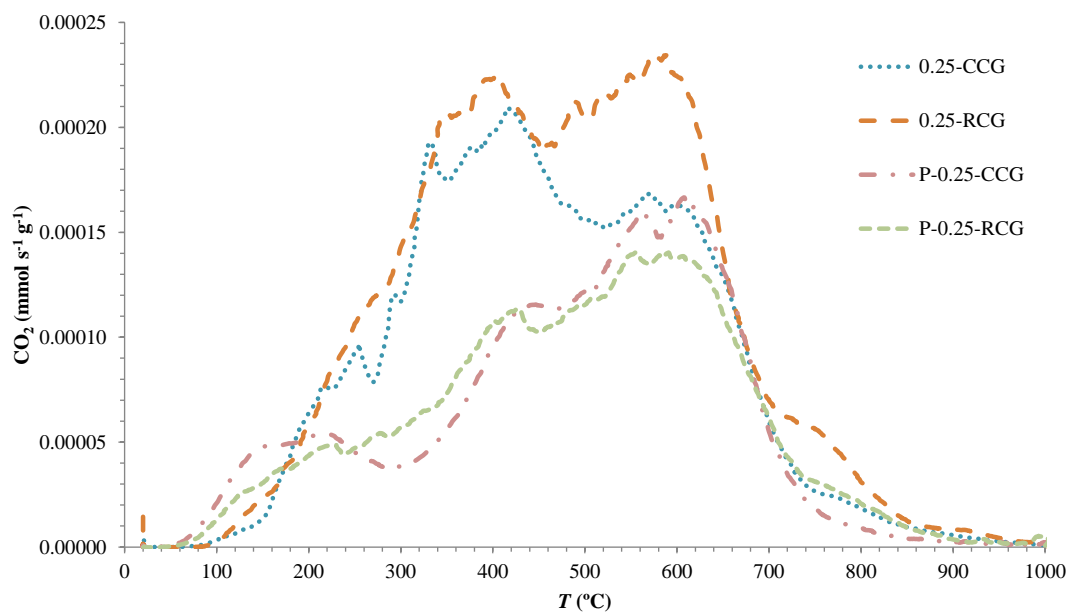
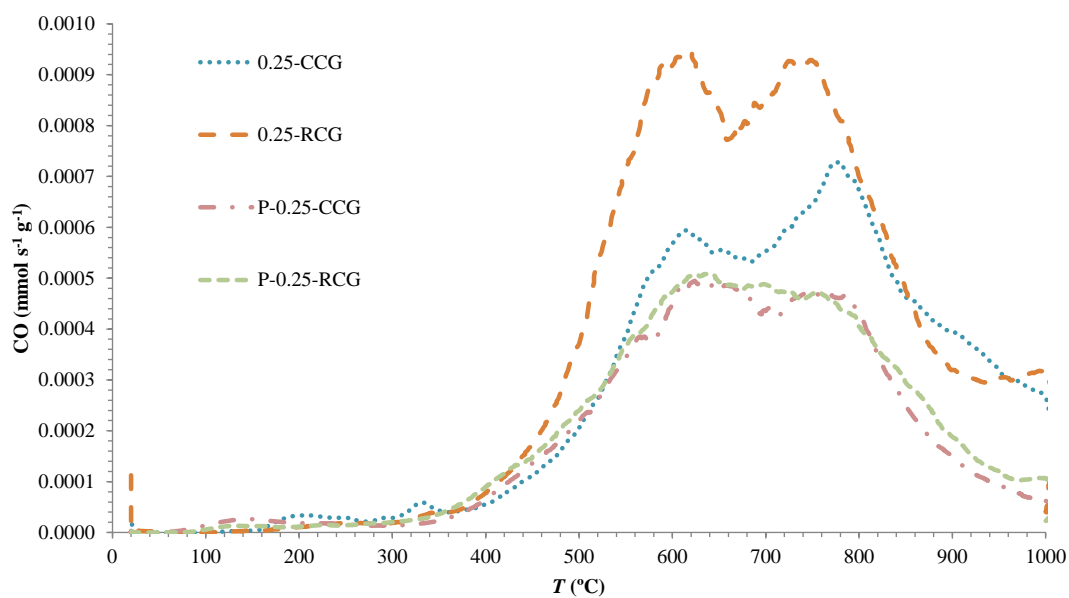
ble 2.2). TPD analyses of these samples are inconclusive as well, as there is a possible bias caused by desorption of the surfactant from the biosorbents' surface.

3.3.3.2 Cork-based activated carbons

An important transformation on the structure of cork occurs through carbonisation. This was reflected in the infrared spectrum of sample 0-CCG (Figure 3.6b). Although regranulated cork suffers a thermal treatment, it does not lead to major changes in chemical composition (Figure 3.6a). At 450 °C and under N₂ flow, however, a degradation of the structural basis of cork (suberin and lignin) occurs, resulting in the reduction of both the –OH “stretching” and –CH₃ “stretching” peaks at 3440-3400 cm⁻¹ and 2920-2850 cm⁻¹ and in the disappearance of the C=O “stretching” bands at 1745-1715 cm⁻¹. On the other hand, the most important band in the spectrum is now the peak at around 1605 cm⁻¹, which corresponds to C=C aromatic ring stretch (Coates, 2000). This is evidence of the formation of coke and the aromatic matrix which characterizes carbon structures. The FTIR spectra of activated carbon samples 0.11-CCG, 0.25-CCG and P-0.25-CCG are also presented in Figure 3.6b. Spectra of corresponding samples using RCG as a precursor were identical and are therefore not shown. The spectra of activated carbons are similar to the 0-CCG spectrum, due to the complete destruction of the cork's structure. The peak at around 1600 cm⁻¹ is still the dominant feature of the spectra. However, there is now another significant peak at around 1230-1210 cm⁻¹, whose broadness covers the previously featureless range of 1450-1200 cm⁻¹. This region of the spectrum can be assigned to C-O vibrations from different surface group species, such as esters, carboxylic acids, carboxylic anhydrides, lactones, alcohols, ethers, phenols and carboxyl-carbonates (Dandekar et al., 1998; Figueiredo et al., 1999; Salame et al., 1999; Marsh and Rodriguez-Reinoso, 2006).

The main problem with interpretation of FTIR spectra of activated carbons is that it is impossible to distinguish surface oxygen groups in the 1450-1200 cm⁻¹ due to superposition. Therefore, TPD is valuable as it can untangle the contributions of different kinds of surface groups, giving both quantitative and qualitative information. CO₂ and CO evolution profiles for activated carbons can be seen in Figure 3.7. Both 0.25-CCG and 0.25-RCG presented a much higher amount of CO-yielding groups than CO₂-yielding ones. CO₂-evolving groups, especially carboxylic acids, were decomposed in the temperature range 200-450 °C during the pyrolysis step. The residual amount detected could have been formed by room temperature oxidation during handling and transport, due to contact with oxygen in air (Dandekar et al., 1998). The CO spectrum is dominated by the presence of two peaks centered at around 600 °C and 750 °C, corresponding to phenols and carbonyl/ether/quinone groups, respectively (Figueiredo et al., 1999).

The amount of surface groups, especially weakly acidic ones, is higher on sample 0.25-RCG than on sample 0.25-CCG. This is not visible qualitatively on the FTIR spectra but could be quantified through integration of the TPD spectra (Table 3.4). This affected the affinities of the carbons to water and methanol. A higher amount of polar groups in 0.25-RCG sample led to higher enthalpy of immersion in water when compared to 0.25-CCG. However, as the latter has higher BET area and pore volume (Table 3.2), indicative of more available porosity, the enthalpy of uptake for

(a) CO_2 (b) CO **Figure 3.7:** TPD profiles of cork-based activated carbons.

methanol was similar in both activated carbons.

The presence of surface functionalities is interrelated with the values of BET area and pore volume. When the surface has more heteroatoms, the groups present at the carbon's surface partially fill the pores, decreasing the pore volume and the area available for adsorption of other molecules. In addition to explaining the differences between samples 0.25-CCG and 0.25-RCG, this pore filling phenomenon also helps describe the decrease of surface groups in propene-treated samples P-0.25-CCG and P-0.25-RCG. [Gonçalves et al. \(2010\)](#) have previously concluded that treatment with propene prevents chemisorption of oxygen with the deposition of carbon on the activated carbons' surface. The cork-based activated carbon samples modified by pyrolysis of propene lost, therefore, part of their surface functionalities when compared to their precursors. Treatment with propene uniformised the activated carbons' surface, as both TPD profiles of P-0.25-CCG and P-0.25-RCG are more similar between them than are those of 0.25-CCG and 0.25-RCG (Figure 3.7). The loss of porosity and surface oxygen groups also led, as expected, to a decrease in the immersion enthalpy (in methanol for both samples and in water for sample P-0.25-CCG).

3.3.4 Application to the sorption of oil from water

The sorption capacities (q) and removal efficiencies (R) of different cork-based materials for sunflower oil emulsified in water were determined in batch tests using a sorbent concentration of 0.5 g L^{-1} , with a starting point of oil concentration between 150 and 200 mg L^{-1} . Results are presented in Figure 3.8.

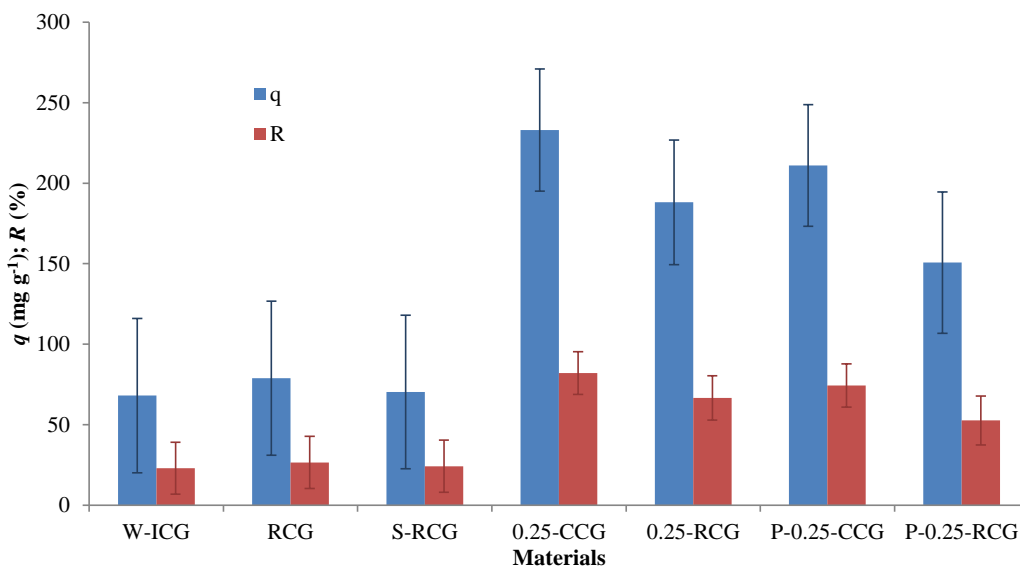


Figure 3.8: Sorption capacities and removal efficiencies of cork-based sorbents for sunflower oil emulsified in water, at pH 7.2 and $25 \text{ }^\circ\text{C}$ (error bars: standard uncertainty).

It is clear from the figure that sorption capacity is increased through transformation of cork granules into activated carbons. The higher surface area in activated carbons facilitates contact between

the sorbent and the oil droplets and, consequently, agglomeration, coalescence and uptake. Nevertheless, surface effects cannot be ignored since the discrepancy between the sorption capacity of biosorbents and of activated carbons is not proportional to surface area. Removal in raw cork sorbent ICG was not presented in Figure 3.8 since the result was not statistically significant due to high experimental uncertainty. However, removal capacities in the other three cork biosorbents (W-ICG, RCG and S-RCG) show that the hydrophobic nature of cork enables some uptake of O&G. The observed increase in capacity after the sorbent is washed (W-ICG) or when it consists of regranulated cork (RCG, S-RCG) is in line with the decrease in CO_2/CO groups ratio and the reduction on the immersion enthalpy in water (Table 3.4). Nevertheless, the increase in hydrophobicity expected after surfactant treatment does not result in an improvement in oil sorption capacity as can be concluded by comparing the results of sorbents RCG and S-RCG.

As far as activated carbons are concerned, 0.25-CCG is the one that achieved higher removal efficiency, of 82%, corresponding to an oil sorption capacity of 233 mg g^{-1} . The better performance of 0.25-CCG when compared to 0.25-RCG can be explained by two factors: the higher surface area of the former and the higher overall presence of surface groups in the latter. Surface groups promote interactions with polar molecules, rather than nonpolar substances as is the case of sunflower oil. Therefore, it should be expected that the more surface groups are present, the more likely a competition between water and oil will occur, lowering the efficiency in the removal of oil.

Pyrolysis under propene did not increase the uptake of oil in activated carbons. Since this treatment decreased the presence of surface groups, the explanation must be assigned to the reduction in surface area that occurred due to inorganic carbon deposition. However, the 10-20% reduction in oil sorption capacity is lower than the 30-40% decrease in surface area, thus indicating that treatment with propene does enhance the affinity to oil in the porosity; but because the porosity is now much less per mass unit, this does not result in an overall increase in oil sorption capacity.

When comparing cork sorbents with cork-based activated carbons for a potential application, one must also take into account the yield of activated carbon per precursor (Table 3.2). Multiplying the sorption capacity of the activated carbon by the yield, one can compare the sorption capacities per mass unit of cork granulate used (either directly or transformed by pyrolysis). Using this conversion, the sorption capacities of 0.25-CCG and 0.25-RCG become 77 and 82 mg g^{-1} of cork granulates, respectively. These are values quite similar to the 79 mg g^{-1} sorption capacity reported for regranulated cork RCG. Considering that the production of activated carbons involves further investments with equipment, energy and reactants, the use of sorbent RCG may achieve the same objectives at a lower cost.

3.4 Conclusions

Textural and surface properties of raw and regranulated cork biosorbents, surfactant-modified biosorbents, phosphoric acid cork-based activated carbons, and activated carbons pyrolysed under propene have been studied, and these materials have been applied to the removal of sunflower

oil from water.

Cork granulates are macroporous solids with very low density. Their surface properties, analysed by FTIR, TPD and potentiometric titration, showed an acidic character with an important presence of carboxylic and phenolic groups. Regranulated cork differs from the raw one in carbon content and presence of carboxylic groups, as these are decomposed upon thermal treatment. This results in a slightly higher removal efficiency of oil from water.

Cork-based carbons activated with phosphoric acid showed interesting textural properties, with BET areas ranging from 270 to 620 m² g⁻¹ and a high content of CO-yielding groups, especially phenols and carbonyls. The increase in surface area caused a great increase in oil sorption capacity, especially in the carbons with less surface groups. Pyrolysis under propene enhanced the affinity to oil in the porosity, but because the surface area decreased due to inorganic carbon deposition, this did not result in an overall higher oil uptake.

Finally, it can be concluded that regranulated cork sorbents and phosphoric acid activated carbons from both precursors, at a 0.25 phosphorus ratio, can be applied to the removal of emulsified oil from water with similar efficiencies per unit mass of cork granulates. Since the objective of this work is to develop environmentally friendly solutions for the removal of O&G from wastewaters, regranulated cork sorbent RCG was selected and used in further studies.

3.5 References

- Alther, G. R. Organically modified clay removes oil from water. *Waste Management*, 15(8):623–628, 1995.
- Bandosz, T. J., Buczek, B., Grzybek, T., and Jagiełło, J. The determination of surface changes in active carbons by potentiometric titration and water vapour adsorption. *Fuel*, 76(14–15):1409–1416, 1997.
- Brunauer, S., Emmett, P. H., and Teller, E. Adsorption of gases in multimolecular layers. *Journal of the American Chemistry Society*, 60:309–319, 1938.
- Cardoso, B., Mestre, A. S., Carvalho, A. P., and Pires, J. Activated carbon derived from cork powder waste by KOH activation: Preparation, characterization, and VOCs adsorption. *Industrial & Engineering Chemistry Research*, 47(16):5841–5846, 2008.
- Carrott, P. J. M., Ribeiro Carrott, M. M. L., and Mourão, P. A. M. Pore size control in activated carbons obtained by pyrolysis under different conditions of chemically impregnated cork. *Journal of Analytical and Applied Pyrolysis*, 75(2):120–127, 2006.
- Coates, J. *Encyclopedia of Analytical Chemistry*, chapter Interpretation of Infrared Spectra, A Practical Approach, pages 10815–10837. John Wiley & Sons Ltd, Chichester, 2000.
- Conde, E., Cadahía, E., Garcia-Vallejo, M. C., and González-Adrados, J. R. Chemical characterization of reproduction cork from Spanish *Quercus suber*. *Journal of Wood Chemistry and Technology*, 18(4):447–469, 1998.
- Dandekar, A., Baker, R. T. K., and Vannice, M. A. Characterization of activated carbon, graphitized carbon fibers and synthetic diamond powder using TPD and DRIFTS. *Carbon*, 36(12):1821–1831, 1998.

- Domingues, V. *Utilização de um produto natural (cortiça) como adsorvente de pesticidas piretróides em águas*. PhD thesis, University of Porto, 2005.
- Dubinin, M. M. *Characterization of Porous Solids*. The Society of Chemical Industry, London, 1979.
- Eaton, A. D., editor. *Standard methods for the examination of water and wastewater*. American Public Health Association, Baltimore, Maryland, 21st edition, 2005. Prepared and published jointly by American Public Health Association, American Water Works Association, Water Environment Federation.
- Figueiredo, J. L., Pereira, M. F. R., Freitas, M. M. A., and Órfão, J. J. M. Modification of the surface chemistry of activated carbons. *Carbon*, 37(9):1379–1389, 1999.
- Fortes, M. A. and Rosa, M. E. Densidade da cortiça: Factores que a influenciam. *Boletim do Instituto dos Produtos Florestais - Cortiça*, 593:65–68, 1988.
- Gil, L. Cork powder waste: An overview. *Biomass & Bioenergy*, 13(1-2):59–61, 1997.
- Gonçalves, M., Molina-Sabio, M., and Rodríguez-Reinoso, F. Modification of activated carbon hydrophobicity by pyrolysis of propene. *Journal of Analytical and Applied Pyrolysis*, 89(1):17–21, 2010.
- Gregg, S. J. and Sing, K. S. W. *Adsorption, Surface Area and Porosity*. Academic Press, London, 2nd edition, 1991.
- Ibrahim, S., Ang, H.-M., and Wang, S. Removal of emulsified food and mineral oils from wastewater using surfactant modified barley straw. *Bioresource Technology*, 100(23):5744–5749, 2009.
- Ibrahim, S., Wang, S., and Ang, H. M. Removal of emulsified oil from oily wastewater using agricultural waste barley straw. *Biochemical Engineering Journal*, 49(1):78–83, 2010.
- Lequin, S., Chassagne, D., Karbowski, T., Gougeon, R., Brachais, L., and Bellat, J.-P. Adsorption equilibria of water vapor on cork. *Journal of Agricultural and Food Chemistry*, 58(6):3438–3445, 2010.
- Lopes, M. H., Rutledge, D., Gil, A. M., Barros, A. S., Delgadillo, I., and Neto, C. P. Variability of cork from Portuguese *Quercus suber* studied by solid-state ^{13}C -NMR and FTIR spectroscopies. *Biopolymers*, 62(5):268–277, 2001.
- Marsh, H. and Rodríguez-Reinoso, F. *Activated Carbon*. Elsevier Science & Technology Books, 2006.
- Milne, C. J., Kinniburgh, D. G., De Wit, J. C. M., Van Riemsdijk, W. H., and Koopal, L. K. Analysis of proton binding by a peat humic acid using a simple electrostatic model. *Geochimica et Cosmochimica Acta*, 59(6):1101–1112, 1995.
- Molina-Sabio, M. and Rodríguez-Reinoso, F. Role of chemical activation in the development of carbon porosity. *Colloids and Surfaces A: Physicochemical and Engineering Aspects*, 241(1-3):15–25, 2004.
- Neto, C. P., Rocha, J., Gil, A., Cordeiro, N., Esculcas, A. P., Rocha, S., Delgadillo, I., De Jesus, J. D. P., and Correia, A. J. F. ^{13}C solid-state nuclear magnetic resonance and Fourier transform infrared studies of the thermal decomposition of cork. *Solid State Nuclear Magnetic Resonance*, 4(3):143–151, 1995.
- Rodríguez-Reinoso, F. and Molina-Sabio, M. Textural and chemical characterization of microporous carbons. *Advances in Colloid and Interface Science*, 76-77:271–294, 1998.

- Rodríguez-Reinoso, F., Molina-Sabio, M., and González, M. T. Effect of oxygen surface groups on the immersion enthalpy of activated carbons in liquids of different polarity. *Langmuir*, 13(8):2354–2358, 1997.
- Salame, I. I. and Bandosz, T. J. Experimental study of water adsorption on activated carbons. *Langmuir*, 15(2):587–593, 1998.
- Salame, I. I., Bagreev, A., and Bandosz, T. J. Revisiting the effect of surface chemistry on adsorption of water on activated carbons. *The Journal of Physical Chemistry B*, 103(19):3877–3884, 1999.
- Silva, S. P., Sabino, M. A., Fernandes, E. M., Correlo, V. M., Boesel, L. F., and Reis, R. L. Cork: properties, capabilities and applications. *International Materials Reviews*, 50(6):345–365, 2005.
- Silvestre-Albero, J., Gómez De Salazar, C., Sepúlveda-Escribano, A., and Rodríguez-Reinoso, F. Characterization of microporous solids by immersion calorimetry. *Colloids and Surfaces A: Physicochemical and Engineering Aspects*, 187-188:151–165, 2001.
- Sips, R. On the structure of a catalyst surface. II. *The Journal of Chemical Physics*, 18:1024–1026, 1950.
- Vilar, V. J. P., Botelho, C. M. S., and Boaventura, R. A. R. Effect of Cu(II), Cd(II) and Zn(II) on Pb(II) biosorption by algae *Gelidium*-derived materials. *Journal of Hazardous Materials*, 154(1–3):711–720, 2008.
- Vilar, V. J. P., Botelho, C. M. S., Pinheiro, J. P. S., Domingos, R. F., and Boaventura, R. A. R. Copper removal by algal biomass: Biosorbents characterization and equilibrium modelling. *Journal of Hazardous Materials*, 163(2-3):1113–1122, 2009.

Chapter 4

Optimisation of a primary gravity separation treatment for vegetable oil refinery wastewaters¹

4.1 Introduction

This chapter focuses on the treatment of vegetable oil refinery wastewaters (VORWs) produced from sunflower oil refining, as this was the selected case study for the application of cork by-products for O&G removal. VORWs have high COD and O&G levels, along with elevated dissolved solids concentrations (Pandey et al., 2003). Depending on their origin inside the industrial plant, they may also present very low pH. Aslan et al. (2009) have evaluated the biodegradability of these wastewaters and concluded that they have a low BOD₅/COD ratio and cannot be decontaminated by a stand-alone biological treatment. Furthermore, their transport presents high risk of clogging in pumps and piping. For these reasons, VORWs cannot be treated in a conventional municipal WWTP.

There are several physical and chemical processes which can be designed to decontaminate VORWs. The most common approach consists in a combination of previously overviewed methods in sections 2.2.3.2 and 2.2.3.4, such as coagulation with aluminum and iron salts and subsequent clarification by sedimentation or DAF. Several authors (Chipasa, 2001; Pandey et al., 2003; Aslan et al., 2009) have demonstrated that this method is efficient in removing O&G and suspended solids and reducing COD; moreover, they have pointed out that the remaining organic matter is mostly soluble and biodegradable, enabling completion of treatment at a final stage using biological reactors. However, a great disadvantage of this methodology consists in the production of chemical sludge, which is unrecoverable to the process and needs proper disposal (Boyer, 1984; Decloux et al., 2007). Tezcan Un et al. (2009) have tested electrocoagulation with aluminum electrodes, but the

¹This chapter is based on the paper: Pintor, A. M. A., Vilar, V. J. P., Botelho, C. M. S., Boaventura, R. A. R. Optimization of a primary gravity separation treatment for vegetable oil refinery wastewaters. *Clean Technologies and Environmental Policy*, 16(8):1725-1734, 2014.

problem of hazardous sludge is not solved with this alternative.

Still, remaining organic matter and emulsified vegetable oil in low concentrations might be biodegradable, which would allow the subsequent application of biological treatment (Kalyanaraman et al., 2013). For the good operation of aerobic reactors for oil and grease degradation, it is necessary to guarantee an adequate oxygen transfer, which might be difficult due to oily superficial films (Campo et al., 2012).

Geetha Devi et al. (2012) proposed treating VORWs through the use of chitosan, an organic substance widely found in crustaceous life. It consists in a process involving mechanisms of both adsorption and coagulation that generates only organic sludge, which is less hazardous and easier to discard than that produced using inorganic salts. Decloux et al. (2007) went further and proposed a membrane filtration unit as a means of separating fat from the effluent and recovering it onto the manufacturing process.

Gravity separation, a simple primary treatment which has often been overlooked in the treatment of VORWs. Its main applications in oily wastewater treatment have been reviewed in section 2.2.3.1. In this chapter, the application of gravity separation in the treatment of real VORW from sunflower oil refining is examined, with the objective of improving the efficiency of the overall treatment line and preventing overload in secondary treatments.

In order to optimise the best conditions to use this technique as a primary treatment for VORWs, the theoretical framework of oil-water separation was analysed and the kinetics of O&G removal were determined experimentally. An empirical model was then articulated with the mathematical equations of theoretical physical principles in the plotting of 3-dimensional (3D) surface graphs representing the process.

4.2 Theoretical framework

The two main processes that affect separation are sedimentation and coalescence (Frising et al., 2006).

Sedimentation is often analysed from the standpoint of discrete particle settling, which is governed by Newton's and Stokes' laws (Hendricks, 2006). In an oily wastewater, the oil is dispersed in the water phase. Considering a simplified system, the oil globules can be considered as spherical discrete particles upon which weight, buoyancy and drag forces are exerted. Since oil is less dense than water, instead of settling, this will result in an upward flotation movement of the droplets, until they reach the surface and merge with the resolved oil phase (API, 1990).

The drag force at the terminal velocity, when the Reynolds number of the particle is very low ($Re < 0.5$), can be determined using the following expression:

$$D_f = 3\pi\mu v_t D \quad (4.1)$$

where D_f is the particle's resistance to motion (drag force) (N), μ is the absolute viscosity of the wastewater (Pa s), v_t is the terminal velocity of the oil droplet in water (m s^{-1}) and D is the

diameter of the oil droplet (m). This drag force equals the effective weight (W_{eff}) of the particle, as described by Newton's equation:

$$W_{eff} = \left(\frac{\pi D^3}{6} \right) (\rho_w - \rho_o) g \quad (4.2)$$

where ρ_w is the density of water (kg m^{-3}), ρ_o is the density of oil (kg m^{-3}), and g is the acceleration of gravity (m s^{-2}).

Hence, the terminal velocity of a given particle can be determined by Stokes' law (Stokes, 1845):

$$v_t = \left(\frac{g}{18\mu} \right) (\rho_w - \rho_o) D^2 \quad (4.3)$$

This version of Stokes' law is often used in dimensioning gravity separators (i.e. flotation units) and settlers as it allows to estimate terminal velocity based on size distribution. From these data it is possible to determine which particles have a rising rate higher than the surface-loading rate of the tank and that can, therefore, reach the surface and be skimmed off the wastewater (API, 1990). Nevertheless, some authors have pointed out that studying an oil-water mixture as a discrete particle suspension is an over-simplification (Hydro-Flo Technologies, 2002; Frising et al., 2006). Stokes' law considers that the particles are all spherical and of the same size, which is often not true, since the droplets are deformed by viscous forces and, as mentioned before, suffer coalescence, growing in size as they rise in the separator. Recent mathematical advances have tried accounting for both coalescence and sedimentation/flotation (Henschke et al., 2002; Grimes, 2012; Noïk et al., 2013), but they require complex manipulations and modelling.

Given the difficulty in describing the gravity separation process by theoretical principles alone, in this study we have tried an approach integrating both empirical models and simple theoretical equations to optimise oil-water separation in VORWs. Empirical data and parameters were collected from the experimental kinetics of O&G removal from a VORW sample in a separation column and the theoretical laws used were Newton's and Stokes' laws for the movement of spherical droplets in a fluid.

4.3 Experimental

4.3.1 Gravity separation column

Gravity separation experiments were carried out in a 1-L glass graduated cylinder (35.7 cm height and 6.0 cm internal diameter) with a lateral sampling port located approximately 7 cm above the bottom. The sampling tube is closed with tweezers and opened only for sample collection at predefined times.

4.3.2 Wastewater samples

Wastewater samples were collected from a vegetable oil refinery in Portugal. At the time of sampling, the facility was operating with sunflower oil.

The first sample was a wastewater from the homogenisation tank of the industrial wastewater treatment plant (TH). It consists of a mixture of all types of wastewaters which are generated in the refinery, namely at the steps of winterization, separation of waxes and washing of centrifuges. The second sample was a wastewater from the removal of waxes line (AW), and therefore represents only part of the wastewater load which is discharged at the homogenization tank. This wastewater was selected due to its acidic properties, which are expected to benefit the separation of oil and grease from water.

Both wastewaters were characterised using the following parameters: pH, conductivity, turbidity, total suspended solids (TSS) and total dissolved solids (TDS), BOD₅, COD, O&G, dissolved organic carbon (DOC), dissolved nitrogen (DN), and inorganic ions.

4.3.3 Experimental methodology

The wastewater sample (1 L) was poured into the graduated cylinder. The wastewaters were previously agitated to promote homogenization. A first sample was taken at time (t) = 0 to determine the initial values of O&G and COD indicators. The cylinder was covered with aluminum foil to prevent evaporation during the experiment.

Samples were taken through the lateral exhaust at predefined times: 5, 15, 30, 60, 120, 240, 480 and 1440 min. Each sample was analysed for both O&G and COD indicators. The removal was calculated according to Equation 4.4:

$$R = \frac{C_0 - C_t}{C_0} \times 100 \quad (4.4)$$

where C_0 corresponds to the initial concentration of O&G or COD (mg L^{-1} or $\text{mg O}_2 \text{ L}^{-1}$, respectively), and C_t is the concentration of O&G or COD at time t .

4.3.4 Analysis methods

pH was measured using a pH meter InoLab WTW Series and conductivity using a conductivity meter LF538 WTW. Turbidity was measured in a turbidimeter Merck® Turbiquant 3000 IR. TSS and TDS were determined according to Standard Methods (2005). BOD₅ was determined by the respirometric method in Standard Methods (2005) using an OXITOP® system. COD was determined by digestion at 148 °C for 2 h and spectrometry using Merck® Spectroquant kits model 1.14541.0001.

DOC was measured in a TC-TOC-TN analyser provided with a NDIR detector and equipped with ASI-V autosampler (Shimadzu, model TOC-VCSN), calibrated with standard solutions of potassium hydrogen phthalate (total carbon) and a mixture of sodium hydrogen carbonate/sodium carbonate (inorganic carbon). DN was measured in the same analyser coupled to a TNM-1 unit (Shimadzu) calibrated with standard solutions of potassium nitrate and provided by thermal decomposition and NO detection by chemiluminescence method. Before analysing in the TC-TOC-TN analyser the samples were filtered using a 0.45 μm nylon filter.

O&G was determined using the partition-infrared method (5520-C) described in Standard Methods (2005), as previously described in section 3.2.5, with carbon tetrachloride (CTC) as the extraction solvent, with a limit of detection of 1.2 mg L^{-1} and whose estimation of uncertainty is presented in Appendix A.

Anions (nitrite, nitrate, sulfate, phosphate, fluoride, chloride and bromide) were quantified by ion chromatography (Dionex ICS-2100; column AS 11-HC $4 \times 250 \text{ mm}$; suppressor ASRS®300 4 mm). Cations (ammonium, lithium, sodium, potassium, magnesium and calcium) were also analysed by ion chromatography (Dionex ICS-2100; column: CS12A $4 \times 250 \text{ mm}$; suppressor: CSRS®300 4 mm). Isocratic elution was achieved with 30 mM NaOH/20 mM methanesulfonic acid, at a flow rate of $1.5/1.0 \text{ mL min}^{-1}$, for anions'/cations' analyses, respectively.

All parameters were assayed in duplicate and the average value was taken. The estimation of uncertainty and its propagation were carried out according to the recommendations of the Eurachem (Ellison and Williams, 2012).

4.3.5 Determination of oil and water properties

Some physical properties of oil and water/wastewater were determined because they were required for the application of some mathematical formulas.

Densities of water and oil were estimated after the visible separation of the two phases, i.e., at the end of the 24-h experiment. Samples were collected from the surface of the column for oil and from the bottom of the column for water (cleared wastewater). They were then measured for volume in 10 or 25 mL graduated cylinders which were previously weighted. The density (ρ) of the liquid sample (kg m^{-3}) was calculated through Equation 4.5:

$$\rho = \frac{m_1 - m_2}{V} \quad (4.5)$$

where m_1 is the mass of cylinder with sample (kg), m_2 is the mass of cylinder (kg) and V is the volume (m^3).

The dynamic viscosity of the wastewater was estimated to be equal to the dynamic viscosity of water at $25 \text{ }^\circ\text{C}$, which is the approximate room temperature at which the experiments were carried out. Referenced values from official sources were used for the viscosity of water at $25 \text{ }^\circ\text{C}$ (IUPAC, 1980) and for the acceleration of gravity (CODATA, 2010).

4.4 Results and discussion

4.4.1 Characterisation of the wastewaters

Table 4.1 shows the characteristics of the two waters used in this study. The wastewater from the homogenisation tank (TH) and the one from removal of waxes (AW) diverge in indicators relating to their different nature and origin. TH wastewater is of white-yellow colour, resembling milk, due to a high concentration of O&G ($0.7 \pm 0.3 \text{ g L}^{-1}$) dispersed homogeneously as a result of mixing

Table 4.1: Characterisation of the wastewater samples under study.

	TH	AW
pH	6.32 ± 0.01	1.62 ± 0.01
Conductivity (mS cm⁻¹)	19.51 ± 0.01	58.6 ± 0.1
T (°C)	24.2 ± 0.1	24.3 ± 0.1
Turbidity (10³ NTU)	2.1 ± 0.2	0.99 ± 0.08
TSS (g L⁻¹)	2.4 ± 0.3	8.9 ± 0.5
TDS (g L⁻¹)	6.2 ± 0.3	8 ± 2
COD (g O₂ L⁻¹)	4.1 ± 0.4	11 ± 4
BOD₅ (g O₂ L⁻¹)	4 ± 4	6 ± 1
O&G (g L⁻¹)	0.7 ± 0.3	3 ± 1
DOC (mg L⁻¹)	(41 ± 2) × 10	(36 ± 2) × 10
DN (mg L⁻¹)	11 ± 6	15 ± 6
Na⁺ (mg L⁻¹)	(2.8 ± 0.2) × 10 ³	62 ± 4
Cl⁻ (mg L⁻¹)	(3.5 ± 0.1) × 10 ³	(0.5 ± 0.1) × 10 ³
SO₄²⁻ (mg L⁻¹)	(3.4 ± 0.1) × 10 ³	(0.2 ± 0.1) × 10 ³
PO₄³⁻ (mg L⁻¹)	(0.9 ± 0.2) × 10 ³	(0.4 ± 0.2) × 10 ³
K⁺ (mg L⁻¹)	60 ± 6	14 ± 6

and turbulence in the equalisation tank. The presence of fine oil droplets causes light scattering and opacity, which is reflected in a high value of turbidity ($(2.1 \pm 0.2) \times 10^3$ NTU). Although this wastewater does not have a great quantity of solids, some of the bigger oil drops are retained in the filter used for TSS determination (2.4 ± 0.3 g L⁻¹), a common problem affecting the reliability of solids determination in VORWs (Boyer, 1984). All effluents from different processing lines suffer pH correction before entering the industrial wastewater treatment plant, leading to a pH value nearly neutral (6.32 ± 0.01) in this sample, which promotes oil emulsion stability.

On the other hand, AW wastewater has a very acid character ($\text{pH} = 1.62 \pm 0.01$) which destabilises emulsions. O&G concentration is higher in this sample (3 ± 1 g L⁻¹), but while the oils present in the homogenisation tank range from crude and neutralised oil to sodium oleates and phospholipids, in this particular effluent only waxes (very saturated esters) are present. These waxes agglomerate easily in bigger blobs, and do not disperse homogeneously in solution, being separated as solids ($\text{TSS} = 8.9 \pm 0.5$ g L⁻¹). Under turbulent mixing, this wastewater exhibits a yellow-orange colour, due to the solid matter in suspension. However, in quiescence, the underlying liquid has a pale yellow translucent appearance.

Both wastewaters present a high organic load, with DOC, COD and BOD₅ values ranging between 0.36-0.41 g C L⁻¹, 4.1-11 g O₂ L⁻¹ and 4-6 g O₂ L⁻¹, respectively. The TH sample presents a higher BOD₅/COD ratio, a sign of higher biodegradability, caused by the presence of edible polar greases. The lower BOD₅/COD ratio for AW wastewater is associated to the fact that waxes are not as prone to biodegradation.

Both effluents present high conductivity along with high concentrations of sodium, sulfate, chloride and phosphate (in the order of a few grams per liter). This is explained by the sequential steps of acidification and neutralisation during chemical refinement, which require the addition of

large amounts of acids (such as HCl, H₂SO₄ and H₃PO₄) and bases (such as NaOH). The ion concentrations are high on the homogenization tank because it collects wastewaters from the whole processing line.

4.4.2 Gravity separation kinetics

Table 4.2 presents the measured concentration values of O&G and COD, along with the corresponding removal percentages calculated using Equation 4.4, illustrating their evolution over time during gravity separation of each of the wastewater samples.

Experiments start as soon as the wastewaters are poured into the column and left in quiescent conditions. A steep decline in both O&G and COD concentrations is observed immediately afterwards, as the biggest particles ascend quickly and reach the surface. This is especially true in AW sample, because acid conditions promote coalescence and rapid separation between the oily and aqueous phases.

After 60 min, the rate of decrease of O&G and COD concentrations slows down considerably and removals begin to stabilise, approaching a maximum value. In AW wastewater both O&G and COD continue to decrease even after 24 h, albeit at a very slow rate. However, in TH wastewater the interparticle forces hold emulsified oil droplets in suspension and no further decrease is observed following the first 4 h of monitoring. The stability of this sample led to an acceptable overall removal of O&G and lower removal of COD (91% and 58% maximum, respectively).

Nevertheless, since maximum O&G removal exceeded 90% in both samples, it can be concluded that most of the oil eliminated with wastewaters is in the free oil form. Gravity separation is effective as a primary treatment for oil removal, even in the absence of pH correction or addition of coagulant aids. Other organics remain emulsified or dissolved, accounting for the residual O&G and COD, and must be subjected to a secondary treatment.

Final values of O&G range between 26 and 65 mg L⁻¹ and of COD between 1.1 and 1.7 g O₂ L⁻¹. These are above the allowable maximum values established by Portuguese legislation for wastewater discharge into water bodies (15 mg L⁻¹ for O&G and 150 mg O₂ L⁻¹ for COD (DL, 1998)). However, these results constitute acceptable values for an effluent from a primary treatment unit. Traditional gravity separators, such as those designed by the API, are expected to achieve a minimum of 100 mg L⁻¹ O&G concentration in the effluent water (API, 1990). Lower concentration objectives require more sophisticated separators, such as corrugated plate interceptors and parallel plate interceptors (Hydro-Flo Technologies, 2002). Nevertheless, regardless of the gravity separator design, O&G concentrations under 50 mg L⁻¹ are rarely achieved.

It can be concluded that gravity separation is a viable primary treatment for both vegetable oil refinery wastewaters under study. The approach is more effective with AW sample, which indicates a possible advantage in implementing a separate treatment strategy for this wastewater. However, the type and efficiency of the secondary treatment must be evaluated before making this decision.

Table 4.2: Results of O&G and COD monitoring over time and corresponding removal efficiency in gravity separation experiments.

<i>t</i> (min)	TH				AW			
	O&G (mg L ⁻¹)	<i>R</i> (O&G) (%)	COD (mg O ₂ L ⁻¹)	<i>R</i> (COD) (%)	O&G (mg L ⁻¹)	<i>R</i> (O&G) (%)	COD (mg O ₂ L ⁻¹)	<i>R</i> (COD) (%)
0	$(7 \pm 3) \times 10^2$		$(4.1 \pm 0.4) \times 10^3$		$(3 \pm 1) \times 10^3$		$(11 \pm 4) \times 10^3$	
5	$(2.4 \pm 0.8) \times 10^2$	$(7 \pm 2) \times 10$	$(2.9 \pm 0.3) \times 10^3$	29 ± 9	$(4 \pm 1) \times 10^2$	88 ± 6	$(2.4 \pm 0.7) \times 10^3$	$(8 \pm 1) \times 10$
15	$(2.1 \pm 0.7) \times 10^2$	$(7 \pm 1) \times 10$	$(2.7 \pm 0.3) \times 10^3$	35 ± 9	$(2.1 \pm 0.7) \times 10^2$	94 ± 3	$(1.7 \pm 0.5) \times 10^3$	85 ± 8
30	$(1.4 \pm 0.5) \times 10^2$	81 ± 9	$(2.4 \pm 0.3) \times 10^3$	42 ± 8	$(1.4 \pm 0.5) \times 10^2$	96 ± 2	$(1.6 \pm 0.3) \times 10^3$	85 ± 7
60	$(1.1 \pm 0.4) \times 10^2$	84 ± 8	$(1.96 \pm 0.07) \times 10^3$	53 ± 5	$(1.4 \pm 0.5) \times 10^2$	96 ± 2	$(1.4 \pm 0.9) \times 10^3$	$(9 \pm 1) \times 10$
120					$(1.1 \pm 0.4) \times 10^2$	97 ± 2	$(1.33 \pm 0.07) \times 10^3$	88 ± 5
145	$(1.0 \pm 0.3) \times 10^2$	87 ± 6	$(1.86 \pm 0.05) \times 10^3$	55 ± 4				
240	$(8 \pm 3) \times 10$	89 ± 5	$(1.73 \pm 0.05) \times 10^3$	58 ± 4	$(7 \pm 3) \times 10$	98 ± 1	$(1.23 \pm 0.05) \times 10^3$	89 ± 5
480	$(8 \pm 3) \times 10$	90 ± 5	$(1.75 \pm 0.05) \times 10^3$	58 ± 4	$(5 \pm 2) \times 10$	98.5 ± 0.7	$(1.17 \pm 0.05) \times 10^3$	89 ± 5
1440	$(7 \pm 2) \times 10$	91 ± 4	$(1.73 \pm 0.05) \times 10^3$	58 ± 4	$(3 \pm 1) \times 10$	99.2 ± 0.4	$(1.07 \pm 0.05) \times 10^3$	90 ± 4

4.4.3 Fitting of empirical model and optimisation of retention time

The mathematical description of the gravity separation process is useful to predict the concentrations and removals that result after a certain retention time. This information is very important when choosing the most adequate retention time for separator design and operation.

The best mathematical formula to fit the data obtained was a hyperbola using the removal efficiency and time as the dependent and independent variables:

$$R = R_{max} \frac{t}{k_t + t} \quad (4.6)$$

The empirical constant parameters can be assigned to a physical meaning: R_{max} is the maximum removal efficiency (%), and k_t is the time interval required to achieve half the maximum removal efficiency (min).

Models were adjusted to experimental data by non-linear curve fitting using Fig. P (Fig. P Software Corporation, distributed by BIOSOFT). Table 4.3 presents the results for model parameters in different datasets (O&G or COD, for both TH and AW wastewaters), along with the corresponding uncertainties and the correlation coefficient.

Table 4.3: Values of model parameters and corresponding correlation coefficients, obtained for O&G and COD removal from two VORWs.

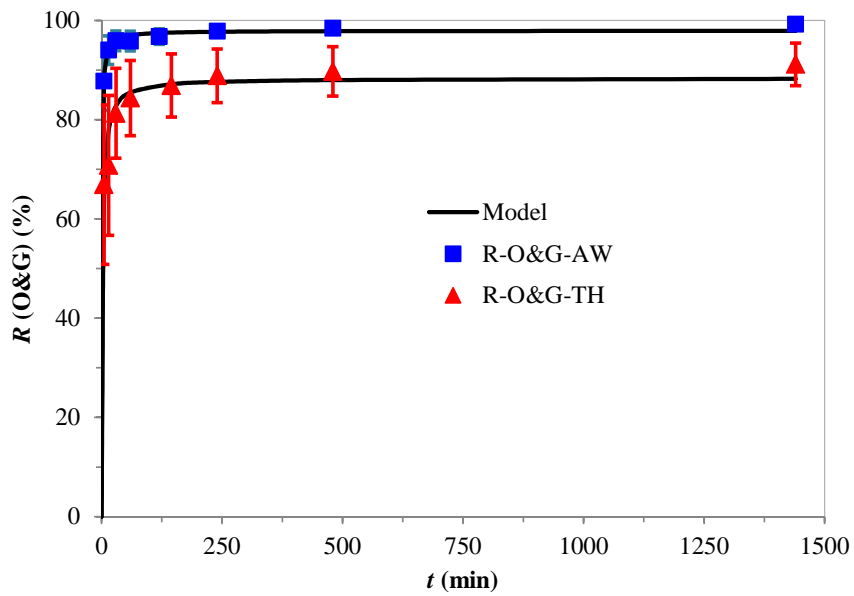
Sample	Parameter	Model parameters for empirical fit (Equation 4.6)		
		R_{max} (%)	k_t (min)	r^2
TH wastewater	O&G	88 ± 4	2.0 ± 0.9	0.988
	COD	58 ± 4	7 ± 3	0.976
AW wastewater	O&G	97.9 ± 0.8	0.6 ± 0.1	0.999
	COD	88.7 ± 0.9	0.7 ± 0.2	0.999

The model curves adjusted according to Equation 4.6 are depicted in Figure 4.1 along with experimental points. The models confirm previous conclusions and comparisons between datasets, namely that removal of O&G is greater than removal of COD, and that removals in AW wastewater are higher than in TH wastewater.

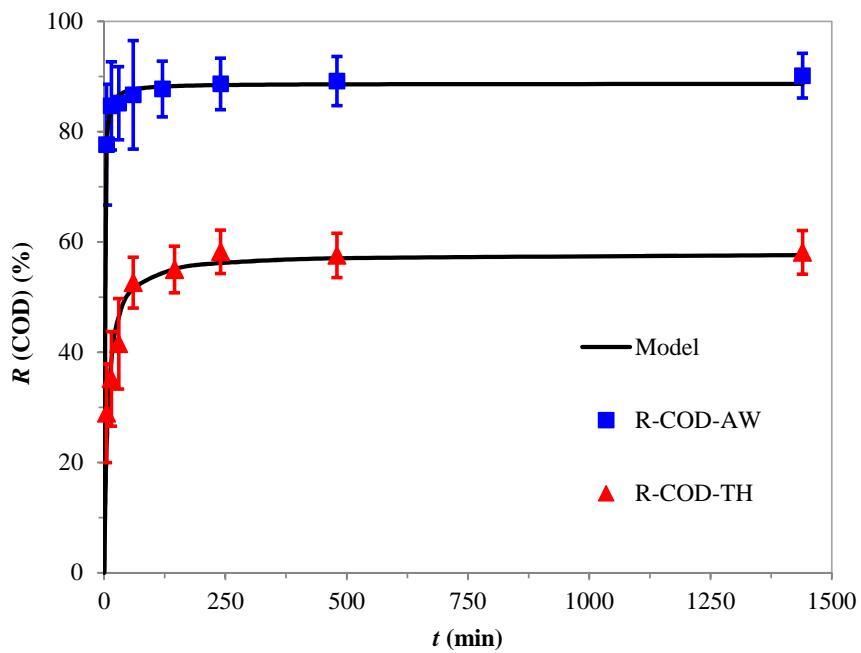
4.4.4 Influence of particle size vs. initial height and treatment time

Particle size in an oil-water dispersion or emulsion can be measured by optical techniques, such as laser diffraction. However, in a real wastewater, the presence of solids and other coloured substances precludes the determination of oil droplet size distribution through these methods.

In this work, the kinetics of the gravity separation process and corresponding empirical models together with the theoretical framework were used as a starting point to estimate the particle size distribution of oil droplets. The available data did not make possible the knowledge of the real particle size distribution, but allowed the plotting of 3D surfaces representing relationships between the different parameters or indicators.



(a) O&G



(b) COD

Figure 4.1: Graphical depiction of experimental removals and the corresponding empirical models adjusted by non-linear regression.

The physical properties used in the calculations, i.e. density of water and oil, viscosity of wastewater, height of the separating column (h_0) and acceleration of gravity, are presented in Table 4.4.

Table 4.4: Physical properties used in theoretical and empirical correlations (ρ_w , ρ_o , μ , h_0 and g).

	TH	AW
ρ_w (kg m^{-3})	$(100 \pm 1) \times 10$	$(99 \pm 1) \times 10$
ρ_o (kg m^{-3})	$(98 \pm 3) \times 10$	$(95 \pm 3) \times 10$
μ (Pa s)	$(8.90 \pm 0.04) \times 10^{-4}$	
h_0 (m)	0.357 ± 0.001	
g (m s^{-2})	9.80665	

Considering the following simplifications:

- an oil particle is a single point in space with initial height h in the separation column, which moves upwards at a constant rate corresponding to its terminal velocity v_t ;
- wall effects on the separation column are negligible;

then, this oil particle is removed after an interval of time t (Equation 4.7):

$$t(h, v_t) = \frac{h_0 - h}{v_t} \quad (4.7)$$

where h_0 is the height of the separating column (m).

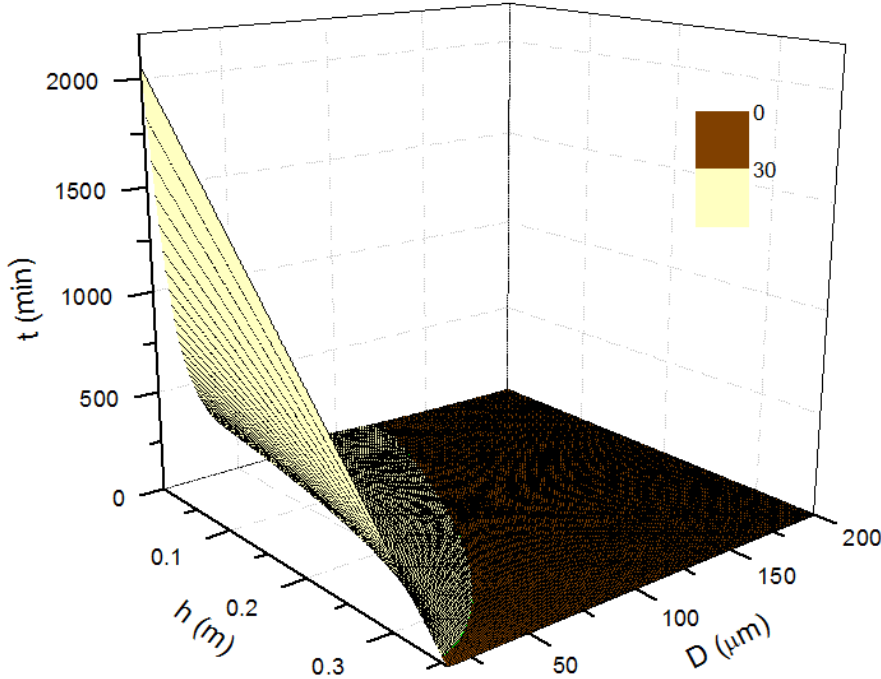
When both the velocity and the initial height come near zero, it is verified that the time of removal increases greatly. However, most dispersed particles have reasonable times of removal. For instance, droplets with velocities higher than 0.1 mm s^{-1} (0.0001 m s^{-1}) are removed in less than 100 min, whatever the initial height is.

Considering that the oil particles are spherical and of constant size, then Stokes' law (Equation 4.3) is valid, and each particle diameter corresponds to a terminal velocity. Substituting the velocity in Equation 4.7 by Equation 4.3, the time of removal t can be expressed in function of initial height h and particle diameter D (Equation 4.8):

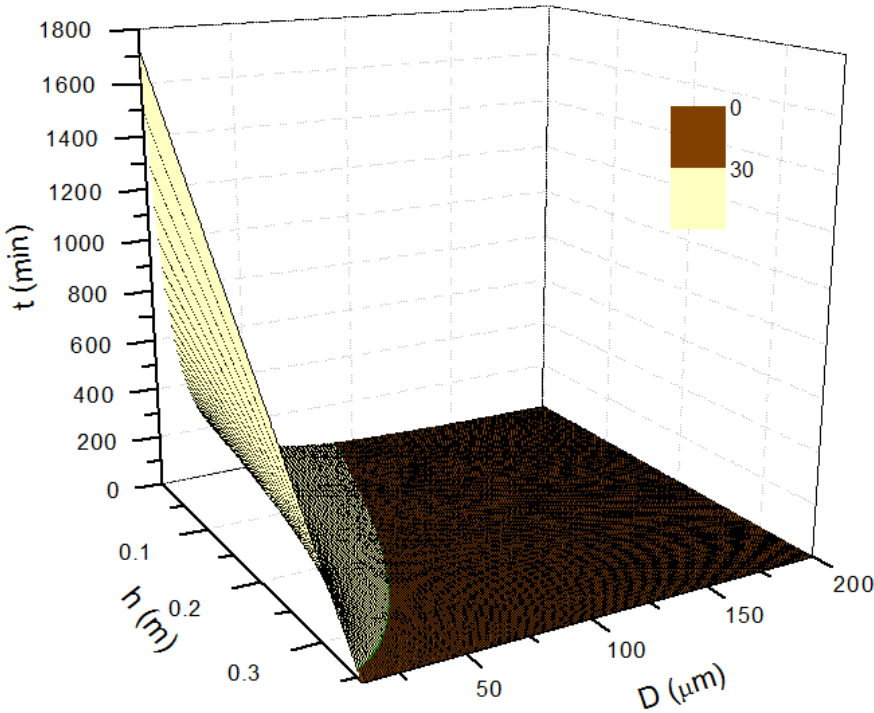
$$t(h, D) = \frac{18\mu(h_0 - h)}{g(\rho_w - \rho_o)D^2} \quad (4.8)$$

This relationship depends on the differential density between water and oil, therefore, the values will be different depending on the characteristics of the wastewater under study. Figure 4.2 presents 3D plots for Equation 4.8 for both TH and AW wastewaters. The time of removal increases for lower diameter and initial height, as has been stated before.

Finally, by using the empirical formula previously adjusted to kinetic data (section 4.4.3) and substituting the time t in Equation 4.6 by the expression of Equation 4.8, the removal R can be



(a) TH wastewater



(b) AW wastewater

Figure 4.2: 3D surface plots of treatment time t (min) as a function of h and D . Colour legend: brown for time of removal lower than 30 min; yellow for time of removal above 30 min.

expressed as a function of the initial height h and diameter D :

$$R(h, D) = \frac{18R_{max}\mu(h_0 - h)}{g(\rho_w - \rho_o)D^2k_t + 18\mu(h_0 - h)} \quad (4.9)$$

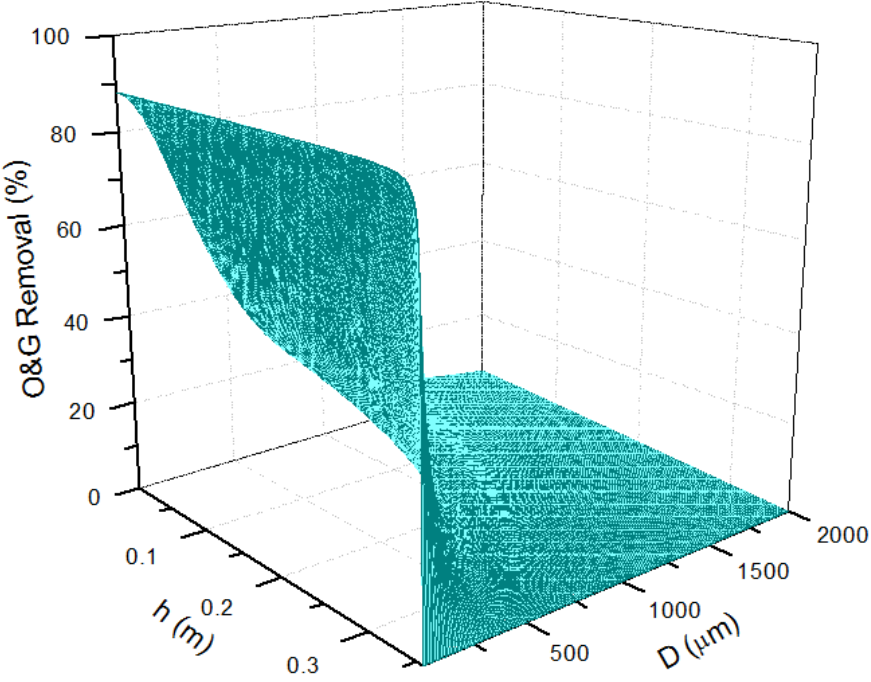
In physical terms, this means that when particles with diameter D at initial height h have reached the top of the column, $R\%$ of the total O&G is removed. Figure 4.3 presents the 3D plots for this relationship (using Equation 4.9) applied to both TH wastewater and AW wastewater. The surface plots are similar between them, except for the value of the maximum removal plateau, which is higher in AW wastewater. Through these graphs, it can be observed that particles with high diameter are removed at the beginning of treatment, while smaller particles reach the top of the column only when R approaches the maximum value, except if their initial height is close to h_0 . This indicates that small particles only make up a minor percentage of total O&G in these wastewaters.

4.4.5 Optimal treatment time

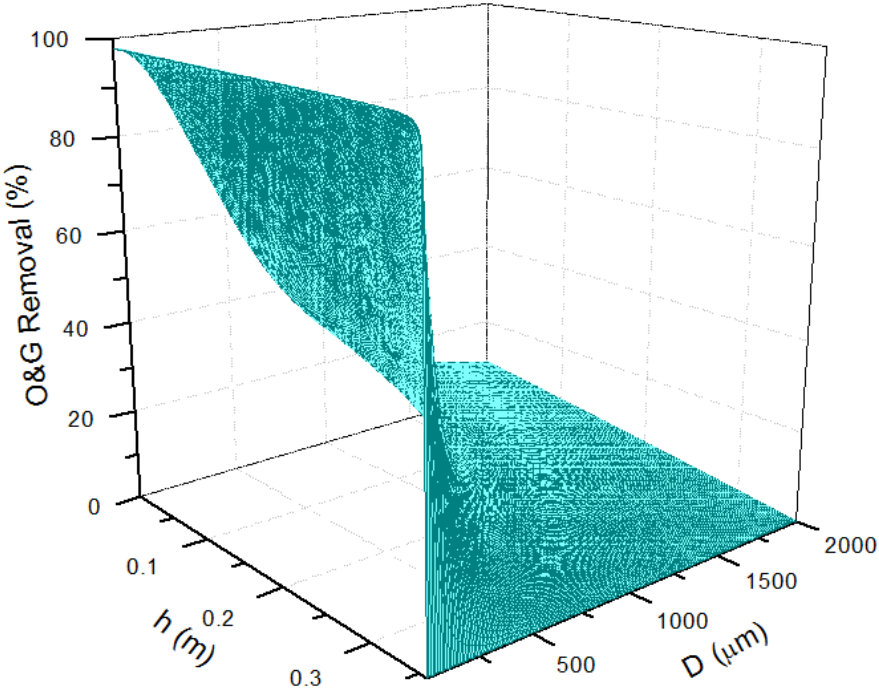
Treatment time optimisation in gravity separator design is usually done by calculating the terminal velocity of particles with a minimum target diameter (e.g., 150 μm , which is considered the threshold for “free oil” (Rhee et al., 1989)) and dimensioning a separator with a lower surface-loading rate (API, 1990). However, in this work, experimental kinetic data were used in the choice of the optimum treatment time, since they may represent the process more accurately, by indirectly accounting for phenomena such as coalescence which are not considered in the theoretical models chosen.

The choice of retention time for the gravity separator was done by observing Figure 4.1a, which represents the evolution of O&G removal in both TH and AW wastewaters, and by analysing the experimental data (Table 4.2) and the empirical model parameters (Table 4.3). Only O&G data were taken into account in this decision because O&G is considered to be the target pollutant of a gravity separation treatment. Other organic matter (which makes up the remaining COD) can be eliminated using a secondary step, which may involve coagulation, sorption, membrane separation or biological treatment, among others.

The rapid increase in removal observed in Figure 4.1a points to a choice of a short treatment time, since high removals and low concentrations can be obtained in 60 min or less. Comparing the treatment times of 15, 30 and 60 min, a significant decrease in O&G concentration is observed between the first two, while the removal seems to approach the stable plateau in the latter two. Bearing in mind that this is a primary treatment, and the wastewater will have to be submitted to a secondary treatment before discharge, it is perhaps unwise to double the retention time at the gravity separator for an improvement of only 1-3% in O&G removal. By choosing 30 min of treatment time, the removal determined experimentally (Table 4.2) is already very close to the maximum removal calculated when fitting the empirical model (Table 4.3). Meanwhile, the experimental O&G concentration (Table 4.2) after 30 min is $\approx 140 \text{ mg L}^{-1}$ in both wastewaters under study, which is an acceptable effluent concentration for primary treatment, especially considering



(a) TH wastewater



(b) AW wastewater

Figure 4.3: 3D surface plots of O&G removal (%) as a function of the treatment of particles with initial height h and diameter D .

that O&G in treated wastewater flowing out of traditional gravity separators is hardly ever under 100 mg L^{-1} (section 4.4.2).

In Figure 4.2, which represents the treatment time as a function of the initial height and diameter of oil particles, the surfaces have been divided to represent the fractions of particles which may be removed (dark brown colour) or not removed (light yellow colour) after the 30-min retention time. By observing these coloured surfaces, it is easy to visualize which particle sizes at which initial heights will be removed in the chosen treatment time. Particles with size as low as $15 \mu\text{m}$ will only be removed if they are close to the top (over 0.35 m height), however, the minimum diameter required for effective removal increases as the initial height in the column decreases. At the bottom of the column (0 m height), only particles over $75 \mu\text{m}$ and $125 \mu\text{m}$ (AW and TH wastewaters, respectively) will reach the surface of the wastewater. These values are compatible with the definition of “free oil” as oil particles under $150 \mu\text{m}$ as reported by Rhee et al. (1989). This type of oil, which is considered to be the main target of gravity separation (API, 1990), is completely removed in the process here optimised.

4.5 Conclusions

In this chapter, it was demonstrated that gravity separation is suitable as a primary treatment for VORWs.

This physical process yielded O&G removals over 90% and COD removals between 58 and 90% after 24 h. The kinetics of oily phase and COD separation, measured throughout the 24-h period, revealed that decrease of O&G and COD concentrations is very quick, stabilising and approaching the minimum after only 60 min. An empirical model of a hyperbola presented a good mathematical fit to the kinetics of O&G and COD removal.

The treatment time of a given particle was also calculated as a function of its initial position in the column and its diameter. The corresponding 3D representation allowed a visualisation of the influence of both variables. It was verified that only a minor portion of O&G present in two different wastewaters corresponds to particles with small diameters, such as those which consist of stable emulsified oil.

Finally, based on both the empirical and theoretical models and the data collected during the study, a treatment time of 30 min was chosen as the optimal retention time. The O&G and COD concentrations in the effluent do not yet comply with the maximum values allowed for discharge, but are adequate for inflowing to a secondary treatment. To design a gravity separator based on the empirical data collected in this study, further studies at pilot plant scale would be necessary to confirm the optimal treatment time, since the geometry and material of the column used can affect the performance of an industrial separator.

The replacement of existing treatment technologies with a two- or three-step strategy in which a 30-min gravity separation is the first operation has numerous advantages, such as downsizing more complex secondary or tertiary treatment methods, reducing chemicals and energy consumption, and improving the overall efficiency.

4.6 References

- API. *Design and Operation of Oil-Water Separators*. American Petroleum Institute, first edition, February 1990. API Publication 421, Monographs on Refinery Environmental Control - Management of Water Discharges.
- Aslan, S., Alyuz, B., Bozkurt, Z., and Bakaoglu, M. Characterization and biological treatability of edible oil wastewaters. *Polish Journal of Environmental Studies*, 18(4):533–538, 2009.
- Boyer, M. J. Current pollution control practices in the United States. *Journal of the American Oil Chemists' Society*, 61(2):297–301, 1984.
- Campo, P., Zhao, Y., Suidan, M. T., and Venosa, A. D. Aerobic fate and impact of canola oil in aquatic media. *Clean Technologies and Environmental Policy*, 14(1):125–132, 2012.
- Chipasa, K. B. Limits of physicochemical treatment of wastewater in the vegetable oil refining industry. *Polish Journal of Environmental Studies*, 10:141–147, 2001.
- CODATA. Recommended values for fundamental physical constants, 2010.
- Decloux, M., Lameloise, M.-L., Brocard, A., Bisson, E., Parmentier, M., and Spiraers, A. Treatment of acidic wastewater arising from the refining of vegetable oil by crossflow microfiltration at very low transmembrane pressure. *Process Biochemistry*, 42(4):693–699, 2007.
- DL. Decree-Law no. 236/98 from 1st August. In *Diario da Republica - I Serie A*. Portugal, 1998.
- Eaton, A. D., editor. *Standard methods for the examination of water and wastewater*. American Public Health Association, Baltimore, Maryland, 21st edition, 2005. Prepared and published jointly by American Public Health Association, American Water Works Association, Water Environment Federation.
- Ellison, S. L. R. and Williams, A., editors. *Eurachem/CITAC guide: Quantifying Uncertainty in Analytical Measurement*. Third edition, 2012.
- Frising, T., Noïk, C., and Dalmazzone, C. The liquid/liquid sedimentation process: From droplet coalescence to technologically enhanced water/oil emulsion gravity separators: A review. *Journal of Dispersion Science and Technology*, 27(7):1035–1057, 2006.
- Geetha Devi, M., Shinoon Al-Hashmi, Z. S., and Chandra Sekhar, G. Treatment of vegetable oil mill effluent using crab shell chitosan as adsorbent. *International Journal of Environmental Science and Technology*, 9(4):713–718, 2012.
- Grimes, B. A. Population balance model for batch gravity separation of crude oil and water emulsions. Part I: Model formulation. *Journal of Dispersion Science and Technology*, 33(4):578–590, 2012.
- Hendricks, D. W. *Water Treatment Unit Processes: Physical and Chemical*. Civil and Environmental Engineering. Taylor & Francis, 2006.
- Henschke, M., Schlieper, L. H., and Pfennig, A. Determination of a coalescence parameter from batch-settling experiments. *Chemical Engineering Journal*, 85(2–3):369–378, 2002.

- Hydro-Flo Technologies, Inc. Oil/water separator theory of operation, 2002. URL <http://www.oil-water-separator.hydroflotech.com/Engineering%20Data/Oil%20Water%20Separator%20Theory%20of%20Operation.htm>. accessed September 2014.
- IUPAC. Section: viscosity. In Marsh, K. N., editor, *Recommended reference materials for realization of physicochemical properties*. IUPAC, 1980.
- Kalyanaraman, C., Sri Bala Kameswari, K., Sudharsan Varma, V., Tagra, S., and Raghava Rao, J. Studies on biodegradation of vegetable-based fat liquor-containing wastewater from tanneries. *Clean Technologies and Environmental Policy*, 15(4):633–642, 2013.
- Noik, C., Palermo, T., and Dalmazzone, C. Modeling of liquid/liquid phase separation: Application to petroleum emulsions. *Journal of Dispersion Science and Technology*, 34(8):1029–1042, 2013.
- Pandey, R. A., Sanyal, P. B., Chattopadhyay, N., and Kaul, S. N. Treatment and reuse of wastes of a vegetable oil refinery. *Resources, Conservation and Recycling*, 37(2):101–117, 2003.
- Rhee, C. H., Martyn, P. C., and Kremer, J. G. Removal of oil and grease in oil processing wastewater. Technical report, Sanitation District of Los Angeles County, 1989.
- Stokes, G. G. On the theories of the internal friction of fluids in motion, and of the equilibrium and motion of elastic solids. *Transactions of the Cambridge Philosophical Society*, 8:287–305, 1845.
- Tezcan Un, U., Kopalal, A. S., and Bakir Ogutveren, U. Electrocoagulation of vegetable oil refinery wastewater using aluminum electrodes. *Journal of Environmental Management*, 90(1):428–433, 2009.

Chapter 5

The role of emulsion properties and stability on vegetable oil uptake by regranulated cork sorbents¹

5.1 Introduction

In the previous chapter, a primary treatment for VORW has been optimised, targeting “free oil” (particles over 150 μm diameter). Subsequently, a secondary treatment must aim to remove the finer, emulsified oily droplets which remain dispersed, because they are stabilised by interparticle interactions that supersede buoyant forces (API, 1990). As it has been reviewed in section 2.2.3.2, a common methodology used at this stage is coagulation/flocculation using inorganic salts, however, a major drawback to this option is the generation of large amounts of hazardous sludge, which must be disposed of accordingly.

Similarly, strictly physical methods, such as those presented in section 2.2.3.4, when in the absence of demulsifiers or coagulant aids, fail to provide adequate treatment. Membrane separation is capable of achieving high effluent purity and of enabling the recovery of the oily retentate, but the large energy requirements and the need for expensive maintenance are great disadvantages for practical application (Rhee et al., 1989; Pandey et al., 2003; Benito et al., 2010).

As shown in section 2.2.4, sorption is emerging as an alternative that combines the advantages of lower cost and possibility of oil recovery. Namely, cork granulates, such as regranulated cork sorbent, which has been shown in chapter 3 to be the most advantageous from a group of eight cork-derived sorbents for sunflower oil removal from water, can be applied for this purpose.

In this chapter, the chemical conditions for improving oil uptake by regranulated cork sorbents are studied further. In order to design successful treatment, it is necessary to understand the interactions occurring between oil droplets and sorbent particles to select operating conditions that

¹This chapter is based on the paper: Pintor, A. M. A., Souza, R. S., Vilar, V. J. P., Botelho, C. M. S., Boaventura, R. A. R. The role of emulsion properties and stability on vegetable oil uptake by regranulated cork sorbents. Working paper, 2014.

promote sorbate-sorbent bonding. There are few studies in the literature focusing on the influence of aqueous medium conditions which induce colloid destabilisation, such as pH and ionic strength, or probing on droplet-sorbent interactions with detailed measurements of droplet size distributions and zeta potential (ζ). This study aims to fill this gap by relating emulsion properties and stability to O&G uptake by regranulated cork sorbents.

5.2 Experimental

5.2.1 Materials

Cork granules used were of type RCG and have been characterised in chapter 3. Refined sunflower oil was collected from a vegetable oil refinery in Portugal. It had a density of $915.5 \pm 0.6 \text{ kg m}^{-3}$ and a viscosity of $(50.3 \pm 0.3) \times 10^{-6} \text{ m}^2 \text{ s}^{-1}$ at ambient conditions ($T = 25 \text{ }^\circ\text{C}$ and $P = 1 \text{ atm}$). These properties were determined by pycnometry and reverse-flow viscometry, respectively. Chemical reagents used for ionic strength adjustments, NaCl (JMGS), Na_2SO_4 (JMGS), and $\text{CaCl}_2 \cdot 2\text{H}_2\text{O}$ (Merck), were of high purity ($> 99.5\%$). Acidification solutions were prepared from concentrated H_2SO_4 (96%, Prolabo).

5.2.2 Analytical methods

The pH and temperature of solutions and emulsions was monitored using a HANNA HI 83141 portable meter coupled to a plastic-body, double-junction, gel, combination pH electrode (HI 1230B) and a stainless steel temperature probe (HI 7669AW). O&G concentrations were determined by the partition-infrared method using PCE as the extraction solvent (estimation of uncertainty in Appendix A).

Droplet size distributions were obtained by laser diffraction and polarization intensity differential scattering (PIDS) in a Beckman Coulter LS 230 equipped with a small volume module. The equipment operated in the range of particle diameters from 0.04 to 2000 μm . Zeta potential was measured in a Malvern Zetasizer Nano using disposable zeta cells.

5.2.3 Emulsion stability tests

The preparation of emulsions was carried out by adding sunflower oil to water in the range of 100-150 mg L^{-1} and submitting the mixture to intensive agitation at 8800 rpm (UltraTurrax MICCRA D-15, ART). Several agitation times were tested, ranging from 5 to 45 min, and the stability was evaluated by measuring the droplet size distribution right after agitation and then after 24 h at rest. Agitation times of over 15 min were divided into one or more cycles separated by intervals of equal duration to avoid overheating of the mixing device.

The stability over 24 h following pH adjustment was then studied. According to the best conditions to achieve a stable emulsion, oil-in-water emulsions were produced by agitation at 8800 rpm during three 10-min cycles separated by 10-min breaks and then pH was adjusted with H_2SO_4 0.05 M, 0.5 M or 5 M in the range of 2.0 to 6.0. Samples were taken after pH correction and

after 24 h in quiescence to determine the initial and final droplet size distributions and O&G concentrations.

5.2.4 Sorption tests

Sorption tests were carried out in 50-mL capped glass tubes containing 45 mL of sunflower oil-in-water emulsion (100-150 mg L⁻¹ O&G) in contact with 45 mg of cork granules. The tubes were placed in a rotating shaker (model SB3, Stuart) at 20 rpm, which was placed inside a thermostatic cabinet at a constant temperature of 25 °C during 24 h (time required to achieve equilibrium).

For the evaluation of the influence of pH on oil sorption, emulsions were produced in three 10-min cycles at 8800 rpm as previously mentioned in section 5.2.3, and the pH was corrected right after emulsification with H₂SO₄. Sorption tests were performed in the pH range of 2.0 to 7.2 (natural pH of the emulsion). No further pH adjustment was done throughout the experiment.

Samples were taken right after pH correction and after 24 h of contact with the sorbent to determine initial and final pH, O&G concentrations, droplet size distributions and zeta potential. Control samples, without sorbent addition, were also analysed. The sorption capacity (q) was calculated from the final O&G concentration values of the control and sorption experiments through a mass balance to the batch contactor:

$$q = \frac{V(C_c - C_f)}{W} \quad (5.1)$$

where V is the volume of emulsion (L), C_c is the final O&G concentration in the control experiment (mg L⁻¹), C_f is the final O&G concentration in the sorption experiment (mg L⁻¹), and W is the mass of sorbent added (g). The percent removal efficiency (R) was determined by the following expression:

$$R = \frac{C_c - C_f}{C_c} \times 100 \quad (5.2)$$

Ionic strength was varied by using different NaCl solutions of known molar concentration (0.02, 0.11 or 0.2 M) instead of distilled water in emulsion preparation. The study of the influence of NaCl concentration and pH on O&G removal efficiency was carried out using a 3-level, 2-factor (3²) full factorial design with duplicate runs, with levels and factors as presented in Table 5.1.

Table 5.1: Factor levels used in the 3² full factorial design.

Coded factor	Factor	Coded levels		
		-1	0	1
x_1	NaCl concentration (M)	0.02	0.11	0.20
x_2	pH	2	4	6

The results were analysed through analysis of variance (ANOVA) and response surface methodology, using software Statistica 5.1 (Statsoft, Inc.). A quadratic regression model taking into account two-way linear interactions was fitted to the experimental data:

$$\hat{y} = \beta_0 + \beta_1 x_1 + \beta_2 x_2 + \beta_{12} x_1 x_2 + \beta_{11} x_1^2 + \beta_{22} x_2^2 \quad (5.3)$$

where \hat{y} is the predicted response in O&G removal efficiency, x_1 and x_2 are the independent variables, or factors (coded as NaCl concentration and pH, respectively), β_0 is the regression coefficient for the intercept, β_1 and β_2 are the regression coefficients for linear effects, β_{12} is the regression coefficient for the two-way linear interaction effect of x_1 and x_2 , and β_{11} and β_{22} are the regression coefficients for quadratic effects (Box et al., 1978).

Additional sorption tests were carried out using emulsions prepared with solutions of Na_2SO_4 0.1 M and CaCl_2 0.1 M and later adjusted to pH 6.0, in order to assess whether the salt source altered the effect of the ionic strength on O&G removal. At the conditions of 0.2 M NaCl and pH of 6.0, zeta potential measurements were also carried out for the initial, control and final samples in order to compare with previous tests.

A sunflower oil sorption isotherm at 25 °C was obtained at the conditions of pH 6.0 and 0.2 M NaCl by changing the dosage of cork sorbent from 0.2 g L⁻¹ to 2.2 g L⁻¹. Assays were carried out using an equilibration time of 24 h. Kinetic studies at the same conditions were carried out using a cork dosage of 1.6 g L⁻¹. Samples were collected (each capped glass tube corresponds to one sample) at predetermined time intervals (0.5, 2, 4, 6, 8 and 24 h). A similar protocol was followed for a second kinetic study which was carried out with the rotating shaker at a speed of 2 rpm, in order to evaluate the influence of agitation conditions on sorption velocity.

All sorption tests were carried out in duplicate or triplicate and the results are presented as the average, including standard deviation as uncertainty.

5.3 Results and discussion

5.3.1 Production of a stable oil-in-water emulsion

Although many emulsification methods are available, by far the most common is mechanical shear. Under violent mixing action, several rupturing mechanisms are bound to occur which decrease the mean diameter of the dispersed phase and increase the homogeneity of the colloidal dispersion. The particle size resulting from this process is affected by a variety of factors, including the applied stress and the shearing protocol (Leal-Calderon et al., 2007).

After emulsification, the stability of the dispersion depends on the repulsion forces between droplets, which may delay or inhibit the occurrence of mechanisms of droplet aggregation such as Ostwald ripening and coalescence (Leal-Calderon et al., 2007). If particles become large enough, they may float by the action of gravity (creaming), ultimately joining a resolved phase separate from the continuous one.

Table 5.2 presents the results of sunflower oil-in-water emulsion production and stability, evaluated by the median droplet diameter (d_{50}) right after mechanical shearing and after 24 h of rest. For low shearing times, d_{50} in the emulsion decreased significantly in the 24-h period, because the larger droplets aggregated and floated to the surface. Leal-Calderon et al. (2007) highlight the importance of spatially homogeneous shear for controlling the droplet size. As this is quite difficult with a rotor-stator mixing device, the mixing times need to be longer for the maximum stress to

be applied to the whole volume. This is why a kinetically stable emulsion with a low droplet size was only achieved for a triple cycle of 10 min (separated by intervals of equal duration). After this shearing protocol, the emulsion still suffered slight creaming during the following 24 h, but the decrease in the median droplet size d_{50} was inferior to 10%.

Table 5.2: Median droplet diameter, measured right after mixing and following 24 h at rest, of emulsions produced during different protocols of mechanical shear.

Shearing Protocol	t (h)	d_{50} (μm)
5 min	0	8.4
	24	4.1
7 min	0	5.2
	24	2.8
10 min	0	4.6
	24	2.9
15 min	0	2.8
	24	2.4
10+10 min	0	2.6
	24	2.2
15+15 min	0	2.4
	24	2
10+10+10 min	0	2.2
	24	1.9

5.3.2 Emulsion stability after pH adjustment

It is believed that oil droplets acquire negative charge when dispersed in water due to the adsorption of hydroxyl ions (Zouboulis and Avranas, 2000; Welz et al., 2007). These charges are responsible for droplet-droplet repulsion and the inhibition of coalescence and Ostwald ripening. Therefore, a means to achieve emulsion destabilisation is to neutralise these charges. A straightforward way to do so is to increase the positive charges in the aqueous medium by lowering the pH (Boyer, 1984; Eckenfelder, 2000).

The destabilisation of sunflower oil-in-water emulsions by acidification was studied through the evaluation of changes in median droplet diameter, concentration of oil and grease (C (O&G)) and pH over a period of 24 h after pH correction. Figure 5.1 represents the changes (Δ) in each parameter, i.e. the difference between the final ($t = 24$ h) and the initial ($t = 0$ h) values of d_{50} , C (O&G) and hydrogen ion concentration (C_H), as a function of the initial pH after acidification. The pH increases over the 24-h quiescent period in all acidified emulsions, so the opposite of ΔC_H , which represents the consumed hydrogen ion concentration during the process, was represented instead in this case.

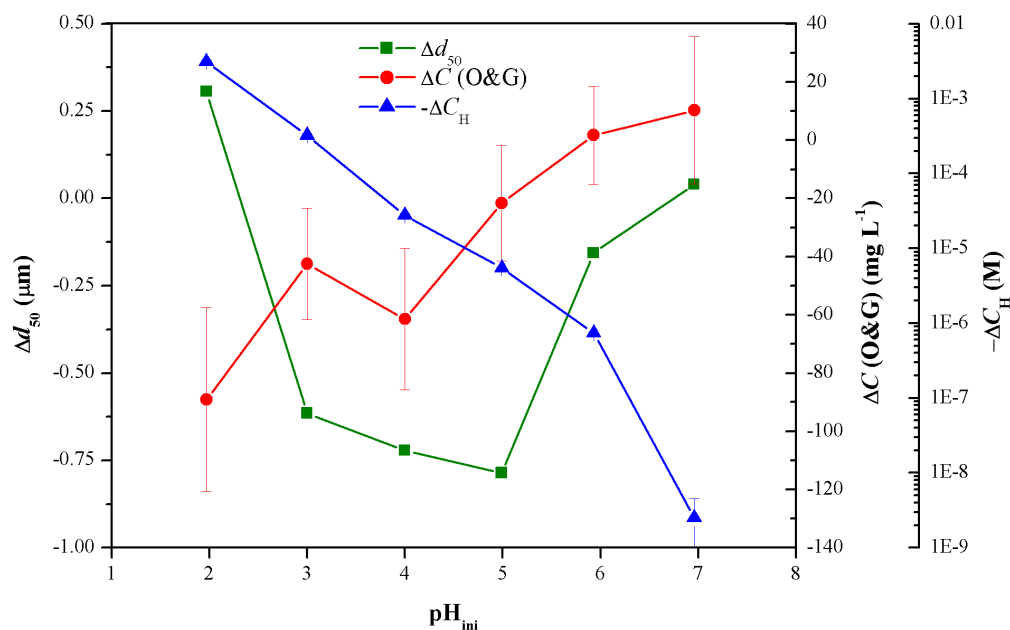


Figure 5.1: Changes (Δ) between final and initial values of oil concentration (C (O&G)), median droplet diameter (d_{50}), and the opposite of the change in hydrogen ion concentration (C_H), as a function of initial pH after acidification, in the study of emulsion stability with varying pH.

It is clear from the graph that acidic conditions favour emulsion destabilisation, since there is a greater decrease in O&G bulk concentration at lower pH, reflecting an increase in creaming. In the range of pH from 3 to 5, the same effect previously reported for unstable emulsions produced by an insufficient shearing protocol is observed: larger droplets aggregate and float towards the resolved oil phase, while smaller droplets remain dispersed, overall resulting in a decrease of d_{50} . At even lower pH, apart from the occurrence of substantial creaming and separation, the droplets which remain dispersed suffer aggregation, increasing d_{50} , and suggesting that further creaming might take place had the assay been extended.

The hydrogen ion concentration consumed increases with decreasing pH, which indicates that part of the positive charges introduced in the emulsion through acidification are used up in the neutralisation of negatively charged oil droplets. It can be concluded that charge neutralisation is the driving mechanism for the occurrence of coalescence, Oswald ripening, aggregation and creaming in these emulsions.

5.3.3 Influence of pH on oil sorption capacity

In the previous section it has been shown that acidification favours emulsion destabilisation, but it remains to be seen whether this is reflected in sorption uptake. Figure 5.2 shows that under acidic conditions the sorption capacity is enhanced, achieving a maximum of 101 mg L⁻¹ (with a cork dosage of 1 g L⁻¹) at pH 2.0.

A marked transition in O&G removal efficiency between pH 4 and 5 is observed due to the steep deflection from lower ranges of O&G removal and sorption capacity (45-50% and 60-70 mg g⁻¹,

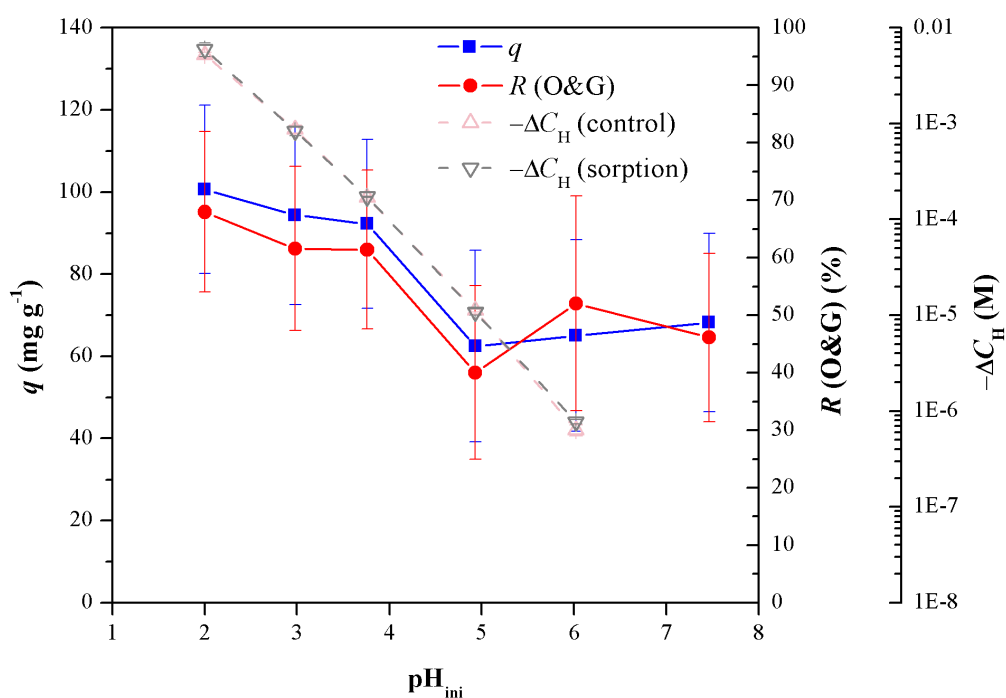


Figure 5.2: Sorption capacities (q) and removal efficiencies (R) of sunflower oil in water (initial concentration: 150-200 mg L^{-1}) onto cork granules (dosage 1 g L^{-1}) as a function of initial pH, along with the opposite of the change in hydrogen ion concentration between final and initial values in control and sorption assays.

respectively) towards improved treatment efficiency at pH below 4.

In previous studies on emulsified oil sorption by fungal biomass, walnut shell (Srinivasan and Viraraghavan, 2010) and chitosan (Ahmad et al., 2005a,b, 2006), it had also been observed that acidic pH improved sorption capacity. Geetha Devi et al. (2012) have later suggested in a study of oil uptake by chitosan that apart from the electrostatic effects on the emulsion, acidic conditions favour sorption due to the protonation of chitosan's amino groups, thereby increasing their attraction towards oil droplets. However, this is probably not the case in cork granules, since the hydrogen ion concentration consumed in the control and sorption assays is similar in the whole range of pH, indicating that the positive charges are used in oil droplet charge neutralisation. Potentiometric titration results shown in section 3.3.3.1 reveal that uptake of hydrogen ions by regranulated cork sorbent in acidic conditions amounts to around 0.2 mmol g^{-1} at pH 3. Such a difference is not found between control and sorption assays in the current study, so it is assumed that the effect of sorbent protonation in O&G uptake by cork granules is negligible.

Changes in droplet surface charge leading to variations in emulsion stability are often detected by measuring the zeta potential. Figure 5.3 presents the zeta potential profile at the initial and final (control and sorption) stages of the experimental assays at different pH. The trend is very clear: as the pH decreases, the zeta potential decreases in absolute value, approaching zero, the point at which surface charge neutralisation occurs and electrostatic repulsion forces no longer inhibit the aggregation of colloidal particles. Similar zeta potential profiles according to pH had already been observed for hydrocarbon oil-in-water emulsions (Shaw, 1991; Stachurski and Michalek, 1996).

Charge neutralisation, expressed by null zeta potential, is also frequently used as a parameter to evaluate the success of oily matter coagulation through metallic salts (Zouboulis and Avranas, 2000; Cañizares et al., 2008; Benito et al., 2010) and has been correlated once to increases in oil sorption uptake (Srinivasan and Viraraghavan, 2010), as it is here observed to occur in the treatment using cork granules.

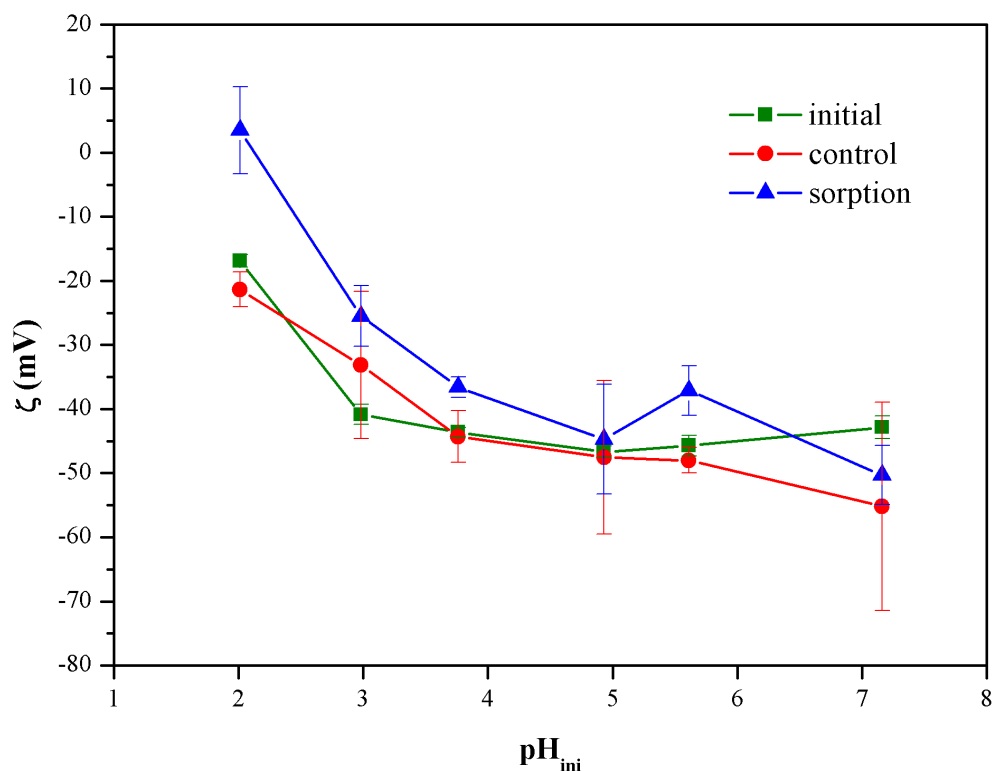


Figure 5.3: Evolution of zeta potential (ζ) (initial, and final in control assays and sorption assays) during 24-h sorption experiments at different pH.

However, even though charge neutralisation would be expected to cause agglomeration and coalescence of oil droplets, as it has been observed on the previous section, the measurements of particle size distribution after a 24-h period under agitation suggest otherwise. Figure 5.4 represents the variations of the median droplet diameter d_{50} from the initial value to final values in control and sorption tests. Since d_{50} is a statistical parameter, instead of representing the average with the standard uncertainty, points representing all replicates are exhibited. Rotating agitation prevents the occurrence of creaming in these conditions, and only coalescence can be expected; however, d_{50} remains the same or even decreases in control experiments, suggesting that even though the particle charge was neutralised, turbulence kept the emulsion stable. Moreover, in sorption tests, droplet diameter decreases significantly. A superficial analysis might suggest that cork granules simply took preference for the larger droplets in sorption, leaving the smaller ones behind; however, a closer look at the cumulative particle size distributions, such as the ones presented in Figure 5.5, reveals that this explanation cannot account entirely for the observed decrease in particle

size. While 100% of oil droplets after the sorption test at pH 6 are below $0.9 \mu\text{m}$ diameter, only 17% and 19% of oil droplets are below this size in the initial and control measurements, respectively. Since at this pH the removal efficiency was 52%, this means that not all of the 81-83% of droplets over $0.9 \mu\text{m}$ were sorbed onto cork, and therefore some (if not most) droplets either suffered breakage or were sorbed partially, causing a reduction in their size. Considering that droplet diameter after sorption decreases with pH, to the point that at pH 2 it is impossible to measure, these observations support the work of other authors (Ahmad et al., 2005a,b; Geetha Devi et al., 2012) which have previously suggested that droplet breakage via agitation might improve sorption due to an increase in the interfacial area available for oil-sorbent contact.

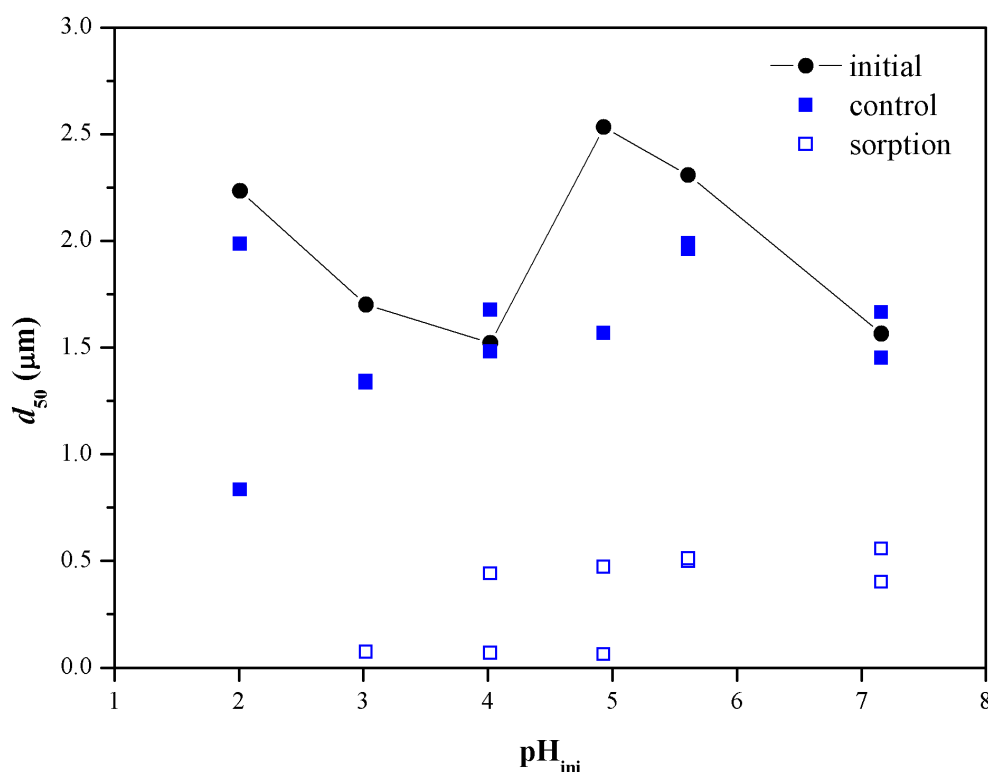


Figure 5.4: Evolution of particle size distribution measurements (initial, and final in control assays and sorption assays), represented by the median droplet diameter d_{50} , during 24-h sorption experiments at different pH.

5.3.4 Influence of ionic strength

Ionic strength is a very important parameter influencing colloid stability. When water contains a high concentration of ions (high ionic strength), the electric double layer of the oil droplets will be compacted, and therefore the zeta potential will be lower, making it easy to neutralise droplet-droplet repulsion forces (Shaw, 1991; Sawyer et al., 2003). Moreover, it is known that in VORWs the salt concentration is high (Pandey et al., 2003), so it may affect the performance of a possible

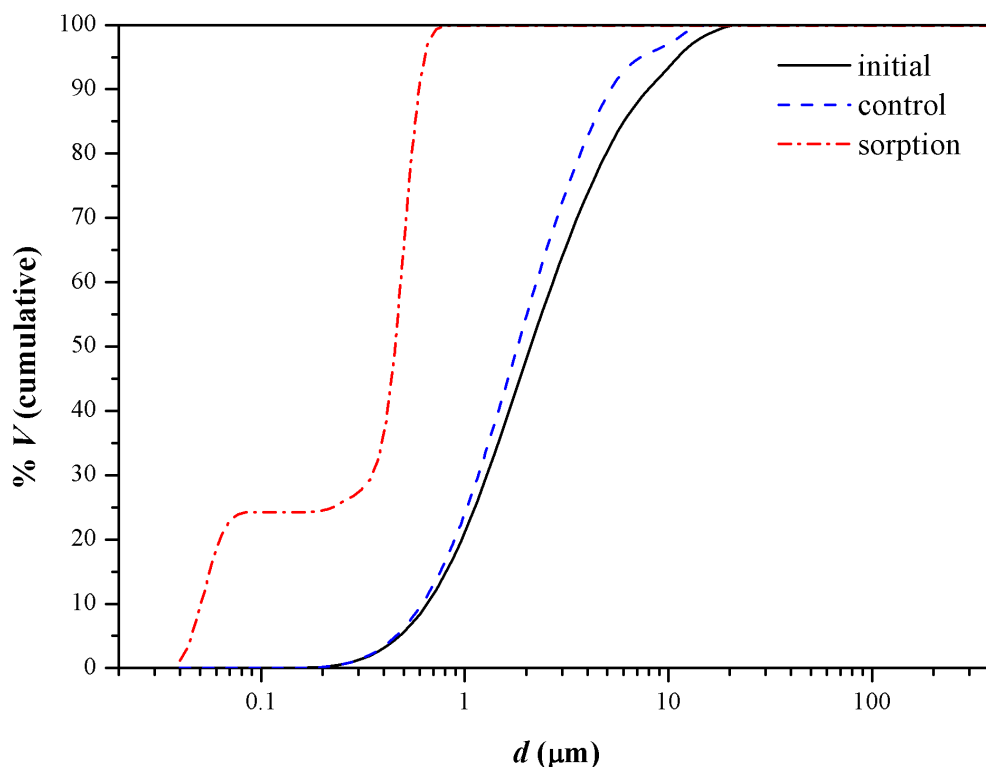


Figure 5.5: Cumulative particle size distributions (initial, and final in control assay and sorption assay) in the 24-h sorption experiment at pH 6.

treatment application. For these reasons, it was imperative to study the influence of ionic strength, by varying the salt concentration, in the sorption of sunflower oil from water using cork granules.

5.3.4.1 Full factorial design with NaCl concentration and pH as factors

The experimental results of the 3^2 full factorial design with duplicate runs used to study the effect of NaCl concentration and pH on O&G removal efficiency are presented in Table 5.3. The regression model of Equation 5.3 yielded the following second order polynomial using coded factors as variables:

$$\hat{y} = 93.1 + 122.7x_1 - 9.4x_2 + 56.7x_1x_2 - 715.0x_1^2 - 0.4x_2^2 \quad (5.4)$$

ANOVA enabled the calculation of the regression coefficient (r^2), and adjusted regression coefficient (adj- r^2), which were 0.890 and 0.844, respectively, indicating a fairly satisfactory fit to the experimental data. The statistical significance of the estimated effects of each factor was determined using the F -value and the p -value. The significance level (α) was set at 0.05, so every effect with a p -value below 0.05 was considered significant. The results are presented in Table 5.4.

It can be observed that only linear effects, of both pH and NaCl concentration and their combination, are significant. The increase in NaCl concentration is the most significant effect, thus confirming the aforementioned proposition that ionic strength plays a very important role in emulsion stability and influences the sorption of sunflower oil from water by cork granules.

Table 5.3: Runs and experimental responses in terms of O&G removal efficiency for the 3^2 full factorial design, along with the predicted values obtained by the quadratic regression model and the corresponding residuals.

x_1 (M)	x_2	y ($R(\text{O\&G})_{\text{exp}}$) (%)	\hat{y} ($R(\text{O\&G})_{\text{pred}}$) (%)	Residual
0.02	6	40.2	34.4	5.8
		35.7	34.4	1.3
0.02	4	43.6	57.2	-13.6
		63.3	57.2	6.1
0.02	2	75.9	77.5	-1.6
		79.7	77.5	2.2
0.11	6	50.6	67.7	-17.1
		72.3	67.7	4.6
0.11	4	84.3	80.3	4.0
		88.6	80.3	8.3
0.11	2	87.8	90.4	-2.6
		93.4	90.4	3.0
0.20	6	87.5	89.5	-2.0
		97.0	89.5	7.5
0.20	4	89.8	91.9	-2.1
		89.3	91.9	-2.6
0.20	2	89.8	91.7	-1.9
		92.7	91.7	1.0

Table 5.4: ANOVA table of the full factorial design, with F -values and p -values for estimating the statistical significance of factors. In bold, significant factors with $p < 0.05$.

	Sum of squares	df	Mean square	F -value	p -value
x_1 (L ^a)	3594.9	1	3594.9	57.1	7×10^{-6}
x_1 (Q ^b)	134.2	1	134.2	2.1	0.17
x_2 (L)	1541.3	1	1541.3	24.4	3.4×10^{-4}
x_2 (Q)	6.4	1	6.4	0.1	0.75
x_1 (L) by x_2 (L)	834.4	1	834.4	13.3	0.0034
Error	755.3	12	62.9		
Total sum of squares	6866.5	17			

^a Linear effect

^b Quadratic effect

Figure 5.6 depicts the 3D response surface as described by Equation 5.4. The graph clearly shows the tendency toward increase in O&G removal efficiency with rising NaCl concentration and decreasing pH. A peak solution is not obtained within the range of levels studied; the mathematical maximum corresponds to limit conditions of NaCl 0.2 M. Increasing the NaCl concentration further or decreasing the pH toward more acid levels would not be recommended in practical applications. Too much salt would cause disturbances in downstream treatment (e.g. biological reactors or membranes), and would increase the demands for salt removal in order to comply with the discharge limits. Furthermore, acidifying the emulsion below 2 might not be adequate in practice because the treatment infrastructure, including pipes, tanks and pumps, would need to be more robust, and, therefore, more expensive, to prevent corrosion by the acid medium.

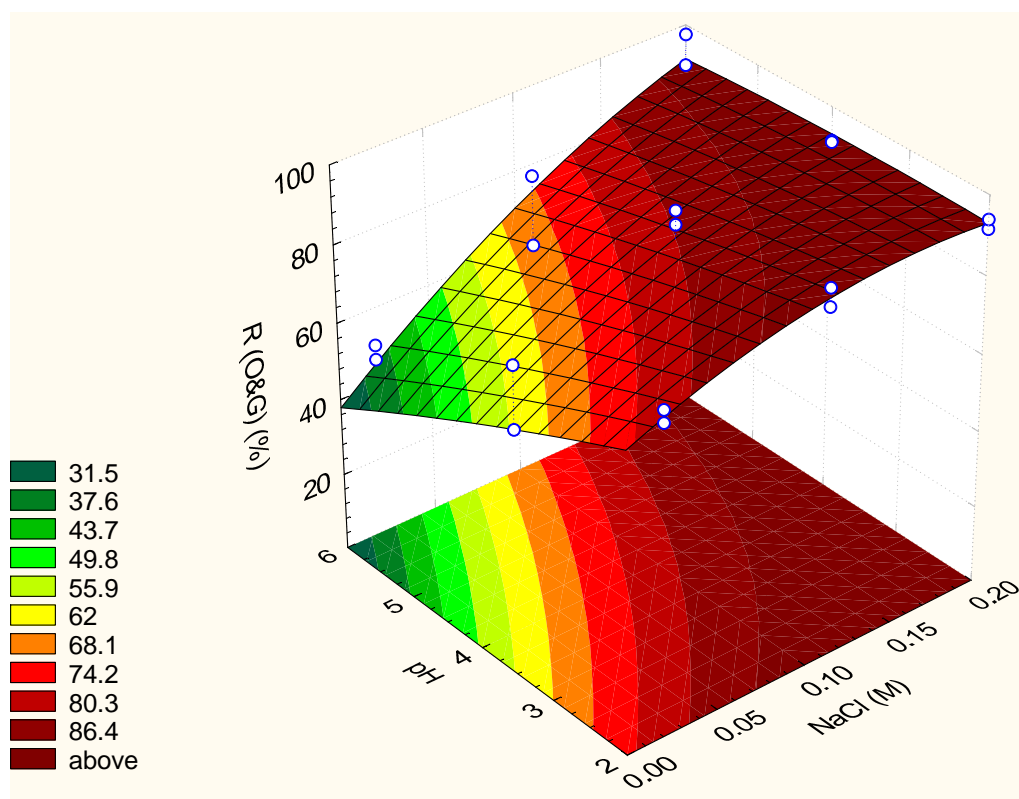


Figure 5.6: 3D response surface of O&G removal efficiency in function of NaCl concentration and pH, as determined by the quadratic regression model. The experimental points are represented in white circles bordered in blue.

The range of levels under study corresponds, therefore, to operating conditions which are feasible in practical applications, and the effects of each factor in O&G removal can be used to infer the best values to apply in further tests. High ionic strength is the most significant factor and, as such, when it is present in oily wastewaters it is beneficial to O&G sorption. When the ionic strength is low, the negative effect of pH is more pronounced, so strong acidification is needed. Alternatively, NaCl can be added to increase the ionic strength up to 0.2 M. It is possible that emulsified oil will be more detrimental to downstream tertiary treatment than higher concentrations of salt, especially in the case of membranes. When salt concentration is high, excessive acidification should be

avoided. At 0.2 M NaCl, O&G uptake is very similar at all three levels of pH (Table 5.3), so the highest value of 6 can be used without considerable loss in removal efficiency. These conditions were used in further sorption experiments reported in this chapter.

5.3.4.2 Emulsion stability at selected operating conditions

The evolution of zeta potential in sorption experiments was measured using the operating conditions selected above. The results are presented in Figure 5.7, where they are compared with similar measurements previously carried out in the absence of NaCl at pH \approx 6 and 2.

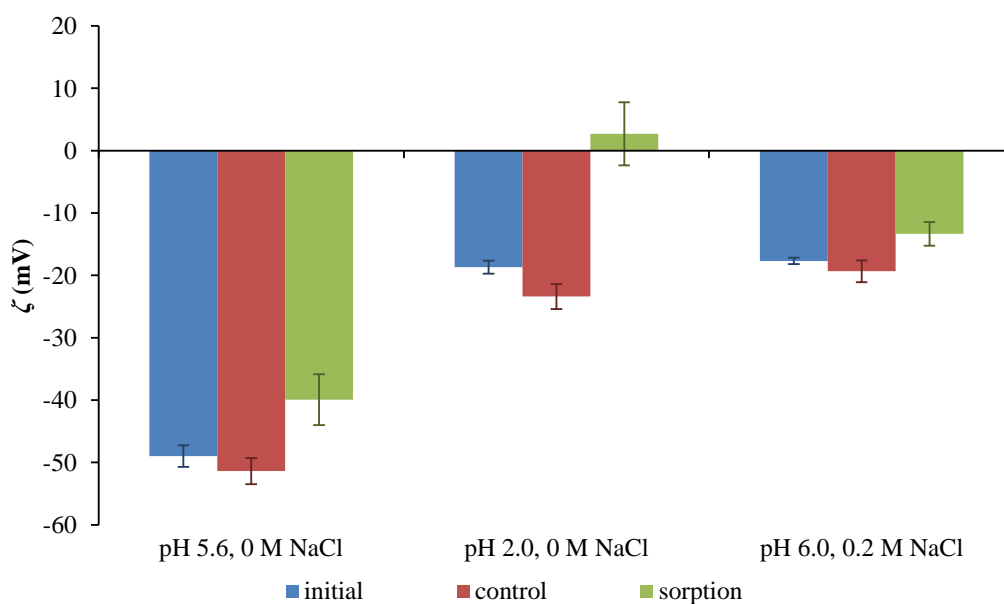


Figure 5.7: Evolution of zeta potential (ζ) (initial, and final in control assays and sorption assays) at the selected operating conditions of 0.2 M NaCl and pH 6, and its comparison with measurements in the absence of salt at pH 5.6 and 2.

It can be observed that the presence of 0.2 M NaCl has a similar effect in zeta potential as the acidification to pH 2 in the absence of salt. However, the mechanism is different in both instances. In acidification, neutralisation of the negative charge of oil droplets occurs, reducing the repulsion forces between them and facilitating their uptake by cork granules. On the other hand, when ionic strength is increased, what occurs is a compression of the double layer, reducing the reach of the repulsive electrostatic forces. Without a repulsive energy barrier, attraction by van der Waals forces becomes the main force of droplet-droplet and droplet-sorbent interaction upon collision in the aqueous medium (Sawyer et al., 2003).

5.3.4.3 Influence of salt source

In order to confirm that the observed effects due to salt concentration are correctly attributed to the increase in ionic strength in the solution, and not by any specific action of NaCl, sorption experiments, at similar operating conditions, were carried out using Na_2SO_4 and CaCl_2 as the

added salts for ionic strength control. NaCl and Na₂SO₄ were used because they are widely available salts, and because sodium, chloride and sulphate are the predominant ions in the VORW samples studied (Chapter 4, Table 4.1). CaCl₂ was used to investigate the effect of a larger cation, calcium, in droplet charge neutralisation. Since Na₂SO₄ is composed by a double-charged anion, and CaCl₂ by a double-charged cation, a concentration of only 0.1 M was used for these salts. O&G removal efficiencies, at pH 6, were 90 ± 3 % and 79 ± 7 % using 0.1 M Na₂SO₄ and 0.1 M CaCl₂ as salt sources, respectively. When comparing to the removal efficiency with NaCl 0.2 M, 92 ± 5 %, at a pH of 6, it can be concluded that the difference between the results is not very significant, so it is assumed that, for the selected operating conditions, the salt source is not an important factor.

5.3.5 Sorption kinetics and isotherm

The study of sorption equilibria was carried out by determining the sorption isotherm at 25 °C in the selected operating conditions of 0.2 M NaCl and pH 6. The Freundlich model, expressed by Equation 5.5, was successfully fitted to the experimental data (Freundlich, 1907).

$$q_{eq} = K_F C_{eq}^{1/n} \quad (5.5)$$

where q_{eq} is the sorbed amount at equilibrium (mg g⁻¹), K_F is the Freundlich constant (mg^(1-1/n) L^{1/n} g⁻¹), C_{eq} is the concentration of O&G at equilibrium (mg g⁻¹) and n is a dimensionless parameter related to sorbate-sorbent affinity.

The fit was carried out using the program Fig. P (Fig. P Software Corporation, Biosoft, USA) and yielded 11 ± 6 mg^(1-1/n) L^{1/n} g⁻¹ for K_F and 1.0 ± 0.2 for n , with an r^2 of 0.830. The experimental points are represented along with the adjusted curve in Figure 5.8.

Since n is close to 1, it can be assumed that the main mechanism of sorption is partitioning, and that K_F is an approach to a sorption partition coefficient. If n is set to 1, the linear sorption isotherm results:

$$q_{eq} = K_p C_{eq} \quad (5.6)$$

where K_p is the partition/sorption coefficient (L g⁻¹; L kg⁻¹). The fitting of the linear model yields a K_p of (10.1 ± 0.6) × 10³ L kg⁻¹ with an r^2 of 0.828.

The partition coefficient K_p can be converted to the organic-carbon-normalized partition coefficient (K_{oc}) if the fraction of organic carbon (f_{oc}) in the solid is known. In the cork granules used for sorption, it can be assumed that all carbon is organic, since the ash content is only 1.24%. Thus the f_{oc} corresponds to the total carbon in the solid, which has been determined to be 70.22% (Table 3.1). Using the following relationship between the partition coefficients (Sawyer et al., 2003):

$$K_{oc} = \frac{K_p}{f_{oc}} \quad (5.7)$$

K_{oc} was calculated to be (14.4 ± 0.8) × 10³ L kg⁻¹. From this organic-carbon-normalized partition coefficient, the octanol-water partition coefficient (K_{ow}), most commonly expressed as log K_{ow} ,

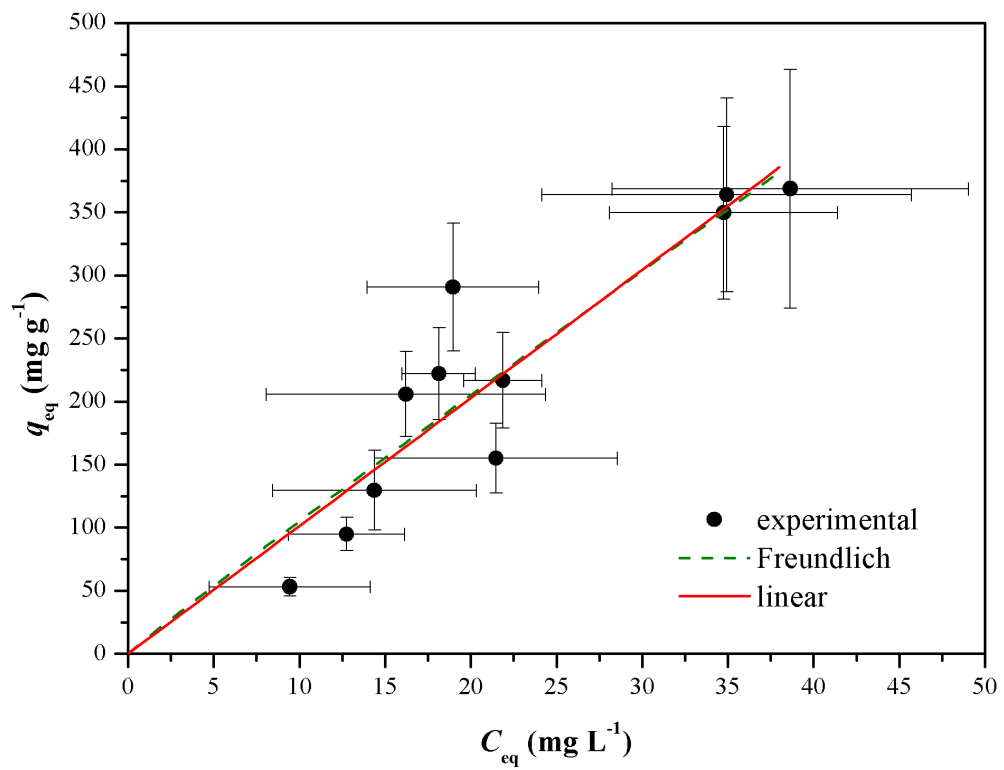


Figure 5.8: Experimental data for isothermal equilibria at 25 °C of the sorption of sunflower oil from water by cork granules, at the selected operating conditions of 0.2 M NaCl and pH 6, along with fitted curves of the Freundlich equation and linear partitioning model.

can be obtained using the following empirical equation (Sawyer et al., 2003):

$$K_{ow} = \frac{K_{oc}}{0.63} \quad (5.8)$$

The calculated value for $\log K_{ow}$ was 4.36 ± 0.02 . The results here obtained are similar to estimates reported in a review of Annex IV of Regulation (EC) no. 1907/2006 (REACH), which document a K_{oc} for sunflower oil of $1.17 \times 10^4 \text{ L kg}^{-1}$ (DHI, 2008).

The final objective in the sorption of sunflower oil from water by cork granules must be the reduction of O&G to concentration values which are compliant with discharge levels defined by legislation. In Portugal, the maximum O&G concentration admitted in discharge is 15 mg L^{-1} (DL, 1998). For the treatment of an oil-in-water emulsion with $\approx 150 \text{ mg L}^{-1}$ O&G, with aqueous phase conditions of pH 6 and 0.2 M NaCl, a dosage of 1.6 g L^{-1} is needed to guarantee with a standard error uncertainty interval that an equilibrium concentration of $13 \pm 2 \text{ mg L}^{-1}$ O&G will be achieved, according to calculations derived from the fit to the Freundlich model (Equation 5.5). Therefore, this dosage was used in further studies on the kinetics of O&G removal.

The results of two kinetic studies, at rotating speeds of 2 and 20 rpm, are presented in Figure 5.9. A theoretical mass transfer model for an isothermal sorption process was developed in order to predict the kinetics of oil uptake by cork granules. Starting with a mass balance to the batch contactor, given by the following expression:

$$-V \frac{dC_b}{dt} = W \frac{dq}{dt} \quad (5.9)$$

where C_b is the O&G concentration in the bulk liquid (mg L^{-1}), V is the volume of liquid in the reactor (L), W is the mass of sorbent (g), t is the contact time (s) and q is the sorbed amount (mg g^{-1}) at time t .

Since the porosity of cork granules consists almost exclusively of external macropores (chapter 3), intraparticle diffusion was estimated to be negligible ($q = q_{eq}$, where q_{eq} is the sorbed amount at the surface) and instantaneous surface equilibrium between q_{eq} and C_{eq} , the O&G concentration near the solid's surface, was assumed to occur according to the linear partitioning model (Equation 5.6). Considering the formation of an external sublayer around the cork particles, in which the oil droplets diffuse from the bulk fluid to the surface of the particles, and assuming the cork granules to be spherical particles, the following equation can be established:

$$\frac{dC_b}{dt} = -\frac{1}{\tau_f} (C_b - C_{eq}); \tau_f = \left(\frac{\varepsilon_b}{1 - \varepsilon_b} \right) \frac{1}{k_f a_p} \quad (5.10)$$

where τ_f is the time constant for film diffusion (s), ε_b is the bulk porosity, k_f is the film mass transfer coefficient ($\text{cm}^3 \text{ cm}^{-2} \text{ s}^{-1}$) and a_p is the external surface area per unit particle volume ($\text{cm}^2 \text{ cm}^{-3}$), given by $a_p = \frac{3}{r_p}$, where r_p is the particle radius (cm). Replacing Equations 5.6 and

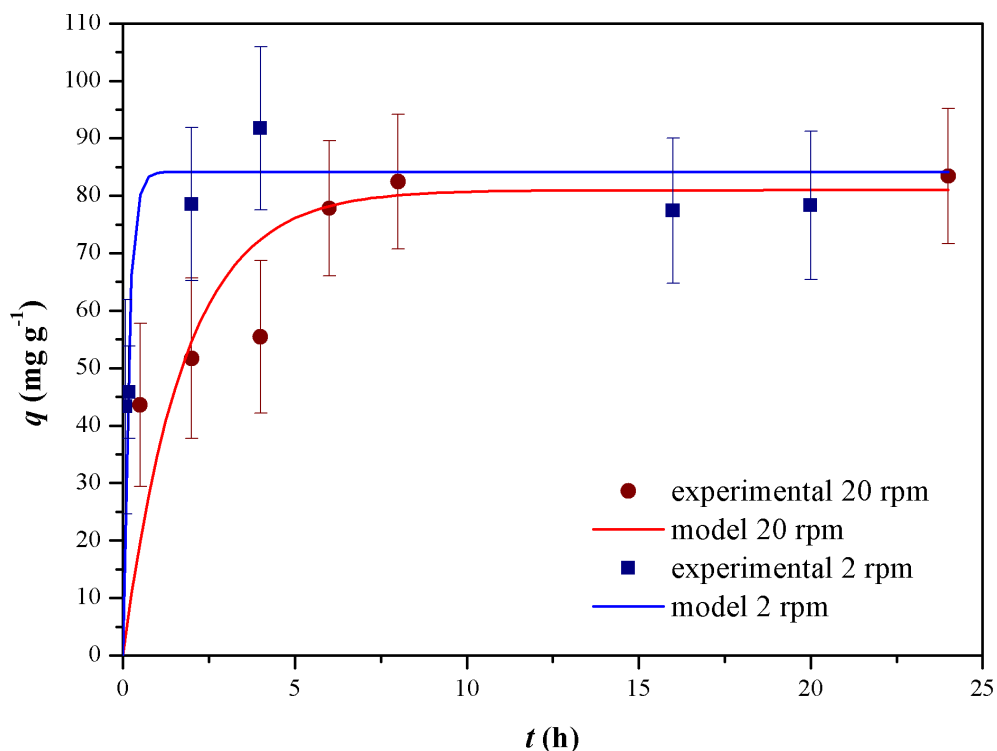


Figure 5.9: Experimental data for the kinetic studies for both rotating speeds of 2 and 20 rpm of the sorption of sunflower oil from water by cork granules (dosage: 1.6 g L^{-1}), at the selected operating conditions of 0.2 M NaCl and $\text{pH } 6$, along with the fitted curves of the mass transfer model.

5.9 in Equation 5.10 and solving for q , the following expression can be obtained:

$$q = \frac{K_p C_{b_0}}{1 + \xi_m} \left(1 - \exp \left(- \left(\frac{1 + \xi_m}{\xi_m} \right) \frac{1}{\tau_f} \right) \right); \xi_m = \frac{W}{V} K_p \quad (5.11)$$

where C_{b_0} is the initial O&G concentration in the bulk liquid (mg L^{-1}) and ξ_m is the batch mass capacity factor.

The model was fitted to the experimental data by nonlinear least squares fitting using Solver, assuming a cork density of 540 g L^{-1} (Table 3.1) and a particle radius of 0.15 cm (average value of the particle size range between 1.0 and 2.0 mm), and considering initial O&G concentrations of 143.2 mg L^{-1} at 2 rpm and 137.7 mg L^{-1} at 20 rpm . The resulting curves can be observed alongside the experimental data in Figure 5.9. The model adequately predicts the experimental data.

It can be observed that the kinetics is faster at the rotating speed of 2 rpm , with a model time diffusion constant τ_f of $(6 \pm 2) \times 10^2 \text{ s}$ and a mass transfer coefficient k_f of $(2.7 \pm 0.7) \times 10^{-2} \text{ cm s}^{-1}$. At 20 rpm , the mass transfer was slower by one order of magnitude, with model parameters of $(7 \pm 3) \times 10^3 \text{ s}$ for τ_f and $(2.5 \pm 1.0) \times 10^{-3} \text{ cm s}^{-1}$ for k_f . The results are counter-intuitive, since it would be expected that faster rotation would improve mass transfer by promoting homogenisation and contact between sorbate and sorbent, leading to a decrease in the film thickness. A possible explanation of this result lies in the creation of excessive turbulence at higher rotating speed. The collisions between oil droplets and cork particles may be too violent in these condi-

tions, with friction in the external fluid film around the sorbent undermining the creation of bonds between oil and the cork surface. Furthermore, previous studies by [Das and Kinsella \(1993\)](#) and [Kumar et al. \(1996\)](#) suggest that gentle stirring of oil-in-water emulsions avoids creaming but accelerates coalescence in bulk. It is possible that the agitation provided at 2 rpm has the same effect, but instead of droplet-droplet aggregation, it promotes sorbate-sorbent bonding.

Finally, while the increase in sorption is very sharp for the kinetics at 2 rpm, with the achievement of equilibrium predicted by the model to occur at less than 2 h of contact time, at 20 rpm removal of O&G is faster at the initial stage, and gradually decreases until it reaches equilibrium between 6 and 8 h.

5.4 Conclusions

In this chapter, it has been shown that sorption of sunflower oil onto regranulated cork granulates can be improved having in consideration the chemistry of the emulsion.

Removal efficiency and sorption capacity are strongly dependent on the electrostatic repulsive forces between oil droplets. Acidification is the most straightforward way to counter negative surface charges and neutralise the zeta potential of the emulsion, causing destabilisation and inhibiting oil uptake by cork sorbents. High ionic strengths facilitate this process by bringing about double layer compression and zeta potential reduction, thus enabling the neutralisation of repulsive forces at higher pH.

Isothermal sorption equilibria could be well described by the Freundlich equation and by a linear model. The main sorption mechanism is partitioning, and the kinetics of the process is governed by an external fluid film resistance, since uptake at the surface is instantaneous and intraparticle diffusion is negligible.

The kinetics were found to be influenced by the speed of the rotating shaker. Slower rotation promoted sorbate-sorbent aggregation, while faster rotation impaired mass transfer due to increased resistance in the external fluid film caused by turbulence and friction. Nevertheless, as it was expected, equilibrium capacity and concentration were similar regardless of agitation speed.

The kinetic mass transfer model assuming a linear partitioning isotherm equation could adequately predict the treatment of sunflower oil-in-water emulsions containing approximately 140 mg L⁻¹ O&G to final concentrations compliant with the maximum limit for O&G imposed by Portuguese legislation for wastewater discharge into water bodies.

5.5 References

Ahmad, A. L., Sumathi, S., and Hameed, B. H. Residual oil and suspended solid removal using natural adsorbents chitosan, bentonite and activated carbon: A comparative study. *Chemical Engineering Journal*, 108(1-2):179–185, 2005a.

Ahmad, A. L., Sumathi, S., and Hameed, B. H. Adsorption of residue oil from palm oil mill effluent using powder and flake chitosan: equilibrium and kinetic studies. *Water Research*, 39(12):2483–2494, 2005b.

- Ahmad, A. L., Sumathi, S., and Hameed, B. H. Coagulation of residue oil and suspended solid in palm oil mill effluent by chitosan, alum and PAC. *Chemical Engineering Journal*, 118(1-2):99–105, 2006.
- API. *Design and Operation of Oil-Water Separators*. American Petroleum Institute, first edition, February 1990. API Publication 421, Monographs on Refinery Environmental Control - Management of Water Discharges.
- Benito, J. M., Cambiella, A., Lobo, A., Gutierrez, G., Coca, J., and Pazos, C. Formulation, characterization and treatment of metalworking oil-in-water emulsions. *Clean Technologies and Environmental Policy*, 12(1):31–41, 2010.
- Box, G. E. P., Hunter, W. G., and Hunter, J. S. *Statistics for experimenters: an introduction to design, data analysis, and model building*. Wiley, 1978.
- Boyer, M. J. Current pollution control practices in the United States. *Journal of the American Oil Chemists' Society*, 61(2):297–301, 1984.
- Cañizares, P., Martínez, F., Jiménez, C., Sáez, C., and Rodrigo, M. A. Coagulation and electrocoagulation of oil-in-water emulsions. *Journal of Hazardous Materials*, 151(1):44–51, 2008.
- Das, K. P. and Kinsella, J. E. Droplet size and coalescence stability of whey protein stabilized milkfat peanut oil emulsions. *Journal of Food Science*, 58(2):439–444, 1993.
- DHI. Review of Annex IV of the Regulation no. 1907/2006 (REACH). Technical report, European Commission, DG Environment, 2008.
- DL. Decree-Law no. 236/98 from 1st August. In *Diario da Republica - I Serie A*. Portugal, 1998.
- Eckenfelder, W. W. *Industrial Water Pollution Control*. McGraw-Hill, 2000.
- Freundlich, H. Ueber die adsorption in loesungen. *Zeitschrift für Physikalische Chemie*, 57:385–470, 1907.
- Geetha Devi, M., Shinoon Al-Hashmi, Z. S., and Chandra Sekhar, G. Treatment of vegetable oil mill effluent using crab shell chitosan as adsorbent. *International Journal of Environmental Science and Technology*, 9(4):713–718, 2012.
- Kumar, S., Narsimhan, G., and Ramkrishna, D. Coalescence in creaming emulsions. Existence of a pure coalescence zone. *Industrial & Engineering Chemistry Research*, 35(9):3155–3162, 1996.
- Leal-Calderon, F., Schmitt, V., and Bibette, J. *Emulsion Science: Basic Principles*. Springer, 2007.
- Pandey, R. A., Sanyal, P. B., Chattopadhyay, N., and Kaul, S. N. Treatment and reuse of wastes of a vegetable oil refinery. *Resources, Conservation and Recycling*, 37(2):101–117, 2003.
- Rhee, C. H., Martyn, P. C., and Kremer, J. G. Removal of oil and grease in oil processing wastewater. Technical report, Sanitation District of Los Angeles County, 1989.
- Sawyer, C., McCarty, P., and Parkin, G. *Chemistry for Environmental Engineering and Science*. McGraw-Hill Education, 2003.
- Shaw, D. J. *Introduction to colloid and surface chemistry*. Butterworth-Heinemann Ltd., Oxford, 4th edition, 1991.

Srinivasan, A. and Viraraghavan, T. Oil removal from water using biomaterials. *Bioresource Technology*, 101(17):6594–6600, 2010.

Stachurski, J. and Michalek, M. The effect of the zeta potential on the stability of a non-polar oil-in-water emulsion. *Journal of Colloid and Interface Science*, 184(2):433 – 436, 1996.

Welz, M. L. S., Baloyi, N., and Deglon, D. A. Oil removal from industrial wastewater using flotation in a mechanically agitated flotation cell. *Water SA*, 33(4):453–458, 2007.

Zouboulis, A. I. and Avranas, A. Treatment of oil-in-water emulsions by coagulation and dissolved-air flotation. *Colloids and Surfaces A: Physicochemical and Engineering Aspects*, 172(1–3):153–161, 2000.

Chapter 6

Treatment of vegetable oil refinery wastewater by sorption of oil and grease onto regranulated cork – a study in batch and continuous mode¹

6.1 Introduction

In the previous chapter, it has been shown that regranulated cork granules are good sorbents for O&G removal from oil-in-water emulsions, as long as high ionic strength and/or low pH conditions are provided. For practical application, a deeper study on whether these conclusions hold in a real wastewater matrix must be carried out.

The main difference between an oil-in-water emulsion and O&G in VORWs is that the latter is more than just neutral vegetable oil; it is also composed of waxes, i.e. esters of longer chain fatty acids with high melting point, and soaps, sodium salts of fatty acids produced in neutralisation steps of refining. Unlike oil and waxes, which are strictly hydrophobic, soaps are amphiphilic molecules with a hydrophilic cation (usually sodium) and a hydrophobic hydrocarbon tail. [Shin and Kim \(2001\)](#) suggest that anionic surfactants, such as the case of sodium oleates, adsorb at the oil-water interface, increasing the negative electrokinetic potential and stabilising emulsions.

The increased stability brought about by the presence of saponified matter is detrimental to O&G removal, particularly to its uptake by hydrophobic sorbents ([Wang et al., 2010, 2012](#)). In the case of cork granules, it has been shown in the previous chapter that emulsion instability is crucial for good removal efficiency in the absence of soap, so it is predicted that the ratio of soap to total O&G will, therefore, affect negatively the sorption process, and determine the extent to which other operating variables will influence oil uptake, since interaction between parameters is to be

¹This chapter is based on the paper: Pintor, A. M. A., Martins, A. G., Souza, R. S., Vilar, V. J. P., Botelho, C. M. S., Boaventura, R. A. R. Treatment of vegetable oil refinery wastewater by sorption of oil and grease onto regranulated cork – a study in batch and continuous mode. *Chemical Engineering Journal*, Accepted paper, 2014.

expected (Stack et al., 2005).

Furthermore, for practical application, a sorption unit for continuous operation must be designed. In the literature, lab and pilot scale columns are the most commonly studied set ups (Ribeiro et al., 2003; Zhou et al., 2008; Mowla et al., 2013; Srinivasan and Viraraghavan, 2014), but in these configurations it can be difficult to account for the mechanism of O&G sorption alone, since other mechanisms, such as coalescence and filtration, may occur simultaneously (Kundu and Mishra, 2013).

Therefore, the main objective of this chapter is to effectively fulfil the premise of this thesis by studying the treatment of real VORWs through O&G removal by sorption onto regranulated cork particles as natural organic sorbents. Sorption process enhancement was evaluated at different pH and ionic strength conditions. O&G sorption studies using synthetic oil-in-water emulsions were also performed in order to elucidate the role of solution pH, ionic strength and soap/oil ratio. Continuous sorption studies were carried out in a stirred tank reactor using a simulated oily wastewater containing sunflower oil, saponified matter and inorganic salt with a composition similar to the real VORWs. A mass transfer model, using a linear partitioning isotherm to describe equilibrium and external fluid film resistance was developed to describe the batch and continuous O&G sorption kinetic profiles.

6.2 Experimental

6.2.1 Materials

Cork granules of type RCG were used as characterised in chapter 3. Refined sunflower oil with the characteristics presented in section 5.2.1 was employed in emulsion preparation. Soap was provided as a concentrate of neutralisation reject in the same vegetable oil refinery; it consisted in a mass of 70% water and 30% sodium oleates and phospholipids.

NaCl of high purity (99.9%, Prolabo) was used to fix ionic strength conditions, and pH adjustments were performed with solutions of H₂SO₄ (96%, Prolabo) and NaOH (99%, Merck).

6.2.2 Analytical methods

pH and temperature were monitored as described in section 5.2.2. Conductivity was measured by a conductivity meter CRISON GLP31.

O&G concentrations were determined by the partition-infrared method using PCE as the extraction solvent (estimation of uncertainty in Appendix A).

COD, DOC and inorganic ions were determined using the same methodologies as presented in section 4.3.4.

6.2.3 Experimental set-up

6.2.3.1 Batch sorption tests

Batch sorption tests were carried out in the same set-up as used in the previous chapter and described in section 5.2.4, with the rotating shaker operating at a speed of 20 rpm. All batch tests were carried out in duplicate.

6.2.3.2 Continuous sorption tests

Experiments in continuous mode were carried out on a 1.5-L cylindrical acrylic reactor with the inlet at the bottom and the outlet at the top, connections in polyvinyl chloride (PVC) tubes and equipped with a temperature-controlled jacket connected to a thermostatic bath at 25 °C. Inside the reactor, a metallic mesh with spacing slightly smaller than 1 mm was placed near the cover to avoid accumulation of cork granules near the top of the reactor and an eventual blockage of the outlet orifice. A 10-L agitated tank was filled with raw emulsion which was fed to the reactor at a flowrate of 10 mL min⁻¹ by a peristaltic pump. Agitation was provided by a mechanical paddle stirrer. A schematic representation of the continuous sorption unit is presented in Figure 6.1.

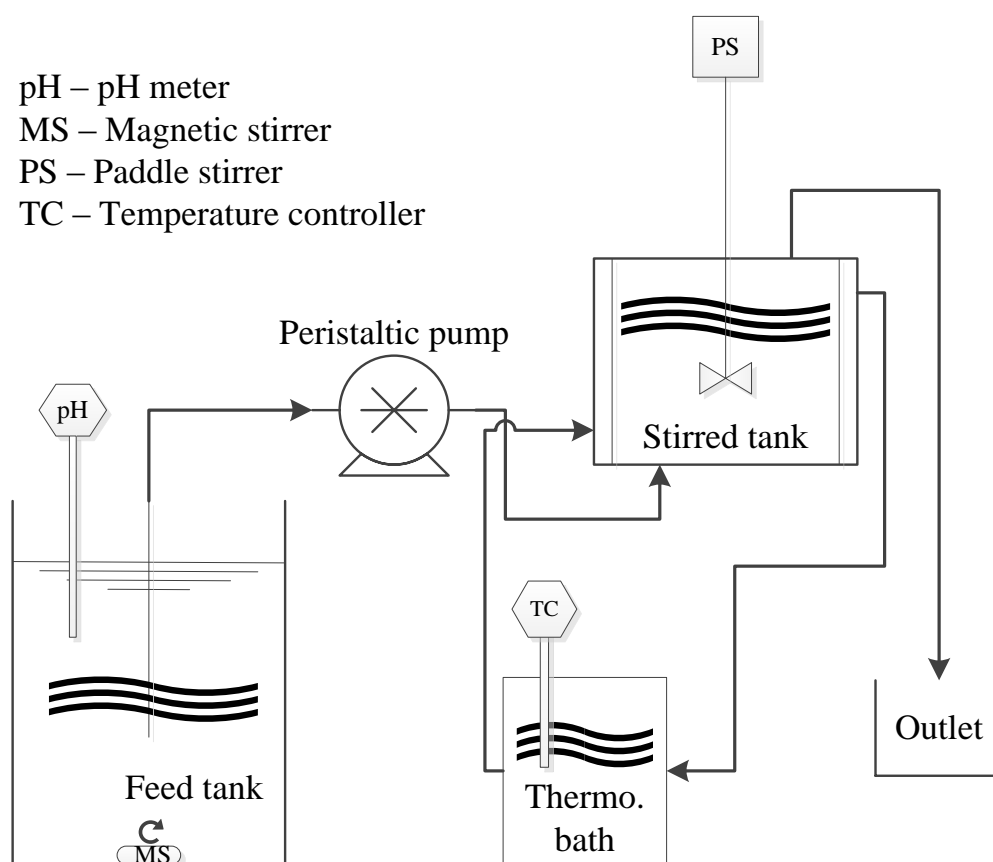


Figure 6.1: Schematic representation of the continuous sorption unit.

6.2.4 Experimental procedure

6.2.4.1 Real VORWs

Two real wastewater samples were studied, AW and TH, with the same provenance as those analysed in chapter 4. After collection, both samples were submitted to gravity separation during 30 min according to the procedure also optimised in chapter 4. The clarified samples were then characterised in terms of pH, conductivity, O&G, COD, DOC and inorganic ions content.

Sorption assays with real VORWs were carried out in batch mode. A preliminary kinetic study was done for both clarified samples without pH or ionic strength adjustments. The tests were performed with a cork dosage of 1 g L^{-1} and contact times varying between 0.25 and 24 h. Control samples, without sorbent addition, were also analysed. The sorption capacity (q) and O&G removal efficiency (R) were calculated according to Equations 5.1 and 5.2 (Chapter 5).

The influence of pH on O&G removal efficiency was evaluated in the range 1.8-7.3, using NaOH (1 M) or H_2SO_4 (0.5 and 5 M) solutions for pH adjustment. For the study of ionic strength effect, NaCl was added to the wastewater samples in the proportion necessary for an increase of 0.1 M ionic strength. In TH sample, salt addition was carried out at the pH values of 2.0 and 7.3 and in AW sample at a pH of 1.8. The tests at variable pH and ionic strength were performed with a cork dosage of 1 g L^{-1} and a contact time of 24 h (to guarantee that equilibrium was reached).

Sorption isotherms at $25 \text{ }^\circ\text{C}$ were obtained at a pH of approximately 2 in both samples by changing the solid/liquid ratio from 0.2 to 1.4 g L^{-1} for AW sample and between 0.5 and 4 g L^{-1} for TH sample. The contact time was kept at 24 h.

6.2.4.2 Oil-in-water emulsions/simulated wastewater

Batch mode Oil-in-water emulsions for studies in batch mode were produced from the mixture of sunflower oil and saponified matter at varying ratios (for an objective of 200 mg L^{-1} total O&G) in NaCl solutions of known molar concentration. The mixtures were sheared in a rotor-stator mixing device (UltraTurrax MICCRA D-15, ART) for three 10-min runs at 8800 rpm separated by 10-min breaks. The pH was adjusted afterward by acidification with H_2SO_4 (0.05, 0.5 or 5 M). The influence of soap ratio, NaCl concentration and pH was studied using a 3-level, 3-factor Box-Behnken design comprising 13 runs and triplicates at the center point. The selected levels for each factor are presented in Table 6.1.

Table 6.1: Factor levels used in the Box-Behnken design.

Coded factor	Factor	Coded levels		
		-1	0	1
x_1	NaCl concentration (M)	0.02	0.11	0.20
x_2	pH	2	4	6
x_3	Soap ratio (%)	30	60	90

Results were analysed using ANOVA and response surface methodology, run in software Statistica 5.1 (Statsoft, Inc.). A second-order regression model including two-way linear interactions was fitted to the experimental data:

$$\hat{y} = \beta_0 + \beta_1x_1 + \beta_2x_2 + \beta_3x_3 + \beta_{12}x_1x_2 + \beta_{13}x_1x_3 + \beta_{23}x_2x_3 + \beta_{11}x_1^2 + \beta_{22}x_2^2 + \beta_{33}x_3^2 \quad (6.1)$$

where x_3 is the independent variable, coded as soap ratio, β_3 is the regression coefficient for the linear effect of x_3 , β_{13} and β_{23} are the regression coefficients for two-way linear interactions effects between x_1 or x_2 and x_3 , and β_{33} is regression coefficient for the quadratic effect of x_3 (Montgomery, 2000).

At the conditions of 0.2 M NaCl, pH 2 and soap/oil ratio of 60%, a sorption isotherm was obtained by varying the cork dosages between 0.4 and 2.2 g L⁻¹ in batch tests with a contact time of 24 h. A kinetic study was then carried out employing a cork dosage of 3.4 g L⁻¹ at 25 °C. Samples were collected at predetermined time intervals up to a contact time of 6 h.

Continuous mode - stirred-tank reactor Oil-in-water emulsions resembling real VORWs (simulated wastewater) were produced by mixing approximately 200 mg L⁻¹ O&G with a soap/O&G ratio of 60% in 0.2 M NaCl solutions with the rotor-stator mixing device at 11600 rpm in three 10-min runs separated by 10-min breaks. The simulated wastewater was produced in parcels of 4 L for each shearing cycle; upon production each parcel was added to the feed tank where pH was adjusted to 2.0 using a 5 M H₂SO₄ solution.

For each experiment in continuous mode, the reactor was filled with distilled water and cork granules at the desired dosage and stirring was initiated. Distilled water was then recirculated for several minutes. Then, the inlet tube was transferred to the feed tank, containing 4 L of simulated wastewater, and the time was registered as $t = 0$. Samples were taken at the feed tank and at the outlet of the stirred-tank reactor in predefined times and analysed for pH and O&G concentration. A first experiment was carried out as a blank, without addition of cork granules, to verify if the residence time distribution response to a step inlet O&G emulsion reflected good agitation conditions inside the reactor. Two experiments were performed with a cork mass of 5.1 g, corresponding to a solid/liquid ratio of 3.4 g L⁻¹, at stirring speeds of 250 and 500 rpm.

6.3 Results and discussion

6.3.1 Real VORWs

6.3.1.1 Characterisation of the wastewaters

The wastewaters were characterized after 30-min gravity separation treatment, achieving an O&G removal efficiency of approximately 74% in AW sample, and 0% in TH sample. The ineffectiveness of treatment for the latter is thought to be related to the existence of a very stable oil-in-water emulsion, probably stemming from the presence of surface-active agents such as sodium soaps.

The characterisation of both pretreated wastewaters is presented in Table 6.2. As expected, TH sample presents a near neutral pH, while AW sample shows an acidic character ($\text{pH} < 2.0$). The acidic conditions in AW wastewater must have enhanced O&G separation in the previous gravity pretreatment. Successful free oil flotation led to a lower value of O&G in pretreated AW when compared to pretreated TH. The latter presents higher values of COD and DOC than AW as well.

Table 6.2: Characterisation of pretreated wastewater samples according to pH, conductivity, O&G, COD, DOC, and inorganic ions.

	TH	AW
pH	7.37 ± 0.01	1.95 ± 0.01
Conductivity (mS cm^{-1})	5.28 ± 0.01	9.84 ± 0.01
O&G (mg L^{-1})	$(1.4 \pm 0.2) \times 10^3$	$(4.8 \pm 0.5) \times 10^2$
COD ($\text{g O}_2 \text{L}^{-1}$)	4.5 ± 0.1	1.68 ± 0.05
DOC (mg L^{-1})	372 ± 2	190 ± 2
Na⁺ (g L^{-1})	1.41 ± 0.07	1.27 ± 0.07
Cl⁻ (g L^{-1})	0.85 ± 0.03	1.36 ± 0.03
SO₄²⁻ (g L^{-1})	0.97 ± 0.05	1.34 ± 0.05
PO₄³⁻ (mg L^{-1})	139 ± 8	114 ± 8

The concentration of sodium, chloride, sulphate and phosphate in both samples was similar, though in total slightly higher in AW wastewater. These four inorganic ions were the most relevant to be quantified in solution in order to estimate the ionic strength of the wastewaters. The hydrogen ion concentration was also taken into account for AW sample. Potassium and nitrate were also detected, but in residual concentrations which were not significant for this purpose. The calculated ionic strength was 0.086 ± 0.002 and 0.069 ± 0.002 M for AW and TH wastewaters, respectively.

The high conductivity of AW sample is mainly associated with the high concentration of inorganic ions combined with acidic pH – H⁺ ions present high ionic conductance (Sawyer et al., 2003).

6.3.1.2 Preliminary sorption tests

An initial evaluation of the treatment using regranulated cork sorbents was carried out by studying the kinetics of O&G uptake in both VORW samples without further chemical adjustments. The results are presented in Figure 6.2.

The sorption capacity at equilibrium q_{eq} , for a solid/liquid ratio of 1 g L^{-1} , was $210 \pm 6 \text{ mg g}^{-1}$ and $84 \pm 6 \text{ mg g}^{-1}$ in AW and TH wastewaters, respectively. Nevertheless, kinetics was faster for the latter, and equilibrium was reached in about 2 h in TH sample and 6 to 8 h in AW sample.

Although regranulated cork granules presented high O&G removal efficiency from AW wastewater, less than 10% of the initial O&G content from the TH wastewater was eliminated. Therefore, further experiments were carried out to try to evaluate the influence of pH and ionic strength in the VORW matrix on O&G sorption by regranulated cork.

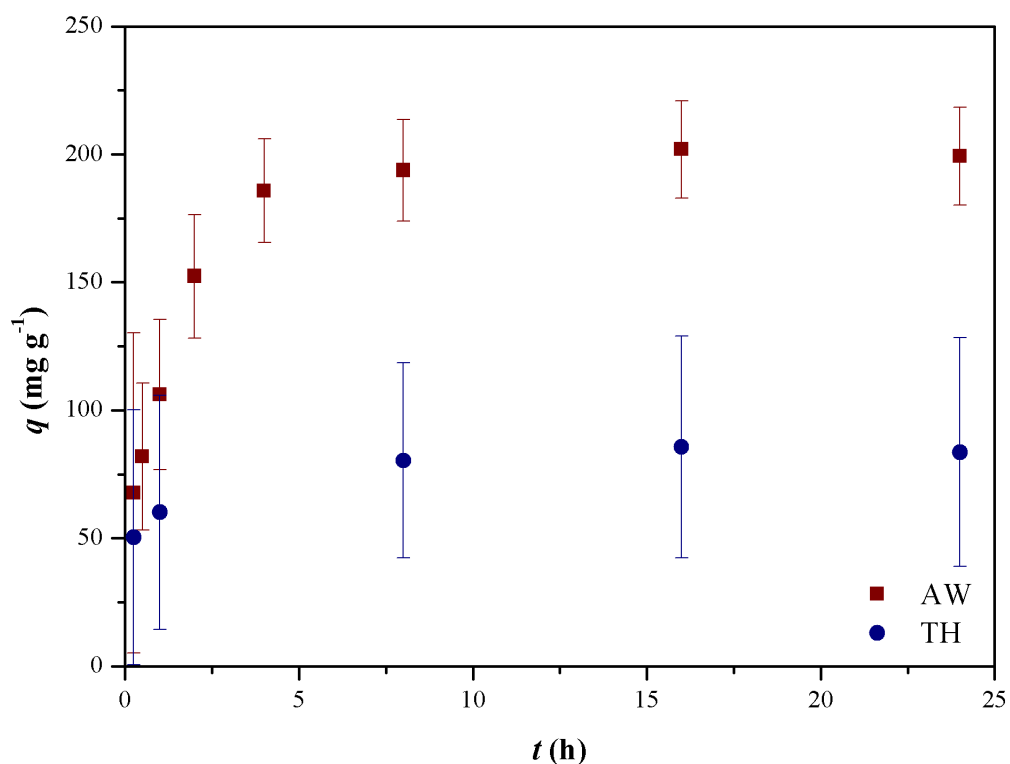


Figure 6.2: Kinetics of O&G sorption by cork granules in real VORW samples AW and TH without chemical adjustment.

6.3.1.3 Influence of pH and ionic strength in O&G sorption onto regranulated cork

The influence of pH and ionic strength in O&G sorption onto regranulated cork was studied by adjusting the chemical conditions of each VORW sample to the desired parameters. To investigate whether the pH was a determining factor, not only the TH wastewater was acidified to values between 1.8 and 6.0 but also the AW wastewater was neutralized to pH values between 3.0 and 7.3, in order to check if that produced an inhibitory effect. The results in terms of O&G sorption capacity under a cork dosage of 1 g L^{-1} are presented in Figure 6.3.

The low values of O&G removal efficiency obtained at neutral pH for AW wastewater and the high values reported for TH wastewater with acid pH support the hypothesis that the pH is a crucial factor in O&G uptake by cork granules. The results are also in line with the results presented in chapter 5 where the neutralisation of negative charges of oil droplets in oil-in-water emulsions by acidification was examined, resulting in enhanced sorbent-sorbate bonding. Furthermore, in the previous chapter it was also reported that ionic strength, in the form of inorganic salts such as sodium chloride, sodium sulphate and calcium chloride, caused emulsion destabilisation through double layer compression, reducing the need for the introduction of hydrogen ions to neutralise droplet-droplet repulsive forces. Therefore it was investigated whether the increase of ionic strength in the VORW matrix resulted in a similar effect.

The obtained results are presented in Figure 6.4. For AW wastewater, the addition of 0.1 M NaCl was only performed at acidic pH (the wastewater's initial pH) since there was no advantage in

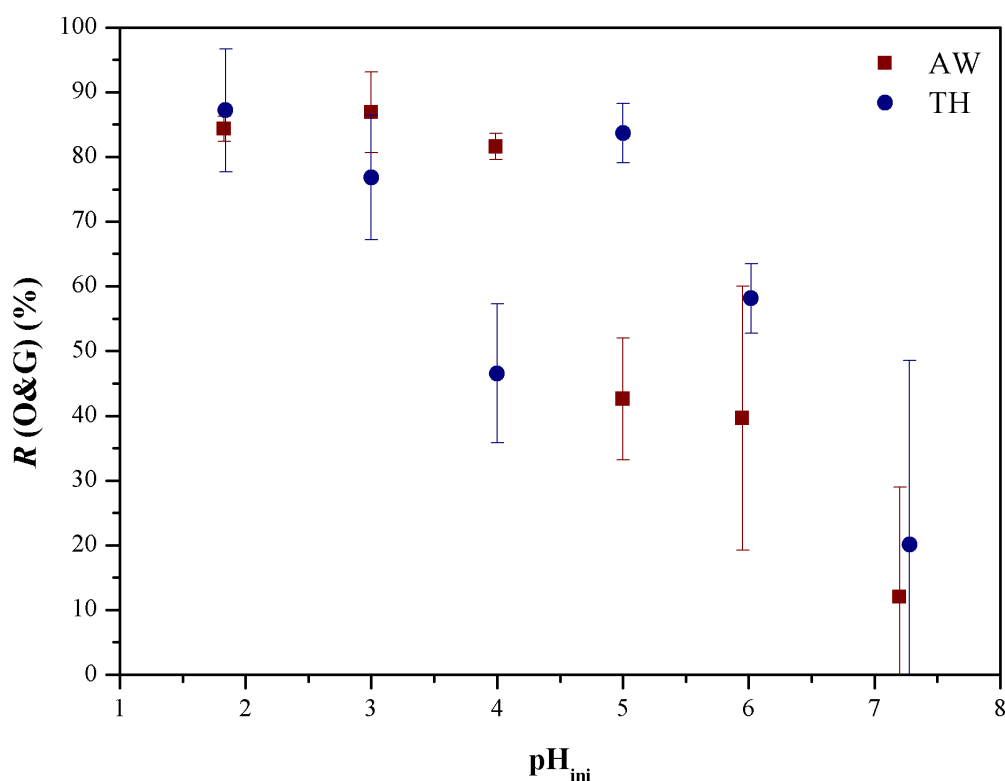


Figure 6.3: O&G removal efficiency R obtained at equilibrium with sorption treatment (cork dosage: 1 g L^{-1}) after pH adjustment of AW and TH real VORW samples.

neutralisation. The effect of NaCl was negligible in this sample and unable to improve upon the removal of $92 \pm 1\%$ obtained without chemical adjustment. For TH wastewater, a positive effect on O&G uptake was perceptible but still not significant if the uncertainty intervals are taken into account.

Since the addition of salt proved to be an inadequate strategy, sorption equilibrium studies were carried out without NaCl addition and at acidic pH in both samples. The TH wastewater was previously acidified to pH 2.0 and no pH adjustment was performed in AW wastewater.

The Freundlich equation (Equation 5.5) was used to fit the equilibrium sorption data obtained for the AW sample. Fitting was performed using software Fig. P (Fig. P Software Corporation, Biosoft, USA) yielding $K_F = 3 \pm 2 \text{ mg}^{(1-1/n)} \text{ L}^{1/n} \text{ g}^{-1}$ and $n = 0.9 \pm 0.1$, with $r^2 = 0.938$. The linear partitioning model (Equation 5.6), which approaches the Freundlich isotherm since n is close to 1, was also fitted to the experimental data, yielding a $K_p = (5.6 \pm 0.3) \times 10^3 \text{ L kg}^{-1}$ and $r^2 = 0.930$. The model curves are presented alongside the experimental data in Figure 6.5.

Both models present good correlations to the experimental equilibrium sorption data. From previous studies, the linear model seems more adequate since it reflects the organic-organic partitioning mechanism between oil and cork; however, the Freundlich model may be more accurate since it also takes into account multilayer sorption caused by aggregation of oil droplets on the cork's surface.

The experimental equilibrium sorption data obtained for the TH wastewater did not allow the out-

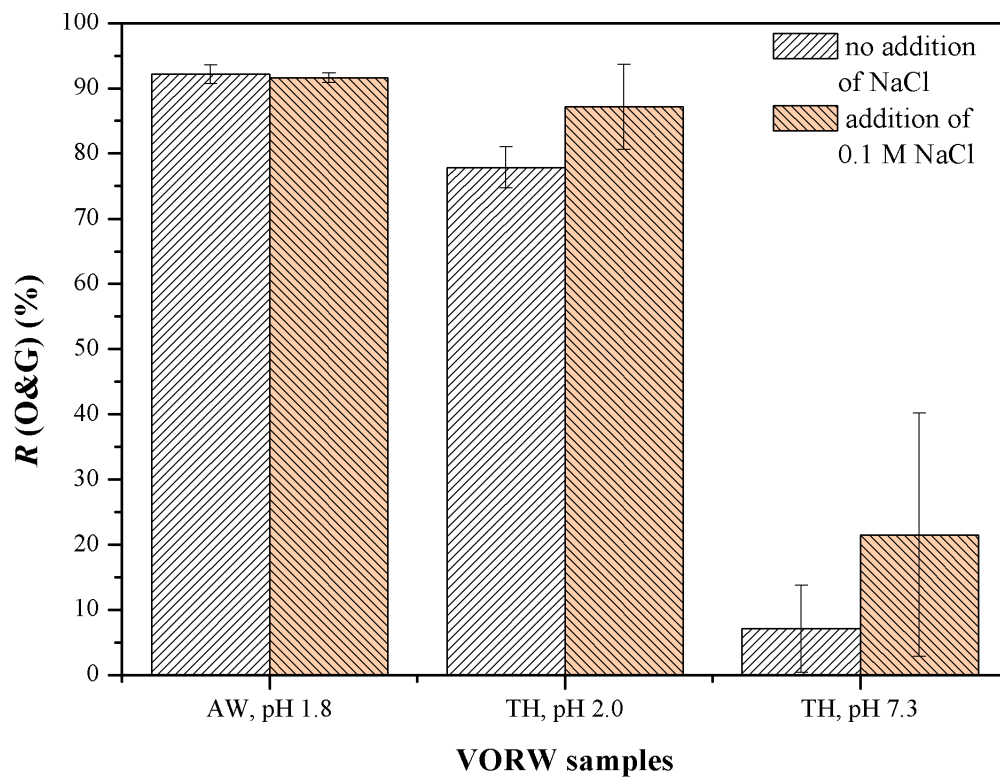


Figure 6.4: Effect of NaCl addition on O&G removal efficiency obtained at equilibrium with sorption treatment (cork dosage: 1 g L^{-1}) in both VORW samples AW and TH, the latter with or without acidification to pH 2.0.

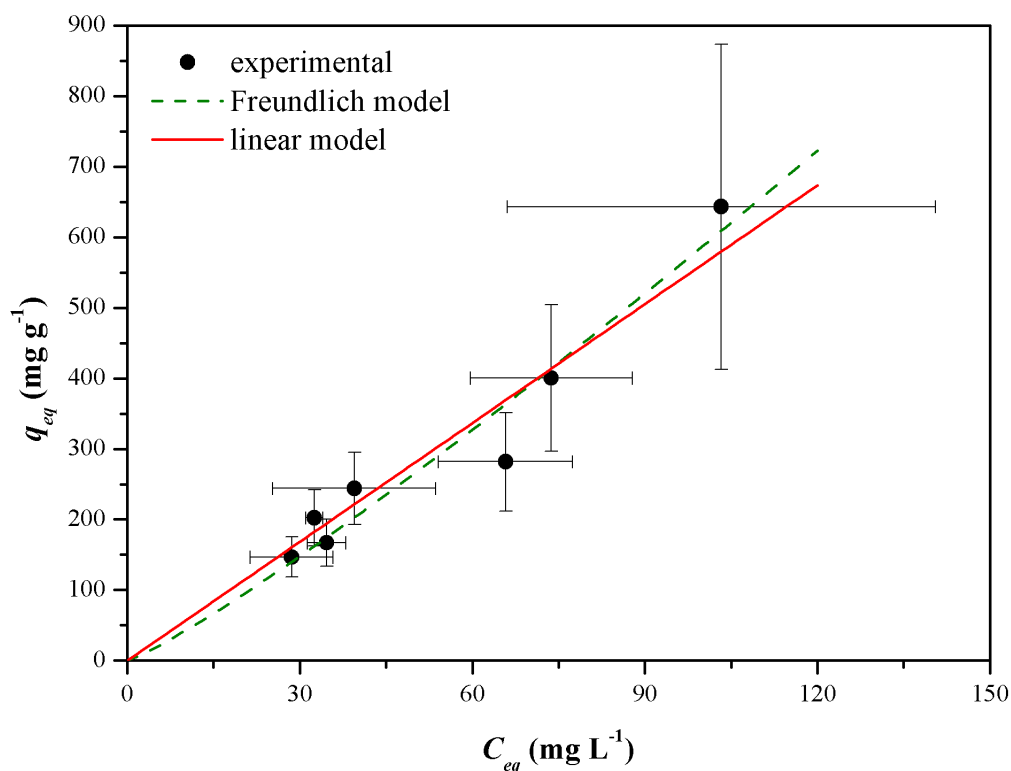


Figure 6.5: Isothermal equilibria at 25 °C for sorption of O&G on regranulated cork in AW sample: experimental data and fitted curves of the Freundlich and linear models.

line of an isotherm curve. O&G removal efficiencies in the range of cork dosages studied (from 0.5 to 4.0 g L⁻¹) were very similar, with a maximum value of $96 \pm 1\%$ for solid/liquid ratios between 1.5 g L⁻¹ and 4.0 g L⁻¹, achieving an O&G equilibrium concentration of 40 ± 10 mg L⁻¹. This means that the O&G sorption capacity decreases with the increase of cork dosage, which can be explained by a combination of two main factors: i) acidification of TH sample, besides improving sorption, also promoted coalescence of oily matter and the formation of agglomerates of fat and cork granules and the action of such mechanisms goes beyond the establishment of a sorption equilibrium; ii) the significant concentration of dissolved organic matter ($DOC = 372 \pm 2$ mg L⁻¹, Table 6.2), a part of which may consist in substances detected in O&G determination, may not be adequately removed by sorption onto cork granules and might account for the residual O&G concentration (40 ± 10 mg L⁻¹), even for the highest cork dosage.

6.3.2 Influence of saponified matter on O&G sorption onto regranulated cork

The inability of salt addition to improve O&G sorption onto regranulated cork particles, especially at neutral pH for TH wastewater, contradicts previous results obtained in oil-in-water emulsions at different NaCl concentrations (section 5.3.4). For an oil-in-water emulsion with 0.2 M NaCl, sunflower oil removal was over 90% for the range of pH between 2.0 and 6.0, using a solid/liquid ratio of 1.0 g L⁻¹ (with an initial O&G concentration of 150 ± 20 mg L⁻¹).

The major difference between synthetic oil-in-water emulsions and the real VORW samples is that while the former were formulated with NaCl solutions in distilled water and neutral sunflower oil, the latter contain many other substances, including saponified matter, which may constitute a significant portion of total O&G. The ratio of soap to neutral oil in the wastewater is unknown, but it should be noted that sodium soaps are produced in large quantities during refining and are washed away to the wastewater homogenisation tank. Due to the amphiphilic nature and emulsifying properties of soaps, which lead to solubilisation, formation of micelles and stabilisation of oil droplets, O&G uptake by sorbents in the presence of saponified matter can be significantly affected, as it has been shown to occur in the presence of other surfactants (Wang et al., 2012).

The 3^3 Box-Behnken experimental design chosen to evaluate the effect of saponified matter in O&G sorption performance takes into account other operating variables, such as pH and ionic strength, which have been proven to influence oil uptake in the absence of soap and in real VORWs (section 6.3.1).

The experimental results of the factorial design are presented in Table 6.3. The fitted second-order regression model according to Equation 6.1 assumed the following form, using coded factors as variables:

$$\hat{y} = 217.7 + 149.6x_1 - 51.5x_2 - 2.5x_3 - 29.2x_1x_2 + 0.02x_1x_3 - 0.05x_2x_3 + 152.3x_1^2 + 6.3x_2^2 + 0.02x_3^2 \quad (6.2)$$

The results of ANOVA for the 15-run dataset are presented in Table 6.4. The regression coefficient (r^2), and adjusted regression coefficient (adj- r^2), were calculated to be 0.978 and 0.938, respectively, indicating a good correlation between the model and the experimental data.

Table 6.3: O&G removal efficiency results for the 15 runs of the Box-Behnken design, along with the predicted values obtained by the second-order regression model and the corresponding residuals.

x_1 (M)	x_2	x_3 (%)	y ($R(\text{O\&G})_{\text{exp}}$) (%)	\hat{y} ($R(\text{O\&G})_{\text{pred}}$) (%)	Residual
0.11	2	30	88.2	91.3	-3.1
0.20	2	60	85.4	80.3	5.1
0.11	2	90	80.6	81.0	-0.4
0.11	6	30	68.4	68.0	0.4
0.20	4	30	59.7	61.7	-2.0
0.02	2	60	56.0	57.6	-1.6
0.02	4	30	54.4	49.7	4.7
0.11	6	90	49.0	45.9	3.1
0.20	6	60	42.2	40.6	1.6
0.20	4	90	40.9	45.6	-4.7
0.02	4	90	35.4	33.4	2.0
0.02	6	60	33.8	38.9	-5.1
0.11	4	60	29.6	27.9	1.7
0.11	4	60	28.1	27.9	0.2
0.11	4	60	26.1	27.9	-1.8

Table 6.4: ANOVA table of the Box-Behnken design with F -values and p -values. Significant factors, with $p < 0.05$, are emphasized in bold.

	Sum of squares	df	Mean square	F -value	p -value
x_1 (L ^a)	295	1	295	10.8	0.022
x_2 (Q ^b)	5.6	1	5.6	0.2	0.67
x_2 (L)	1705	1	1705	62.5	5.2×10^{-4}
x_2 (Q)	2342	1	2342	85.9	2.5×10^{-4}
x_3 (L)	525	1	525	19.2	7.1×10^{-3}
x_3 (Q)	1255	1	1255	46.0	1.1×10^{-3}
x_1 (L) by x_2 (L)	111	1	111	4.0	0.1
x_2 (L) by x_3 (L)	0.01	1	0.01	3.7×10^{-4}	0.99
x_1 (L) by x_2 (L)	35	1	35	1.3	0.31
Error	136	5	27.3		
Total sum of squares	6172	14			

^a Linear effect

^b Quadratic effect

The significance of effects was evaluated by the statistical parameters F -value and p -value (significance level $\alpha = 0.05$). It can be concluded from Table 6.4 that all factors, when considered individually, are significant. The strongest effect is that of pH, and the weakest is that of NaCl concentration; in the latter only the linear effect presents a p -value below 0.05.

The weak effect of NaCl concentration in the presence of soap is in agreement with the results obtained for this parameter in real VORWs (Figure 6.3). This observation corroborates the hypothesis that NaCl contribution towards O&G removal is lessened by the presence of soap. Since anionic surfactants are thought to adsorb at the oil-water interface, increasing the electrokinetic potential of droplets (Shin and Kim, 2001), it is possible that a higher concentration of salt would be needed to achieve a significant double layer compression effect. However, further addition of salt could cause problems in complying with discharge limits regarding inorganic ions concentrations.

Figure 6.6 presents a response surface of O&G removal efficiency, according to the regression model, vs pH and soap/O&G ratio, at a fixed value of 0.11 M NaCl. The 3D surface indicates a response with a minimum value, which reflects the inhibitory effect of saponified matter content up to 60%, regardless of pH. However, above this value, the sorption process is improved. This behaviour suggests that emulsion stability is most influential when the soap ratio to total O&G is 60%, which can be explained by a stronger adsorption at the interface and formation of superficial films around the oil droplets at this ratio. Above this value, the decrease in the amount of neutral oil means less droplets enclosed in soap micelles, and it seems to be easier to convert the solubilised soap to free fatty acids than to neutralise strong repulsive forces between emulsified colloidal particles.

In spite of O&G removal being more difficult at 60% soap, and of the weakened effect of ionic strength adjustment in these conditions, the pH is certainly the determining factor to guarantee successful O&G uptake by cork granules. Acidification to pH 2.0 leads to over 67% O&G re-

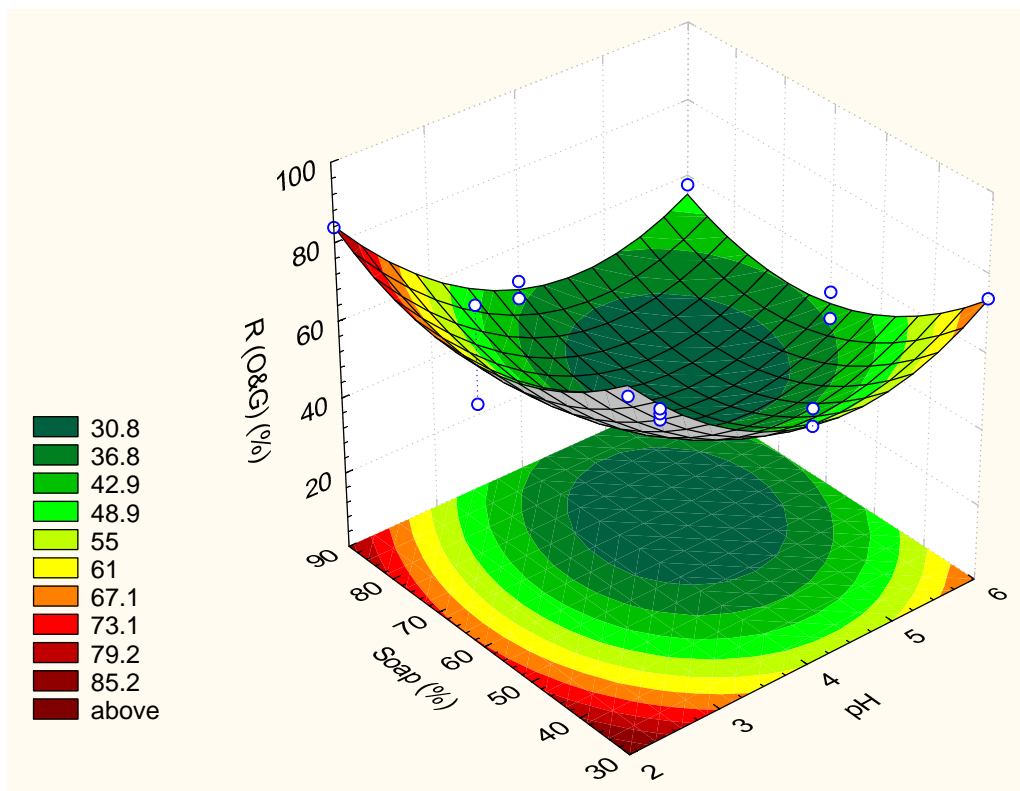


Figure 6.6: 3D response surface, determined by the second-order regression model, of O&G removal efficiency as a function of pH and soap ratio (%), at a fixed NaCl concentration of 0.11 M. Experimental points are represented in white circles bordered in blue.

removal over all the range of soap when NaCl concentration is set at 0.11 M. The results show a similar sorption efficiency to that obtained for TH sample, for which the addition of acid is the most effective methodology to improve O&G removal (Figures 6.2 and 6.3).

Kinetic and equilibrium sorption studies were carried out for a simulated wastewater produced with 60% soap, 0.2 M NaCl and adjusted to pH 2.0, which are representative conditions of real VORWs, considering the previous results.

The equilibria points along with the adjusted isotherm curves according to the Freundlich (Equation 5.5) and linear partitioning (Equation 5.6) models are presented in Figure 6.7. Both models showed good correlation to the experimental data with r^2 of 0.942 and 0.941, respectively. In the Freundlich model, $n = 1.0 \pm 0.1$, indicating a close equivalence to the linear model. The Freundlich constant K_F was $6 \pm 3 \text{ mg}^{(1-1/n)} \text{ L}^{1/n} \text{ g}^{-1}$ and the partition coefficient K_p was $(6.5 \pm 0.3) \times 10^3 \text{ L kg}^{-1}$. These values present similarities to those obtained for O&G uptake in AW sample (section 6.3.1.3).

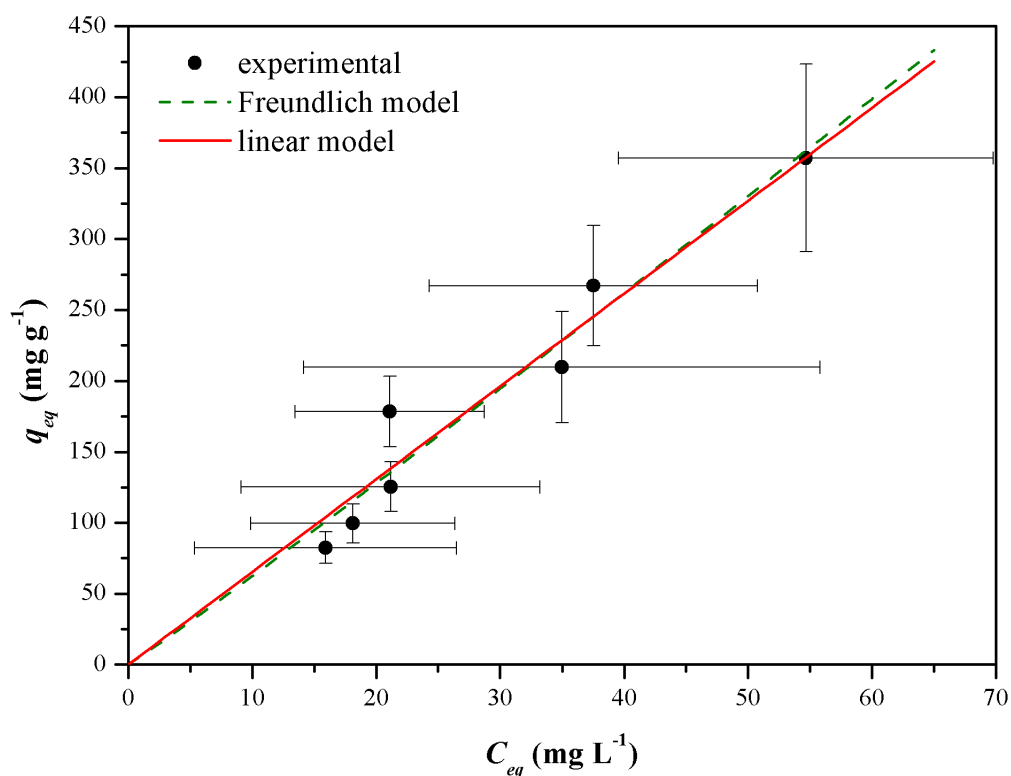


Figure 6.7: Isothermal equilibria at 25 °C for sorption of O&G on regranulated cork in simulated wastewater: experimental data and fitted curves of the Freundlich and linear models.

Sorption kinetics was followed up to 6 h contact time at a cork dosage of 3.4 g L^{-1} . This dosage was chosen after calculations from the Freundlich model in order to guarantee with a standard error uncertainty interval that an equilibrium concentration of $13 \pm 2 \text{ mg L}^{-1}$ O&G would be achieved in the treatment of a $\approx 200 \text{ mg L}^{-1}$ O&G simulated wastewater. The concentration goal was selected for compliance with the O&G discharge limit of 15 mg L^{-1} defined in Portuguese legislation (DL, 1998). The results are presented in Figure 6.8.

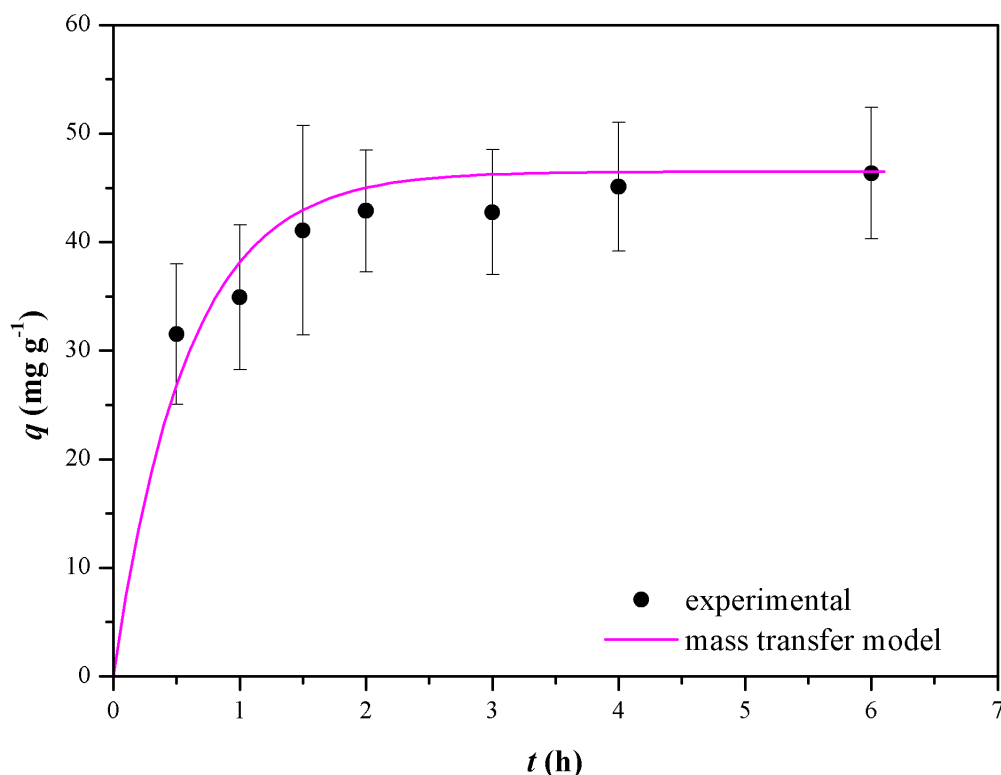


Figure 6.8: Kinetics of O&G sorption by cork granules in simulated wastewater: experimental data and fitted curve of mass transfer model.

A mass transfer model (Equation 5.11), whose derivation has been presented in section 5.3.5, was fitted to experimental data. The parameters obtained were a time constant for film diffusion τ_f of $(2.2 \pm 0.3) \times 10^3$ s and a film mass transfer coefficient k_f of $(3.6 \pm 0.6) \times 10^{-3}$ cm s⁻¹ ($r^2 = 0.691$). These values are in the same order of magnitude as those obtained in a previous study for oil sorption in oil-in-water emulsions in the absence of soap, at a similar agitation speed.

6.3.3 Continuous sorption tests

For adequate study of O&G sorption in continuous mode, a first experiment was carried out without sorbent and at a stirring speed of 250 rpm, in order to assess the agitation conditions in the stirred-tank reactor by measuring the response to a step inlet O&G concentration of ≈ 200 mg L⁻¹ in a simulated wastewater with 60% soap ratio, 0.2 M NaCl and adjusted to pH 2.0. The normalised response $F(t) = \frac{C_{out}}{C_0}$, with C_{out} as the outlet O&G concentration (mg L⁻¹) and C_0 as the average feed concentration (mg L⁻¹), was equalled to the Danckwerts curve for an ideal continuous stirred-tank reactor (CSTR), expressed by:

$$F(t) = 1 - \exp\left(-\frac{1}{\tau}t\right) \quad (6.3)$$

where t is the time of operation (h) and τ is the mean residence time (h) (Fogler, 2006).

The fitting of Equation 6.3 to the measured normalised response showed good correlation ($r^2 = 0.995$),

and yielded an experimental mean residence time (τ_{exp}) of 2.91 ± 0.09 h. The experimental normalised response, along with the adjusted curve for $F(t)$ and the normalised $\frac{C_{out}}{C_0}$ responses in the two sorption experiments in the continuous reactor, is presented in Figure 6.9.

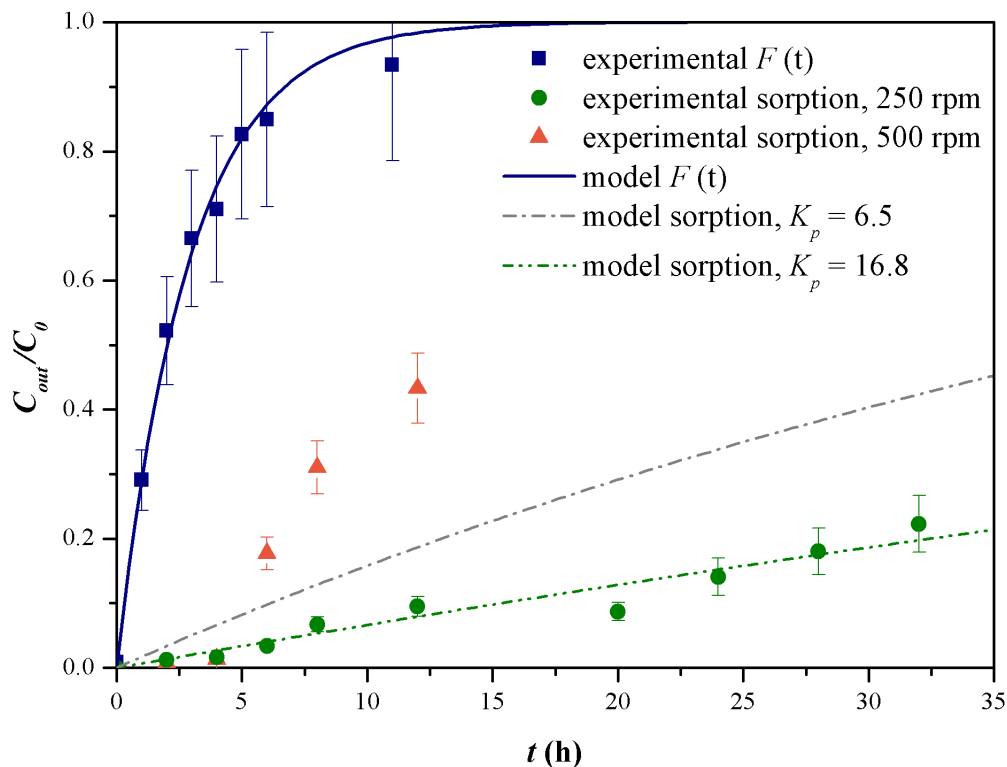


Figure 6.9: Evolution of normalised responses $\frac{C_{out}}{C_0}$ for the step experiment and the two sorption experiments in the continuous reactor, along with the fitted Danckwerts curve (Equation 6.3 and the model curves of the continuous stirred-tank operation, using the partition coefficient K_p of batch sorption equilibria (6.5) and an adjusted value (16.8) to the experimental data of the best performing sorption experiment (stirring speed 250 rpm).

The experimental residence time is slightly higher than the theoretical (2.5 h), however this is to be expected in non-ideal conditions, due to small losses of O&G by contact with the connection tubes and the vessel's walls, and uncertainties in the analytical method for O&G measurement. It is assumed, therefore, that the continuous reactor provides good agitation and homogenisation conditions without dead volumes and by-passes.

A second experiment was carried out at a dosage of 3.4 g L^{-1} of cork granules employed in previous batch kinetic studies (section 6.3.2), at the same stirring speed. In these conditions, significant O&G sorption could be achieved, as it is reflected in a very slow increase in the outlet O&G concentration through time. During 8 h of operation, the outlet O&G concentration was below discharge limits according to Portuguese legislation ($< 15 \text{ mg L}^{-1}$) (DL, 1998).

A third experiment was designed with the objective of improving the treatment further by enhancing the mass transfer using a stirring speed of 500 rpm. However, the observed effect was the opposite, with a rapid increase in outlet O&G concentration after 4 h of operation. Excessive turbulence was produced inside the reactor, leading to sorbent disintegration and mass loss, and vio-

lent collisions and friction between oil droplets and sorbent particles that impaired sorbate-sorbent bonding. The latter had already been observed in batch kinetic sorption studies in oil-in-water emulsions (section 5.3.5). Moreover, at the speed of 250 rpm, due to slower mixing and cork's low density, a short layer of cork granules formed near the metallic mesh at the top of the reactor, and the packing of sorbent particles in this zone may have enhanced O&G removal by acting like a filter.

In the best operating conditions of 3.4 g L⁻¹ cork and 250 rpm, the successful operation during 8 h with outlet concentration under O&G discharge limits corresponded to the successful treatment of 4.8 L of simulated wastewater. The sorbed amount during this operating time was 192 ± 2 mg g⁻¹. A mass transfer model was developed to describe the sorption process in the continuous reactor. The mass balance to the CSTR can be expressed by the following equation:

$$QC_0 = QC_b + \varepsilon_b V \frac{dC_b}{dt} + (1 - \varepsilon_b) V \rho_{ap} \frac{dq}{dt} \quad (6.4)$$

where Q is the flowrate (L s⁻¹), q (mg g⁻¹) is the sorbed amount at time t (s), C_b is the bulk O&G concentration in the reactor at time t (mg L⁻¹), equal to C_{out} , ε_b is the bulk porosity inside the reactor, V is the reactor volume (L) and ρ_{ap} is the apparent density of the sorbent particles (540 g L⁻¹, Table 3.1).

As in the batch mass transfer model, it is assumed that the cork particles are spherical, and there is an external sublayer around the cork particles, in which the oil droplets diffuse from the bulk to the surface. The mass balance to this fluid film surrounding the particles can be established by the following equation:

$$k_f a_p (C_b - C_p) = \rho_{ap} \frac{dq}{dt} \quad (6.5)$$

where k_f is the film mass transfer coefficient (cm³ cm⁻² s⁻¹), a_p is the external surface area per unit particle volume (cm² cm⁻³) and C_p is the O&G concentration in the liquid phase at the sorbent surface at time t (mg L⁻¹).

It is further assumed that intraparticle diffusion is negligible (since cork has no internal porosity) and equilibrium at the surface is instantaneous and described by the linear partitioning model (Equation 5.6). Combining Equations 6.4, 6.5 and 5.6, introducing dimensionless variables and solving for C_b , the following expression results:

$$C_b = C_0 \left[- \left(\frac{\lambda_2 + 1}{\lambda_2 - \lambda_1} \right) \exp(\lambda_1 \theta) + \left(\frac{\lambda_1 + 1}{\lambda_2 - \lambda_1} \right) \exp(\lambda_2 \theta) + 1 \right] \quad (6.6)$$

where

$$\theta = \frac{t}{\tau}; \tau = \frac{\varepsilon_b V}{Q}$$

$$\lambda_1 = \frac{-\left(1 + N_f + \frac{N_f}{\xi}\right) + \sqrt{\left(1 + N_f + \frac{N_f}{\xi}\right)^2 - 4\frac{N_f}{\xi}}}{2}$$

$$\lambda_2 = \frac{-\left(1 + N_f + \frac{N_f}{\xi}\right) - \sqrt{\left(1 + N_f + \frac{N_f}{\xi}\right)^2 - 4\frac{N_f}{\xi}}}{2}$$

$$\xi = \frac{(1 - \varepsilon_b)}{\varepsilon_b} \rho_{ap} K_p; N_f = \frac{\tau}{\tau_f}; \tau_f = \frac{\varepsilon_b}{(1 - \varepsilon_b) k_f a_p}$$

and θ is the dimensionless time, τ is the mean residence time (s), λ_1 and λ_2 are coefficients of the resolution of a second order homogeneous differential equation expressed by

$$\frac{d^2 y_b}{d\theta^2} + \left(1 + N_f + \frac{N_f}{\xi}\right) \frac{dy_b}{d\theta} + \frac{N_f}{\xi} y_b = 0$$

where $y_b = \frac{C_b}{C_0}$ is the dimensionless O&G bulk concentration, N_f is the number of mass transfer units by film diffusion, ξ is the mass capacity of the reactor, and τ_f is the time constant for film diffusion (s).

When fitting the model to the experimental data using τ_f as the variable, it approaches the experimental data better when τ_f tends to zero. The fact that the fluid film resistance is negligible in the continuous reactor when compared to the batch sorption tests may be related to the type of agitation used in each case. While the rotating agitation used in batch simply promoted a slow contact between the cork granules and the liquid sample, the mechanical agitation in the continuous reactor guaranteed an excellent mixture between the particles and the liquid. Therefore, a simplified model without fluid film resistance was applicable to the continuous reactor. In this case, $C_b = C_p$ and Equations 6.5 and 5.6 are replaced by:

$$q = K_p C_b \quad (6.7)$$

which, substituting in Equation 6.4 and solving for C_b , gives:

$$C_b = C_0 \left[1 - \exp\left(-\frac{\theta}{1 + \xi}\right) \right] \quad (6.8)$$

However, as it can be observed in Figure 6.9, the application of the model using the partition coefficient obtained in batch sorption tests (section 6.3.2), of 6.5 L g⁻¹, largely overestimates the outlet concentration in the second experiment, by about a factor of 2. If fitting of Equation 6.8 is carried out defining K_p as the variable, a good adjustment is obtained with an r^2 of 0.939 yielding $K_p = 16.8$ L g⁻¹. This partition coefficient is much higher than the one obtained in batch sorption tests. The formation of a packed layer of cork particles near the top of the reactor may

have caused this deviation and promoted enhanced sorption mechanisms which are impossible to account for. The occurrence of improved removal gives important directions for future work: while shifting toward a packed bed reactor can result in problems of clogging and flow and pressure loss, increasing the concentration of sorbent particles and adjusting the agitation conditions in stirred-tank reactors may result in improved filter-like mechanisms with fast O&G removal from oily wastewaters.

6.4 Conclusions

In this chapter, successful treatment of real VORW by O&G sorption onto regranulated cork granules was achieved by acidification to a pH of 2.0. Under these favourable conditions, it was possible to treat, in batch mode, a wastewater containing emulsified oil from $1.4 \pm 0.2 \text{ g L}^{-1}$ to $40 \pm 10 \text{ mg L}^{-1}$.

In the presence of soap, the effect of ionic strength is weakened, and no significant double layer compression is observed, even with the addition of 0.1 M NaCl to VORWs. In oil-in-water emulsions with saponified matter, the inhibitory effect of soap could be verified to increase up to 60% soap to total O&G, then decreasing for higher ratios. Therefore, in the presence of soap, only the introduction of positive charges via acidification could successfully neutralise the electrokinetic potential of the emulsion in order to promote sorption. In simulated wastewater, at a pH of 2.0, O&G removal efficiency exceeded 60% regardless of NaCl concentration or soap ratio.

In a stable simulated wastewater with 60% soap and 0.2 M NaCl, sorption at pH 2.0 was shown to be successful in both batch and continuous modes. In batch mode, equilibria could be well described by both the Freundlich and linear partitioning models, and the time required to achieve equilibrium was between 2 to 4 h. In continuous mode in a stirred-tank reactor, successful treatment exceeding that predicted by the equilibrium isotherm could be achieved with a stirring speed of 250 rpm and a cork dosage of 3.4 g L^{-1} . Higher stirring speed impaired sorbate-sorbent bonding.

At the best operating conditions, simulated wastewater with $205 \pm 30 \text{ mg L}^{-1}$ O&G could be treated to achieve $\text{O\&G} < 15 \text{ mg L}^{-1}$, the discharge limit defined by Portuguese legislation.

6.5 References

DL. Decree-Law no. 236/98 from 1st August. In *Diario da Republica - I Serie A*. Portugal, 1998.

Fogler, H. S. *Elements of Chemical Reaction Engineering*. Prentice Hall PTR, 2006.

Kundu, P. and Mishra, I. M. Removal of emulsified oil from oily wastewater (oil-in-water emulsion) using packed bed of polymeric resin beads. *Separation and Purification Technology*, 118:519 – 529, 2013.

Montgomery, D. C. *Design and Analysis of Experiments*. Wiley, 2000.

- Mowla, D., Karimi, G., and Salehi, K. Modeling of the adsorption breakthrough behaviors of oil from salty waters in a fixed bed of commercial organoclay/sand mixture. *Chemical Engineering Journal*, 218:116–125, 2013.
- Ribeiro, T. H., Rubio, J., and Smith, R. W. A dried hydrophobic aquaphyte as an oil filter for oil/water emulsions. *Spill Science & Technology Bulletin*, 8(5–6):483–489, 2003.
- Sawyer, C., McCarty, P., and Parkin, G. *Chemistry for Environmental Engineering and Science*. McGraw-Hill Education, 2003.
- Shin, S. H. and Kim, D. S. Studies on the interfacial characterization of O/W emulsion for the optimization of its treatment. *Environmental Science & Technology*, 35(14):3040–3047, 2001.
- Srinivasan, A. and Viraraghavan, T. Oil removal in a biosorption column using immobilized *M. rouxii* biomass. *Desalination and Water Treatment*, 52(16-18):3085–3095, 2014.
- Stack, L. J., Carney, P. A., Malone, H. B., and Wessels, T. K. Factors influencing the ultrasonic separation of oil-in-water emulsions. *Ultrasonics Sonochemistry*, 12(3):153–160, 2005.
- Wang, D., Silbaugh, T., Pfeffer, R., and Lin, Y. S. Removal of emulsified oil from water by inverse fluidization of hydrophobic aerogels. *Powder Technology*, 203(2):298–309, 2010.
- Wang, D., McLaughlin, E., Pfeffer, R., and Lin, Y. S. Adsorption of oils from pure liquid and oil–water emulsion on hydrophobic silica aerogels. *Separation and Purification Technology*, 99:28–35, 2012.
- Zhou, Y.-B., Tang, X.-Y., Hu, X.-M., Fritschi, S., and Lu, J. Emulsified oily wastewater treatment using a hybrid-modified resin and activated carbon system. *Separation and Purification Technology*, 63(2):400–406, 2008.

Chapter 7

Oil desorption and recovery from cork sorbents¹

7.1 Introduction

In section 2.2.4.3, a brief overview of the chemical and physical methods which have been studied for the desorption and recovery of oil from sorbents has been presented. In this chapter, the objective is to study several methods of oil desorption and recovery from oil-impregnated cork sorbents. Since it is difficult to produce oil-saturated sorbents by treatment of oil-in-water emulsions or VORWs in large quantities with homogeneous characteristics, the study focuses on the application of recovery methods to cork saturated with oil from pure oil medium, i.e. as derived from an oil spill application.

For elution, a variety of aqueous solutions (acid, basic, and anionic and cationic surfactants) were tested, since organic solvents are bound to have high recovery, but are less environmentally friendly. On the other hand, the performance of physical recovery by mechanical compression was also studied. Finally, all methods were compared, and by interpretation of the experimental data important conclusions are drawn about the most effective and practical methods for oil recovery and cork sorbent regeneration.

7.2 Experimental

7.2.1 Materials

The cork granules used in this study were provided by Corticeira Amorim, SGPS (Portugal) and were of regranulated type (as RCG) but with particle size between 2 and 4 mm. Refined sunflower oil with the characteristics presented in section 5.2.1 was used for the impregnation of cork granules.

¹This chapter is based on the paper: Pintor, A. M. A., Ferreira, C. I. A., Pereira, J. P. C., Souza, R. S., Silva, S. P., Vilar, V. J. P., Botelho, C. M. B., Boaventura, R. A. R. Oil desorption and recovery from cork sorbents. Working paper, 2014.

Tap water was used for recovery studies. Aqueous elution solutions were prepared with distilled water and H₂SO₄ (96%, Prolabo), NaOH (99%, Merck), HDTMA bromide (Acrós Organics, > 99%) and sodium dodecyl sulphate (SDS) (> 99%, Merck).

7.2.2 Analytical methods

O&G in aqueous solution was determined by the partition-infrared method using PCE as the extraction solvent (estimation of uncertainty in Appendix A).

7.2.3 Impregnation of cork granules

Cork granules were impregnated with sunflower oil by contact with oil in excess in a beaker for 15 h. Then, the solids were removed from the oil medium and left in a steel mesh to drain the oil which was entrained by the particles. After drainage was completed the steel mesh was contacted with absorbing paper to remove all the excess oil which was not sorbed by the solid.

The cork granules were weighed before and after impregnation and the sorption capacity q (g g⁻¹) was calculated as:

$$q = \frac{m_{oc} - m_c}{m_c} \quad (7.1)$$

where m_{oc} is the mass of oil-impregnated cork (g) and m_c is the mass of cork (g).

In the cases where impregnation was done for several cycles, the total sorption capacity (q_{total}) was calculated using Equation 7.1, but the sorption capacity in each cycle was determined by the following expression:

$$q_{cycle} = \frac{m_{oc} - m_{ocd}}{m_c} \quad (7.2)$$

where m_{ocd} is the mass of oil-impregnated cork after the previous desorption cycle (g).

7.2.4 Desorption by elution

Elution tests were carried out in 50-mL capped glass tubes containing 45 mg of oil-impregnated cork granules and 45 mL of desorbing solutions: tap water, acid solution (0.1 M H₂SO₄), basic solution (0.1 M NaOH), cationic surfactant solution (10 mM HDTMA bromide) and anionic surfactant solution (10 mM SDS). They were agitated in a rotary shaker (model SB3, Stuart) for 3 h inside a thermostatic cabinet which ensured a constant operating temperature of 25 °C.

After contact the cork granules were separated manually from the desorbing solution and the liquid was analysed for O&G. The O&G removal efficiency R (%) was calculated using the following relationship:

$$R = \frac{C(O\&G) \times V}{m_o}; m_o = \frac{m_{oc} \times q}{q + 1} \quad (7.3)$$

where C (O&G) is the concentration of oil and grease in the eluting solution (mg L⁻¹), V is the volume of the batch reactor (L), and m_o is the mass of oil initially sorbed by cork (mg).

Control tests were done in cationic and anionic surfactant solutions, since these substances may

also be detected in O&G determination. No surfactant was detected in O&G determination in both initial solutions nor after their contact with 45 mg of non-impregnated cork granules for 3 h.

7.2.5 Recovery by compression

Compression tests were carried out using an extruder (CAMOZZI 368-905), comprised of a conical piston, a control panel for compression/decompression and a metallic cylinder where the sample is placed. The tip of the metallic cylinder can be replaced with several types of perforated conical heads (Figure 7.1). In this work, only the head represented in the middle in Figure 7.1 was used for all experiments.



Figure 7.1: Extruder CAMOZZI 368-905 used in compression tests along with its three types of metallic conical heads.

Oil-impregnated cork was placed in the extruder and compressed at the desired pressure for a determined period of time. The mass of the oil-impregnated cork was measured before and after compression and the removal efficiency in each cycle R (%) was calculated by the expression:

$$R = \frac{m_{oc} - m_{ocd}}{m_o} \times 100; m_o = \frac{m_{oc} \times q}{q + 1} \quad (7.4)$$

Preliminary compression studies were carried out with the extruder in the horizontal position and evaluated the compression of 0.5 g of oil-impregnated cork at the pressures of 2, 5 and 7 bar. The sorbents were compressed two times during 1 min per compression. Regenerated sorbents were then applied in three consecutive sorption/desorption cycles at the selected compression protocol. A comparison between the efficiency of interrupted compression and continuous compression was done by carrying out two different compression protocols at 2 bar. The first consisted in four compressions of 1 min each, and the latter was a single continuous compression of 4 min.

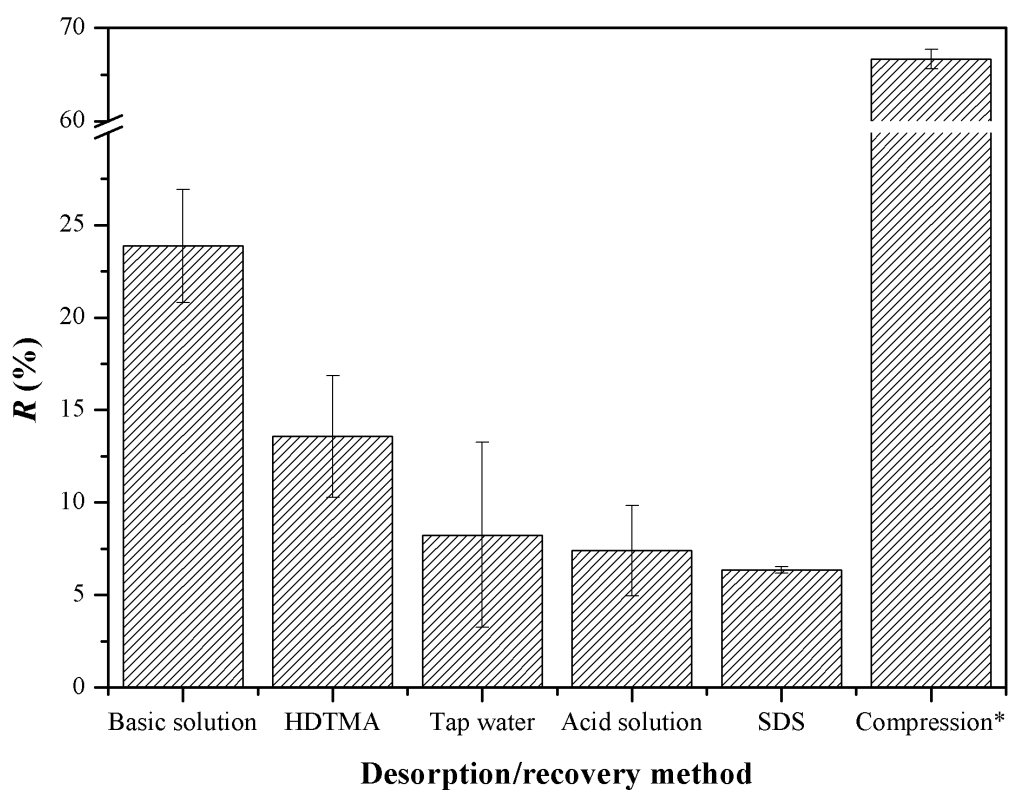
For the following experiments, the extruder was used in the vertical position since this guaranteed more homogeneous compression. The influence of the amount of oil-saturated sorbent inside the extruder was studied by varying the mass of oil-loaded granules from (0.5, 1, 3, 5 and 10 g) for a compression protocol of 4 compressions of 1 min at 2 bar. Using a mass of 10 g the influence of the pressure was again evaluated by performing a similar protocol but at 7 bar.

Finally, the sorption/desorption behaviour of cork sorbents for 10 cycles was evaluated using a regeneration protocol of four 1-min compressions at 7 bar with a sorbent load of 10 g. The partial and total sorption capacities were determined for each cycle.

7.3 Results and discussion

7.3.1 Desorption by elution

Figure 7.2 presents the results for oil recovery efficiency using different aqueous solutions. Elution with tap water yielded an efficiency of $8 \pm 5\%$, a value which is slightly higher than others reported in the literature for the elution of sorbed oil from organic sorbents using distilled water (Ibrahim et al., 2009). Still, it is a low value, as it could be expected since cork is a hydrophobic material and oil, as a hydrophobic substance, has much higher affinity toward its surface than toward water. The acid solution of 0.1 M H_2SO_4 and the anionic surfactant solution of 10 mM SDS did not improve upon the recovery obtained with tap water. Acidity does not favour the dispersion of oil in water. In fact, previous chapters 5 and 6 showed that vegetable oil sorption from oil-in-water emulsions by cork granules is increased at lower values of pH. The elution with SDS solution did not improve oil recovery. On the contrary, the surfactant solution of 10 mM HDTMA bromide yielded better results. The reason why elution with SDS solution did not improve oil recovery is not so clear. It would be expected that the addition of surfactant would decrease the surface tension and thus improve the oil removal from the saturated cork. The difference between the effects of cationic and anionic surfactant solutions on the desorption of sorbed oil suggests that charge mechanisms may be at play. In fact, oil droplets acquire negative charge when dispersed in water and this may hamper the interaction between oil and the anionic surfactant, leading to a decrease in the dispersion of oil in the aqueous medium. On the other hand, the quaternary ammonium ions of HDTMA bromide not only neutralize negative charges enabling dispersion, but they may also dissolve more readily the hydrophobic tail into the oil medium due to its longer chain, when compared to SDS.



* 4 compressions of 1 min at 7 bar

Figure 7.2: Recovery efficiencies for the different aqueous solution elutions, along with the recovery efficiency of the most successful compression procedure (4 compressions of 1 min at 7 bar).

Finally, the use of NaOH solution led to the highest desorbing efficiency of all considered eluents, $24 \pm 3\%$. The better performance of the basic solution can be explained by the occurrence of saponification of the sorbed oil and subsequent solubilization in the water matrix. It is possible that stronger NaOH solutions could improve this result further. However, when considering the process from the point of view of sorbent regeneration, the use of strong basic solutions may cause partial destruction of the cork structure and reuse of the sorbent may be impaired. Pitakpoonsil and Hunsom (2014) have observed a decrease in the sorption of oil and grease and organic substances by chitosan flakes following several cycles of sorption and regeneration using NaOH solutions.

7.3.2 Recovery by compression

7.3.2.1 Preliminary tests

Preliminary tests on compression of oil loaded cork granules were carried out to evaluate the effect of the pressure on oil recovery for four cycles. The results are presented in Figure 7.3.

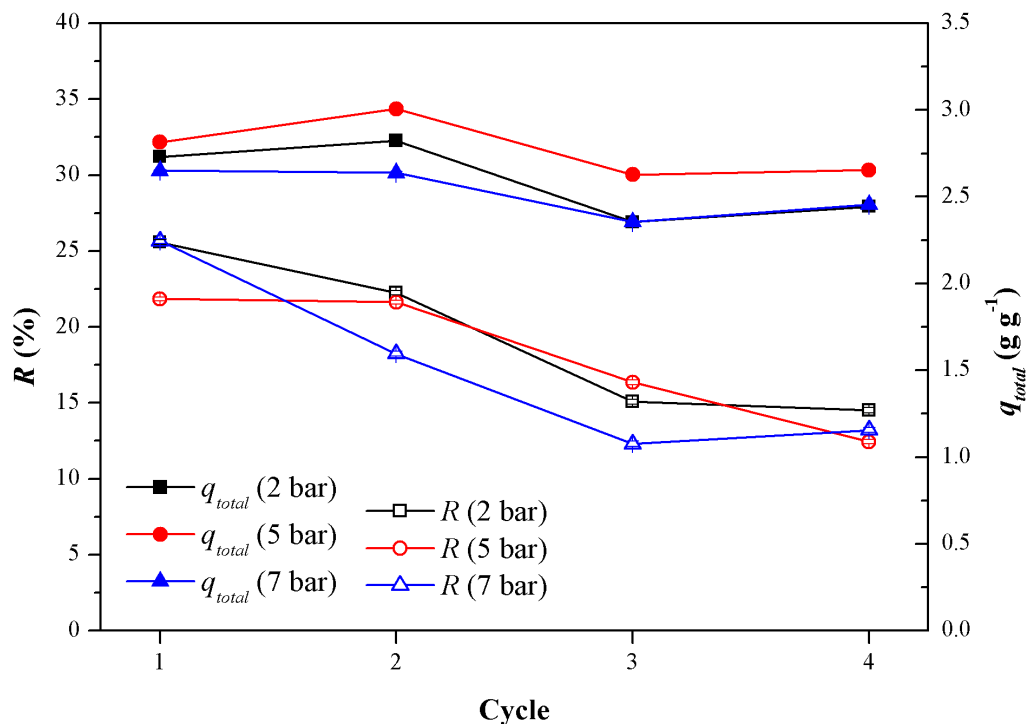


Figure 7.3: Sorbed amount in total and recovery efficiency by compression during 4 cycles of sorption/compression at three different pressures (2, 5 and 7 bar) ($m_{oc} = 0.5$ g, 2 compressions of 1 min per cycle).

First cycle recovery is not very high in the selected conditions, and pressure does not seem to have a significant effect on oil removal, which varies between 21.8 ± 0.1 and $25.7 \pm 0.2\%$ with no correlation to the variable conditions. Over four cycles, however, other conclusions can be drawn. Recovery decreases after each cycle of sorption/regeneration regardless of the operating pressure. The overall sorption capacity (q_{total}) also decreases slightly, especially after the second compression. It is likely that the pressure applied partially damages the cork structure, leading to

a decrease in the sorption capacity. The decrease in recovery efficiency is also more pronounced for an operating pressure of 7 bar, supporting the notion that increased pressure could cause more damage to the sorbent's capacity. It is also believed that operating the extruder in the horizontal position may not provide homogeneous conditions of compression thus enhancing this effect.

7.3.2.2 Optimisation of the compression protocol

For the optimisation of the compression protocol, the first operating parameter to be examined was the compression mode. Interrupted compression consists in pressing the piston for a determined amount of time and then alleviating the pressure for an equally spaced interval, for several rounds. Continuous compression, on the other hand, considers only one round of piston pressure for an amount of time equivalent to the sum of the compression times in the interrupted mode. Figure 7.4 presents the results that compare interrupted and continuous compression for a time of 4 min, in which the interrupted procedure consisted of four 1-min compressions.

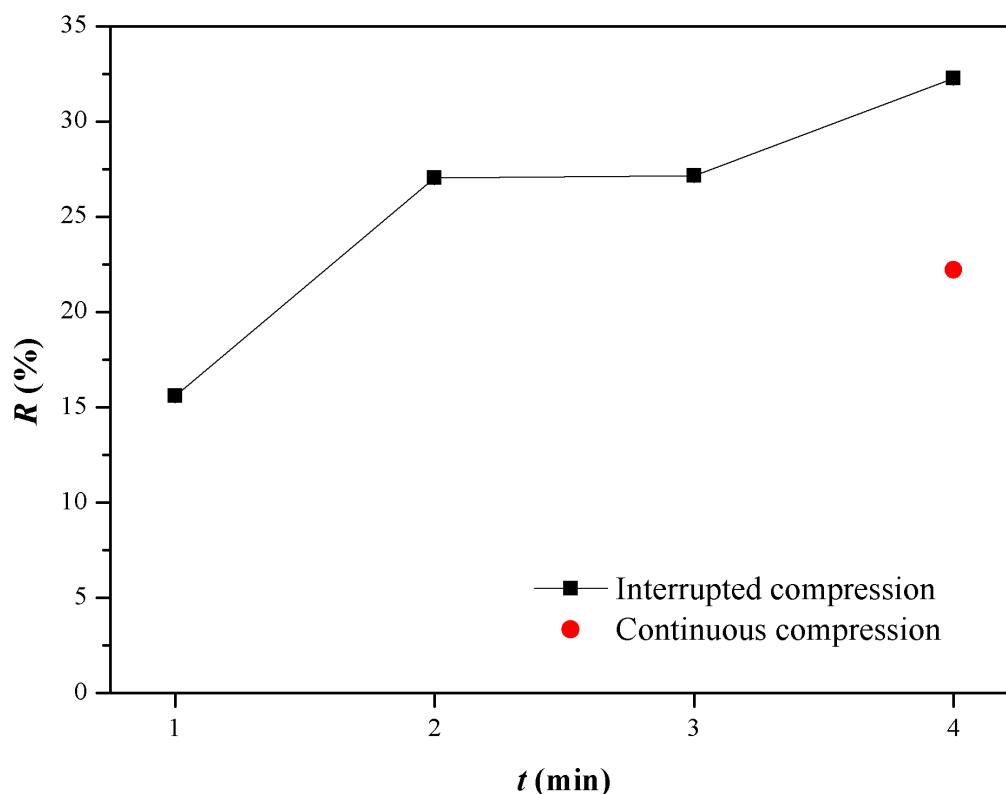


Figure 7.4: Recovery efficiency during interrupted compression and with continuous compression for 4 min.

It can be seen that interrupted compression is more efficient than the continuous one for a same overall compression time. This can be explained by the fact that when pressure is alleviated in interrupted compression, the oil flows out of the interparticular spaces between the cork sorbents, releasing these spaces for the next round of applied pressure and allowing the squeezing of more oil from the sorbent. Recovery increases in particular from the first to the second round of applied

pressure, and then further on the fourth round. Therefore, four 1-min compressions were used as the protocol for further experiments.

Afterwards, the influence of the mass of oil-saturated sorbent in the extruder was evaluated. The results are presented in Figure 7.5. It can be seen that increasing the mass of oil-saturated sorbent increases oil recovery up to 5 g, then stabilising for the maximum load of 10 g. This occurs because the presence of a higher amount of cork sorbent causes a “pillow effect”, enabling higher overall squeezing of the material. Furthermore, the fact that a higher mass of oil is flowing out of the compressed amount of sorbent leads to an easier separation of the oily phase from the solid phase between successive rounds of applied pressure.

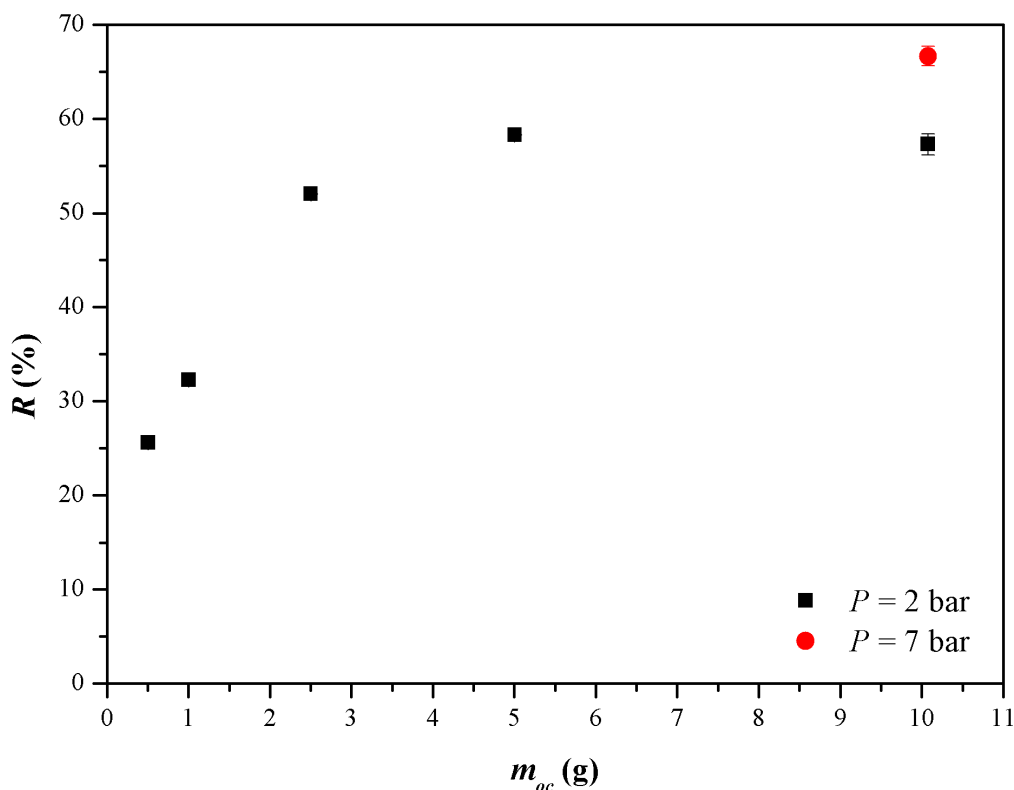


Figure 7.5: Recovery efficiencies according to the mass load of oil-saturated sorbent in the extruder at the operating pressures of 2 bar and 7 bar (four 1-min compressions).

The occurrence of the “pillow effect” is further confirmed by examining the recovery efficiency at the maximum mass load, 10 g, in both operating pressures of 2 and 7 bar. While in previous tests with a 0.5 g mass load no significant difference in recovery was observed between operating pressures (Figure 7.3), this was not the case with a 10 g load, where the recovery increased from $57 \pm 1\%$ to $67 \pm 1\%$ with the increase in pressure.

The recovery efficiency obtained at the optimised conditions for compression ($m_{oc} = 10$ g, $P = 7$ bar, and a protocol of four 1-min compressions) is compared in Figure 7.2 with the recoveries obtained with desorbing solutions. It is clear that, in these conditions, compression is a much more efficient method for recovering oil from cork sorbents.

7.3.2.3 Sorption/recovery behaviour for 10 cycles

For the optimised conditions of compression, the behaviour of cork sorbents during 10 cycles of oil sorption and recovery was evaluated. The results are presented in Figure 7.6. It is shown that the sorption/recovery behaviour of the cork sorbents is generally stable over 10 cycles, even though slight modifications occur.

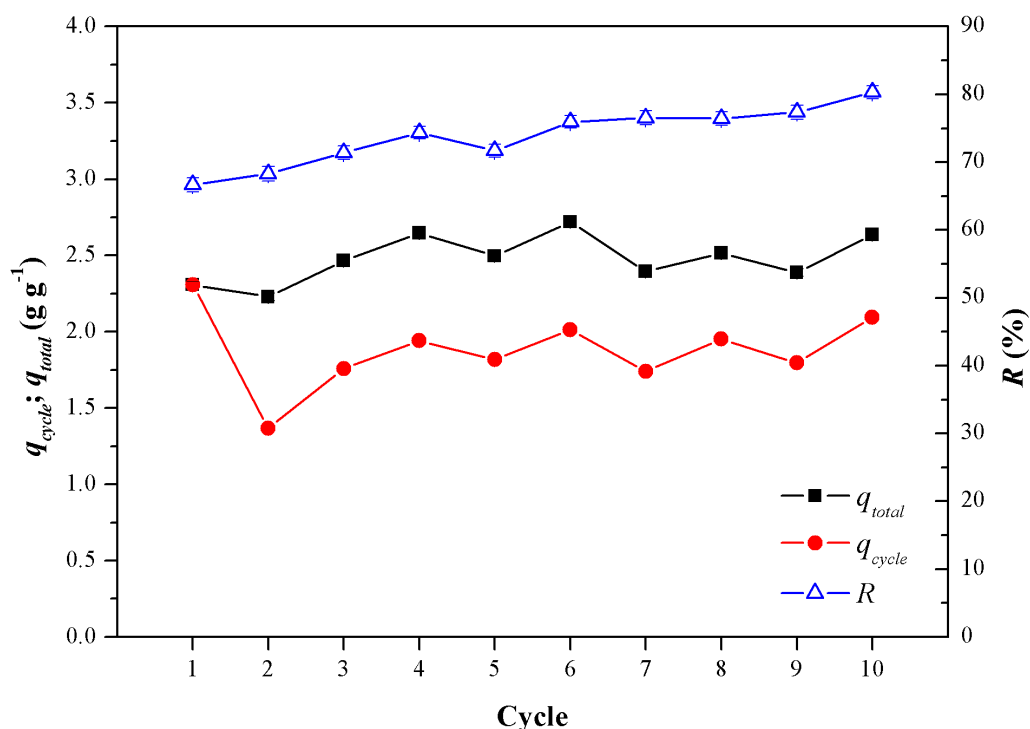


Figure 7.6: Overall sorption capacity (q_{total}), sorption capacity per cycle (q_{cycle}) and recovery efficiency by compression (R) ($m_{oc} = 10$ g, $P = 7$ bar, four 1-min compressions) during 10 cycles of sorption/recovery.

Unlike what has been observed previously (Figure 7.3), in these conditions the oil recovery increased over the sorption/recovery cycles. The overall increase in recovery efficiency from the first to the tenth cycle was from $67 \pm 1\%$ to $80 \pm 1\%$. However, the total sorption capacity also increased through the cycles, even though not so steadily. In the first cycle the oil sorption capacity was 2.31 ± 0.02 g g⁻¹ while in the tenth cycle it was 2.64 ± 0.03 g g⁻¹.

The results relate well to the “pillow effect” described previously. When the oil-saturated sorbent load in the extruder was 0.5 g (Figure 7.3), and it was operated in the horizontal, it is likely that, as it has been previously mentioned, slight structural damage may have occurred in the sorbent, since the overall oil sorption capacity decreased in the 4 cycles of operation. However, for the 10-cycle study with a sorbent load of 10 g, and operating the extruder in the vertical, the type of modifications suffered by the cork sorbent was completely different, since compression was possibly not so damaging due to the “pillow effect”. In this scenario, compression occurs more from the contact of the cork granules between themselves and less from the squeezing of cork granules between the conical head and the cylindrical piston, so the damage of the structure was lessened. However, fragmentation of the cork granules was observed, and this helps in explaining

the increase in sorption capacity, since surface area was also increased.

After the tenth cycle the extent of fragmentation was already too high to allow for an effective regeneration of the sorbent without significant mass loss. Figure 7.7 illustrates this phenomenon by comparing the visual aspect of the cork sorbents after the first and the tenth cycle.

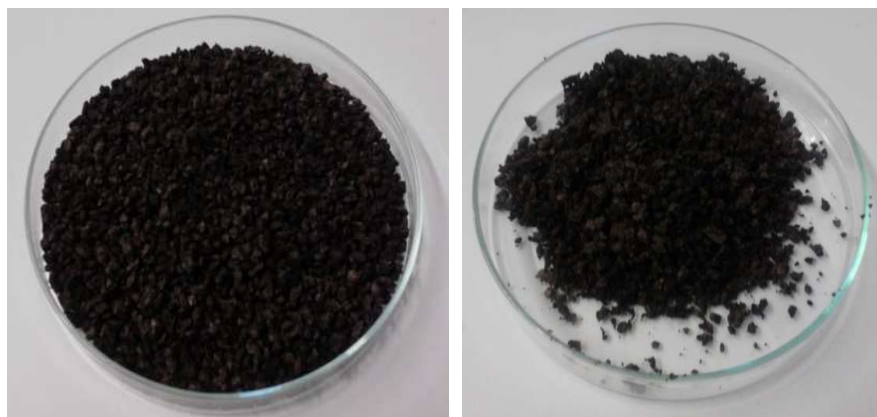


Figure 7.7: Visual aspect of the cork sorbents after the first (left) and the tenth (right) cycles of sorption/recovery.

7.4 Conclusions

Recovery of oil from cork sorbents was studied by elution using several eluent solutions and by mechanical compression using a cylindrical extruder.

It was found that the extent of desorption using tap water is very limited (under 10%), as it would be expected in a hydrophobic sorbent. Acid and anionic surfactant solutions did not improve recovery, and cationic surfactant only increased desorption slightly. The best performing eluent was the basic solution of 0.1 M NaOH, however, the use of this method may damage the cork sorbent structure.

Recovery by mechanical compression was more efficient than desorption as long as the operating conditions were optimised. It was found that interrupted compression instead of continuous compression for a same period of time favoured the overall recovery. The sorbent mass load to the extruder also influenced the oil recovery causing a “pillow effect” which maximized oil recovery up to the maximum load of 10 g. With this mass, better results were achieved employing an operating pressure of 7 bar; the maximum recovery was $67 \pm 1\%$.

It was demonstrated that, for the best method for oil recovery (10 g mass load, operating pressure of 7 bar and a protocol of four 1-min compressions), the cork sorbents were stable during 10 cycles of oil sorption and recovery.

7.5 References

- Ibrahim, S., Ang, H.-M., and Wang, S. Removal of emulsified food and mineral oils from wastewater using surfactant modified barley straw. *Bioresource Technology*, 100(23):5744–5749, 2009.
- Pitakpoolsil, W. and Hunsom, M. Treatment of biodiesel wastewater by adsorption with commercial chitosan flakes: Parameter optimization and process kinetics. *Journal of Environmental Management*, 133: 284–292, 2014.

Chapter 8

Conclusions and Future Work

8.1 General conclusions

This thesis presents a novel methodology for oil and grease removal from industrial wastewaters using sorption onto regranulated cork granulates. Current technologies for O&G removal include coagulation/flocculation, which produces hazardous sludge needing to be disposed of, and membrane processes, which are often too expensive and suffer quick fouling in the presence of high O&G concentrations. Sorption onto regranulated cork sorbents can be considered as an alternative, due to its potential to be cheaper, cleaner and more environmentally friendly. In addition, the methodology proposed in this thesis may provide added value to regranulated cork granulates, a byproduct of the cork industry, a very important economic activity in Portugal and in other Mediterranean countries.

The reviewed literature indicated that successful oil sorbents usually present low density and high hydrophobicity and in this work it has been confirmed that this applies in the case of cork granulates. In chapter 3, textural and surface characterisation of both cork biosorbents and phosphoric acid cork-based activated carbons was presented. The activated carbons were produced with the objective of improving surface area and porosity. Hydrophobicity was also enhanced in both cork biosorbents and cork-based activated carbons, in the former by impregnation with cationic surfactant HDTMA bromide and in the latter by a second pyrolysis with propene. Through the determination of the N₂ adsorption isotherms, it was found that surface area was increased and micro and mesoporosity were developed in activated carbon. Potentiometric titration, TPD, FTIR and immersion calorimetry provided insights into the surface chemistry of both biosorbents and activated carbons. Nevertheless, even though activated carbons showed increased sorption capacity toward sunflower oil in water, this did not compensate the low yields of carbonisation and energy requirements for their production, since cork biosorbents, in particular regranulated cork granulates, also showed significant sorption capacity in the same conditions.

The selected case study focused on the industrial wastewaters from a vegetable oil refinery (VORWs). Due to a high presence of free oil in these wastewaters, a gravity separation pretreatment was optimised (chapter 4) before proceeding with the studies regarding sorption treatment. It was found

that a simple gravity treatment of 30 min could yield very high removals of both O&G and COD in the studied samples, in particular in the more acidic one. The application of an empirical model and the plotting of 3D surfaces based on theoretical principles of droplet motion in a fluid allowed to conclude that all particles classified as free oil floated to the surface in less than 30 min. The application of a primary gravity separation treatment to VORWs and other oily wastewaters can be a very important strategy for downsizing secondary and tertiary treatment methods, improving treatment efficiency and achieving better effluent quality.

O&G sorption onto regranulated cork sorbents was then studied as a secondary treatment. First of all, in chapter 5, the chemistry of sunflower oil-in-water emulsions and the influence of electrostatic interactions in vegetable oil uptake by cork sorbents was examined. Droplet size distributions and zeta potential measurements allowed to establish the stability of emulsions and relate this to sorption performance. Both pH and ionic strength were shown to be very influential in O&G removal efficiency, due to their effect in neutralising droplet-droplet repulsive forces. The addition of acid led to the introduction of positive charges which neutralised the adsorbed layer of hydroxyl ions on the colloidal oil droplets, while the increase in sodium chloride concentration caused a double layer compression effect, reducing the need for such strong acidification. Moreover, in chapter 6, the influence of saponified matter was also analysed and it was confirmed that its stabilising influence inhibited O&G sorption onto regranulated cork granulates, probably due to adsorption of sodium oleates at the oil/water interface leading to the formation of micelles and increasing the electrokinetic potential. In these conditions, only strong acidification to a pH of 2.0 guaranteed effective O&G removal by sorption.

In favourable conditions for sunflower oil sorption, both in the absence and in the presence of soap, it was found that the uptake mechanism was organic-organic partitioning by hydrophobic interactions between O&G and cork. The equilibrium isotherms could be well described by both Freundlich and linear models, since in the Freundlich isotherm the parameter n was always close to 1. A mass transfer model was developed to describe the sorption kinetics by assuming that the oil-in-water emulsion behaved as a homogeneous solution and that the process was governed by an external fluid film resistance, since intraparticle diffusion was considered to be negligible because cork has no internal porosity. In the absence of soap, kinetics were slowed down by an order of magnitude when increasing the rotating agitation speed, a counter-intuitive result that indicated that turbulence kept the emulsion stable and impaired mass transfer from the bulk liquid to the solid surface.

Still in chapter 6, the secondary treatment of VORWs by O&G sorption onto regranulated cork granulates was effectively carried out. The treatment was successful in acidic conditions (pH of 2.0 or lower) in both wastewater samples studied, and for the naturally acidic wastewater from the removal of waxes (AW) an equilibrium isotherm could also be drawn. In the case of the wastewater from the homogenisation tank of the industrial wastewater treatment plant (TH) the treatment could never exceed a certain removal efficiency due to the presence of dissolved organic matter which could not be removed by sorption and requires further treatment. Nevertheless, in this VORW sample it was possible to reduce the emulsified O&G load from over 1 g L^{-1} to only

$40 \pm 10 \text{ mg L}^{-1}$.

The continuous treatment of a simulated wastewater produced with sunflower oil, saponified matter, sodium chloride and acid pH adjustment with sulphuric acid by sorption of O&G onto regranulated cork granulates was demonstrated in a continuous stirred-tank reactor. At the best operating conditions, 4.8 L of simulated wastewater containing $205 \pm 30 \text{ mg L}^{-1}$ O&G were treated during 8 h to values below the O&G discharge limit defined in the Portuguese legislation (15 mg L^{-1}). Mathematical models were developed to describe the sorption process in continuous mode. The study in the CSTR demonstrated the feasibility of applying sorption onto cork granulates as the secondary treatment of VORWs at lab scale. The stirred-tank set-up has advantages over a column setup due to the prevention of problems of clogging and flow and pressure loss; furthermore, it was observed that a filter layer can still occur in the stirred-tank due to the high buoyancy of low-density cork granulates and enhance O&G removal when compared to the results obtained in batch sorption tests.

Finally, an exploratory study on desorption and recovery of oil from regranulated cork sorbents was presented in chapter 7. Even in oil-saturated sorbents from contact with pure oil medium, the leaching of oil using tap water is low, as well as with acid and anionic surfactant solutions. The best performing elution was achieved with a basic solution which caused a partial saponification of the sorbed oil leading to its solubilisation. Still, recovery was much higher using mechanical compression, as long as favourable conditions of high pressure, interrupted compression, and maximum sorbent load to the extruder were provided. Using this regeneration procedure, regranulated cork granulates remained stable for 10 cycles of oil sorption/recovery, suffering only partial fragmentation due to mechanical compression. Sorbent disintegration eventually led to the inability to reuse it after the 10th cycle.

8.2 Suggestions for future work

This thesis mainly consisted in an exploratory study on the application of cork byproducts as sorbents of O&G in VORWs. Since the feasibility of this methodology has been confirmed and optimised at lab scale, future work should address the challenges posed by the scale up of the process, having in view pilot and industrial scale units for a marketable application.

First of all, a more in-depth study of the continuous lab-scale unit would have to be carried out. In spite of the predicted problems with clogging and pressure loss, the operation of a fixed-bed column at lab scale would be beneficial if only for the sake of comparison with CSTR results. Furthermore, in the best performing unit, optimisation studies would need to be carried out. The effect of mechanical stirring speed was briefly considered in this thesis, but many other parameters can influence the process, such as the sorbent mass load, the flowrate, the inlet O&G concentration, and the operating temperature. The latter is particularly relevant since VORWs can reach temperatures as high as $80 \text{ }^\circ\text{C}$ upon generation in the facility. Studies with real VORW, instead of simulated wastewater, should be carried out, ideally *in situ*, to prove the applicability of the methodology before investing on a pilot or industrial scale unit.

Moreover, O&G sorption onto regranulated cork granulates should be investigated as a treatment methodology for other types of wastewaters. As it was mentioned in chapter 2, there are many industrial activities which generate wastewaters heavily loaded with O&G, not only from the food processing, e.g., fish canning, slaughterhouses, olive mills, but also from petroleum refineries and metalworking industries. The specifics of each case need to be studied but the successful treatment of VORW which has been demonstrated in this thesis is a good indicator that the methodology could also be advantageous in other applications.

Oil recovery and sorbent regeneration is a topic which was only superficially considered in this thesis and which needs to be studied in more detail. Experimental studies need to be carried out with oil-saturated sorbents from wastewater treatment (instead of by contact with pure oil medium) to verify if the conclusions taken from this study still hold in those conditions. The regeneration conditions and procedure in a continuous unit also need to be considered for optimal operation of a larger scale system. Furthermore, the fate of exhausted cork sorbents must be taken into account, whether it is deposition on sanitary landfill, incineration or any other application. For cork granulates saturated with vegetable oil, an interesting possibility would be to apply it as soil conditioner, in the perspective of resource recovery.

Finally, the confirmation from this work that cork granulates are hydrophobic sorbents with good affinity for oil and hydrophobic substances in aqueous medium also opens up other possibilities for this kind of byproducts. Micropollutants are an emerging concern in the environment and, particularly, in water matrices and their removal by sorption is a clean and simple methodology with high potential for a real application. Many of these organic pollutants, from PAHs to organochloride pesticides or personal care products like polycyclic musks have high octanol-water partition coefficients and as such it could be expected that their partition onto cork is highly favoured. Recent studies (mentioned in chapter 2) also indicate this since it has been demonstrated that successful sorption of PAHs from water onto cork granulates is possible. Exploratory studies on the removal of other hydrophobic pollutants could be very interesting topics to explore in current times.

Appendix A

Uncertainty in the analytical method used for O&G determination

A.1 Introduction

This appendix presents the results for the estimation of uncertainty in the analytical method used for O&G determination in water throughout this thesis. The selected methodology is described in Standard Methods (2005) as the partition-infrared method for the determination of O&G (5520-C). The method is based on liquid-liquid extraction which causes the partition of oils onto between water and an organic solvent phase; the solvent used must be transparent to infrared radiation at the C-H bond. When a scan of the extract is read in a FTIR spectrophotometer, the height of the C-H peak (between 2900 and 2950 cm^{-1} , approximately) is calculated and it is from the values of peak heights (PHs) that quantification is carried out.

Standard Methods recommends trichlorotrifluoroethane as the infrared-transparent extraction solvent, however, due to phase out of its production after regulation by the Montreal Protocol (UNEP, 2009), the solvent in use at the beginning of the project was carbon tetrachloride (CTC). This solvent was used in the first two years of this project.

Nevertheless, production of CTC was also phased out in 2010, therefore the stock was used up and an alternative solvent had to be sought. For this purpose, infrared-transparent tetrachloroethylene (PCE) was chosen. Even though the use of PCE for O&G determination in water matrices is not endorsed by any standard, recent studies by Farmaki et al. (2007) and Almeida et al. (2013) have shown successful validation and application of this solvent.

In this appendix the results of the estimation of analytical uncertainty of the method with both CTC and PCE as extraction solvents are presented.

A.2 Experimental

A primary standard of 2 g L^{-1} O&G was produced in the laboratory by dissolving a known mass of sunflower oil in CTC or PCE. Even though Standard Methods recommends a mixture of isooc-

tane, hexadecane and benzene as the reference oil, sunflower oil was selected in this work since it focused on sunflower oil-in-water emulsions and VORWs from sunflower oil refining. A comparison between the spectrum of reference oil (mixture of isooctane, hexadecane and benzene), the spectrum of sunflower oil, and the spectrum of an extracted VORW sample is presented in Figure A.1. It can be seen that the spectra of both VORW samples is much more similar in shape to the spectrum of the sunflower oil standard than to that of the reference oil standard mixture.

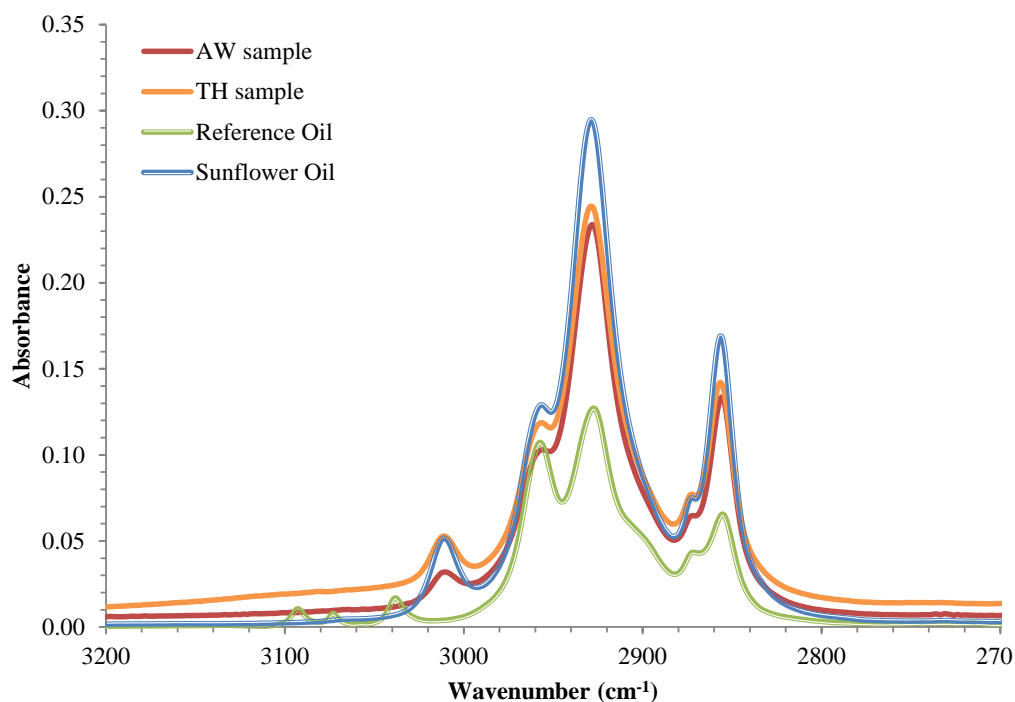


Figure A.1: Comparison between FTIR spectra of AW and TH VORW samples, a reference oil standard of 50 mg L⁻¹ and a sunflower oil standard of 130 mg L⁻¹.

From the primary standard of sunflower oil in CTC or PCE, a range of standards were prepared to obtain the calibration curves, with the following concentrations: 0.2 mg L⁻¹, 0.5 mg L⁻¹, 1 mg L⁻¹, 2 mg L⁻¹, 3 mg L⁻¹, 5 mg L⁻¹, 10 mg L⁻¹, 15 mg L⁻¹, 20 mg L⁻¹, 35 mg L⁻¹, 50 mg L⁻¹, 75 mg L⁻¹, 100 mg L⁻¹, 150 mg L⁻¹, 200 mg L⁻¹, 250 mg L⁻¹ and 350 mg L⁻¹. The standards were read in triplicate in a FTIR spectrophotometer (IRAffinity-1, Shimadzu) on the range 2700-3200 cm⁻¹ (30 scans, resolution 2.0), and the PH for the C-H band, between 2900 and 2950 cm⁻¹, approximately, was calculated using the IRAffinity software.

Two different quartz cells, with optical paths of 50 and 10 mm, were used for standard and extract reading in the spectrophotometer. The calibration done with the cell with the longer optical path (50 mm) is thus denominated as “Low Range” and comprises a range up to 50 mg L⁻¹ with more sensibility. The calibration with the cell of 10 mm optical path is denominated as “High Range” and covers a wider range, up to 350 mg L⁻¹.

The calibration and uncertainty parameters of all four methods (carbon tetrachloride - low range (CTC-LR), carbon tetrachloride - high range (CTC-HR), tetrachloroethylene - low range (PCE-LR), and tetrachloroethylene - high range (PCE-HR)) were carried out according to the recom-

recommendations of Ellison and Williams (2012). The repeatability was evaluated by calculating the standard deviation of the triplicate determination of the PH of standards. The intermediate precision was determined at three levels for each analytical method by the quantification of six samples of the same oil-in-water emulsion. Since this analytical method is considered “empirical” or “operationally defined” because the result is not independent of the choice of method conditions, namely the extraction solvent, estimation of bias was not carried out. Ellison and Williams (2012) consider that, in this case, “It is not meaningful to consider correction for bias intrinsic to the method, since the measurand is defined by the method used.”

Sunflower oil-in-water emulsions for intermediate precision tests were produced by mixing sunflower oil in water in order to achieve a desired concentration level and agitating at 8800 rpm (UltraTurrax MICCRA D-15, ART) during three 10-min cycles alternated with 10-min breaks.

A.3 Results

A.3.1 Carbon tetrachloride - low range

Figure A.2 presents the calibration curve for the method with carbon tetrachloride - low range. At first, the calibration was done with the readings of the standards of 0.2 mg L⁻¹, 0.5 mg L⁻¹, 1 mg L⁻¹, 2 mg L⁻¹, 3 mg L⁻¹, 5 mg L⁻¹, 10 mg L⁻¹, 15 mg L⁻¹, 20 mg L⁻¹ and 50 mg L⁻¹, but since the limit of detection (LOD) calculated with this method was approximately 0.9 mg L⁻¹, a new calibration curve was defined without the readings of the first two standards.

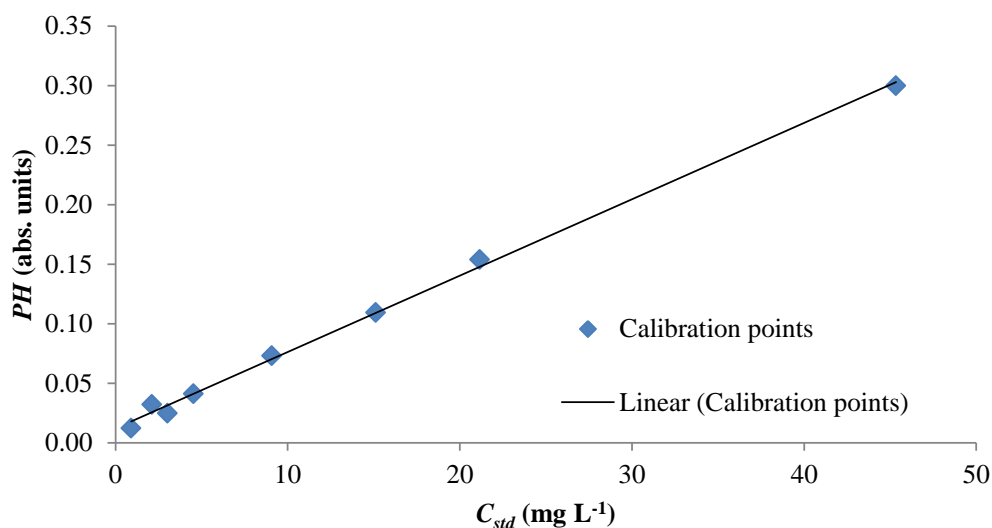


Figure A.2: Calibration curve for the CTC-LR method.

Table A.1 presents the calibration parameters for the CTC-LR method, including the slope of the calibration curve (a), the intercept of the calibration curve (b), the correlation coefficient, the LOD and the limit of quantification (LOQ). The estimation of total uncertainty was then carried out taking into account two sources of uncertainty: the calibration curve and the intermediate precision.

As mentioned before, bias was not taken into consideration since this is an empirical method. The uncertainty from the calibration curve (S_{x_0}) was determined according to the following equation:

$$S_{x_0} = \frac{S_{y/x}}{a} \sqrt{\frac{1}{p_{rep}} + \frac{1}{n_{std}} + \frac{(C_{pred} - C_{av})^2}{\sum_{j=1}^{n_{std}} (C_{stdj} - C_{av})^2}} \quad (\text{A.1})$$

where $S_{y/x}$ is the standard deviation of the residuals, p_{rep} is the number of repetitions of each analysis, n_{std} is the number of standards used in the calibration curve, C_{pred} is the predicted concentration of standard according to the calibration curve, C_{av} is the average concentration of standards in the calibration curve, and C_{std} is the concentration of standards.

Table A.1: Calibration parameters for the CTC-LR method.

a (L mg⁻¹)	6.42×10^{-3}
b (abs. units)	1.20×10^{-2}
r^2	0.997
n_{std}	8
p_{rep}	3
df	6
$S_{y/x}$	5.38×10^{-3}
S_a (L mg⁻¹)	1.36×10^{-4}
S_b (abs. units)	2.56×10^{-3}
LOD (mg L⁻¹)	1.199
LOQ (mg L⁻¹)	3.996

The intermediate precision consists in the relative standard deviation between the O&G determinations of the six sample readings. Finally, the overall uncertainty (u) was calculated by:

$$u = \sqrt{\left(\frac{S_{x_0}}{C_{pred}}\right)^2 + (Int.Precision)^2} \quad (\text{A.2})$$

The results are presented in Table A.2.

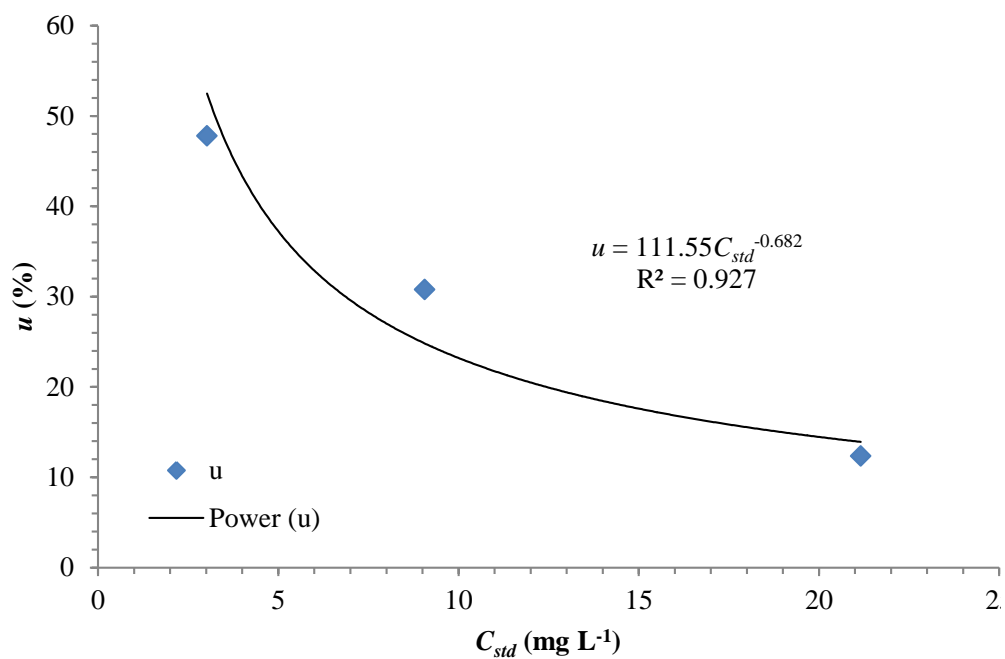
Finally, the uncertainty was plotted against the concentration of standard (C_{std}) so that a power function could be fitted to predict the uncertainty all over the calibration curve. The result is presented in Figure A.3 and the fitted function was used to estimate the uncertainty for all O&G determinations using this analytical method.

A.3.2 Carbon tetrachloride - high range

Figure A.4 presents the calibration curve for the method with carbon tetrachloride - high range. This calibration was done with the readings of the standards of 1 mg L⁻¹, 5 mg L⁻¹, 10 mg L⁻¹, 15 mg L⁻¹, 20 mg L⁻¹, 50 mg L⁻¹, 75 mg L⁻¹, 100 mg L⁻¹, 150 mg L⁻¹, 200 mg L⁻¹, 250 mg L⁻¹ and 350 mg L⁻¹.

Table A.2: Determination of the uncertainty associated to the calibration, for the the analytical method CTC-LR.

C_{std} (mg L ⁻¹)	PH_{meas} (abs. units)	PH_{calc} (abs. units)	C_{pred} (mg L ⁻¹)	S_{x_0} (mg L ⁻¹)	Repeat. (%)	Int. Prec. (%)	u (%)	u (mg L ⁻¹)
0.907	0.012	0.018	0.02					
2.116	0.032	0.026	3.14					
3.023	0.025	0.031	1.97	0.61	7.6	36.4	47.8	1.44
4.534	0.041	0.041	4.54					
9.068	0.073	0.070	9.51	0.57	2.9	30.2	30.8	2.79
15.113	0.109	0.109	15.15					
21.158	0.154	0.148	22.07	0.60	2.1	12.0	12.3	2.61
45.339	0.300	0.303	44.85					

**Figure A.3:** Estimation of uncertainty for the CTC-LR method.

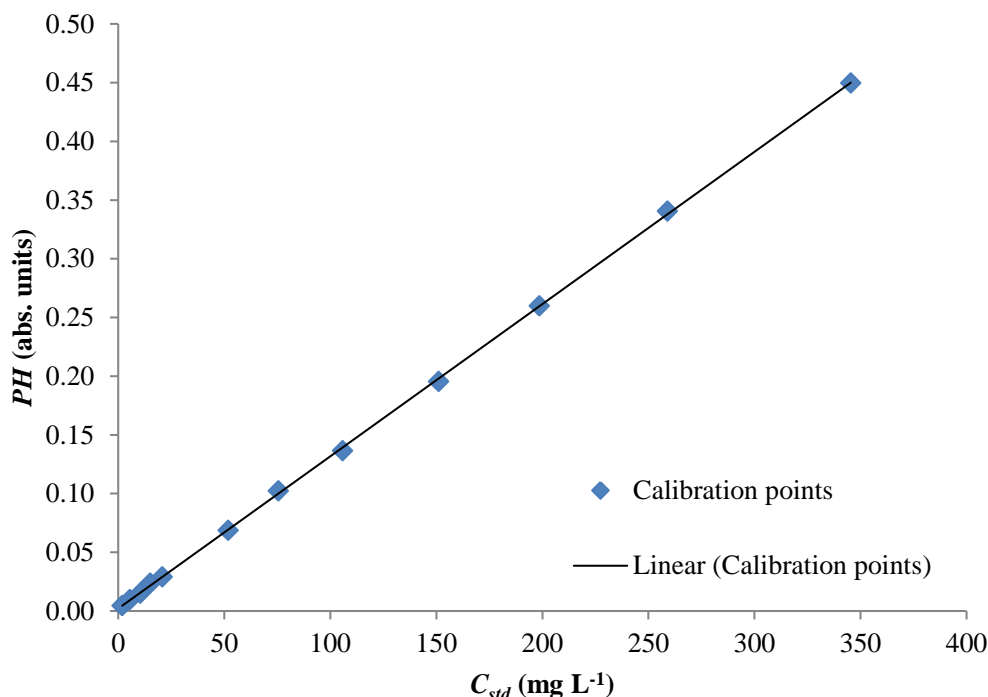


Figure A.4: Calibration curve for the CTC-HR method.

Tables A.3 and A.4 present the calibration and uncertainty estimation parameters for the CTC-HR method. S_{x_0} and u were also calculated using Equations A.1 and A.2, respectively. Figure A.5 shows the fitted function to estimate uncertainty in this method.

A.3.3 Tetrachloroethylene - low range

Figure A.6 presents the calibration curve for the method with tetrachloroethylene - low range. In this calibration, the readings of the standards of 0.2 mg L⁻¹ and 0.5 mg L⁻¹ did not even produce enough signal for the peak height to be determined, therefore the calibration was initially done with the readings of the standards of 1 mg L⁻¹, 2 mg L⁻¹, 3 mg L⁻¹, 5 mg L⁻¹, 10 mg L⁻¹, 15 mg L⁻¹, 20 mg L⁻¹, 35 mg L⁻¹ and 50 mg L⁻¹. Since the LOD here was estimated to be approximately 1.3 mg L⁻¹, a new calibration curve was defined without the reading of the first standard.

As for the previous methods, the calibration and uncertainty estimation parameters are presented in table form in Tables A.5 and A.6, and Equations A.1 and A.2 were used for the calculation of S_{x_0} and u . Figure A.7 shows the fitted function to estimate uncertainty in the PCE-LR method.

A.3.4 Tetrachloroethylene - high range

Finally, Figure A.8 presents the calibration curve for the method with tetrachloroethylene - high range. This calibration was done with the readings of the standards of 2 mg L⁻¹, 5 mg L⁻¹,

Table A.3: Calibration parameters for the CTC-HR method.

a (L mg ⁻¹)	1.30×10^{-3}
b (abs. units)	2.09×10^{-3}
r^2	1.000
n_{std}	12
p_{rep}	3
df	10
$S_{y/x}$	1.70×10^{-3}
S_a (L mg ⁻¹)	4.52×10^{-6}
S_b (abs. units)	6.77×10^{-4}
LOD (mg L ⁻¹)	1.566
LOQ (mg L ⁻¹)	5.220

Table A.4: Determination of the uncertainty associated to the calibration, for the analytical method CTC-HR.

C_{std} (mg L ⁻¹)	PH_{meas} (abs. units)	PH_{calc} (abs. units)	C_{pred} (mg L ⁻¹)	S_{x_0} (mg L ⁻¹)	Repeat. (%)	Int. Prec. (%)	u (%)	u (mg L ⁻¹)
1.926	0.005	0.005	1.92					
5.527	0.010	0.009	5.77					
10.363	0.015	0.016	10.06					
15.113	0.024	0.022	16.57	0.90	4.2	16.7	17.5	2.65
20.726	0.029	0.029	20.64					
51.816	0.069	0.069	51.35					
75.565	0.102	0.100	77.15					
105.791	0.136	0.139	103.63	0.84	1.1	17.3	17.3	18.32
151.130	0.196	0.198	149.16					
198.628	0.260	0.260	198.74	0.91	0.3	16.8	16.8	33.35
259.080	0.340	0.338	260.93					
345.440	0.450	0.450	345.18					

Table A.5: Calibration parameters for the PCE-LR method.

a (L mg ⁻¹)	6.29×10^{-3}
b (abs. units)	2.40×10^{-2}
r^2	0.997
n_{std}	8
p_{rep}	3
df	6
$S_{y/x}$	5.90×10^{-3}
S_a (L mg ⁻¹)	1.30×10^{-4}
S_b (abs. units)	3.09×10^{-3}
LOD (mg L ⁻¹)	1.472
LOQ (mg L ⁻¹)	4.905

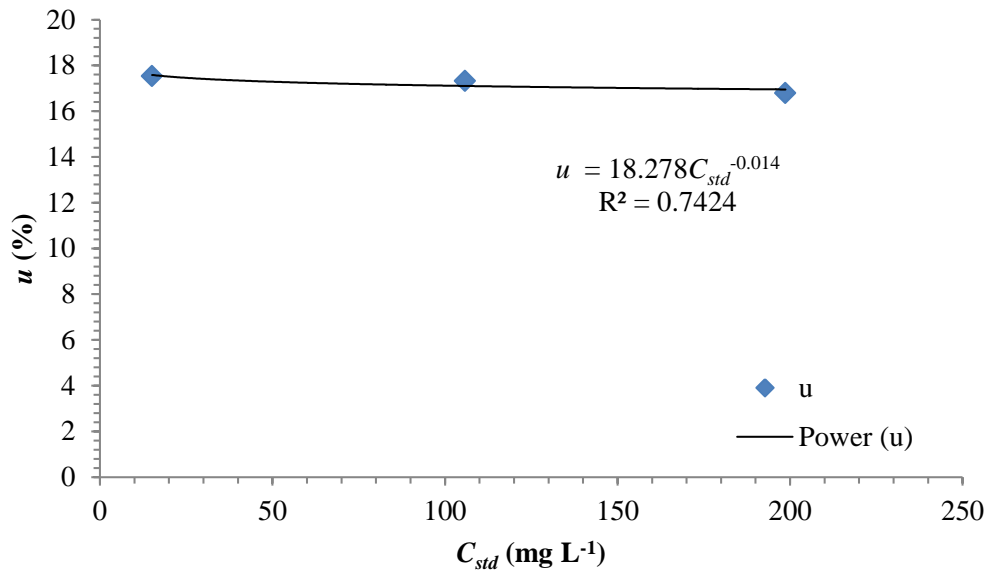


Figure A.5: Estimation of uncertainty for the CTC-HR method.

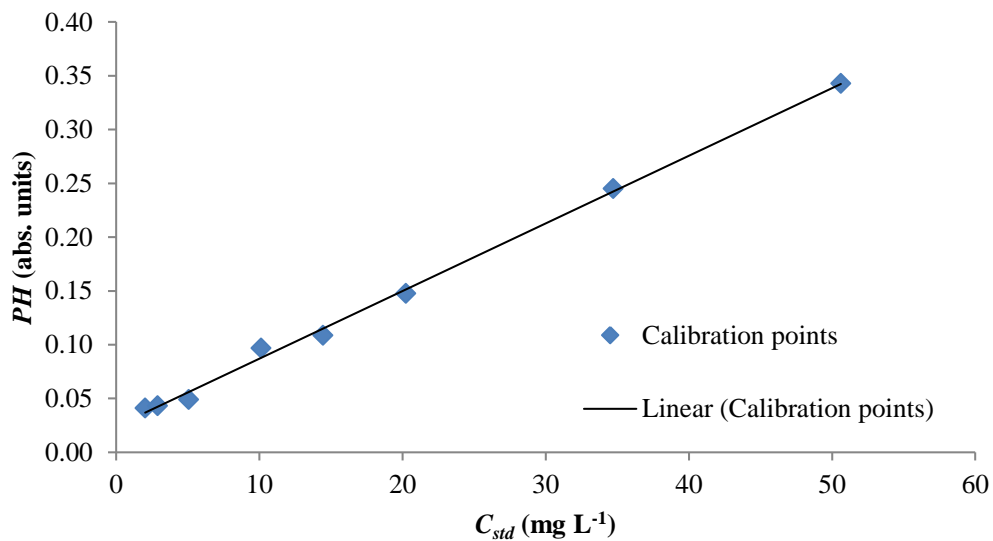
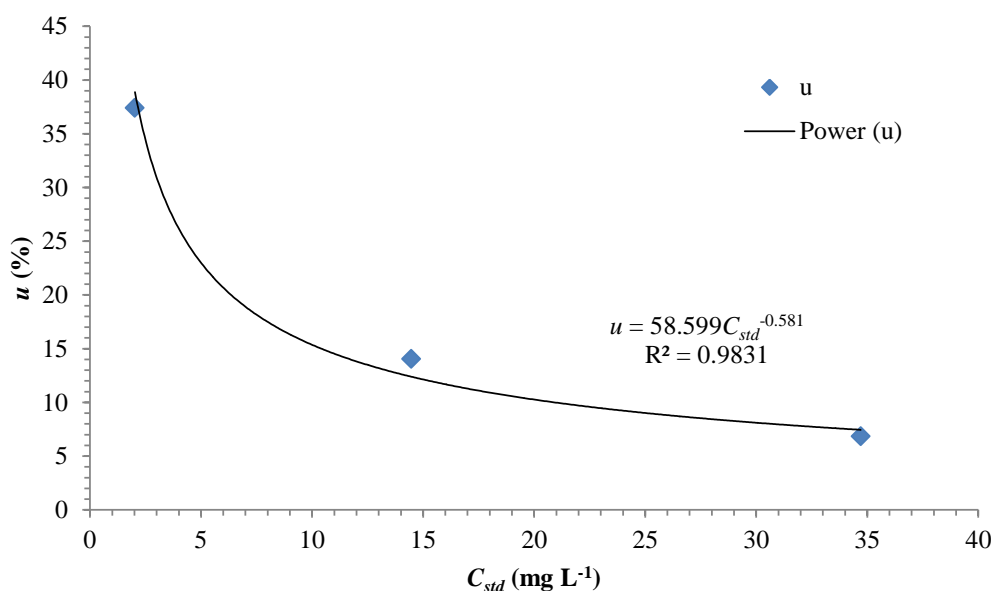


Figure A.6: Calibration curve for the PCE-LR method.

Table A.6: Determination of the uncertainty associated to the calibration, for the analytical method PCE-LR.

C_{std} (mg L ⁻¹)	PH_{meas} (abs. units)	PH_{calc} (abs. units)	C_{pred} (mg L ⁻¹)	S_{x_0} (mg L ⁻¹)	Repeat. (%)	Int. Prec. (%)	u (%)	u (mg L ⁻¹)
2.025	0.041	0.037	2.70	0.71	7.3	26.8	37.4	0.76
2.892	0.043	0.042	3.05	0.70				
5.062	0.049	0.056	3.98	0.69				
10.123	0.097	0.088	11.56	0.65				
14.462	0.109	0.115	13.45	0.64	2.7	13.2	14.0	2.03
20.247	0.147	0.151	19.62	0.64				
34.709	0.245	0.242	35.12	0.73	1.0	6.5	6.8	2.37
50.617	0.343	0.342	50.66	0.93				

**Figure A.7:** Estimation of uncertainty for the PCE-LR method.

10 mg L⁻¹, 15 mg L⁻¹, 20 mg L⁻¹, 35 mg L⁻¹, 50 mg L⁻¹, 75 mg L⁻¹, 100 mg L⁻¹, 150 mg L⁻¹, 200 mg L⁻¹, 250 mg L⁻¹ and 350 mg L⁻¹.

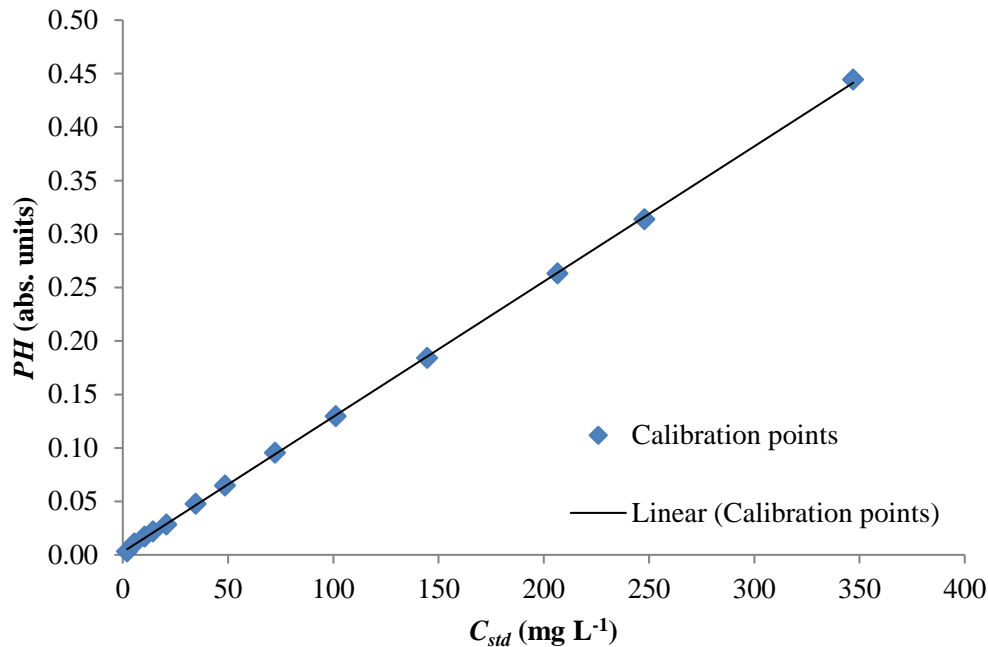


Figure A.8: Calibration curve for the PCE-HR method.

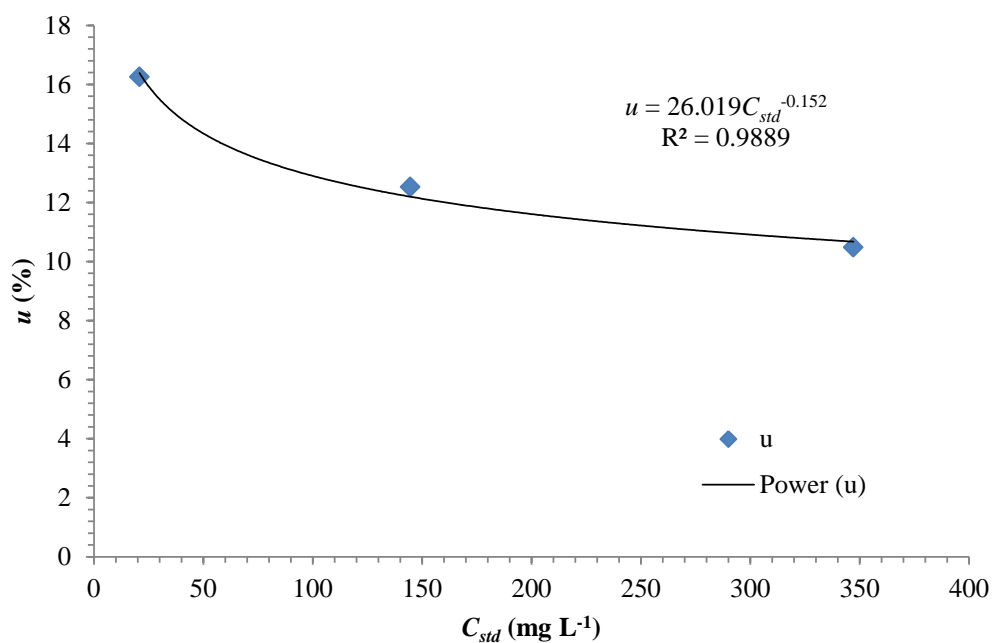
The calibration and uncertainty estimation parameters were calculated as previously mentioned and are presented in Tables A.7 and A.8. The fitted function for the estimation of uncertainty is presented in Figure A.9.

Table A.7: Calibration parameters for the PCE-HR method.

a (L mg ⁻¹)	1.29×10^{-3}
b (abs. units)	2.69×10^{-3}
r^2	1.000
n_{std}	13
p_{rep}	3
df	11
$S_{y/x}$	1.58×10^{-3}
S_a (L mg ⁻¹)	4.16×10^{-6}
S_b (abs. units)	5.94×10^{-4}
LOD (mg L⁻¹)	1.409
LOQ (mg L⁻¹)	4.697

Table A.8: Determination of the uncertainty associated to the calibration, for the analytical method PCE-HR.

C_{std} (mg L ⁻¹)	PH_{meas} (abs. units)	PH_{calc} (abs. units)	C_{pred} (mg L ⁻¹)	S_{x_0} (mg L ⁻¹)	Repeat. (%)	Int. Prec. (%)	u (%)	u (mg L ⁻¹)
2.083	0.003	0.005	0.46					
5.553	0.011	0.010	6.32					
10.413	0.017	0.016	11.36					
14.462	0.022	0.021	15.06					
20.825	0.028	0.029	20.29	0.84	2.5	15.7	16.3	3.38
34.709	0.048	0.047	35.57					
48.592	0.065	0.064	49.15					
72.310	0.095	0.094	73.21					
101.234	0.130	0.131	100.38					
144.620	0.184	0.186	143.50	0.81	0.3	12.5	12.5	18.11
206.600	0.263	0.264	205.86					
247.920	0.314	0.316	246.05					
347.088	0.444	0.442	349.20	1.15	0.3	10.5	10.5	36.38

**Figure A.9:** Estimation of uncertainty for the PCE-HR method.

A.3.5 Comparison between methods with CTC and PCE

Table A.9 shows a comparison between the intermediate precision measurements using the two different extraction solvents. A single sunflower oil-in-water emulsion was produced for each concentration level to carry out the estimation of intermediate precision for both solvents. This allowed for a comparison of the concentrations obtained.

Table A.9: Comparison between the intermediate precision measurements using PCE and CTC.

	<i>C</i> (O&G) PCE (mg L ⁻¹)	<i>C</i> (O&G) CTC (mg L ⁻¹)	PCE/CTC (%)
Low Range	2.06	2.99	68.7
	13.2	11.2	118.3
	29.4	22.4	131.3
High Range	20.5	16.0	128.3
	151.9	110.0	138.1
	326.5	194.8	167.6

It can be seen that, as expected, the concentration of oil and grease obtained using CTC or PCE are different. Moreover, a relationship between the results of CTC and PCE, e.g. a direct proportionality, cannot be established. A trend exists in that the concentrations obtained with PCE get relatively higher to the CTC concentrations as the overall O&G content increases. This suggests that PCE has a higher extraction capacity than CTC, but is less sensitive at lower concentrations.

A.4 References

- Almeida, C. M. M., Silverio, S., Silva, C., Paulino, A., Nascimento, S., and Revez, C. A. Optimization and validation of FTIR method with tetrachloroethylene for determination of oils and grease in water matrices. *Journal of the Brazilian Chemical Society*, 24(9):1403–1413, 2013.
- Eaton, A. D., editor. *Standard methods for the examination of water and wastewater*. American Public Health Association, Baltimore, Maryland, 21st edition, 2005. Prepared and published jointly by American Public Health Association, American Water Works Association, Water Environment Federation.
- Ellison, S. L. R. and Williams, A., editors. *Eurachem/CITAC guide: Quantifying Uncertainty in Analytical Measurement*. Third edition, 2012.
- Farmaki, E., Kaloudis, T., Dimitrou, K., Thanasoulas, N., Kousouris, L., and Tzoumerkas, F. Validation of a FT-IR method for the determination of oils and grease in water using tetrachloroethylene as the extraction solvent. *Desalination*, 210(1–3):52–60, 2007. Ninth Environmental Science and Technology Symposium September 1–3, 2005, Rhodes, Greece.
- UNEP. Montreal protocol on substances that deplete the ozone layer - Report of the Technology and Economic Assessment Panel. Volume 1, UNEP, May 2009.